UNIVERSIDAD DE SANTIAGO DE COMPOSTELA

FACULTAD DE FARMACIA

Departamento de Farmacia y Tecnología Farmacéutica

NANOCÁPSULAS POLICATIÓNICAS: NUEVOS SISTEMAS PARA LA LIBERACIÓN INTRACELULAR DE FÁRMACOS ANTITUMORALES

Mª Victoria Lozano López.

Santiago de Compostela, 2009

DOÑA MARÍA JOSÉ ALONSO FERNÁNDEZ Y DOÑA DOLORES TORRES LÓPEZ, CATEDRÁTICA Y PROFESORA TITULAR, RESPECTIVAMENTE, DEL DEPARTAMENTO DE FARMACIA Y TECNOLOGÍA FARMACÉUTICA DE LA UNIVERSIDAD DE SANTIAGO DE COMPOSTELA.

INFORMAN

Que la presente Memoria Experimental titulada: "Nanocápsulas policatiónicas: nuevos sistemas para la liberación intracelular de fármacos antitumorales", elaborada por la Licenciada en Farmacia **Mª Victoria Lozano López**, ha sido realizada bajo su dirección en el Departamento de Farmacia y Tecnología Farmacéutica y, hallándose concluida, autorizan su presentación a fin de que pueda ser juzgada por el tribunal correspondiente.

Y para que conste, expiden y firman el presente certificado en Santiago de Compostela, el 4 de Mayo de 2009.

Fdo. María José Alonso Fernández. Fdo. Dolores Torres López.

A mis padres.

La sencillez es algo tan complicado que sólo se puede ver con una mirada simple.

Fernando Pereira. “Discurso abstracto”.

AGRADECIMIENTOS

Sin lugar a dudas, para realizar una tesis doctoral (y no quedarse en el intento), es necesario recibir apoyo desde dos planos realmente importantes: En primer lugar desde un aspecto profesional/financiero, y en segundo lugar en el sentido personal/afectivo. Por lo tanto, hay muchas personas que han formado parte de esta tesis doctoral de uno u otro modo, y a las cuales quería agradecer su ayuda.

En primer lugar, y desde mi experiencia personal, en el aspecto profesional/financiero han intervenido un gran número de personas.

- A mis directoras de tesis, las profesoras Mª José Alonso y Dolores Torres, por haberme dado la oportunidad de realizar esta tesis doctoral y por enseñarme no sólo el significado de la investigación, sino también a desenvolverme en este campo.

- Al Ministerio de Ciencia y Tecnología así como a la USC por facilitarme el apoyo económico necesario para realizar esta tesis.

- Al Departamento de Farmacia y Tecnología Farmacéutica en general, así como a los profesores Ángel Concheiro y Carmen Álvarez.

- Al profesor Fernando Domínguez y Daniel Torrecilla del Departamento de Fisiología de la Facultad de Medicina. Muy especialmente quería agradecer a Anxo Vidal su dedicación, paciencia y disponibilidad.

- A la profesora Mabel Loza, a Pepo, Mónica, Silvia, Salva y Fátima del Departamento de Farmacología de la Facultad de Farmacia.

- A los profesores Ricardo Riguera y Eduardo Fernández-Megía, así como a Enrique Lallana y Ramón Novoa del Departamento de Química Orgánica de la Facultad de Química.

- Al profesor Stefan Schneider, a Volker, Christian, Eva, Elwira, Birgit y Susana de la Hautklinik Münster, por los maravillosos meses que pasé con ellos y por enseñarme otra forma de ver la investigación. *Danke schön!*

- A los profesores Juan Luis Ortega, Delfi Bastos, J. M. Peula y así como a Manuel Santander del Departamento de Coloides de la Universidad de Granada.

- A Miro, Merche y Raquel del Servicio de Microscopía de la Universidad de Santiago de Compostela.

- Al profesor Antonio Rabasco y a la profesora Mª Luisa González, del Departamento de Tecnología Farmacéutica de la Universidad de Sevilla, gracias a ellos tuve la oportunidad de contactar con el grupo de la profesora Alonso.

Y ahora le toca el turno a mi apoyo personal que ha sido mucho, muy intenso y necesario durante estos años:

- Muchísimas gracias a mis padres, por el apoyo y por la educación que me han dado, me ha sido de gran ayuda siempre y especialmente durante esta tesis. Además, no sería justo olvidarme de la excepcional paciencia de mi padre al teléfono, ¡casi serías capaz de defender esta tesis por mi! Muchas gracias a mis hermanos y a Juani, por su punto de vista "extracientífico" y por lo que disfruto estando con ellos; y por supuesto a mi Tía Geny (nunca me imaginé que las clases de mecanografía de verano me fueran a servir para tanto).

- Gracias también a Manolo, Carmen, Jose, Rocío, María, Mª Carmen y Javi, por su cariño y acogida.

- Dentro de todos mis amigos santiagueses, tengo que destacar en primer lugar a Nela, especialmente ella es la que entiende qué han supuesto estos años de tesis, quizás por todo el tiempo que hemos pasado juntas. Por supuesto otro apoyo esencial ha sido Manolo, principalmente por su cariño, paciencia (sobre todo informática) y por sus ánimos. ¡Has sido el mejor descubrimiento de esta tesis! Y luego hay un montón de amigos más, a los que no les puedo dedicar un párrafo a cada uno, pero que no puedo dejar de nombrar: María Álvarez, Noelia, Ivana, Sascha, Daya, Chachi, Mª Alonso, Marcos, Noemi, Mª de la Fuente, Desi, Pablo, Rafa, Puri, Francisco, Jenny, Giovanna, Sandra y Helena, y por supuesto a todos los demás que han pasado o continúan en el laboratorio. ¡Arriba Snakers!

- Por último a mis amigas Marina, Mª José, Ali, Ángeles y Mabel, a las que veo muy poco, pero que siempre están ahí.

Mª Victoria Lozano López.
4 de Mayo de 2009.

ÍNDICE

RESUMEN

RESUMEN

La mayoría de los fármacos anticancerosos se caracterizan por su baja solubilidad en agua, y por lo tanto frecuentemente se necesitan solubilizantes para mejorar su formulación. Los mayores inconvenientes de estos solubilizantes, como el Cremophor EL o el Tween 80, son los graves efectos secundarios que producen en los pacientes, lo cual limita la dosis de fármaco que puede ser administrada. Por lo tanto, recientemente se han propuesto formulaciones alternativas basadas en la Nanotecnología las cuales no requieren la utilización de estos compuestos tensoactivos y que mejoran la liberación intracelular de los fármacos que transportan.

En este contexto, las nanocápsulas poliméricas, sistemas vesiculares constituidos por un núcleo oleoso y una cubierta catiónica, son candidatos prometedores debido a la eficiente encapsulación de moléculas hidrofóbicas en sus núcleos oleosos. Por lo tanto, el principal objetivo de esta tesis es el desarrollo de nanocápsulas poliméricas como sistemas de liberación intracelular de fármacos anticancerígenos, poniendo especial atención a su evaluación biológica en modelos tumorales. Adicionalmente, en base a la crucial importancia de la cubierta polimérica en la estabilidad y en el comportamiento físico-químico de las nanocápsulas, en este trabajo hemos investigado el desarrollo de las nanocápsulas poliméricas con una cubierta de materiales que promueven el paso a través de barreras biológicas, como son el polisacárido quitosano o el poliaminoácido poliarginina. Además, se utilizó una estrategia de direccionamiento selectivo de los sistemas mediante el anticuerpo monoclonal anti-TMEFF-2, para facilitar su interacción con las células tumorales que sobreexpresan el antígeno en su superficie.

ABSTRACT

Most anticancer drugs are characterized for their low water solubility and hence solubilizers are frequently required to facilitate their formulation. The main drawback of these solubilizers, such as Cremophor EL or Tween 80, are their severe side-effects, which limit the amount of drug that can be safely administrated. Therefore, alternative nanotechnology-based formulations, which do not require these solubilizers and are able to improve the intracellular drug delivery, have recently been proposed.

In this context, polymeric nanocapsules, which are vesicular systems constituted by an oil core and a cationic shell, are promising candidates due to the efficient encapsulation of hydrophobic molecules in their oil cores. Thus, the main objective of this thesis has been the design of polymeric nanocapsules as intracellular drug delivery systems for anticancer drugs, paying special attention to their biological evaluation in tumor models. Moreover, based on the crucial role of the polymeric shell on the stability and behaviour of the nanocapsules, in this work we have deeply investigated the development of polymeric nanocapsules surface-modified with materials that efficiently translocate through biological barriers, such as the polysaccharide chitosan or the polyaminoacid polyarginine. In addition, an active targeting approach was employed for the selective modification of polymeric nanocapsules with the monoclonal antibody anti-TMEFF-2, aimed to facilitate the interaction of the nanosystems with the tumor cells that overexpress the antigen in their surfaces.

INTRODUCCIÓN

INTRODUCCIÓN

La Nanotecnología está repercutiendo considerablemente en los avances experimentados por diversas áreas científicas. Así, su aplicación en Biomedicina ha dado lugar a la Nanomedicina, una rama que está actualmente en pleno desarrollo. De hecho, el creciente interés en esta área, tanto académico como industrial, se muestra reflejado en el incesante número de publicaciones y patentes [1]. Un aspecto característico y de gran importancia de la Nanomedicina es que engloba los esfuerzos de múltiples disciplinas, con el fin de diseñar nuevas estrategias para el diagnóstico y tratamiento de enfermedades. Así pues, la investigación en cáncer está siendo especialmente intensa y ha dado lugar a importantes avances en inmunodiagnóstico, diagnóstico por imagen, quimioterapia y radioterapia [2; 3]. Más concretamente, ha contribuido a la mejora de la eficacia y a la disminución de los efectos secundarios de los fármacos utilizados en la quimioterapia del cáncer.

Dentro de la Nanomedicina podemos encontrar un gran número de sistemas tales como nanopartículas poliméricas, micelas, liposomas, dendrímeros, conjugados, nanopartículas magnéticas, nanopartículas de silicio y quantum dots [4-7]. Una descripción pormenorizada sobre algunos de estos sistemas se recoge en el artículo de revisión incluido en esta memoria [1]. Por lo tanto, en esta introducción nos centraremos en el caso concreto de la evolución de las nanopartículas poliméricas en el tratamiento del cáncer.

Nanopartículas poliméricas y tratamiento del cáncer

Nanopartículas de albúmina

Las primeras nanopartículas poliméricas diseñadas para el tratamiento del

---

[1] **Hervella P.; Lozano V.; Garcia-Fuentes M.; Alonso M.J.** (2008). J. Biomed. Nanotechnol. 4: 276-292.
[2] **Ferrari M.** (2005). Nat. Rev. Cancer. 5: 161-171.
[3] **Peer D.; Karp J.M.; Hong S.; Farokhzad O.C.; Margalit R.; Langer R.** (2007). Nat. Nanotechnol. 2: 751-760.
[4] **Zamboni W.C.** (2005). Clin. Cancer Res. 11: 8230-8234.
[5] **Couvreur P.; Vauthier C.** (2006). Pharm. Res. 23: 1417-1450.
[6] **Duncan R.** (2006). Nat. Rev. Cancer. 6: 688-701.
[7] **Juzenas P.; Chen W.; Sun Y.P.; Coelho M.A.N.; Generalov R.; Generalova N.; Christensen I.L.** (2008). Adv. Drug Deliv. Rev. 60: 1600-1614.

cáncer fueron las elaboradas a base de albúmina, conteniendo mercaptopurina, y obtenidas mediante emulsificación y posterior desnaturalización por calor de la proteína [8]. Posteriormente, Sugibayashi y *col.* [9-11] utilizaron este mismo sistema para la encapsulación del fármaco anticancerígeno 5-fluorouracilo. Asimismo Widder y *col.* [12-14] emplearon las nanopartículas de albúmina para la encapsulación de doxorubicina junto a partículas de magnetita. En este último caso se observó que la acción de un campo magnético externo al animal inducía la acumulación de las nanopartículas en el tejido tumoral, permitiendo la liberación selectiva del fármaco en el tejido diana. Ello supuso un éxito en aquel momento, que más adelante fue cuestionado por la falta de aproximación a la realidad del modelo *in vivo*, en donde el tumor se implantaba en la cola de las ratas, hacia donde se focalizaba el campo magnético [15].

A finales de los años 70, Marty *et al.* [16] desarrollaron una formulación de nanopartículas de albúmina obtenidas por un procedimiento distinto al anteriormente comentado. En esta ocasión, se consiguió la formación de las nanopartículas mediante un proceso de desolvatación y posterior reticulación del sistema. Este procedimiento ha sido optimizado 20 años después, y se ha utilizado para la obtención de nanopartículas de albúmina modificadas con Herceptin® para el transporte intracelular de oligonucleótidos en células tumorales [17, 18].

Es de destacar que la primera formulación de nanopartículas poliméricas comercializada ha sido la de nanopartículas de albúmina para la vehiculización de paclitaxel. Esta formulación, denominada Abraxane®, fue aprobada por la FDA (*Food and Drug Administration*) en 2005 para el tratamiento del cáncer de mama metastásico. El mecanismo de acción propuesto para estas nanopartículas es su acumulación en el tumor debido al efecto de aumento de la permeabilidad y retención *(enhanced permeability and retention, EPR)* [19]. Asimismo, también

[8] **Kramer P.A.** (1974). J. Pharm. Sci. 63: 1646-1647.
[9] **Sugibayashi K.; Morimoto Y.; Nadai T.; Kato Y.** (1977). Chem. Pharm. Bull. 25: 3433-3434.
[10] **Sugibayashi K.; Akimoto M.; Morimoto Y.** (1979). J. Pharmacobio-dyn. 2: 350-355.
[11] **Sugibayashi K.; Morimoto Y.; Nadai T.** (1979). Chem. Pharm. Bull. 27: 204-209.
[12] **Widder K.J.; Senyei A.E.; Ranney D.F.** (1979). Adv. Pharmacol. Chemother. 16: 213-271.
[13] **Widder K.J.; Marino P.A.; Morris R.M.** (1983). Eur. J. Cancer Clin. Oncol. 19: 141-147.
[14] **Widder K.J.; Morris R.M.; Poore G.A.** (1983). Eur. J. Cancer Clin. Oncol. 19: 135-139.
[15] **Kreuter J.** (1983). Pharm. Acta Helv. 58: 242-250.
[16] **Marty J.J.; Oppenheim R.C.; Speiser P.** (1978). Pharm. Acta Helv. 53: 17-23.
[17] **Wartlick H.; Michaelis K.; Balthasar S.; Strebhardt K.; Kreuter J.; Langer K.** (2004). J. Drug Target. 12: 461-471.
[18] **Wartlick H.; Spankuch-Schmitt B.; Strebhardt K.; Kreuter J.; Langer K.** (2004). J. Control. Release. 96: 483-495.
[19] **Maeda H.; Matsumura Y.** (1989). Crit. Rev. Ther. Drug Carrier Syst. 6: 193-210.

interviene un mecanismo de internalización transendotelial a través de la proteína gp60, que reconoce a la albúmina. Los estudios clínicos demostraron que el Abraxane® consigue ralentizar el curso de la enfermedad, aumentando la supervivencia de los pacientes de cáncer de mama [20]. Abraxis Bioscience ha empleado esta misma tecnología para la formulación de nanopartículas de albúmina con el fármaco citostático docetaxel (ABI-008) y con el antibiótico rapamicina (ABI-009), que se encuentran actualmente en fase clínica II y I, respectivamente [21].

Nanopartículas de poli(cianoacrilato) de alquilo

Estas nanopartículas fueron desarrolladas también a finales de los años 70 por el grupo de P. Couvreur, en la Universidad de Paris Sud. Más adelante, en 1983, el trabajo publicado por Grislain *et al*. [22] demostró que las nanopartículas de poli(cianoacrilato) de isobutilo se concentraban de forma significativa en los tumores primarios de cáncer de pulmón. Estos resultados apuntaban ya la capacidad de los nanosistemas para ser extravasados y acumulados en los tejidos tumorales, por medio del efecto EPR anteriormente comentado. Posteriormente, las nanopartículas de poli(cianoacrilato) de isohexilo, que encapsulaban doxorucibina, demostraron mayor índice terapéutico en comparación con el fármaco libre y capacidad para superar los fenómenos de resistencia celulares. Estas nanopartículas, denominadas Doxorubicin-Transdrug® y desarrolladas por la compañía BioAlliance, fueron evaluadas en fase clínica para el tratamiento del hepatocarcinoma. Sin embargo, a pesar de los prometedores resultados obtenidos, los estudios de fase II/III se suspendieron al manifestarse daño pulmonar en los pacientes tratados [23].

---

[20] **Farokhzad O.C.; Langer R.** (2006). Nanomedicine: Developing smarter therapeutic and diagnostic modalities. Adv. Drug Del. Rev. 58: 1456-1459.

[21] **Hawkins M.J.; Soon-Shiong P.; Desai N.** (2008). Protein nanoparticles as drug carriers in clinical medicine. Adv. Drug Del. Rev. 60: 876-885.

[22] **Grislain L.; Couvreur P.; Lenaerts V.** (1983). Pharmacokinetics and distribution of a biodegradable drug-carrier. Int. J. Pharm. 15: 335-345.

[23] "BioAlliance Pharma suspends the Phase II/III trial of doxorubicin Transdrug® in primary liver cancer, following advice from the Drug Safety Monitoring Board and the Steering Committee" (2008) http://www.bioalliancepharma.com/eng/content/advancedsearch?SearchText=doxorubicin%20transdrug&startSearch=1.

Nanopartículas de poliésteres

Desde que en 1981 Gurny *et al*. [24] desarrollaron por primera vez las nanopartículas de ácido poli(láctico) (PLA), este polímero y su copolímero ácido poli(láctico-glicólico) (PLGA) han sido ampliamente utilizados para la formulación de nanosistemas en Tecnología Farmacéutica. Ambos polímeros presentan características muy atractivas, como su baja toxicidad y su carácter biodegradable, por lo que han sido autorizados por la FDA para la administración en humanos. Asimismo, fueron las nanopartículas de PLGA las primeras en ser modificadas en superficie con el polímero polietilenglicol (PEG) [25; 26]. Esta estrategia resultó ser clave en el desarrollo de nanosistemas capaces de evitar el reconocimiento por los macrófagos circulantes del sistema retículo endotelial (SRE), prolongando así el tiempo de circulación de los nanosistemas en sangre y disminuyendo su acumulación en los órganos del SRE.

Nanopartículas lipídicas

Las nanopartículas lipídicas como vehículos de fármacos citotóxicos surgieron en la década de los 90. En comparación a otros sistemas coloidales, las nanopartículas lipídicas poseen una corta historia, razón por la cual ninguna formulación ha superado todavía las barreras que le permitan acceder a la fase de estudios clínicos. No obstante, los resultados obtenidos de los estudios preclínicos están siendo muy prometedores [27-29]. Por lo tanto, es esperable que en el futuro las nanopartículas lipídicas desempeñen un papel importante en la mejora de los tratamientos de cáncer.

---

[24] **Gurny R.; Peppas N.A.; Harrington D.D.; Banker G.S.** (1981). Drug Dev. Ind. Pharm. 7: 1-25.

[25] **Gref R.; Minamitake Y.; Peracchia M.T.; Trubetskoy V.; Torchilin V.; Langer R.** (1994). Science. 263: 1600-1603.

[26] **Bazile D.; Prud'Homme C.; Bassoullet M.T.; Marlard M.; Spenlehauer G.; Veillard M.** (1995). J. Pharm.Sci. 84: 493-498.

[27] **Yang S.C.; Lu L.F.; Cai Y.; Zhu J.B.; Liang B.W.; Yang C.Z.** (1999). J. Control. Release. 59: 299-307.

[28] **Zara G.P.; Bargoni A.; Cavalli R.; Fundaro A.; Vighetto D.; Gasco M.R.** (2002). J. Pharm. Sci. 91: 1324-1333.

[29] **Harivardhan R.L.; Sharma R.K.; Chuttani K.; Mishra A.K.; Murthy R.S.R.** (2005). J. Control. Release. 105: 185-198.

Nanocápsulas poliméricas

Estos sistemas vesiculares, que surgieron a mediados de los años 80 [30], están constituidos por un núcleo hidrófobo o hidrófilo recubierto por una capa de polímero. Sus aplicaciones se dirigen fundamentalmente a la encapsulación de moléculas poco solubles, en la terapia del cáncer [31; 32]. De este modo, la encapsulación de dichos fármacos en el núcleo oleoso del nanosistema evita la utilización de otro tipo de disolventes causantes de graves efectos secundarios [33]. Actualmente no hay formulaciones de nanocápsulas poliméricas disponibles en el mercado. No obstante, existen estudios en la literatura que avalan el uso de esta tecnología para la terapia del cáncer [34; 35].

Puesto que las nanocápsulas poliméricas son el objeto de estudio de esta tesis doctoral, en las siguientes secciones se presentará información más detallada sobre este nanosistema.

---

[30] **Al Khouri Fallouh N.; Roblot-Treupel L.; Fessi H.** (1986). Int. J. Pharm. 28: 125-132.
[31] **Khalid M.N.; Simard P.; Hoarau D.; Dragomir A.; Leroux J.C.** (2006). Pharm. Res. 23: 752-758.
[32] **Bae K.H.; Lee Y.; Park T.G.** (2007). Biomacromolecules. 8: 650-656.
[33] **Gelderblom H.; Verweij J.; Nooter K.; Sparreboom A.** (2001). Eur. J. Cancer. 37: 1590-1598.
[34] **Burger K.N.J.; Staffhorst R.W.H.M.; De Vijlder H.C.; Velinova M.J.; Bomans P.H.; Frederik P.M.; De Kruijff B.** (2002). Nat. Med. 8: 81-84.
[35] **Cahouet A.; Denizot B.; Hindre F.; Passirani C.; Heurtault B.; Moreau M.; Le Jeune J.J.; Benoit J.P.** (2002). Int. J. Pharm. 242: 367-371.

Article I

Nanomedicine: new challenges and opportunities in cancer therapy

Pablo Hervella[#], Victoria Lozano[#], Marcos Garcia-Fuentes[#], Maria Jose Alonso*.

NANOBIOFAR group, Dep. Pharmacy and Pharmaceutical Technology, School of Pharmacy, University of Santiago de Compostela, 15782 Santiago de Compostela, Spain

[#] These authors contributed equally to this manuscript

* Corresponding author: Prof. Maria Jose Alonso

Adapted from: Journal of Biomedical Nanotechnology. (2008). 4: 276-292.

ABSTRACT

Nanomedicine contribution to cancer therapy is notoriously improving survival and quality of life of cancer patients. Currently there are several products already available on the market, and many others are in the preclinical-to clinical pipeline. Nanomedicine could bring the tools necessary to improve inherent limitations of classical pharmacotherapy. In this review, we offer a comprehensive analysis of the progress made in the design of biodegradable nanocarriers particularly adapted for the delivery of anticancer drugs, including classical low molecular weight drugs, peptides and nucleic acid based therapeutics. Furthermore, we analyze the benefits provided by these drug delivery platforms, such as long-term stability, the solubility, the biodistribution and the efficacy of anticancer drugs.

Keywords: Nanomedicine, cancer, passive targeting, active targeting, intracellular delivery

1. INTRODUCTION

Nanotechnology is pointed out as one of the disciplines with the highest future impact in pharmacotherapy. This assessment is inspired in the possibility of integrating bioactive compounds (drugs, gene medicines, etc.) into nanoscale devices, the resulting products being nowadays called nanomedicines. In conventional drugs, their pharmacological activity is inextricably linked to other characteristics of the drug: toxicity, biodistribution pattern, capacity to cross biological membranes, solubility, stability, etc. Through the formation of nanomedicines, the pharmacological activity of a drug can be dissociated from their toxic, pharmaceutical and biopharmaceutical profile [1; 2]. Nanomedicines are very flexible systems because of their modular makeup that integrates a drug in a nanoscale delivery platform. In this way, a drug can be integrated in different delivery platforms, which can be optimized to meet the requirements of specific therapeutic approaches.

The interest of nanomedicine is best perceived in cancer therapy [3], because the efficacy of current treatments is still very limited owing to the unspecific biodistribution, to the suboptimal cell internalization of many injected drugs, and to the toxicity of standard excipients required for drug solubilization. Table 1 summarizes the main biopharmaceutical advantages that can be achieved through the use of nanotechnology platforms in cancer therapy. Benefits from the application of nanotechnology to drug delivery of anticancer drugs are not only related to some of the major challenges in drug biodistribution that have been widely covered by the literature of the field [4], but also to other issues of a more technical nature. For instance, nanotechnologies that allow the formulation of many hydrophobic drugs in solvent-free media have resulted in very relevant advances for pharmaceutical practice [5; 6].

Table 1: Summary of the main therapeutical advantages that can be achieved through the use of nanotechnology in cancer.

Challenge	Effect	Examples
Storage	Improved chemical stability of the drug	59, 64
Formulation	Reduced toxicity of formulation excipients	40
Mucosal administration	Higher bioavailability. Less inter-individual variability	75
Biodistribution	Enhanced residence time in the blood	17, 94
	Passive or active targeting to tumors	28, 113
Cell trafficking	Enhanced cell penetration	77, 128, 140
	Reduced expulsion of the drug	153,154
	Efficient intracellular trafficking to the drug action site	138, 169

The expectations being raised by nanotechnology in cancer therapy have boosted interest in the academic world, in governments' scientific policy, and in industry alike. In academia, this can be exemplified by the considerable increase observed in the number of publications related to this field (e.g. see Figure 1). Indeed, over the last years, the application of nanotechnology for the improvement of anticancer drugs has attracted the attention of scientists from a broad range of disciplines -pharmacists, physicians, physicists, chemists, engineers. The intensity of the research activity initiated in this topic has also resulted in an important number of patents in this topic.

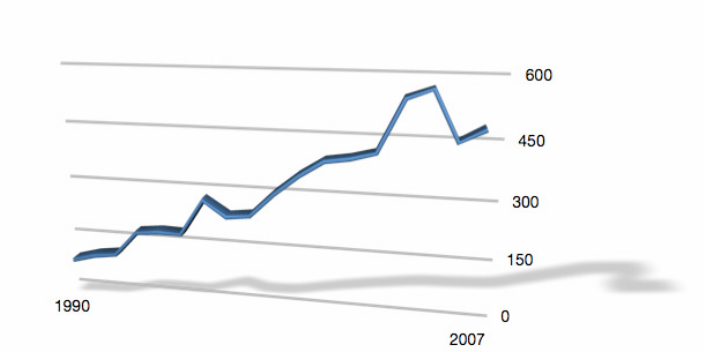

Figure 1: Number of publications related to nanotherapeutics in cancer therapy. Search performed in Scopus® (Copyright © 2008 Elsevier BV), search terms used: liposomes, nanoparticles, nanocapsules, nanoemulsions, nanocrystals, micelles and cancer.

Governments have also realized the importance of bridging together nanotechnology and cancer therapy. In the US, the National Cancer Institute (NCI) -a part of the National Institute of Health- has created the NCI Alliance for Nanotechnology in Cancer. This initiative is engaged in efforts to harness the power of nanotechnology to radically change the way we diagnose, treat and prevent cancer [7]. The European Science Foundation (ESF) has also issued a report analyzing the situation of nanomedicine in Europe [8], and it has designated nanotechnology and its applications to biomedicine as one of its major priority research areas.

The major interest in cancer therapy is also reflected in an important industry-related activity. As a matter of fact, cancer therapy is the application that has led to the highest number of "nanotherapeutic" products on the market. Table 2 summarizes which, to the best of our knowledge, are the current marketed

products for cancer treatment. There are 6 nanomedicines currently approved for cancer therapy, mostly based on liposomes. Other products are in advanced clinical trials, for example: Xyotax® (paclitaxel-polymer conjugate), Genexol-PM™ (paclitaxel in polymer micelles) and SP1049C (Doxorubicin in polymer micelles). Several others are at earlier stages of clinical trials or in preclinical phase. Considering the increasing interest that this area has undergone over the last years, we can predict a much larger amount of products on the market pipeline in the next years.

Table 2: Nanotherapeutics for cancer treatment currently in the market. Information dates from March 2008.

Name	Type of nanosystems	Drug	Company
Doxil	Liposome	Doxorubicin	Ortho Biotech
Caelyx	Liposome	Doxorubicin	Schering-Plough
Myocet	Liposome	Doxorubicin	Cephalon
DaunoXome	Liposome	Daunorubicin	Diatos S.A.
Depocyt	Liposome	Cytarabine	Enzon Pharmaceutical, Inc.
Abraxane	Albumin bound nanoparticle	Paclitaxel	Abraxis Bioscience, Inc. /AstraZeneca Pharmaceutical LP

In this review, we summarize the benefits that nanomedicines could confer to cancer therapeutics. First we describe the different biodegradable nanocarriers used as drug delivery platforms of anticancer molecules (section 2). Then, we analyze the benefits of these drug delivery platforms at different stages (section 3): (a) upon storage of the nanomedicines (subsection 3.1), (b) after their administration to the patient (subsection 3.2), (c) once they are in the systemic circulation (subsection 3.3), (d) and once they reach the tumor/cancer cells (subsection 3.4). We also review the current technologies that can be applied to achieve drug release at the desired target site (subsection 3.5).

2. NANOSTRUCTURES USED AS DRUG DELIVERY PLATFORMS

Anticancer nanomedicines require the integration of drugs into nanostructured drug delivery platforms [3; 9; 10]. Drug delivery platforms can be classified by their physical form or functional properties, both of which should be tailored according to the specific needs of the drug to be delivered and the intended therapeutic use [11; 12].

Cancer is a general term used for more than 100 different types of pathologies characterized by uncontrolled growth of abnormal cells with capacity to invade healthy tissues [7]. The arsenal available in chemotherapy includes a wide range of drugs generally aimed to revert or prevent the progression of the disease. Treatments on the market are mostly based on low molecular weight drugs, which are usually very low-soluble molecules. However, large biomolecules, such as proteins and genes, are gaining increasing attention [13-15]. As the number and variety of anticancer molecules is increasing, there is a higher pressure to deliver specific formulation solutions to their intrinsic limitations.

Nanocarriers are in constant evolution towards more sophisticated and effective systems. Current drug delivery systems enclose characteristics such as biodegradability, stimuli-sensitive behavior, and functionalization. The purpose of this review is to specifically focus on biodegradable nanocarriers which have been applied to cancer therapy. In the next paragraphs we present the advantages and limitations of the most widely applied drug delivery platforms.

2.1. Polymer therapeutics

Polymer therapeutics is a general term that includes polymer-drug or polymer-protein conjugates. Incorporation of hydrophobic drugs to polymer chains enhances their water-solubility and changes their biodistribution pattern. Examples are the polyglutamate-paclitaxel conjugate, Xyotax®, currently in clinical evaluation (phase III), and the PEGylation of proteins as L-asparaginase (Oncaspar), which improves the efficacy of this enzyme, in the treatment of acute lymphoblastic leukaemia. Polymer therapeutics for cancer has been the subject of a recent excellent review [16] and, thus, will not be covered herein.

2.2. Polymeric micelles

Polymeric micelles are nanostructures formed by the self-assembly of amphiphilic block copolymers. They present a typical organization with a hydrophobic core surrounded by a hydrophilic shell. Because of this organization, hydrophobic drugs are easily associated to their core. The integration of hydrophobic drugs to polymeric micelles results in a number of benefits such as enhanced water-solubility of hydrophobic drugs, drug protection against harsh environment, and prolonged blood circulation times [17]. Moreover, the small size of polymeric micelles, between 10-100nm, is sufficiently large to avoid renal

excretion (>50kDa) but yet small enough (<200 nm) to bypass filtration by interendothelial cell slits in the spleen [18]. As potential drawbacks, polymeric micelles are characterized by their low physical stability leading to a premature drug release after intravenous administration. There have been some recent attempts to overcome this limitation by changing the composition, physical state or cohesion of the micelle core [19-21]. Currently, there are several formulations of polymeric micelles in clinical trials, most of them, based on PEGylated copolymers, aimed at extending the drug circulation times. Doxorubicin-containing micelles, (SP1049 and NK911) [22; 23], and Genexol-PM™ containing paclitaxel [24], are some representative examples of this category of nanomedicines.

2.3. Nanoemulsions

Nanoemulsions are nanodispersions of an immiscible liquid phase in an external liquid phase, which are stabilized by an emulsifier agent [25]. Typically, they are oil-in-water nanoemulsions and they have an excellent capacity to encapsulate hydrophobic drugs [26]. Nanoemulsions are suitable for intravenous administration [27], as they are amenable to sterilization by autoclaving or filtration through a 0.22µm. Their main limitation is the lack of controlled drug release characteristics [28]. A vitamin E-based nanoemulsion of paclitaxel (TOCOSOL™ paclitaxel) is currently in Phase III, and the clinical data gathered so far have indicated enhanced efficacy compared to Taxol® [28].

2.4. Nanocapsules

Nanocapsules are vesicular systems formed by an inner cavity, aqueous or oily, surrounded by a polymeric shell [29]. These nanosystems have been used for the encapsulation of a variety of drugs, from hydrophobic compounds (e.g. paclitaxel) [30] to large hydrophilic molecules (e.g. siRNA) [31]. Nanocapsules offer several advantages as compared to nanoemulsions, such as their versatility in terms of surface modification, their improved stability in biological media [32], and a limited capacity to control drug release [33]. On the other hand, the polymeric coating of nanocapsules might result in increased toxicity compared to nanoemulsions. At present there are no anticancer drug formulations on the market based on nanocapsules, however, there are very promising data in the literature which support the interest of this formulation strategy [34].

2.5. Liposomes

Liposomes are spherical nanovesicles formed by lipid bilayers with an aqueous phase inside. This feature enables them to entrap hydrophilic or hydrophobic drugs, depending whether they associate to the internal water compartment or to the lipid membrane [35]. Liposomes are interesting nanosystems for solubilizing drugs and to prolong drug circulation times. Nevertheless, these nanosystems present limitations in their capacity to control drug release [10]. Doxil®, PEGylated liposomes containing doxorubicin, was one of the first nanosystems approved for medical use that clearly improved cancer treatment [36].

2.6. Nanoparticles

Nanoparticles are solid matrix systems in which the drug is dispersed within the particle or conjugated to the polymeric backbone. The biomaterials used and the preparation technique allows the modulation of the drug release to the required rate [37], and the modification of their surface can introduce further functionality to the system [38]. The concerns of nanoparticles relates to their limited drug loading and the small variety of biodegradable and low-toxic polymers that can be used for their formation. Among the numerous nanoparticles in pre-clinical or clinical development [39], is worth to mention Abraxane®, an albumin-based nanoparticulate formulation currently on the market [40].

2.7. Nanosuspensions

Nanosuspensions are sub-micron colloidal dispersions of drug particles in an outer liquid phase [41]. Nanosuspensions can be used to formulate compounds that are insoluble in both water and hydrophobic solvents and to reformulate existing drugs to remove toxicologically less favorable excipients [28; 42]. The main advantage of this technology is related to its simplicity [43]. However, their composition (drug particles) precludes the possibility of achieving drug targeting and/or controlled drug release. The formulation of nanosuspension EMEND® has already been approved by the FDA for oral coadjuvant therapy in cancer treatment [10].

3. THE BENEFITS OF ANTICANCER NANOMEDICINES

In the next subsections, we cover the different phases and challenges in the design of an antitumor nanomedicine, all the way from the pharmacy shelf to its final (intra-)cellular target. A schematic sketch of the different barriers in anticancer delivery is depicted in Figure 2.

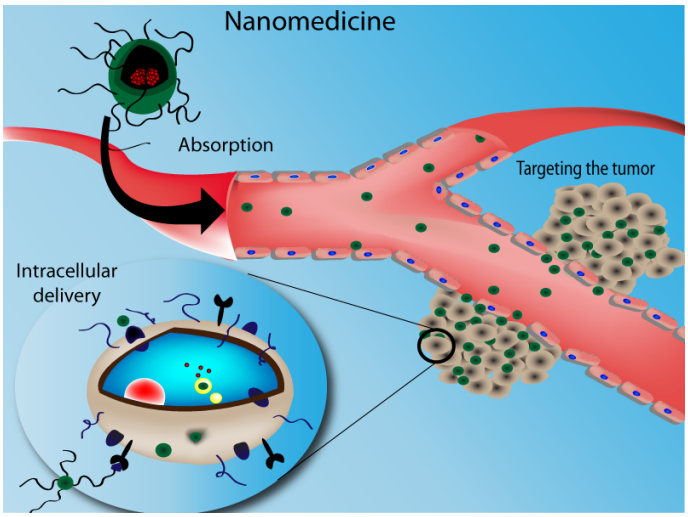

Figure 2: Illustration of the different biopharmaceutical steps in the delivery of an anticancer nanomedicine.

3.1. Increase of stability during storage

The first limitation to the successful delivery of an antitumor drug arises even before the drug is administered to a patient. Many drugs used in anticancer therapy are unstable even under mild conditions. Low molecular weight drugs suffer degradation by diverse mechanisms: e.g. photochemical reactions, oxidation, hydrolysis, etc. [44-50]. Polypeptidic drugs can be partially denatured during storage, thus loosing their activity [51-53]. Gene medicines can also be degraded by the environmental conditions, particularly by enzymes present in the environment (i.e. DNAases, RNAses) [54-58]. Nanocarriers can increase the stability of many anticancer drugs by integrating them into their structure, which is typically a more inert environment for the drug. For instance, doxorubicin is quickly degraded upon exposure to light [47], whereas doxorubicin entrapped into nanoparticles maintains its biological activity under the same conditions [59]. The

stability of doxorubicin has also been increased through its incorporation into liposomes [60]. Similarly, the antineoplastic drug paclitaxel formulated in a surfactant/alcohol mixture has a shelf-live of 71 days at 25ºC, and its stability is reduced even further upon dilution [61]. Fortunately, its shelf-live can be markedly improved up to at least 12 months upon incorporation into liposomes and further freeze-drying [62].

An enhanced preservation of the biological activity during storage has also been observed for gene medicines that are integrated in a drug delivery platform. For instance, plasmid DNA remains stable upon storage at 4º and 37ºC when it is entrapped in polylysine-PEG nanoparticles [63]. Hayes *et al*. [64] demonstrated that lipid-nucleic acid nanoparticles (Genospheres) could be stored under a variety of conditions, including a lyophilized state where no appreciable increase in particle size or DNA degradation was observed following reconstitution. Miyata *et al*. [65] also observed a beneficial effect on long-term DNA stability when this molecule was complexed to polymeric micelles, and this polyplex was lyophilized.

3.2. The improvement of drug administration and absorption

Oral administration

Mucosal administration of anticancer drugs is almost neglected in current practice because of low drug bioavailability and variable and erratic drug absorption. This problem is stressed in the case of molecules such as genes or peptides, for which, mucosal bioavailability is negligible. However, there is an emerging interest in mucosal delivery of anticancer drugs, particularly in the case of long-term treatments, for whose it is a more economic and convenient route.

In general terms anticancer drugs have low oral bioavailability. For large macromolecules this is related to their fast enzymatic degradation and their inefficiency in crossing biological barriers. For hydrophobic drugs, their main limitation is their low solubility at the absorption site, but also their biodegradation. The case of many conventional hydrophobic drugs is finely illustrated by paclitaxel. This molecule has less than 10% oral bioavailability in conventional formulations [66], because most of the drug is eliminated through the cytochrome P450-dependent metabolism, and excreted by the P-glycoprotein (P-gp) pump present in the intestinal wall [66-70]. Indeed, the bioavailability of this drug can be

improved by the addition of P-gp inhibitors, such as cyclosporine A, to the formulation [71-73].

Nanosystems may improve drug absorption in oral chemotherapy by protecting the drug, enhancing its residence time at the absorption site, or through the inhibition of efflux pumps. Many of these approaches rely on the use of drug nanocarriers with mucoadhesive properties. Examples of mucoadhesive polymers used for nanocarrier formation are those with pendent carboxylic groups, such as poly(acrylic acid) PAA or poly(methacrylic acid) PMAA [74]. This research group reported that the oral administration of several drugs in mucoadhesive poloxamer-PAA micelles results in enhanced drug bioavailability, primary due to prolonged residence time at the absorption site, and to the inhibition of the membrane efflux pumps such as P-gp [75]. Mu *et al*. [76] suggested new d-α-tocopheryl-PEG succinate nanoparticles for oral delivery of paclitaxel. On the other hand, liposomes formed by a blend of collagen and carrageenan polymeric core were also found to enhance the permeability of 5-fluoracil (5-FU), and methotrexate across the Caco-2 and TC7 monolayers [77], a result that suggest their potential for oral anticancer treatments.

Other very representative example of the benefits of nanotechnology to oral administration of drugs in cancer chemotherapy is EMEND®, which has been recently approved by the FDA for the prevention of chemotherapy-induced nausea and vomiting. The active ingredient of EMEND®, MK-0869 (aprepitant), a potent substance P antagonist, have show better bioavailabilty when it is formulated as drug nanoparticle (NanoCrystal®, Elan/Nanosystems, King of Prussia, PA, USA) [78].

Parenteral administration

Parenteral administration is usually preferred over mucosal administration for the administration of antineoplastic drugs. Anticancer drugs present narrow therapeutic ranges and a high toxicity, a fact that makes imperative to control the delivery of the drug to the target site [11; 79]. Parenteral formulations have the additional advantage of circumventing any problem related to drug absorption; however, the preparation of injectable formulations of many hydrophobic drugs is not trivial due to their very low water solubility. Indeed, intravenous injection of these drugs may cause embolization of blood vessels due to drug aggregation, and ultimately, local toxicity as a result of high drug concentrations at the site of deposition [37]. Moreover, most of these drugs need to be solubilized in toxic

solvent/surfactant mixtures, adding up this indiscriminative toxicity to the already important secondary effects of anticancer drugs.

This situation is well illustrated by the antineoplastic family of the taxanes, which have very low water-solubility, and therefore, the use of surfactants and alcohols to administrate these compounds is necessary. Cremophor EL (Taxol®) has been the standard solvent system for paclitaxel, but a great number of pharmacologic and biologic effects related to this drug formulation have been described, including clinically relevant acute hypersensitivity reactions, and peripheral neuropathy [80-82]. Besides, polyvinyl chloride (PVC)-free equipment for Cremophore EL administration is obligatory, since cremophor EL is known to leach plasticizers from PVC infusion bags and polyethylene-lined tubing sets which can cause severe hepatic toxicity [80]. These negative effects have been successfully solved by incorporating the drug into several nanocarriers, and currently a great number of formulations of Cremophor-free taxanes have been developed. They include glycol chitosan nanoparticles, polyglutamic acid-paclitaxel conjugates, nanoemulsions and liposomes [83; 28; 84]. Moreover, paclitaxel-loaded albumin nanoparticles (Abraxane® or ABI-007) [40; 85] have recently been approved by FDA for the treatment of metastatic breast cancer.

3.3. Increase in blood circulation time

The inefficacy of classical chemotherapy has been associated primarily with the inadequate biodistribution of the drugs, which partially accumulate into non-target tissues, leading to severe side effects. Changes in drug biodistribution and accumulation in the target tissues can be achieved through the incorporation of these drugs into specific nanocarriers. Classical non-selective nanocarriers are known to be opsonized and rapidly cleared by the mononuclear phagocitic systems (MPS), which is predominantly distributed in liver, lungs, spleen, and bone marrow. This uptake can be very advantageous for the chemotherapeutic treatment of MPS-localized tumors like hepatocarcinoma or hepatic metastasis. This therapeutical benefit has been observed with doxorubicin in a murine hepatic metastases model, when this drug was incorporated into biodegradable poly(alkylcyanoacrylate) nanoparticles [86]. Apart from these specific cases, nanocarriers should avoid uptake by the MPS. Presently, it is know that in order to prevent this uptake, nanocarriers should be small and provided of a neutral and hydrophilic surface coating [87]. The technology most frequently applied to prevent the uptake by the MPS has been the modification of the nanocarrier surface with polyethylene glycol [88]. This technology is usually referred as PEGylation, and the

surface-modified carriers as "Stealth®" or "long-circulating" [89-91]. PEGylation works by preventing the opsonization of the nanocarriers through a combination of mechanisms that include: (1) the shielding of the nanocarrier charged surface, (2) the increase of its hydrophilicity, (3) the enhancement of the repulsive interaction between nanocarrier and blood components, (4) and the formation of a polymeric layer around the particle's surface, which makes it impermeable to other solutes [92]. PEGylation has been applied to enhance the plasmatic half-life of several nanocarriers, including liposomes [36], nanoparticles [89] and micelles [93].

Passive tumor targeting

Healthy tissues have tight, continuous blood vessel walls with pores that are approximately 9 nm in diameter. Therefore, the size of blood vessel pores restricts the extravasation of large molecules and nanomedicines [94]. In contrast, the blood vessels formed in solid tumors are irregular and dilated, the endothelial cells are poorly aligned and disorganized, there is an irregular or an absence of a basal lamina, an there are a large number of pores with sizes up to 400 nm depending on the specific tumor. This particular blood vessel structure results from the rapid formation of a vascular network in solid tumors, which is necessary to provide oxygen and nutrients for its fast growing mass [95]. This differentiated structure of the tumor blood vessels results in a facilitated access of macromolecules and nanomedicines. Indeed, nanosystems are too large to penetrate through the vascular wall of healthy tissues, while they can easily penetrate to solid tumors [96]. Besides, tumor tissues lack a functional lymphatic system for draining lipophilic and polymeric materials [97; 98], thus making the elimination of the nanocarriers from the tumor very difficult. This phenomenon of facilitated intake and prolonged retention of nanometric materials was first identified by Maeda *et al*. [97; 98] and named "enhanced permeability and retention effect" (EPR). The EPR allows the passive targeting of nanomedicines with a suitable size to tumoral tissues, and it is the reason behind the enhanced activity and reduced toxicity of many anticancer nanomedicines in comparison to free drugs. There are numerous examples of the application of this concept to anticancer drugs. A recent one was from Constantinides *et al.* [28], who observed that the antitumor activity of paclitaxel was increased when the drug was encapsulated in nanoemulsions in comparison with the drug solubilized in Cremophor. This research group attributed this effect to the higher tumor accumulation of the drug delivered in the nanoemulsion. Similar enhancements in therapeutic efficacy of antitumor agents have been obtained with doxorubicin in liposomes [99], chitosan nanoparticles [100], and block copolymer micelles [93]. All of

these systems have been suggested to accumulate in solid tumors by the EPR effect.

Active targeting

Since Paul Ehrlich envisioned the concept of the "magic bullet", many efforts have been directed towards the design of therapeutic agents with the capacity to actively target cancer cells. Active targeting of cancer cells based on specific molecular recognition interactions between a nanometric carrier and the target cells has been researched profusely [101]. The ultimate goal is to achieve a drug delivery system that selectively accumulates in cancer tissues, where a loaded cytotoxic agent can exert its effect, while avoiding undesirable side-effects.

To achieve molecular recognition of cancer cells, different kind of ligands have been conjugated to drug delivery platforms: (1) ligands for receptors overexpressed in cancer cells (e.g. folate), (2) ligands that target cells/tissues where the tumor is located (e.g. mannose), and (3) ligands capable of recognizing cancer-specific receptors (e.g. antibodies or aptamers) [102; 103]. Some considerations need to be taken into account with actively targeted nanomedicines. First, the incorporation of ligands may increase the complexity and the particle size of the nanomedicines, hindering their preparation and enhancing the risk of biological side-effects [3]. Moreover, it is essential that the targeting agents used to functionalize the nanocarriers bind with high selectivity to its receptor in the cancer tissue, and that this receptor is either uniquely expressed on cancer cells, or at least overexpressed to a great extent in these. Finally, once the functionalized nanosystems interact with the target receptors, other processes might be necessary to achieve the full benefit from this active targeting: e.g. tumor-site triggered drug release, intracellular drug delivery, etc. [104].

Active targeting to tumor vasculature

Typically, initial tumors proliferate until they reach a steady state where their growth is subordinated to the supply of nutrients and to the excess of excretory products in the tumor mass. This situation is overcome by the formation of new blood vessels that will provide the necessary exchange of molecules between the blood and the tumor tissue, thus ensuring a continuous tumor growth. For that reason, the angiogenic process is a promising target for the development of new

therapeutic agents that control tumor expansion [13]. The vascular network is highly accessible to parenterally delivered therapeutic agents, and therefore, nanosystems can easily target proliferating tumor vessels. Moreover, due to the reduced area of the tumor vasculature compared to tumor interstitium, lower doses are needed to achieve therapeutic responses [14].

Angiogenesis is a complex process which is regulated by many molecular mediators. These mediators bind to cell receptors that are frequently overexpressed in cancer vasculature. Therefore, these receptors can be used as specific receptors to target functionalized nanosystems. One of the most prominent proangiogenic regulators is epidermal growth factor (EGF), which has been used to derivatize silicon nanoparticles loaded with the pore-forming protein melittin that lyses the cell membranes of tumor endothelium [105]. αvß3-Integrin receptor is another molecule expressed in the neovasculature during angiogenesis. This specific ligand has been coupled to cationic nanoparticles for gene therapy directed to angiogenic blood vessels. Systemic injection of the nanosystem into mice led to sustained regression of tumors due to the apoptosis of the tumor-associated endothelium [106]. Similarly positive results have been obtained with other type of nanocarriers that are not covered in detail in this review, e.g. αv-integrin targeted doxorubicin-conjugated peptides [107].

Active targeting to the cancer cells

Nanomedicines designed to actively target cancer cells have complex design requirements. On one hand, in order to achieve high tumor specificity, the targeting moiety should have a high binding affinity for its receptor on cancer cells. On the other hand, it is known that in the case of solid tumors, the use of very high affinity ligands may impede the penetration of the nanocarriers into the inner tumor mass [108]. Another choice that must be made when designing an actively-targeted nanomedicine is the cell receptor, which may help or not internalization upon binding. For many drugs, intracellular delivery is necessary [109], as we discuss in more detail in the following section. For other drugs with receptors on the plasmatic membrane, or for those that penetrate freely into cells, binding to a non-internalizing receptor might be more adequate [110]. In the next paragraphs we discuss some of the most widely used targeting ligands.

Monoclonal antibodies were the first targeting ligands able to bind to specific tumor antigens. At present, there are several formulations comprising antibodies approved or undergoing clinical trials. For example, Mylotarg®, a

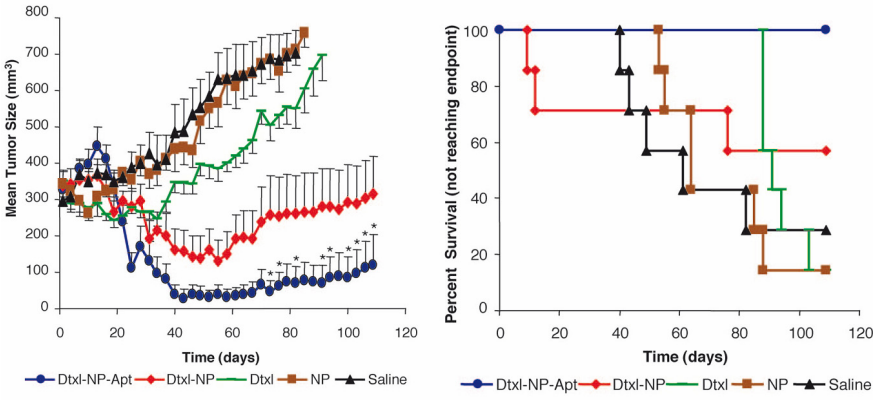

Figure 3: Comparative efficacy study of docetaxel-encapsulated nanoparticle-aptamer bioconjugates in xenografts nude mouse model (left) and corresponding Kaplan-Meier survival curve (right) (reproduced from Ref [115] with permission, PNAS Copyright (2006) National Academy of Sciences, U.S.A).

CD33-antibody conjugated drug, Zevalin® and Bexxar®, two CD20 antibody radionuclide conjugates, have already been approved by the FDA [111]. A liposome-plasmid DNA formulation (SGT-53) that uses an antibody fragment for tumor targeting is currently in Phase I clinical trials [112]. Besides, there are a significant number of animal studies in the literature that support the efficacy of antibody targeted nanocarriers. For instance, anti-HER-2 immunoliposomes with doxorubicin were more efficient against breast cancer than PEGylated liposomes [113]. In a different work, a scFv antibody fragment was used to deliver small interfering RNA (siRNA) to lymphocytes, achieving a 10,000-fold increase in affinity for the target receptors compared to the control [103]. Another impacting work is that from MacDiarmid *et al.*, who encapsulated antineoplastic drugs in bacterially-derived nano-sized particles (minicells) and targeted them using antibodies. Actively targeted minicells resulted in very marked antitumor effects, and in an enhanced efficacy even compared to other less sophisticated nanomedicines (i.e. Doxil®) [114]. Despite this recognized efficacy, the incorporation of antibodies to nanomedicines is a complex issue, because the number of associated molecules should be enough for receptor recognition, but not too high to activate the MPS.

Aptamers are short single-stranded DNA or RNA oligonucleotides selected *in vitro* to bind to a wide variety of targets, like receptors on cancer cells [3]. For instance, docetaxel loaded poly(D, L-lactic-co-glycolic acid)-block-poly(ethylene glycol) (PLGA-b-PEG) were functionalized by aptamers and a complete regression of the tumor was fulfilled [115] (see Figure 3).

Small peptides show reduced immunogenicity compared to antibodies and can distribute more homogeneously to the tumor tissue [116]. A prototypical example is the consensus sequence arginine-glycine-aspartic acid (RGD), which binds to integrin receptors and has been used to target nanomedicines to tumor neovasculature [117]. However, the lack of selectivity of RGD for cancer-related integrins limits the interest of this system.

Transferrin is a very useful ligand that presents the advantage of being intracellularly internalized by its own receptor [118]. Transferrin receptors are overexpressed on cell surfaces when metabolic processes are increased. Therefore, cancer cells –like pancreatic, colon, lung and bladder cancer- will present a higher density of this receptor. Unfortunately, other fast-growing but healthy cells might also overexpress transferrin receptors, reducing the effectiveness of this targeting moiety [119]. Currently there are two formulations of transferrin-modified nanosystems in clinical trials: MBP-426, liposomes containing oxaliplatin that are in phase I [120], and CALAA-01, a polymer-siRNA conjugate, with transferrin receptor triggered drug release. This formulation has just begun phase I clinical trials in 2007 [121].

Folate has been used as well as targeting ligand due to the up-regulation of folate receptors on the tumor cell surface. Liu *et al.* performed *in vivo* experiments that showed how doxorubicin containing micelles were targeted towards breast cancer xenografts. In this work higher tumor accumulation of the drug was achieved with folate-conjugated micelles compared to non-conjugated micelles [93].

Carbohydrates like **mannose** and **galactose** have also been used as targeting ligands. Nevertheless, these ligands are limited because of their broad distribution on the healthy cells. For example, PK-2 a polymer-doxorubicin conjugate was stopped at phase I clinical trials due to the accumulation of the nanosystems in the healthy hepatocytes [16].

Other targeting molecules like epidermal growth factor (EGF), heparin sulphate, chondroitin sulphate, hyaluronan, vitamin B_{12} or wheat germ agglutinin have also been investigated for cancer therapy [104].

Tumor extravasation and distribution

Tumors are characterized by heterogeneous blood flow in non-necrotic regions, and for slow and unpredictable blood flow in necrotic and semi-necrotic regions. Moreover, unlike most normal tissues, tumor interstitium has high

interstitial pressure that may hinder the extravasation of drugs and nanocarriers alike [122]. As the homogenous distribution of nanosystems throughout the tumor is crucial for an optimal response, some drug delivery strategies have been developed to overcome this issue. For instance, PEGylated-liposomes have been administered systemically with low doses of tumor necrosis factor-α, a combination therapy that is aiming at increasing the permeability of tumor vessels and ultimately to facilitate the distribution of liposomes in the tumor [123].

3.4. Intracellular delivery and trafficking

Once an antitumor nanomedicine arrives to the tumor site, the associated drug might be directly effective through a receptor on the cell surface. If not, the nanomedicine will have to make its way through to the intracellular space. For some drugs, this access to the intracellular space is a considerable challenge. Indeed, internalization through the cell membrane and trafficking to the correct cellular compartment represents a critical challenge [124]. Prototypical drugs that show restricted cell internalization and inefficient transport to its target cell compartment are gene medicines. For these, it is imperative to ensure their penetration through the cell membrane, and their stability from degradation in lysosomes. RNA-based therapeutics need to be addressed to the cytosol, while DNA-based therapeutics need to reach the cell nucleus to become effective. Other kind of drugs that are also limited by their ineffective cell internalization are peptides that act as interferents of intracellular pathways necessary for cancer development [125; 126], and hydrophobic drugs that undergo intensive degradation in lysosomes, and/or extensive expulsion through efflux mechanisms i.e. P-gp or multidrug resistance protein (MRP).

Cell Internalization

Nanomedicines are internalized into eukariotic cells through endocytic pathways; the best characterized are clathrin-mediated endocytosis, caveolae-mediated endocytosis, and macropinocytosis. All of these endocytic mechanisms share a common feature: they require the adhesion to the cell membrane of the nanostructure to be internalized. Despite this, these mechanisms have several differences regarding their mechanism and characteristics, which are reviewed in more detail elsewhere [127; 128]. Depending on the size of the internalizing vesicles we could distinguish between macropinocytosis, which leads to the largest

vesicles (0.5-5 μm) [129], clathrin-mediated endocytosis (≈150 nm) [130], and caveolae-mediated endocytosis (≈80 nm) [131].

Cell penetration of the nanoparticles by endocytosis can be triggered either by non-specific adhesion to the cell surface or through the binding to specific cell receptors on the cell membrane. Endocytosis of non-bioconjugated nanocarriers has been described for carriers with very different biomaterial compositions. For instance, nanocapsules can enter cells though an endocytic pathway, and this can lead to a more effective intracellular delivery of the drug carboplatin [132]. Endocytic transport of nanoparticles from the hydrophobic polyester PLGA alone or forming blends with the hydrophilic polymer poloxamer have been described [133; 134]. Similarly, endocytic uptake was described for mesoporous silica nanoparticles in HeLa cells, allowing the delivery of a membrane-impermeable protein to the cytosol [126]. Studies have shown that size is a critical parameter for the internalization of these carriers: up to a 27-fold increase in nanoparticle internalization was found for PLGA nanoparticles with a particle size below 100 nm compared to PLGA nanoparticles with a particle size above 100 nm [135].

A particular case of non-specific binding and internalization of nanocarriers is that from cationic polyaminoacids and some cell-penetrating peptides. These polypeptides are internalized after association to anionic glycosaminoglycans present on the plasmatic membrane. The complex between these polycations and the glycosaminoglycans trigger the endocytic process [136]. Initially, these materials were thought to cross the plasmatic membrane through clathrin-mediated endocytosis [137], but some later evidence has shown that, at least some of them –e.g. TAT peptide-, might be mainly translocated through caveolae-mediated endocytosis or through macropinocytosis [138; 139]. Although the importance of this pathway for all cationic polymers has not been demonstrated, recent findings point to the relevance of the interaction of glycosaminoglycans with another widely used cationic polymer, polyethylenimine [140]. In cancer therapy, cationic polymers have found their most notable application as carriers for gene medicines [141; 142].

Many of the nanocarriers investigated for intracellular delivery of anticancer agents incorporate specific moieties capable of interacting with the cell surface receptors, which are known to be overexpressed in cancer cells. The most widely used ligands known to promote intracellular penetration are: antibodies [64; 114; 143], transferrin [144], tocopherol [145; 146], and folic acid [30; 147]. Other ligands that have been used recently are galactose -for hepatic cell uptake- [148], lectins [149; 150], and anisamide [151].

A very particular approach for improving cell internalization is based on the use of bacteria. More concretely, in this approach, gene loaded-nanoparticles were adsorbed onto the surface of bacteria, which acted as an absorption promoting micro-robot. This complex system achieved high nanoparticle penetration that translates into promising levels of gene expression in mammal organs after the administration of this carrier to mice [152]. Other relevant systems are those combining a targeting/cellular binding moiety with a cell penetration system. Examples of those are liposomes having a PEG-antibody as targeting/binding group, and a cell penetrating peptide to promote intracellular penetration [153; 154]. To maximize the effect of these carriers, the PEG-antibody coating is designed to be cleaved by the acidic pH once the nanomedicine arrives to the tumor site.

The capacity of nanomedicines to improve cell penetration of drugs is very explicit. For instance, up to a 1000-fold reduction in the IC_{50} of carboplatin was observed when this drug was delivered in non-actively targeted nanocapsules to a panel of carcinoma cell lines. These promising results were attributed to higher cell penetration of the drug [132]. Conjugation to a specific ligand can improve this performance even further; for instance, liposomes targeted with an anti-HER2 antibody fragment showed a 6-fold increase in nanocarrier internalization [143] compare to non-conjugated liposomes. Similar increases, but in gene expression levels, were observed by Hood *et al*. for targeted nanoparticles incubated with receptor-expressing cells and non-receptor expressing cells [106]. This enhanced intracellular penetration of the antitumor molecule typically translates into improved efficacy of the treatment in vivo [106; 151] (see Figure 4).

Overcoming efflux pumps

Once a drug has penetrated through the plasmatic membrane, there is still another substantial barrier towards its intracellular penetration: the presence of efflux pumps [155; 156]. Integration of drugs into nanomedicines can help to overcome this barrier. An example is the association of anticancer drugs to polymeric micelles based on the copolymer poloxamer. These systems can inhibit the activity of some efflux pumps, thus enhancing the intracellular penetration of some drugs [157]. Other recent examples illustrate the potential of nanocarrier-mediated intracellular delivery in this area. Yi *et al*. administered doxorubicin encapsulated in nanoparticles conjugated with tocopherol [145], and the most notable improvements in cellular penetration were found in drug-resistant cells (i.e. MCF-7/ADR and MES-SA/Dx-5). Similarly, van Vierken *et al*. co-

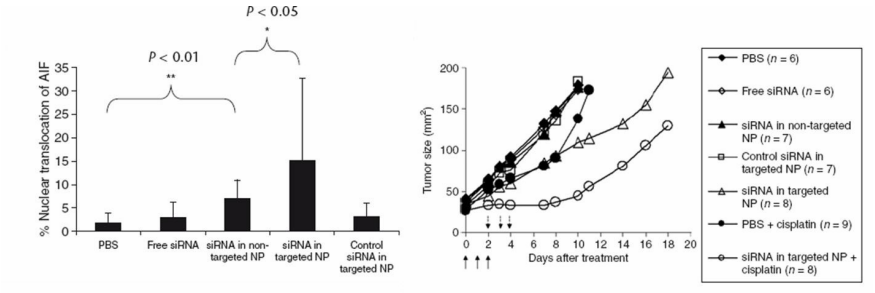

Figure 4: Quantitative analysis of the nuclear translocation of the apoptosis inducing factor (left) and xenografts tumor growth inhibition (right) in tumor bearing mice after treatment with siRNA formulations (Reprinted by permission from Macmillan Publishers Ltd: Molecular Therapy (ref 151), copyright (2008)).

encapsulated ceramide and paclitaxel in poly(epsilon-caprolactone)-PEG nanoparticles. This co-therapy integrated in a nanomedicine presented a cytotoxic effect that was far above that of the free drugs in solution or paclitaxel alone. As a matter of fact, IC_{50} of the nanomedicine was similar to the IC_{50} observed for paclitaxel alone in non-MRP (drug sensitive) cells. This result implies a 100-fold increase in chemosensitation, which has been attributed to the capacity of the system to overcome the efflux mechanisms of these cell lines [158].

Endosomal/lysosomal escape

Classical clathrin-mediated endocytic pathway leads to the entrapment of the cargo in digestive vesicles (endosomes/lysosomes) [124]. Caveolae-mediated endocytosis and macropinocytosis, on the other hand, can lead to direct cytosolic release of the nanomedicine [131; 139]. However, there is evidence that even these pathways may lead also to a partial delivery to the endosomal compartment [159; 160]. For that reason, and considering that lysosome enzymatic activity is a prime cause for the degradation of active molecules, promoting endosomal escape is very important to achieve cytosolic or organelle-specific delivery of drugs. Two main strategies have been proposed for promoting endosomal escape: (1) pH-sensitive polymers, and (2) the use of membrane-disruptive compounds

The use of polymers that are sensitive to pH are based on the so-called “proton-sponge” hypothesis. According to this hypothesis, a basic polymer could buffer the protons being pumped into the lysosomal compartment. While the polymer is absorbing these protons, chlorides are being co-transported inside the lysosome. The increased concentration of ions, together with the swelling of these polymers in acid pH creates an increased osmotic pressure inside the

lysosomes that leads to its rupture [161]. Some authors are still challenging this particular mechanism [162]; nevertheless, it is clear that some basic polymers have lysosomolytic properties, and that their use can increase the cytosolic delivery of drugs [142; 163; 164].

A second approach for endosomal escape is the use of membrane disruptive agents [165]. In order for them to be effective, the release of these membrane disruptive agents should be triggered by their presence in the endosomal compartment (i.e. typically by the low pH of this compartment). Alternatively, specific molecules can be used that form membrane-disrupting structures only in these conditions. Excellent examples are some peptides that undergo a transition towards a hydrophobic alpha-helix at the low pH typical of lysosomes, such as the peptides GALA [166; 167] and KALA [168].

Another current example of membrane disruptive strategies relies on the use of photochemical internalization agents. In this strategy, photosensitizers are used in combination with light radiation to induce the formation of reactive oxygen species. These reactive oxygen species destroy the endosomal membrane, leading to the cytosolic delivery of drugs [169]. Increases above 100-fold in the biological activity of a variety of compounds (i.e. proteins, peptides, oligonucleotides, genes and low molecular weight drugs) have been achieved through the use of this strategy with cancer cell lines [170].

Intracellular trafficking

Cytosolic delivery can be achieved through endosomal/lysosomal escape or through an internalization mechanism that leads to direct cytosolic delivery (e.g. macropinocitosis), and it represents the end of the journey for many drugs such as siRNAs [151; 168; 171; 172]. However, other molecules still need to reach a target organelle. The most typical cellular compartment to which drugs need to be addressed is the nucleus, although delivery to other organelles such as mitochondria has also been reported [173]. The delivery to the cell nucleus is very important for applications such as DNA delivery, to which it represents a substantial barrier. Nanomedicines can increase nuclear delivery of genes, what has been mainly achieved through the use of specific aminoacid sequences called nuclear localization signals. An example of this strategy was reported by Park *et al*., who condensed DNA with low molecular weight protamine, a polypeptide sequence that has been argued to posses a certain nuclear localization signal effect through its homology to HIV-TAT [174]. Nuclear targeting

has been mostly explored with liposomal carriers [175], and it currently represents an area of intensive research.

3.5. Drug release

Nanomedicines are modular nanodevices containing drugs. Hence, a control over the dissociation of the drug from the carrier is critical for the efficacy of the system. As a matter of fact, the benefits of the improved biodistribution, or intracellular penetration achieved through the integration of the drug in a nanomedicine might not be realized in case of an inadequate drug release, as it has been already observed with several liposome and nanoparticle carriers [36; 176-178]. Moreover, in order to take full advantage of the benefits of these carriers it is often not enough to have a sustained release of the drug [179], but rather, a triggered release at the target site. This target site can be the tumor extracellular space for drugs that do not require an intracellular carrier, and it will be a specific intracellular compartment for drugs with intracellular target sites and poor cell penetration. Methods for triggering drug release can be subdivided in those based on external stimuli and those based on internal stimuli.

Drug release triggered by external sources relies on the localized application of outer stimulus at the tumor site that will initiate the release of the drug from the nanomedicine. Controlled release systems triggered by external sources are particularly adequate to achieve release at the tumor extracellular space. The reason is that triggering the release through stimuli-responsive materials that are sensitive to the different conditions between tumors and healthy tissues is very difficult. This difficulty is due to the physicochemical conditions found in the extracellular space of tumors, which are not radically different from those of healthy tissues.

Typical examples of systems that are triggered by external stimuli are those which work through induction by physical energy sources, for example: some micellar systems that release their cargo in response to focused ultrasounds [180], nanoparticles that release drug in response to magnetic fields [181], and liposomes sensitive to electromagnetic radiation [182]. A frequent approach is the use of thermosensitive delivery systems (e.g. thermosensitive liposomes) [177; 183; 184], to combine these delivery systems with external heating of the tumor area. A very interesting and original approach is that reported by Cheong *et al.* [185]; these authors combined the administration of the anaerobic bacterium *Clostridium novyi-NT* with liposomal doxorubicin (Doxil®). C. novyi-NT, like other anaerobic

bacteria, colonize preferentially the tumor sites because of their anaerobic nature [186], and there, they express a specific lipase. This lipase triggers the release of doxorubicin from the liposomes at the tumor site, greatly enhancing the effectiveness of the treatment [185].

Two are the main drawbacks of triggered-release nanocarriers for cancer therapy: (1) they are inadequate for intracellular delivery; (2) their application is mainly restricted to its use in solid tumors that are accessible to the external stimulus. Such tumors can often be removed with surgery. On the other hand, this approach is ineffective for metastases, which are the main cause of cancer mortality [187].

Controlled release systems triggered by internal stimuli are particularly useful for intracellular delivery, and thus, they are extensively used for gene therapy. Classical stimuli-sensitive nanomedicines based on this principle are nanogels or liposomes with pH-sensitive release, which is particularly interesting for endosome/lysosome delivery [188; 189]. Release can also be triggered by other stimulus such as the redox potential (i.e. glutathione concentration) [190]. Some of the most promising systems combine a certain degree of sensitivity to two stimuli. For instance, several polymeric carriers have been prepared that present a pH-dependent lower critical solution temperature. Therefore, polymers that swell and release cargo at acid pH can be prepared based on this concept [93; 191-193]. A similar, but more sophisticated approach is that from Sonoda *et al*., who designed a thermosensitive polymer with a lower critical solution temperature that is controlled by the phosporylation of the polymer by an intracellular enzyme [194]. Indeed, sensitivity to specific enzymes present in tumors is one of the most intriguing mechanisms that are currently being explored. For example, liposome carriers can be designed to release their cargo in the presence of the enzyme alkaline phosphatase [195], or to other enzymes overexpressed in tumors such as phosphatase A_2 [196].

4. CONCLUSIONS

Cancer therapy is beginning to enjoy the results from implementing classical pharmacotherapy with nanotechnology-based approaches. Several products are already on the market and many others in the preclinical-to-clinical pipeline. These achievements, together with the understanding of the potential held by

nanomedicine for cancer treatment, has created a conjuncture where both the resources being invested and the clinical expectations are high.

A probable bottleneck for cancer nanomedicines before they achieve wide clinical application is our still limited knowledge on their toxicity, particularly after chronic administration. As a matter of fact, some side effects related to the use of PEG-liposomes have been observed, like dose-limiting palmar–plantar erythrodysesthesia. This is caused by the tendency of liposomes to diffuse out of the capillaries of the hands and feet (hand-foot syndrome) [197; 198]. It is necessary to find out whether such chronic side-effects are inherent to nanomedicines or carrier-specific.

Nanomedicine has the potential to radically improve current pharmacotherapy in cancer, achieving less indiscriminately toxic effects, and more effective and easier to administer treatments. We believe that it is within the reach of current pharmaceutical practice the design of nanomedicines that allow solvent-free administration of poorly-soluble drugs, that enhance the stability of some drugs upon storage, and that are passively targeted towards solid tumors. For a more distant (and hypothetical) future we envisage nanomedicines able to target to metastatic cells, and nanomedicines for gene therapy. Indeed, overcoming these challenges will require the design of nanocarriers capable of a very sophisticated behavior, probably beyond current technical possibilities.

ACKNOWLEDGEMENTS

This work was supported by the Spanish Ministry of Science and Technology (SAF 2004-08319-CO2-01). Victoria Lozano acknowledges the fellowship received from the Spanish Government (AP2005-1701).

REFERENCES

1. Alonso M.J. (2004). Nanomedicines for overcoming biological barriers. Biomed. Pharmacother. 58: 168-172.
2. Wagner V.; Dullaart A.; Bock A.K.; Zweck A. (2006). The emerging Nanomedicine landscape. Nat. Biotechnol. 24: 1211-1217.
3. Ferrari M. (2005). Cancer nanotechnology: Opportunities and challenges. Nat. Rev. Cancer. 5: 161-171.
4. Cho K.; Wang X.; Nie S.; Chen Z.G.; Shin D.M. (2008). Therapeutic nanoparticles for drug delivery in cancer. Clin. Cancer Res. 14: 1310-1316.
5. Koo O.M.; Rubinstein I.; Onyuksel H. (2005). Camptothecin in sterically stabilized phospholipid micelles: a novel Nanomedicine. Nanomed. 1: 77-84.
6. Lobo C.; Lopes G.; Silva O.; Gluck S. (2007). Paclitaxel albumin-bound particles (abraxane) in combination with bevacizumab with or without gemcitabine: early experience at the University of Miami/Braman Family Breast Cancer Institute. Biomed. Pharmacother. 61: 531-533.
7. National Cancer Institute, NCI Alliance for Nanotechnology in Cancer. http://nano.cancer.gov (2008).
8. European Science Foundation, Nanomedicine. An ESF-European medical research councils (EMRC) forward look report. http://www.esf.org/publications/ medical-sciences.html (2005).
9. Cuenca A.G.; Jiang H.B.; Hochwald S.N.; Delano M.; Cance W.G.; Grobmyer S.R. (2006). Emerging implications of nanotechnology on cancer diagnostics and therapeutics. Cancer. 107: 459-466.
10. Heath J.R.; Davis M.E. (2008). Nanotechnology and cancer. Annu. Rev. Med. 59: 251-265.
11. Barratt G. (2003). Colloidal drug carriers: achievements and perspectives. Cell Mol. Life Sci. 60: 21-37.
12. Sahoo S.K.; Labhasetwar V. (2003). Nanotechnologycal approaches to drug delivery and imaging. Drug Discov. Today. 8: 1112-1120.
13. Brannon-Peppas L.; Ghosn B.; Roy K.; Cornetta K. (2007). Encapsulation of nucleic acids and opportunities for cancer treatment. Pharm. Res. 24: 618-627.
14. Dass C.R.; Choong P.F.M. (2006). Selective gene delivery for cancer therapy using cationic liposomes: In vivo proof of applicability. J. Control. Release. 113: 155-163.
15. Engels F.K.; Mathot R.A.; Verweij J. (2007). Alternative drug formulations of docetaxel: a review. Anticancer Drugs. 18: 95-103.

16. Duncan R. (2006). Polymer conjugates as anticancer nanomedicines. Nat. Rev. Cancer. 6: 688-701.
17. Torchilin V.P. (2001). Structure and design of polymeric surfactant-based drug delivery systems. J. Control. Release. 73: 137-172.
18. Kwon G.S. (2003). Polymeric micelles for delivery of poorly water-soluble compounds. Crit. Rev. Ther. Drug Carrier Syst. 20: 357-403.
19. Gaucher G.; Dufresne M.H.; Sant V.P.; Kang N.; Maysinger D.; Leroux J.C. (2005). Block copolymer micelles: preparation, characterization and application in drug delivery. J. Control. Release. 109: 169-188.
20. Huo Q.S.; Liu J.; Wang L.Q.; Jiang Y.B.; Lambert T.N.; Fang E. (2006). A new class of silica cross-linked micellar core-shell nanoparticles. J. Am. Chem. Soc. 128: 6447-6453.
21. Read E.S.; Armes S.P. (2007). Recent advances in shell cross-linked micelles. Chem. Commun. 29: 3021-3035.
22. Danson S.; Ferry D.; Alakhov V.; Margison J.; Kerr D.; Jowle D.; Brampton M.; Halbert G.; Ranson M. (2004). Phase I dose escalation and pharmacokinetic study of pluronic polymer-bound doxorubicin (SP1049C) in patients with advanced cancer. Br. J. Cancer. 90: 2085-2091.
23. Matsumura Y.; Hamaguchi T.; Ura T.; Muro K.; Yamada Y.; Shimada Y.; Shirao K.; Okusaka T.; Ueno H.; Ikeda M.; Watanabe N. (2004). Phase I clinical trial and pharmacokinetic evaluation of NK911, a micelle-encapsulated doxorubicin. Br. J. Cancer. 91: 1775-1781.
24. Kim T.Y.; Kim D.W.; Chung J.Y.; Shin S.G.; Kim S.C.; Heo D.S.; Kim N.K.; Bang Y.J. (2004). Phase I and pharmacokinetic study of Genexol-PM, a cremophor-free, polymeric micelle-formulated paclitaxel, in patients with advanced malignancies. Clin. Cancer Res. 10: 3708-3716.
25. Solans C.; Izquierdo P.; Nolla J.; Azemar N.; Garcia-Celma M. (2005). Nano-emulsions. Curr. Opin. Colloid Interface Sci. 10: 102-110.
26. Yang S.C.; Benita S. (2000). Enhanced Absorption and Drug Targeting by Positively Charged Submicron Emulsions. Drug Dev. Res. 50: 476-486.
27. Wu W.H. (2007). Parenteral nanoemulsions- composition, preparation and cellular uptake. PhD Thesis, Freiburg (Germany). http://www.freidok.uni-freiburg.de /volltexte/3110/
28. Constantinides P.P.; Chaubal M.V.; Shorr R. (2008). Advances in lipid nanodispersions for parenteral drug delivery and targeting. Adv. Drug Deliv. Rev. 60: 757-767.

29. Couvreur P.; Barratt G.; Fattal E.; Legrand P.; Vauthier C. (2002). Nanocapsule technology: a review. Crit. Rev. Ther. Drug Carrier Syst. 19: 99-134.
30. Bae K.H.; Lee Y.; Park T.G. (2007). Oil-encapsulating PEO-PPO-PEO/PEG shell cross-linked nanocapsules for target-specific delivery of paclitaxel. Biomacromolecules. 8: 650-656.
31. Lambert G.; Fattal E.; Pinto-Alphandary H.; Gulik A.; Couvreur P. (2000). Polyisobutylcyanoacrylate nanocapsules containing an aqueous core as a novel colloidal carrier for the delivery of oligonucleotides. Pharm. Res. 17: 707-714.
32. Rübe A. (2006). Development and physico-chemical characterization of nanocapsules. PhD Thesis, Halle (Germany), http://sundoc.bibliothek.uni-halle.de/diss-online/06/06H083/prom.pdf.
33. Lamprecht A.; Bouligand Y.; Benoit J.P. (2002). New lipid nanocapsules exhibit sustained release properties for amiodarone. J. Control. Release. 84: 59-68.
34. Burger K.N.; Staffhorst R.W.; de Vijlder H.C.; Velinova M.J.; Bomans P.H.; Frederik P.M.; de Kruijff B. (2002). Nanocapsules: lipid-coated aggregates of cisplatin with high cytotoxicity. Nat. Med. 8: 81-84.
35. Torchilin V.P. (2005). Recent advances with liposomes as pharmaceutical carriers. Nat. Rev. Drug Discov. 4: 145-160.
36. Andresen T.L.; Jensen S.S.; Jorgensen K. (2005). Advanced strategies in liposomal cancer therapy: Problems and prospects of active and tumor specific drug release. Prog. Lipid Res. 44: 68-97.
37. Park J.H.; Lee S.; Kim J.H.; Park K.; Kim K.; Kwon I.C. (2008). Polymeric Nanomedicine for cancer therapy. Prog Polym Sci. 33: 113-137.
38. Parveen S.; Sahoo S.K. (2008). Polymeric nanoparticles for cancer therapy. J. Drug Target. 16: 108-123.
39. Brigger I.; Dubernet C.; Couvreur P. (2002). Nanoparticles in cancer therapy and diagnosis. Adv. Drug Deliv. Rev. 54: 631-651.
40. Sparreboom A.; Scripture C.D.; Trieu V.; Williams P.J.; De T.; Yang A.; Beals B.; Figg W.D.; Hawkins M.; Desai N. (2005). Comparative preclinical and clinical pharmacokinetics of a cremophor-free, nanoparticle albumin-bound paclitaxel (ABI-007) and paclitaxel formulated in Cremophor (Taxol). Clin. Cancer Res. 11: 4136-4143.
41. Moschwitzer J.; Achleitner G.; Pomper H.; Muller R.H. (2004). Development of an intravenously injectable chemically stable aqueous omeprazole formulation using nanosuspension technology. Eur. J. Pharm. Biopharm. 58: 615-619.

42. Kocbek P.; Baumgartner S.; Kristl J. (2006). Preparation and evaluation of nanosuspensions for enhancing the dissolution of poorly soluble drugs. Int. J. Pharm. 312: 179-186.
43. Muller R.H.; Jacobs C.; Kayser O. (2001). Nanosuspensions as particulate drug formulations in therapy. Rationale for development and what we can expect for the future. Adv. Drug Deliv. Rev. 47: 3-19.
44. Cheung Y.W.; Cradock J.C.; Rao Vishnuvajjala B.; Flora K.P. (1987). Stability of cisplatin, iproplatin, carboplatin, and tetraplatin in commonly used intravenous solutions. Am. J. Hosp. Pharm. 44: 124-130.
45. Dordunoo S.K.; Burt H.M. (1996). Solubility and stability of taxol: Effects of buffers and cyclodextrins. Int. J. Pharm. 133: 191-201.
46. Elsabahy M.; Perron M.E.; Bertrand N.; Yu G.E.; Leroux J.C. (2007). Solubilization of Docetaxel in Poly(ethylene oxide)-block-poly(butylene/styrene oxide) Micelles. Biomacromolecules. 8: 2250-2257.
47. Le Bot M.A.; Riche C.; Guedes Y.; Kernaleguen D.; Simon S.; Begue J.M.; Berthou F. (1988). Study of doxorubicin photodegradation in plasma, urine and cell culture medium by HPLC. Biomed. Chromatogr. 2: 242-244.
48. Rao B.M.; Chakraborty A.; Srinivasu M.K.; Devi M.L.; Kumar P.R.; Chandrasekhar K.B.; Srinivasan A.K.; Prasad A.S.; Ramanatham J. (2006). A stability-indicating HPLC assay method for docetaxel. J. Pharm. Biomed. Anal. 41: 676-681.
49. Tardi P.; Choice E.; Masin D.; Redelmeier T.; Bally M.; Madden T.D. (2000). Liposomal Encapsulation of Topotecan Enhances Anticancer Efficacy in Murine and Human Xenograft Models. Cancer Res. 60: 3389-3393.
50. Williams D.A.; Lokich J. (1992). A review of the stability and compatibility of antineoplastic drugs for multiple-drug infusions. Cancer Chemother. Pharmacol. 31: 171-181.
51. Bi M.; Singh J. (2000). Effect of buffer pH, buffer concentration and skin with or without enzyme inhibitors on the stability of [Arg8]-vasopressin. Int. J. Pharm. 197: 87-93.
52. Nuijen B.; Nuijen B.; Bouma M.; Talsma H.; Manada C.; Jimeno J.M.; Lopez-Lazaro L.; Bult A.; Beijnen J.H. (2001). Development of a lyophilized parenteral pharmaceutical formulation of the investigational polypeptide marine anticancer agent kahalalide F. Drug Dev. Ind. Pharm. 27: 767-780.
53. Roberts M.J.; Bentley M.D.; Harris J.M. (2002). Chemistry for peptide and protein PEGylation. Adv. Drug Deliv. Rev. 54: 459-476.

54. Fewell J.G.; Matar M.; Slobodkin G.; Han S.O.; Rice J.; Hovanes B.; Lewis D.H.; Anwer K. (2005). Synthesis and application of a non-viral gene delivery system for immunogene therapy of cancer. J. Control. Release. 109: 288-298.
55. Harder J.; Schroder J.M. (2002). RNase 7, a novel innate immune defense antimicrobial protein of healthy human skin. J. Biol. Chem. 277: 46779-46784.
56. Jacobson A.; Peltz S.W. (1996). Interrelationships of the pathways of mRNA decay and translation in eukaryotic cells. Annu. Rev. Biochem. 65: 693-739.
57. Kim S.H.; Jeong J.H.; Lee S.H.; Kim S.W.; Park T.G. (2006). PEG conjugated VEGF siRNA for anti-angiogenic gene therapy. J. Control Release. 116: 123-129.
58. Leong K.W.; Mao H.Q.; Truong-Le V.L.; Roy K.; Walsh S.M.; August J.T. (1998). DNA-polycation nanospheres as non-viral gene delivery vehicles. J. Control. Release. 53: 183-193.
59. Wong H.L.; Rauth A.M.; Bendayan R.; Manias J.L.; Ramaswamy M.; Liu Z.; Erhan S.Z.; Wu X.Y. (2006). A new polymer-lipid hybrid nanoparticle system increases cytotoxicity of doxorubicin against multidrug-resistant human breast cancer cells. Pharm. Res. 23: 1574-1585.
60. Xiang G.; Wu J.; Lu Y.; Liu Z.; Lee R.J. (2008). Synthesis and evaluation of a novel ligand for folate-mediated targeting liposomes. Int. J. Pharm. 356: 29-36.
61. Nornoo A.O.; Chow D.S.L. (2008). Cremophor-free intravenous microemulsions for paclitaxel. II. Stability, in vitro release and pharmacokinetics. Int. J. Pharm. 349: 117-123.
62. Zhang J.A.; Anyarambhatla G.; Ma L.; Ugwu S.; Xuan T.; Sardone T.; Ahmad I. (2005). Development and characterization of a novel Cremophor® EL free liposome-based paclitaxel (LEP-ETU) formulation. Eur. J. Pharm. Biopharm. 59: 177-187.
63. Rimann M.; Luhmann T.; Textor M.; Guerino B.; Ogier J.; Hall H. (2008). Characterization of PLL-g-PEG-DNA nanoparticles for the delivery of therapeutic DNA. Bioconjug. Chem. 19: 548-557.
64. Hayes M.E.; Drummond D.C.; Kirpotin D.B.; Zheng W.W.; Noble C.O.; Park J.W.; Marks J.D.; Benz C.C.; Hong K. (2006). Genospheres: self-assembling nucleic acid-lipid nanoparticles suitable for targeted gene delivery. Gene Ther. 13: 646-651.
65. Miyata K.; Kakizawa Y.; Nishiyama N.; Yamasaki Y.; Watanabe T.; Kohara M.; Kataoka K. (2005). Freeze-dried formulations for in vivo gene

delivery of PEGylated polyplex micelles with disulfide crosslinked cores to the liver. J. Control. Release. 109: 15-23.

66. Malingre M.M.; Schellens J.H.M.; Tellingen O.V.; Ouwehand M.; Bardelmeijer H.A.; Rosing H.; Koopman F.J.; Schot M.E.; Huinink W.W.; Beijnen J.H. (2001). The co-solvent Cremophor EL limits absorption of orally administered paclitaxel in cancer patients. Br. J. Cancer. 85: 1472-1477.
67. Malingre M.M.; Meerum Terwogt J.M.; Beijnen J.H.; Rosing H.; Koopman F.J.; Van Tellingen O.; Duchin K.; Ten Bokkel Huinink W.W.; Swart M.; Lieverst J.; Schellens J.H.M. (2000). Phase I and pharmacokinetic study of oral paclitaxel. J. Clin. Oncol. 18: 2468-2475.
68. Malingre M.M.; Schellens J.H.M.; Van Tellingen O.; Rosing H.; Koopman F.J.; Duchin K.; Ten Bokkel Huinink W.W.; Swart M.; Beijnen J.H. (2000). Metabolism and excretion of paclitaxel after oral administration in combination with cyclosporin A and after i.v. administration. Anti-Cancer Drugs. 11: 813-820.
69. Sparreboom A.; Van Asperen J.; Mayer U.; Schinkel A.H.; Smit J.W.; Meijer D.K.F.; Borst P.; Nooijen W.J.; Beijnen J.H.; Van Tellingen O. (1997). Limited oral bioavailability and active epithelial excretion of paclitaxel (Taxol) caused by P-glycoprotein in the intestine. Proc. Natl. Acad. Sci. U.S.A. 94: 2031-2035.
70. Yang S.; Gursoy R.N.; Lambert G.; Benita S. (2004). Enhanced Oral Absorption of Paclitaxel in a Novel Self-Microemulsifying Drug Delivery System with or without Concomitant Use of P-Glycoprotein Inhibitors. Pharm. Res. 21: 261-270.
71. Malingre M.M.; Beijnen J.H.; Schellens J.H.M. (2001). Oral delivery of taxanes. Invest. New Drugs. 19: 155-162.
72. Meerum Terwogt J.M.; Malingre M.M.; Beijnen J.H.; Ten Bokkel Huinink W.W.; Rosing H.; Koopman F.J.; Van Tellingen O.; Swart M.; Schellens J.H.M. (1999). Coadministration of oral cyclosporin A enables oral therapy with paclitaxel. Clin. Cancer Res. 5: 3379-3384.
73. Woo J.S.; Lee C.H.; Shim C.K.; Hwang S.J. (2003). Enhanced oral bioavailability of paclitaxel by coadministration of the p-glycoprotein inhibitor KR30031. Pharm. Res. 20: 24-30.
74. Bromberg L.; Temchenko M.; Alakhov V.; Hatton T.A. (2004). Bioadhesive properties and rheology of polyether-modified poly(acrylic acid) hydrogels. Int. J. Pharm. 282: 45-60.
75. Bromberg L. (2008). Polymeric micelles in oral chemotherapy. J. Control. Release. 128: 99-112.

76. Mu L.; Feng S.S. (2003). A novel controlled release formulation for the anticancer drug paclitaxel (Taxol®): PLGA nanoparticles containing vitamin E TPGS. J. Control. Release. 86: 33-48.
77. Moutardier V.; Tosini F.; Vlieghe P.; Cara L.; Delpero J.R.; Clerc T. (2003). Colloidal anticancer drugs bioavailabilities in oral administration models. Int. J. Pharm. 260: 23-38.
78. Wu Y.; Loper A.; Landis E.; Hettrick L.; Novak L.; Lynn K.; Chen C.; Thompson K.; Higgins R.; Batra U.; Shelukar S.; Kwei G.; Storey D. (2004). The role of biopharmaceutics in the development of a clinical nanoparticle formulation of MK-0869: A Beagle dog model predicts improved bioavailability and diminished food effect on absorption in human. Int. J. Pharm. 285: 135-146.
79. Jaehde U.; Liekweg A.; Simons S.; Westfeld M. (2008). Minimising treatment-associated risks in systemic cancer therapy. Pharm. World Sci. 30: 161-168.
80. Gelderblom H.; Verweij J.; Nooter K.; Sparreboom A. (2001). Cremophor EL: The drawbacks and advantages of vehicle selection for drug formulation. Eur. J. Cancer. 37: 1590-1598.
81. Hennenfent K.L.; Govindan R. (2006). Novel formulations of taxanes: a review. Old wine in a new bottle? Ann. Oncol. 17: 735-749.
82. Singla A.K.; Garg A.; Aggarwal D. (2002). Paclitaxel and its formulations. Int. J. Pharm. 235: 179-192.
83. Li C. (2002). Poly(L-glutamic acid)-anticancer drug conjugates. Adv. Drug Deliv. Rev. 54: 695-713.
84. Treat J.; Damjanov N.; Huang C.; Zrada S.; Rahman A. (2001). Liposomal-encapsulated chemotherapy: Preliminary results of a phase I study of a novel liposomal paclitaxel. Oncology. 15: 44-48.
85. Ibrahim N.K.; Desai N.; Legha S.; Soon-Shiong P.; Theriault R.L.; Rivera E.; Esmaeli B.; Ring S.E.; Bedikian A.; Hortobagyi G.N.; Ellerhorst J.A. (2002). Phase I and pharmacokinetic study of ABI-007, a Cremophor-free, protein-stabilized, nanoparticle formulation of paclitaxel. Clin. Cancer Res. 8: 1038-1044.
86. Chiannilkulchai N.; Ammoury N.; Caillou B.; Devissaguet J.P.; Couvreur P. (1990). Hepatic tissue distribution of doxorubicin-loaded nanoparticles after i.v. administration in reticulosarcoma M 5076 metastasis-bearing mice. Cancer Chemother. Pharmacol. 26: 122-126.
87. Vonarbourg A.; Passirani C.; Saulnier P.; Benoit J.P. (2006). Parameters influencing the stealthiness of colloidal drug delivery systems. Biomaterials. 27: 4356-4373.

88. Jeon S.I.; Lee J.H.; Andrade J.D.; De Gennes P.G. (1991). Protein-surface interactions in the presence of polyethylene oxide. I. Simplified theory. J. Colloid Interface Sci. 142: 149-158.
89. Gref R.; Minamitake Y.; Peracchia M.T.; Trubetskoy V.; Torchilin V.; Langer R. (1994). Biodegradable long-circulating polymeric nanospheres. Science. 263: 1600-1603.
90. Moghimi S.M.; Hunter A.C.; Murray J.C. (2001). Long-circulating and target-specific nanoparticles: Theory to practice. Pharmacol. Rev. 53: 283-318.
91. Storm G.; Belliot S.O.; Daemen T.; Lasic D.D. (1995). Surface modification of nanoparticles to oppose uptake by the mononuclear phagocyte system. Adv. Drug Deliv. Rev. 17: 31-48.
92. Torchilin V.P. (2006). Multifunctional nanocarriers. Adv. Drug Deliv. Rev. 58: 1532-1555.
93. Liu S.Q.; Wiradharma N.; Gao S.J.; Tong Y.W.; Yang Y.Y. (2007). Bio-functional micelles self-assembled from a folate-conjugated block copolymer for targeted intracellular delivery of anticancer drugs. Biomaterials. 28: 1423-1433.
94. Fukumori Y.; Ichikawa H. (2006). Nanoparticles for cancer therapy and diagnosis. Adv. Powder. Tech. 17: 1-28.
95. Yuan F.; Dellian M.; Fukumura D.; Leunig M.; Berk D.A.; Torchilin V.P.; Jain R.K. (1995). Vascular permeability in a human tumor xenograft: Molecular size dependence and cutoff size. Cancer Res. 55: 3752-3756.
96. Maeda H. (2001). The enhanced permeability and retention (EPR) effect in tumor vasculature: The key role of tumor-selective macromolecular drug targeting. Adv. Enzyme Regul. 41: 189-207.
97. Iwai K.; Maeda H.; Konno T. (1984). Use of oily contrast medium for selective drug targeting to tumor: Enhanced therapeutic effect and X-ray image. Cancer Res. 44: 2115-2121.
98. Matsumura Y.; Maeda H. (1986). A new concept for macromolecular therapeutics in cancer chemotherapy: Mechanism of tumoritropic accumulation of proteins and the antitumor agent smancs. Cancer Res. 46: 6387-6392.
99. Moghimi S.M.; Hunter A.C.; Murray J.C. (2005). Nanomedicine: Current status and future prospects. FASEB J. 19: 311-330.
100. Jae H.P.; Kwon S.; Lee M.; Chung H.; Kim J.H.; Kim Y.S.; Park R.W.; Kim I.S.; Sang B.S.; Kwon I.C.; Seo Y.J. (2006). Self-assembled nanoparticles based on glycol chitosan bearing hydrophobic moieties as carriers for doxorubicin: In vivo biodistribution and anti-tumor activity. Biomaterials. 27: 119-126.

101. Marcucci F.; Lefoulon F. (2004). Active targeting with particulate drug carriers in tumor therapy: fundamentals and recent progress. Drug Discov. Today. 9: 219-228.
102. Allen T.M. (2002). Ligand-targeted therapeutics in anticancer therapy. Nat. Rev. Cancer. 2: 750-763.
103. Peer D.; Zhu P.; Carman C.V.; Lieberman J.; Shimaoka M. (2007). Selective gene silencing in activated leukocytes by targeting siRNAs to the integrin lymphocyte function-associated antigen-1. Proc. Natl. Acad. Sci. U. S. A. 104: 4095-4100.
104. Peer D.; Karp J.M.; Hong S.; FaroKHzad O.C.; Margalit R.; Langer R. (2007). Nanocarriers as an emerging platform for cancer therapy. Nat. Nanotechnol. 2: 751-760.
105. Cohen M.H.; Melnik K.; Boiasrki A.; Ferrari M.; Martin F.J. (2003). Microfabrication of silicon-based nanoporous particulates for medical applications. Biomed. Microdevices. 5: 253-259.
106. Hood J.D.; Bednarski M.; Frausto R.; Guccione S.; Reisfeld R.A.; Xiang R.; Cheresh D.A. (2002). Tumor regression by targeted gene delivery to the neovasculature. Science. 296: 2404-2407.
107. Arap W.; Pasqualini R.; Ruoslahti E. (1998). Cancer treatment by targeted drug delivery to tumor vasculature in a mouse model. Science. 279: 377-380.
108. Adams G.P.; Schier R.; McCall A.M.; Simmons H.H.; Horak E.M.; Alpaugh R.K.; Marks J.D.; Weiner L.M. (2001). High affinity restricts the localization and tumor penetration of single-chain fv antibody molecules. Cancer Res. 61: 4750-4755.
109. Sapra P.; Allen T.M. (2002). Internalizing antibodies are necessary for improved therapeutic efficacy of antibody-targeted liposomal drugs. Cancer Res. 62: 7190-7194.
110. Allen T.M. (1994). Long-circulating (sterically stabilized) liposomes for targeted drug delivery. Trends Pharmacol. Sci. 15: 215-220.
111. Stern M.; Herrmann R. (2005). Overview of monoclonal antibodies in cancer therapy: Present and promise. Crit. Rev. Oncol. Hematol. 54: 11-29.
112. Clinical Trials, Safety study of infusion of SGT-53 to treat solid tumors. http://www.clinicaltrials.gov/ct/show/NCT00355888 (2007).
113. Park J.W.; Kirpotin D.B.; Hong K.; Shalaby R.; Shao Y.; Nielsen U.B.; Marks J.D.; Papahadjopoulos D.; Benz C.C. (2001). Tumor targeting using anti-her2 immunoliposomes. J. Control. Release. 74: 95-113.
114. MacDiarmid J.A.; Mugridge N.B.; Weiss J.C.; Phillips L.; Burn A.L.; Paulin R.; Haasdyk J.E.; Dickson K.A.; Brahmbhatt V.N.; Pattison S.T.;

James A.C.; Al Bakri G.; Straw R.C.; Stillman B.; Graham R.M.; Brahmbhatt H. (2007). Bacterially Derived 400 nm Particles for Encapsulation and Cancer Cell Targeting of Chemotherapeutics. Cancer Cell. 11: 431-445.

115. Farokhzad O.C.; Cheng J.J.; Teply B.A.; Sherifi I.; Jon S.; Kantoff P.W.; Richie J.P.; Langer R. (2006). Targeted nanoparticle-aptamer bioconjugates for cancer chemotherapy in vivo. Proc. Natl. Acad. Sci. U.S.A. 103: 6315-6320.
116. Shadidi M.; Sioud M. (2003). Selective targeting of cancer cells using synthetic peptides. Drug Resist. Updat. 6: 363-371.
117. Ruoslahti E. (1994). Cell adhesion and tumor metastasis. Princess Takamatsu Symp. 24: 99-105.
118. Hatakeyama H.; Akita H.; Maruyama K.; Suhara T.; Harashima H. (2004). Factors governing the in vivo tissue uptake of transferrin-coupled polyethylene glycol liposomes in vivo. Int. J. Pharm. 281: 25-33.
119. Ekblom P.; Thesleff I.; Lehto V.P.; Virtanen I. (1983). Distribution of the transferrin receptor in normal human fibroblasts and fibrosarcoma cells. Int. J. Cancer. 31: 111-117.
120. Clinical Trials, Safety study of MBP-426 (liposomal oxaliplatin suspension for injection) to treat advanced or metastatic solid tumors. http://www.clinicaltrials. gov/ct/show/NCT00355888. (2006).
121. Heidel J.D.; Yu Z.; Liu J.Y.; Rele S.M.; Liang Y.; Zeidan R.K.; Kornbrust D.J.; Davis M.E. (2007). Administration in non-human primates of escalating intravenous doses of targeted nanoparticles containing ribonucleotide reductase subunit M2 siRNA. Proc. Natl. Acad. Sci. U.S.A. 104: 5715-5721.
122. Brannon-Peppas L.; Blanchette J.O. (2004). Nanoparticle and targeted systems for cancer therapy. Adv. Drug Deliv. Rev. 56: 1649-1659.
123. Seynhaeve A.L.B.; Hoving S.; Schipper D.; Vermeulen C.E.; De Wiel-Ambagtsheer G.A.; Van Tiel S.T.; Eggermont A.M.M.; Ten Hagen T.L.M. (2007). Tumor necrosis factor a mediates homogeneous distribution of liposomes in murine melanoma that contributes to a better tumor response. Cancer Res. 67: 9455-9462.
124. Vasir J.K.; Labhasetwar V. (2007). Biodegradable nanoparticles for cytosolic delivery of therapeutics. Adv. Drug Deliv. Rev. 59: 718-728.
125. Katz B.A. (1997). Structural and mechanistic determinants of affinity and specificity of ligands discovered or engineered by phage display. Annu. Rev. Biophys. Biomol. Struct. 26: 27-45.

126. Slowing I.I.; Trewyn B.G.; Lin V.S.Y. (2007). Mesoporous silica nanoparticles for intracellular delivery of membrane-impermeable proteins. J. Am. Chem. Soc. 129: 8845-8849.
127. Rawat A.; Vaidya B.; Khatri K.; Goyal A.K.; Gupta P.N.; Mahor S.; Paliwal R.; Rai S.; Vyas S.P. (2007). Targeted intracellular delivery of therapeutics: an overview. Pharmazie. 62: 643-658.
128. Torchilin V.P. (2008). Tatp-mediated intracellular delivery of pharmaceutical nanocarriers. Adv. Drug Deliv. Rev. 60: 548-558.
129. Khalil I.A.; Kogure K.; Akita H.; Harashima H. (2006). Uptake pathways and subsequent intracellular trafficking in nonviral gene delivery. Pharmacol. Rev. 58: 32-45.
130. Takei K.; Haucke V. (2001). Clathrin-mediated endocytosis: membrane factors pull the trigger. Trends Cell Biol. 11: 385-391.
131. Panyam J.; Labhasetwar V. (2004). Targeting intracellular targets. Curr. Drug Deliv. 1: 235-247.
132. Hamelers I.H.L.; van Loenen E.; Staffhorst R.W.H.M.; de Kruijff B.; de Kroon A.I.P.M. (2006). Carboplatin nanocapsules: a highly cytotoxic, phospholipid-based formulation of carboplatin. Mol. Cancer Ther. 5: 2007-2012.
133. Csaba N.; Sanchez A.; Alonso M.J. (2006). PLGA:poloxamer and PLGA:poloxamine blend nanostructures as carriers for nasal gene delivery. J. Control. Release. 113: 164-172.
134. Panyam J.; Labhasetwar V. (2003). Dynamics of endocytosis and exocytosis of poly(D,L-lactide-co-glycolide) nanoparticles in vascular smooth muscle cells. Pharm. Res. 20: 212-220.
135. Prabha S.; Zhou W.Z.; Panyam J.; Labhasetwar V. (2002). Size-dependency of nanoparticle-mediated gene transfection: studies with fractionated nanoparticles. Int. J. Pharm. 244: 105-115.
136. Lundberg M.; Wikstrom S.; Johansson M. (2003). Cell surface adherence and endocytosis of protein transduction domains. Mol. Ther. 8: 143-150.
137. Console S.; Marty C.; Garcia-Echeverria C.; Schwendener R.; Ballmer-Hofer K. (2003). Antennapedia and HIV transactivator of transcription (TAT) "protein transduction domains" promote endocytosis of high molecular weight cargo upon binding to cell surface glycosaminoglycans. J. Biol. Chem. 278. 35109-35114.
138. Rothbard J.B.; Jessop T.C.; Lewis R.S.; Murray B.A.; Wender P.A. (2004). Role of membrane potential and hydrogen bonding in the mechanism of translocation of guanidinium-rich peptides into cells. J. Am. Chem. Soc. 126: 9506-9507.

139. Wadia J.S.; Stan R.V.; Dowdy S.F. (2004). Transducible TAT-HA fusogenic peptide enhances escape of TAT-fusion proteins after lipid raft macropinocytosis. Nat. Med. 10: 310-315.
140. Burke R.S.; Pun S.H. (2008). Extracellular barriers to in Vivo PEI and PEGylated PEI polyplex-mediated gene delivery to the liver. Bioconjug. Chem. 19: 693-704.
141. Ogris M.; Wagner E. (2002). Tumor-targeted gene transfer with DNA polyplexes. Somat. Cell Mol. Genet. 27: 85-95.
142. Sethuraman V.A.; Na K.; Bae Y.H. (2006). pH-responsive sulfonamide/PEI system for tumor specific gene delivery: An in vitro study. Biomacromolecules. 7: 64-70.
143. Kirpotin D.B.; Drummond D.C.; Shao Y.; Shalaby M.R.; Hong K.L.; Nielsen U.B.; Marks J.D.; Benz C.C.; Park J.W. (2006). Antibody targeting of long-circulating lipidic nanoparticles does not increase tumor localization but does increase internalization in animal models. Cancer Res. 66: 6732-6740.
144. Anabousi S.; Bakowsky U.; Schneider M.; Huwer H.; Lehr C.M.; Ehrhardt C. (2006). In vitro assessment of transferrin-conjugated liposomes as drug delivery systems for inhalation therapy of lung cancer. Eur. J. Pharm. Sci. 29: 367-374.
145. Yi Y.W.; Kim J.H.; Kang H.W.; Oh H.S.; Kim S.W.; Seo M.H. (2005). A polymeric nanoparticle consisting of mPEG-PLA-Toco and PLMA-COONa as a drug carrier: Improvements in cellular uptake and biodistribution. Pharm. Res. 22, 200-208.
146. Zhang Z.P.; Feng S.S. (2006). The drug encapsulation efficiency, in vitro drug release, cellular uptake and cytotoxicity of paclitaxel-loaded poly(lactide)-tocopheryl polyethylene glycol succinate nanoparticles. Biomaterials. 27: 4025-4033.
147. Lee Y.K. (2006). Preparation and characterization of folic acid linked poly(L-glutamate) nanoparticles for cancer targeting. Macromol. Res. 14: 387-393.
148. Liang H.F.; Yang T.F.; Huang C.T.; Chen M.C.; Sung H.W. (2005). Preparation of nanoparticles composed of poly(gamma-glutamic acid)-poly(lactide) block copolymers and evaluation of their uptake by HepG2 cells. J. Control. Release. 105: 213-225.
149. Mo Y.; Lim L.Y. (2005). Paclitaxel-loaded PLGA nanoparticles: Potentiation of anticancer activity by surface conjugation with wheat germ agglutinin. J. Control. Release. 108: 244-262.

150. Mo Y.; Lim L.Y. (2005). Preparation and in vitro anticancer activity of wheat germ agglutinin (WGA)-conjugated PLGA nanoparticles loaded with paclitaxel and isopropyl myristate. J. Control. Release. 107: 30-42.
151. Li S.D.; Chen Y.C.; Hackett M.J.; Huang L. (2008). Tumor-targeted delivery of siRNA by self-assembled nanoparticles. Mol. Ther. 16: 163-169.
152. Akin D.; Sturgis J.; Ragheb K.; Sherman D.; Burkholder K.; Robinson J.P.; Bhunia A.K.; Mohammed S.; Bashir R. (2007). Bacteria-mediated delivery of nanoparticles and cargo into cells. Nat. Nanotechnol. 2: 441-449.
153. Kale A.A.; Torchilin V.P. (2007). Design, synthesis, and characterization of pH-sensitive PEG-PE conjugates for stimuli-sensitive pharmaceutical nanocarriers: the effect of substitutes at the hydrazone linkage on the ph stability of PEG-PE conjugates. Bioconjug. Chem. 18: 363-370.
154. Sawant R.M.; Hurley J.P.; Salmaso S.; Kale A.; Tolcheva E.; Levchenko T.S.; Torchilin V.P. (2006). "SMART" drug delivery systems: double-targeted pH-responsive pharmaceutical nanocarriers. Bioconjug. Chem. 17: 943-949.
155. Gottesman M.M.; Fojo T.; Bates S.E. (2002). Multidrug resistance in cancer: role of ATP-dependent transporters. Nat. Rev. Cancer. 2: 48-58.
156. Kruh G.D.; Belinsky M.G. (2003). The MRP family of drug efflux pumps. Oncogene. 22: 7537-7552.
157. Kabanov A.V.; Batrakova E.V.; Alakhov V.Y. (2002). Pluronic (R) block copolymers as novel polymer therapeutics for drug and gene delivery. J. Control. Release. 82: 189-212.
158. van Vlerken L.E.; Duan Z.F.; Seiden M.V.; Amiji M.M. (2007). Modulation of intracellular ceramide using polymeric nanoparticles to overcome multidrug resistance in cancer. Cancer Res. 67: 4843-4850.
159. Hansen S.H.; Sandvig K.; van Deurs B. (1993). Molecules internalized by clathrin-independent endocytosis are delivered to endosomes containing transferrin receptors. J. Cell. Biol. 123: 89-97.
160. Racoosin E.L.; Swanson J.A. (1993). Macropinosome maturation and fusion with tubular lysosomes in macrophages. J. Cell. Biol. 121: 1011-1020.
161. Behr J.P. (1997). The proton-sponge-a trick to enter cells the viruses did not exploit. Chimia. 51: 34-36.
162. Funhoff A.M.; van Nostrum C.F.; Koning G.A.; Schuurmans-Nieuwenbroek N.M.; Crommelin D.J.; Hennink W.E. (2004). Endosomal escape of polymeric gene delivery complexes is not always enhanced by polymers buffering at low pH. Biomacromolecules. 5: 32-39.

163. Murthy N.; Campbell J.; Fausto N.; Hoffman A.S.; Stayton P.S. (2003). Bioinspired pH-responsive polymers for the intracellular delivery of biomolecular drugs. Bioconjug. Chem. 14: 412-419.
164. Wang Y.; Gao S.J.; Ye W.H.; Yoon H.S.; Yang Y.Y. (2006). Co-delivery of drugs and DNA from cationic core-shell nanoparticles self-assembled from a biodegradable copolymer. Nat. Mater. 5: 791-796.
165. Wagner E.; Plank C.; Zatloukal K.; Cotten M.; Birnstiel M.L. (1992). Influenza virus hemagglutinin HA-2 N-terminal fusogenic peptides augment gene transfer by transferrin-polylysine-DNA complexes: toward a synthetic virus-like gene-transfer vehicle. Proc. Natl. Acad. Sci. U.S.A. 89: 7934-7938.
166. Choi H.S.; Huh J.; Jo W.H. (2006). pH-induced helix-coil transition of amphipathic polypeptide and its association with the lipid bilayer: electrostatic energy calculation. Biomacromolecules. 7: 403-406.
167. Futaki S.; Masui Y.; Nakase I.; Sugiura Y.; Nakamura T.; Kogure K.; Harashima H. (2005). Unique features of a pH-sensitive fusogenic peptide that improves the transfection efficiency of cationic liposomes. J. Gene Med. 7: 1450-1458.
168. Lee S.H.; Kim S.H.; Park T.G. (2007). Intracellular siRNA delivery system using polyelectrolyte complex micelles prepared from VEGF siRNA-PEG conjugate and cationic fusogenic peptide. Biochem. Biophys. Res. Commun. 357: 511-516.
169. Berg K.; Selbo P.K.; Prasmickaite L.; Tjelle T.E.; Sandvig K.; Moan J.; Gaudernack G.; Fodstad Ø.; Kjølsrud S.; Anholt H.; Rodal G.H.; Rodal S.K.; Høgset A. (1999). Photochemical internalization: A novel technology for delivery of macromolecules into cytosol. Cancer Res. 59: 1180-1183.
170. Høgset A.; Prasmickaite L.; Selbo P.K.; Hellum M.; Engesæter B.Ø.; Bonsted A.; Berg K. (2004). Photochemical internalisation in drug and gene delivery. Adv. Drug Deliv. Rev. 56: 95-115.
171. Pal A.; Ahmad A.; Khan S.; Sakabe I.; Zhang C.B.; Kasid U.N.; Ahmad I. (2005). Systemic delivery of RafsiRNA using cationic cardiolipin liposomes silences Raf-1 expression and inhibits tumor growth in xenograft model of human prostate cancer. Int. J. Oncol. 26: 1087-1091.
172. Peer D.; Park E.J.; Morishita Y.; Carman C.V.; Shimaoka M. (2008). Systemic leukocyte-directed siRNA delivery revealing cyclin D1 as an anti-inflammatory target. Science. 319: 627-630.
173. Yamada Y.; Akita H.; Kamiya H.; Kogure K.; Yamamoto T.; Shinohara Y.; Yamashita K.; Kobayashi H.; Kikuchi H.; Harashima H. (2008). MITO-Porter: A liposome-based carrier system for delivery of macromolecules

into mitochondria via membrane fusion. Biochim. Biophys. Acta. 1778: 423-432.

174. Park Y.J.; Liang J.F.; Ko K.S.; Kim S.W.; Yang V.C. (2003). Low molecular weight protamine as an efficient and nontoxic gene carrier: in vitro study. J. Gene Med. 5: 700-711.
175. Vaysse L.; Gregory L.G.; Harbottle R.P.; Perouzel E.; Tolmachov O.; Coutelle C. (2006). Nuclear-targeted minicircle to enhance gene transfer with non-viral vectors in vitro and in vivo. J. Gene. Med. 8: 754-763.
176. Cheong I.; Huang X.; Thornton K.; Diaz L.A.; Zhou S.B. (2007). Targeting cancer with bugs and liposomes: Ready, aim, fire. Cancer Res. 67: 9605-9608.
177. Kong G.; Anyarambhatla G.; Petros W.P.; Braun R.D.; Colvin O.M.; Needham D.; Dewhirst M.W. (2000). A new temperature-sensitive liposome for use with mild hyperthermia: Characterization and testing in a human tumor xenograft model. Cancer Res. 60: 1197-1201.
178. Ulbrich K.; Subr V. (2004). Polymeric anticancer drugs with pH-controlled activation. Adv. Drug Deliv. Rev. 56: 1023-1050.
179. Kim J.H.; Kim Y.S.; Kim S.; Park J.H.; Kim K.; Choi K.; Chung H.; Jeong S.Y.; Park R.W.; Kim I.S.; Kwon I.C. (2006). Hydrophobically modified glycol chitosan nanoparticles as carriers for paclitaxel. J. Control. Release. 111: 228-234.
180. Rapoport N. (2004). Combined cancer therapy by micellar-encapsulated drug and ultrasound. Int. J. Pharm. 277: 155-162.
181. Sonvico F.; Dubernet C.; Colombo P.; Couvreur P. (2005). Metallic colloid nanotechnology, applications in diagnosis and therapeutics. Curr. Pharm. Des. 11: 2095-2105.
182. Bondurant B.; Mueller A.; O'Brien D.F. (2001). Photoinitiated destabilization of sterically stabilized liposomes. Biochim. Biophys. Acta. 1511: 113-122.
183. Chen Q.; Tong S.; Dewhirst M.W.; Yuan F. (2004). Targeting tumor microvessels using doxorubicin encapsulated in a novel thermosensitive liposome. Mol. Cancer Ther. 3: 1311-1317.
184. Hauck M.L.; LaRue S.M.; Petros W.P.; Poulson J.M.; Yu D.; Spasojevic I.; Pruitt A.F.; Klein A.; Case B.; Thrall D.E.; Needham D.; Dewhirst M.W. (2006). Phase I trial of doxorubicin-containing low temperature sensitive liposomes in spontaneous canine tumors. Clin. Cancer Res. 12: 4004-4010.
185. Cheong I.; Huang X.; Bettegowda C.; Diaz L.A.Jr.; Kinzler K.W.; Zhou S.; Vogelstein B. (2006). A bacterial protein enhances the release and efficacy of liposomal cancer drugs. Science. 314: 1308-1311.

186. Ryan R.M.; Green J.; Lewis C.E. (2006). Use of bacteria in anti-cancer therapies. Bioessays. 28: 84-94.
187. Kong G.; Dewhirst M.W. (1999). Hyperthermia and liposomes. Int. J. Hyperthermia. 15, 345-370.
188. Connor J.; Yatvin M.B.; Huang L. (1984). pH-sensitive liposomes: acid-induced liposome fusion. Proc. Natl. Acad. Sci. U.S.A. 81: 1715-1718.
189. Das M.; Mardyani S.; Chan W.C.W.; Kumacheva E. (2006). Biofunctionalized pH-responsive microgels for cancer cell targeting: Rational design. Adv. Mater. 18: 80-83.
190. Kommareddy S.; Amiji M. (2005). Preparation and evaluation of thiol-modified gelatin nanoparticles for intracellular DNA delivery in response to glutathione. Bioconjug. Chem. 16: 1423-1432.
191. Seow W.Y.; Xue J.M.; Yang Y.Y. (2007). Targeted and intracellular delivery of paclitaxel using multi-functional polymeric micelles. Biomaterials. 28: 1730-1740.
192. Wei J.S.; Zeng H.B.; Liu S.Q.; Wang X.G.; Tay E.H.; Yang Y.Y. (2005). Temperature- and Ph-sensitive core-shell nanoparticles self-assembled from poly(N-isopropylacrylamide-CO-acrylic acid-CO-cholesterylacrylate) for intracellular delivery of anticancer drugs. Front. Biosci. 10: 3058-3067.
193. Zhang L.Y.; Guo R.; Yang M.; Jiang X.Q.; Liu B.R. (2007). Thermo and pH dual-responsive nanoparticles for anti-cancer drug delivery. Adv. Mater. 19: 2988-2995.
194. Sonoda T.; Nogami T.; Oishi J.; Murata M.; Niidome T.; Katayama Y. (2005). A peptide sequence controls the physical properties of nanoparticles formed by peptide-polymer conjugates that respond to a protein kinase A signal. Bioconjug. Chem. 16: 1542-1546.
195. Davis S.C.; Szoka F.C.Jr. (1998). Cholesterol phosphate derivatives: synthesis and incorporation into a phosphatase and calcium-sensitive triggered release liposome. Bioconjug. Chem. 9: 783-792.
196. Wymer N.J.; Gerasimov O.V.; Thompson D.H. (1998). Cascade liposomal triggering: light-induced Ca^{2+} release from diplasmenylcholine liposomes triggers PLA2-catalyzed hydrolysis and contents leakage from DPPC liposomes. Bioconjug. Chem. 9: 305-308.
197. Hussein M.A.; Wood L.; Hsi E.; Srkalovic G.; Karam M.; Elson P.; Bukowski R.M. (2002). A phase II trial of pegylated liposomal doxorubicin, vincristine, and reduced-dose dexamethasone combination therapy in newly diagnosed multiple myeloma patients. Cancer. 95: 2160-2168.

198. Gordon K.B.; Tajuddin A.; Guitart J.; Kuzel T.M.; Eramo L.R.; VonRoenn J. (1995). Hand-foot syndrome associated with liposome-encapsulated doxorubicin therapy. Cancer. 75: 2169-2173.

ANTECEDENTES, HIPÓTESIS Y OBJETIVOS

ANTECEDENTES

1.- Las nanocápsulas poliméricas, constituidas por un núcleo oleoso y una cubierta polimérica, permiten mejorar la formulación de fármacos anticancerosos de naturaleza hidrofóbica [1-3], evitando la utilización de otros excipientes que producen graves efectos secundarios [4; 5].

2.- Las nanocápsulas de quitosano han demostrado su efectividad para mejorar la absorción vía oral y nasal del péptido calcitonina, principalmente debido a la mucoadhesividad y capacidad promotora de la absorción del quitosano [6; 7].

3.- Se han planteado diversas estrategias para conseguir la acumulación selectiva de los fármacos anticancerosos en el tumor, siendo una de ellas la funcionalización de la superficie de los nanosistemas con anticuerpos monoclonales frente a antígenos expresados en las células tumorales [8-10].

4.- Recientemente, dada la capacidad que presenta la poliarginina para atravesar membranas [11], se han descrito nanosistemas constituidos por este poliaminoácido que favorecen la internalización del fármaco que transportan [12-14].

---

[1] **Peltier S.; Oger J.M.; Lagarce F.; Couet W.; Benoit J.P.** (2006). Pharm. Res. 23: 1243-1250.
[2] **Bae K.H.; Lee Y.; Park T.G.** (2007). Biomacromolecules. 8: 650-656.
[3] **Khalid M.N.S.; Hoarau D.; Dragomir A.; Leroux J.C.** (2007) Pharm. Res. 23: 752-758.
[4] **Van Zuylen L.; Verweij J.; Sparreboom A.** (2001). Invest. New Drugs. 19: 125-141.
[5] **Engels F.K.; Mathot R.A.A.; Verweij J.** (2007). Anticancer Drugs. 18: 95-103.
[6] **Prego C.; Torres D.; Alonso M.J.** (2006). J. Nanosci. Nanotechnol. 6: 2921-2928.
[7] **Prego C.; Torres D.; Alonso M.J.** (2006). J.D.D.S.T. 16: 331-337.
[8] **Kirpotin D.B.; Drummond D.C.; Shao Y.; Shalaby M.R.; Hong K.; Nielsen U.B.; Marks J.D.; Benz C.C.; Park J.W.** (2006). Cancer Res. 66: 6732-6740.
[9] **Chen H.; Gao J.; Lu Y.; Kou G.; Zhang H.; Fan L.; Sun Z.; Guo Y.; Zhong Y.** (2008). J. Control. Release. 128: 209-216.
[10] **Debotton N.; Parnes M.; Kadouche J.; Benita S.** (2008). J. Control. Release. 127: 219-230.
[11] **Lundberg M.W.; Johansson M.** (2003). Mol. Ther. 8: 143-150.
[12] **Firbas C.; Jilma B.; Tauber E.; Buerger V.; Jelovcan S.; Lingnau K.; Buschle M.; Frisch J.; Klade C.S.** (2006). Vaccine. 24: 4343-4353.
[13] **Zhang C.; Tang N.; Liu X.; Liang W.; Xu W.; Torchilin V.P.** (2006). J. Control. Release. 112: 229-239.
[14] **Suzuki R.; Yamada Y.; Harashima H.** (2007). Biol. Pharm. Bull. 30: 758-762.

HIPÓTESIS

1.- El desarrollo de nanocápsulas, constituidas por un núcleo oleoso y una cubierta de quitosano, puede resultar una estrategia adecuada para la incorporación eficaz del fármaco citostático docetaxel, debido al marcado carácter hidrofóbico de esta molécula. Por otro lado, la cubierta de quitosano puede favorecer la interacción biológica de los sistemas, potenciando la acción del fármaco.

2.- La funcionalización de las nanocápsulas de quitosano con el anticuerpo monoclonal antitomoregulina puede facilitar el direccionamiento selectivo y la captura de los nanosistemas por parte de células tumorales que sobreexpresen el antígeno tomoregulina en su superficie. De este modo se pretende conseguir una liberación específica del fármaco vehiculizado en las nanocápsulas de quitosano, en el interior de las células diana.

3.- Tomando en consideración la capacidad de la poliarginina para atravesar las membranas celulares, el recubrimiento con poliarginina de los núcleos oleosos que contienen el fármaco puede mejorar la internalización de los nanosistemas, favoreciendo la penetración intracelular del fármaco.

OBJETIVOS

Teniendo en cuenta lo anteriormente expuesto, el objetivo global de este trabajo se ha dirigido a evaluar el potencial que presentan distintas nanoestructuras poliméricas para vehiculizar y promover la internalización celular de fármacos anticancerosos de carácter hidrofóbico, como el docetaxel. Para cubrir este objetivo, se han seguido las siguientes etapas:

1.- Desarrollo de nanocápsulas de quitosano y evaluación de su potencial en la terapia del cáncer.

Esta parte de la memoria se ha dirigido a la caracterización de sistemas de tipo nanocapsular constituidos por oligómeros de quitosano, así como al estudio de su capacidad para incorporar y liberar eficazmente el fármaco citostático docetaxel. Por otro lado también se ha pretendido profundizar en el estudio de la interacción de las nanocápsulas con cultivos de células tumorales, así como en el potencial de estos vehículos para favorecer la liberación intracelular del docetaxel.

Los resultados de este apartado se recogen en el artículo II:

Highly efficient systems to deliver taxanes into tumor cells: docetaxel-loaded chitosan oligomer colloidal carriers. Biomacromolecules. (2008). 9: 2186–2193.

2.- Estudio de liofilización de las nanocápsulas de quitosano conteniendo docetaxel.

Esta etapa se planteó con un doble objetivo: en primer lugar, la optimización del proceso de liofilización de la formulación de nanocápsulas de quitosano y, en una segunda parte, la evaluación del mantenimiento de la actividad biológica del liofilizado de nanocápsulas conteniendo docetaxel.

Los resultados de este apartado se recogen en el artículo III:

Freeze-dried chitosan nanocapsules: efficient vehicles for the intracellular delivery of docetaxel. Pendiente de publicación.

3.- Desarrollo de nanocápsulas de quitosano modificadas con el anticuerpo monoclonal antitomoregulina y evaluación de su eficacia *in vivo*.

Los estudios llevados a cabo en esta etapa se han dirigido hacia la obtención y evaluación biológica de un sistema de nanocápsulas de quitosano modificado en superficie con el anticuerpo monoclonal antitomoregulina, que reconozca selectivamente a las células tumorales que sobreexpresen el antígeno.

Los resultados de este apartado se recogen en el Anexo I:

In vivo efficacy of anti-TMEFF-2 modified nanocapsules in non-small cell lung cancer tumors.

4.- Desarrollo de nanocápsulas de poliarginina y evaluación de su potencial en la terapia del cáncer.

El objetivo de esta etapa ha consistido en el diseño y desarrollo de una nueva formulación de nanocápsulas, en la que la cubierta polimérica está constituída por el poliaminoácido catiónico poliarginina. En concreto, se evaluó la versatilidad del sistema encapsulando el fármaco docetaxel, y asociando ADN plasmídico, así como realizando estudios en cultivos celulares.

Los resultados de este apartado se recogen en el artículo IV:

Polyarginine nanocapsules: a new platform for intracellular drug delivery. Pendiente de publicación.

ARTICLES

Article II

Highly efficient systems to deliver taxanes into tumor cells: docetaxel-loaded chitosan oligomer colloidal carriers

M. V. Lozano[1#], D. Torrecilla[2#], D. Torres[1], A. Vidal[2], F. Domínguez[2*], M. J. Alonso[1].

[1] Department of Pharmaceutical Technology, Faculty of Pharmacy.
[2] Department of Physiology. Faculty of Medicine. University of Santiago de Compostela (USC) 15782 Santiago de Compostela, Spain

# Both authors equally contributed to the paper.

* Corresponding author: Prof. Fernando Domínguez

Adapted from: Biomacromolecules. (2008). 9: 2186-2193.

ABSTRACT

Chitosan (CS) colloidal carriers, which consist of an oily core and a CS coating, were developed to facilitate a controlled intracellular delivery of docetaxel. The systems presented a particle size of <200 nm and a positive surface charge. As shown by the flow cytometry analysis, fluorescent CS carriers were rapidly internalized by human tumor cells. Fluorescence was observed in more than 80% of MCF7 (human breast adenocarcinoma) and almost 100% of A549 (human lung carcinoma) cells when a 2h treatment with fluorescent CS carriers was given. A total of 24 h after treatment, docetaxel-loaded CS carriers had an effect on cell proliferation that was significantly greater than that of free docetaxel. These results indicate that docetaxel remains fully active upon its encapsulation into the colloidal carriers and that these systems actively transport docetaxel into cancer cells and, thus, result in a significant increase in its antiproliferative effect.

INTRODUCTION

Taxanes (paclitaxel, docetaxel) are potent chemotherapeutic agents that have greatly contributed to the improvement in cancer patient survival and have proven clinical efficacy against a wide range of solid tumors, such as advanced breast, ovarian, or nonsmall cell lung cancer [1-3]. Recent reports on antitumor activity regarding survival in patients with metastatic breast cancer suggest the superiority of docetaxel over paclitaxel [4]. Irrespective of their specific activity, these drugs are characterized by their hydrophobic character and a resulting necessity to use solubilizers for their intravenous administration. So far, Cremophor EL and Tween 80, both of which combined with ethanol, have been the only pharmaceutical formulation vehicles used for administration of paclitaxel and docetaxel, respectively. These vehicles, however, are responsible for severe side effects, which limit the amount of drug that can be safely administered [5; 6]. To overcome these problems, alternative nanotechnology-based formulations, which do not require solubilization, have recently been proposed. These formulations consist of nanostructures, such as polymer conjugates, polymeric micelles, liposomes, or nanoparticles [7; 8].

The rationale behind the nanotechnological approach is the so-called "passive targeting", which is produced after the intravenous administration of nanosystems and their subsequent accumulation in the tumor interstitium due to the known "enhanced permeability and retention effect". This process, which is typical in cancer tissues, enables the achievement of high drug levels in the target site and prevents the indiscriminate biodistribution of antitumor drugs [9]. The potential of nanoformulated taxanes was reinforced by the Food and Drug Administration's approval of Abraxane®, which are nanoparticles containing albumin-bound paclitaxel [10].

Lipid nanosystems based on a core-shell structure consisting of an oil-filled interior with a surrounding polymer layer (nanocapsules) are known to be promising vehicles for the delivery of hydrophobic drugs like taxanes. Depending on the coating polymer and on the specific ligands coupled to their surface, a variety of exciting possibilities have been described. For example, Leroux *et al*. [11] reported on the potential of long circulating PEG-decorated lipid nanocapsules as vehicles for the delivery of docetaxel to solid tumors. This was the first report to demonstrate that docetaxel physically entrapped in a colloidal carrier could be passively targeted to neoplastic tissues. What is more, nanocapsules showed an enhanced drug deposition in mice tumors when compared to the control

formulation (Taxotere®). Similarly, docetaxel encapsulated in micronized droplets (about 2 μm) of olive oil coated with fibrinogen [12] was found to be more effective than Taxotere® for the treatment of melanoma-bearing mice. The enhancement of the antitumor effect was partially attributed to the retention of the coated droplets within the fibrin-rich tumor microenvironment. A successful targeting was also achieved by a nanosystem based on oil-encapsulating PEO-PPO-PEO/PEG nanocapsules conjugated with folic acid. These nanocapsules loaded with paclitaxel showed a significant enhancement of the cellular and apoptotic effect against folate receptor overexpressing cancer cells when compared with the commercial formulation (Taxol®) [13].

Previous studies performed by our research group have shown that CS nanocapsules were able to improve the intestinal, nasal, and ocular transport of poorly absorbed molecules mainly due to their intimate interaction with the different epithelia [14-16]. Previous studies have also suggested that the polymer properties, such as molecular weight, may affect the mode of action of the polymer. More specifically, it has been indicated that low molecular weight CS has a facilitated interaction with epithelial cells when compared to high molecular weight CS [17]. In addition, it has been reported that CS oligomers exhibit angioinhibitory and tumor cell apoptotic properties [18].

Taking this information into account, the aim of this work was to evaluate the potential of CS oligomer nanocapsules as vehicles for anticancer drugs, using docetaxel as a model drug.

MATERIALS AND METHODS

Chemicals

Docetaxel (from Fluka) and poloxamer 188 (Pluronic® F-68) were purchased from Sigma-Aldrich (Spain). Miglyol® 812, which is neutral oil formed by esters of caprylic and capric fatty acids and glycerol, was donated by Sasol Germany GmbH (Germany). The surfactant Epikuron® 145V, which is a phosphatidylcholine-enriched fraction of soybean lecithin, was donated by Cargill (Spain), and fluorescein-DHPE was supplied by Molecular Probes (Spain). Protasan Cl 113, medium molecular weight CS chloride salt with a deacetylation degree of 85%, was purchased from FMC Biopolymer Novamatrix (Norway). Sodium nitrite was purchased from Probus (Spain).

Preparation of CS Oligomers

CS oligomers were prepared from medium molecular weight CS by oxidative degradation using sodium nitrite ($NaNO_2$) following a previously described procedure [19]. Briefly, 0.1 mL of $NaNO_2$ (0.1 M) were added to 2 mL of a CS solution (1% w/v) at room temperature under magnetic stirring. Overnight reaction ensured complete degradation, and finally, the resulting CS solution was freeze-dried and the CS oligomers were obtained. The molecular size of CS oligomers was verified by size exclusion chromatography (SEC).

Preparation of CS Carriers

Blank CS oligomer carriers were prepared by the solvent displacement technique following the procedure described previously [14]. Consequently, 40 mg of Epikuron® 145V were dissolved in 0.5 mL of ethanol before adding 125 µL of Miglyol® 812 and 9.5 mL of acetone. This organic phase was immediately poured into an aqueous phase composed of CS oligomers (0.05% w/v) and Pluronic® F-68 (0.25% w/v). The formation of the system was instantaneous, which was evident due to the milky appearance of the mixture, and provided a CS carriers concentration of 21.75 mg/mL.

The incorporation of docetaxel, or the fluorescent probe in CS oligomer structures, required the previous dissolution of the molecule in ethanol to obtain a final concentration of 2 mg/mL. Next, an aliquot of the stock solution was added to the oily core of the carriers and the same procedure was followed. The final docetaxel concentration obtained in CS oligomer carriers was 12.4 µM.

CS Carriers Characterization

Size, ζ-Potential, and Morphology of CS Oligomer Carriers

Particle size and polydispersion index were determined by photon correlation spectroscopy (PCS). Samples were diluted to the appropriate concentration with filtered water. Each analysis was performed at 25 °C with an angle detection of 90°. The *ζ*-potential values were calculated from the mean electrophoretic mobility values, which were determined by laser Doppler anemometry (LDA). Samples were diluted with KCl 1 mM and placed in the electrophoretic cell, where a potential of ±150 mV was established. PCS and LDA analysis were performed using a Zetasizer 3000HS (Malvern Instruments, Malvern, U.K.). Each batch was

analyzed in triplicate.

The morphological characterization of the systems was performed using the transmission electron microscopy technique (TEM, CM12 Philips, The Netherlands). Samples were stained with 2% (w/v) phosphotungstic acid solution and placed on copper grids with Formvar films for viewing by TEM.

Encapsulation Efficiency of Docetaxel-Loaded CS Oligomer Carriers

The encapsulation efficiency of docetaxel in the CS carriers was determined indirectly by the difference between the total amount of docetaxel in the formulation and the free drug found in the supernatant of the formulation. Therefore, the total amount of drug was estimated by dissolving an aliquot of nonisolated docetaxel-loaded CS carriers with acetonitrile. This sample was centrifuged during 20 min at 4000 × *g* and the supernatant was measured with a high-performance liquid chromatography (HPLC) system. The nonencapsulated drug was determined by the same method following separation of the CS structures from the aqueous medium by ultracentrifugation.

Docetaxel was assayed by a slightly modified version of the method proposed by Lee *et al*. [20]. The HPLC system consisted of an Agilent 1100 series instrument equipped with a UV detector set at 227 nm and a reverse phase Zorbax Eclipse XDB-C8 column (4.6 × 150 mm i.d., pore size 5 μm Agilent, U.S.A.). The mobile phase consisted of a mixture of acetonitrile and 0.1% v/v orthophosphoric acid (55:45, v/v) and the flow rate was 1 mL/min. The standard calibration curves of docetaxel were linear (r^2 > 0.999) in the range of concentrations between 0.3-2 μg/mL.

In Vitro Release Studies

The release studies of docetaxel from CS carriers were performed by incubating a sample of the formulation with acetate buffer (pH = 5) at an appropriate concentration to ensure sink conditions. The vials were placed in an incubator at 37°C with horizontal shaking. A total of 4 mL of the suspension were collected and centrifuged by using Amicon Ultra devices (Millipore, Spain) at different time intervals (1, 3, 6, 24, and 48 h). The docetaxel released was calculated indirectly by determining how much of it was left in the system by processing the isolated CS carriers with acetonitrile before HPLC analysis.

Cell Culture, MTT Assay, Flow Cytometry and Estimation of GI_{50}

Cell Culture

MCF7 tumor cell line, human breast adenocarcinoma derived, was cultured in Dulbecco′s Modified Eagle′s Medium (DMEM, Sigma), supplemented with 10% (v/v) of fetal bovine serum (FBS, GIBCO-Invitrogen) and 1% (v/v) of L-glutamine, penicillin, and streptomycin solution (GPS, Sigma). The human lung carcinoma-derived A549 tumor cell line was cultured in a 1:1 mixture of DMEM and Ham′s F12 Medium (Sigma) with the same supplements.

MTT Assay and GI_{50} Estimation

Cells were plated in a multiwell-96 plate (Iwaki) at 4×10^3 cells/well, and 24 h later, the medium was changed for the following three treatments: docetaxel, docetaxel-loaded CS carriers, and blank CS carriers. Tetrazolium salt 3-(4,5-dimethylthiazol-2-yl)-2,5-diphenyltetrazoliumbromide (MTT, Acros Organics) was used for mitochondrial activity evaluation in cell viability studies 24 and 48 h post-treatments. Plates were measured in MicroPlate Reader Model 550 (BIO-RAD) and data were processed with Excel and SPSS software. Using absorbance measurements [time zero, (Az), control growth, (C), and test growth in the presence of drug at the various concentration levels (Ai)], the percentage growth was calculated at each of the drug concentration levels.

Growth inhibition of 50% (GI_{50}) was calculated from $[(Ai - Az) / (C - Az)] \times 100 = 50$, which is the drug concentration resulting in a 50% reduction in absorbance in control cells during the drug incubation.

Uptake Studies

Cells were plated in a multiwell-6 plate (Falcon) at 5×10^5 cells/well, and 24 h later, the medium was changed for treatments: fluorescently-labeled CS carriers with fluorescein-derivatized dihexadecanoylglycerol phosphoethanolamine (fluorescein-DHPE, Fisher Scientific) and fluorescent dye as a control. After 2 h of incubation, cells were washed with acidic phosphate saline buffer (PBS, Sigma), detached, and resuspended in PBS supplemented with 3% (v/v) of FBS. Living cell suspensions were analyzed for green fluorescence by flow cytometry in a FACScan (Becton Dickinson) and fluorescent microscopy (Leica).

Cell Cycle Analysis

Cell cycle phase distribution was determined by measuring DNA content by flow cytometry of propidium iodide-stained cells, as described [21]. Briefly, whole cell suspensions were washed in PBS, fixed in 70% ethanol, stained in 50 µg/mL propidium iodide, 1 mg/mL RNase, 0.1% Triton X-100, and analyzed using the ModFit software.

RESULTS AND DISCUSSION

The main aim of this project was to evaluate the potential of CS oligomer carriers of nanometric size, so-called nanocapsules [14], for the transport of the anticancer drug docetaxel. CS oligomer carriers were proposed because they are supposedly able to improve the stability of the drug included in their core, as well as promoting a tight interaction with the cancer cells due to their CS corona. As a first step, the physicochemical, morphological and encapsulation properties of these systems, as well as the docetaxel *in vitro* release characteristics, were determined. Subsequently, the cell viability assays with breast (MCF-7) and nonsmall lung (A-549) cancer cell lines were performed so as to follow the antiproliferative activity of the encapsulated docetaxel. Additionally, flow cytometry and immunofluorescence microscopy assays on cell lines pretreated with the docetaxel-loaded carriers were carried out to elucidate the internalization capacity of the systems. Finally, the cellular effects of CS oligomer carriers in both cell lines were investigated more deeply by cell cycle analysis.

CS Carriers Characterization

CS oligomer carriers were prepared using the solvent displacement technique previously reported [14]. The CS coating around the oily nanodroplets was formed due to the ionic interactions between the negatively charged tensoactive agent, lecithin, and the positively charged CS oligomers (MW = 10 KDa). Blank CS oligomer carriers formed a homogeneous population of a mean particle size smaller than 200 nm and a high positive surface charge (Table 1). The positive charge was due to the CS oligomer layer disposed over the hydrophobic core formed by lecithin and the oil Miglyol® 812.

Docetaxel is a noncharged drug with a very low water solubility, which makes it an attractive candidate for inclusion in the hydrophobic core of a lipidic system like that of the CS nanocapsules. Furthermore, this reservoir structure allowed an encapsulation efficiency of 72% for docetaxel. Several authors have also reported high encapsulation efficiencies for docetaxel or paclitaxel in oil containing nanostructures, which is mainly due to the affinity of these drugs to the core components [11]. As expected, the encapsulation of docetaxel hardly modified the size and the charge of blank CS carriers.

Table 1: Physicochemical properties of blank, fluorescent and docetaxel (DCX)-loaded CS carriers. PI: polydispersity index. Values are given as mean ± s.d.; n=3.

Carrier	Size (nm)	PI	-Potential (mV)
Blank CS carriers	151 ± 1	0.1	+47 ± 1
DCX-loaded CS carriers	162 ± 4	0.1	+47 ± 3
Fluorescent CS carriers	185 ± 3	0.1	+38 ± 2

The morphological appearance of the systems was observed by transmission electron microscopy. The CS carriers have a round shape and a size of less than 200 nm (Figure 1), a result that corresponds to that observed by photonic correlation spectroscopy (Table 1).

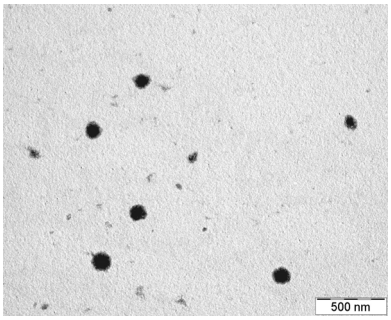

Figure 1: Transmission electron micrograph of blank CS carriers.

The results of the *in vitro* release studies of docetaxel from CS carriers are presented in Figure 2. The biphasic profile, typically observed in these types of delivery systems, is composed of an initial release phase (50% of drug released in 8 h), followed by a second phase characterized by the absence of drug release. The initial phase could be related to the partition of the drug between the

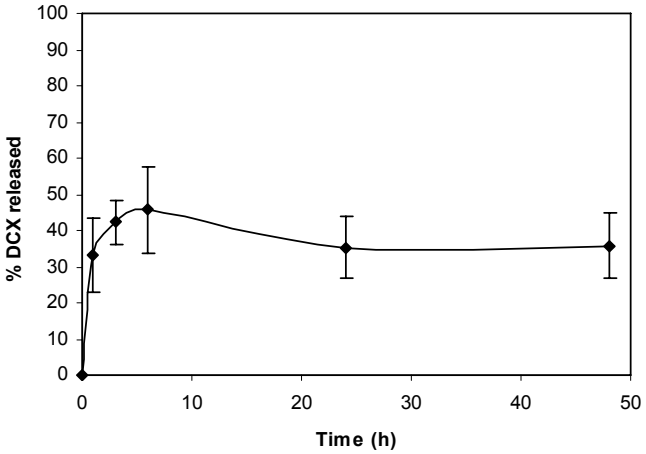

Figure 2: In vitro docetaxel release from docetaxel-loaded CS carriers (mean ± s.d.; n=3).

oily core and the external aqueous release medium, whereas the second phase illustrates the important affinity of the drug to the oily core. An important additional observation from these studies was that the drug delivered from CS carriers remains stable. These results suggest that, following *in vivo* administration, the structures slowly deliver the encapsulated drug in an active form.

In Vitro Cellular Proliferation and Uptake Studies in Human Tumor Cell Lines

The results indicate that docetaxel loaded CS carriers reduced the rate of proliferation of MCF7 and A549 human tumor cells with faster kinetics than free docetaxel. Indeed, at 24 h after treatment, the encapsulated docetaxel had an effect on cell proliferation that was significantly greater than that of free docetaxel (Figure 3A1, B1). The GI_{50} values calculated for docetaxel-loaded carriers (24 h after treatment) were predictably lower than those estimated for free docetaxel both in MCF7 and A549 cell lines (Table 2).

On the other hand, blank CS carriers had no significant effects on the cell growth (Figure 3). Indeed, the differences in viability observed after exposure to this formulation and the nontreated cells were not statistically significant. These negligible toxicity results observed for CS carriers, which are consistent with other toxicity results reported for CS [22; 23], could be justified by the low concentration of CS presented in the experimental conditions of the study.

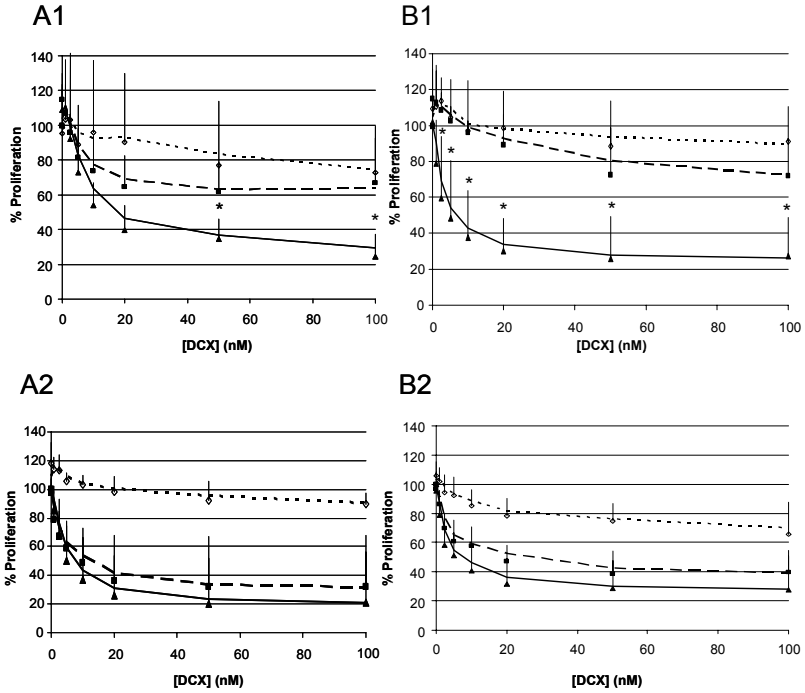

Figure 3: Effect on MCF7 and A549 cell proliferation of docetaxel (DCX, dash line), docetaxel (DCX)-loaded CS carriers (solid line) and blank CS carriers (dotted line) at different incubation times and concentrations. MCF7 after 24h (A1) and 48h (A2), A549 after 24h (B1) and 48h (B2). Mean values of four independent experiments. * $p<0.05$, DCX-loaded CS carriers vs. DCX.

Table 2: GI_{50} values (Growth inhibitory 50, drug concentration resulting in a 50% reduction in absorbance in control cells), expressed in nM, were estimated as described in material and methods. Blank CS carriers, docetaxel (DCX) and docetaxel (DCX)-loaded CS carriers. Mean values of 4 independent experiments; n.d.: none of the concentrations tested resulted in a 50% reduction of the absorbance.

	MCF7		**A549**	
	24h	**48h**	**24h**	**48h**
Blank CS carriers	n.d.	n.d.	n.d.	n.d.
DCX	62.5	5.6	36.5	12.8
DCX-loaded CS carriers	4.7	2.7	5.3	4.5

After 48 h incubation, the effects on cell proliferation observed for docetaxel-loaded CS carriers and free docetaxel were similar (Figure 3A2, B2), which suggests that the differential effect found at 24 h was due to an accelerated uptake of the encapsulated docetaxel in CS structures. Both docetaxel-loaded CS carriers and free docetaxel had a cytostatic effect, which arrested proliferating cells without noticeable effects on cell viability (data not shown) at any given moment. In theory, the observed antiproliferative effect of docetaxel-loaded CS carriers could be attributed to the uptake of the systems followed by the intracellular delivery of docetaxel. However, the possibility that a certain amount of docetaxel may have been released from the oily reservoir before the uptake took place cannot be ruled out. To provide evidence of the uptake intensity of the CS carriers, a fluorescent dye was encapsulated and its uptake was estimated by flow cytometry. This encapsulated fluorescent dye was detected inside almost every cell 2 h, or possibly sooner, after addition to the cell medium, while the nonencapsulated dye remained mostly excluded (Figure 4). Consequently, these results suggest that the internalization of the CS carriers most probably occurs before a significant amount of docetaxel is released from the system.

Fluorescence microscopy showed that the dye localization inside the cell was in the cytoplasm without staining the nucleus. Moreover, the dye was found in vesicles (Figure 4B), suggesting that the encapsulated dye had entered the cell via an endocytic pathway. Docetaxel, like most tumor drugs, is not selective of tumors and affects both normal and cancer cells equally. Unfortunately, encapsulation does not make docetaxel more selective, but it does accelerate its entry into the cell, as we have shown here. Therefore, tumors rather than normal tissues will be more exposed to the action of the drug because they have a greater blood flow than their normal neighbor tissue.

We postulated that the enhanced antiproliferative effect of docetaxel on the tumor cells observed at 24 h post-treatment is subsequently related to rapid uptake by the cells. This improved uptake could be related to a favored interaction of the CS carriers surface with the cancer cells, which may well be due to the CS coating [24]; this was also found for different cell types, such as those of corneal epithelium [16]. Moreover, it has been shown that the charge plays a role in passive tumor targeting because cationic nanoparticles are better at concentrating in the tumor environment than similarly designed anionic particles: it was found that an increase in the charge content doubled the accumulation of cationic liposomes in tumor vessels of two different tumor types [25].

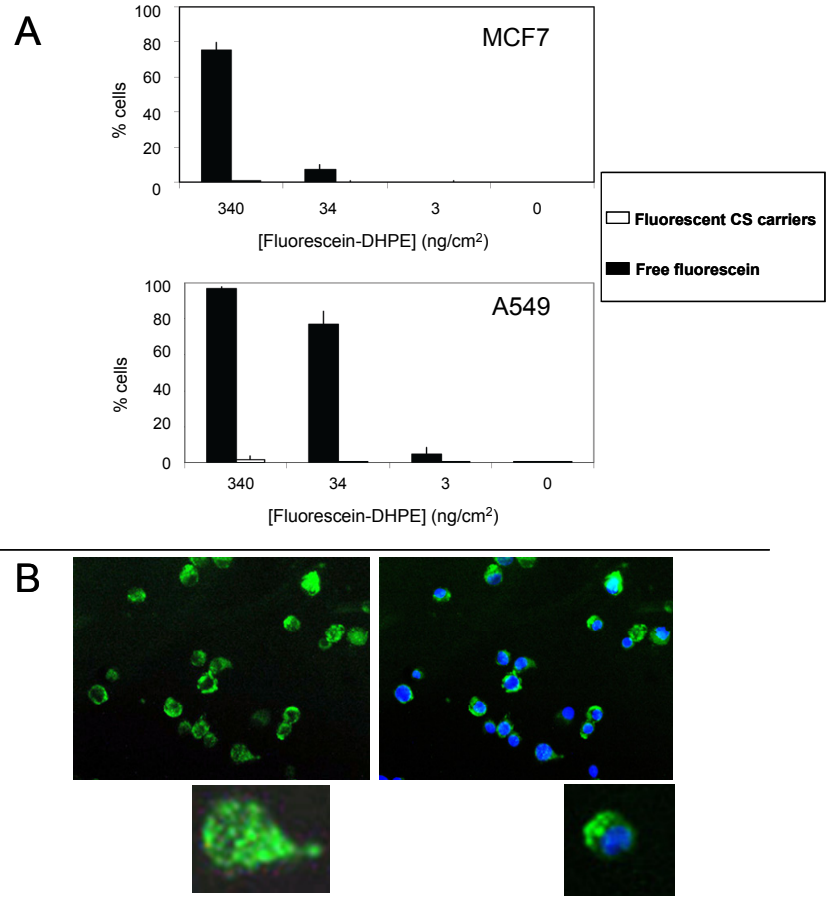

Figure 4: Uptake studies of fluorescent CS carriers assessed by flow cytometry in MCF7 and A549 cells. (A) Percentage of stained cells after 2 h incubation with fluorescein-DHPE CS carriers, black bars, or free fluorescein-DHPE, white bars. Mean values of 3 independent experiments. (B) Fluorescence microscopy image of MCF7 cells treated with fluorescent CS carriers. On the left, green label corresponds to fluorescent CS carriers loaded with fluorescein-DHPE. On the right, merged imagine of nuclei stained with DAPI (blue) and fluorescein (green). The insert is a magnification of the same image and it shows that the dye was found in vesicles inside the cells.

The next step was to rule out the possibility that the procedure of encapsulation or the mechanism of cellular uptake could affect the biological activity of docetaxel. Taxanes have been shown to target tubulin causing stabilization of microtubules, which results in cell-cycle arrest and apoptosis [26]. As a result, attention was given to the well-studied effects of docetaxel on tumor cells, such as cell cycle distribution and α-tubulin distribution and aggregation. Flow cytometry analysis of the effects of docetaxel on the cell cycle of the two

types of cancer cells showed that both docetaxel-loaded CS carriers and free docetaxel were able to accumulate cells in the G2/M phase (Figure 5), which suggests an arrest in the cell cycle, which is consistent with the data obtained by MTT analysis.

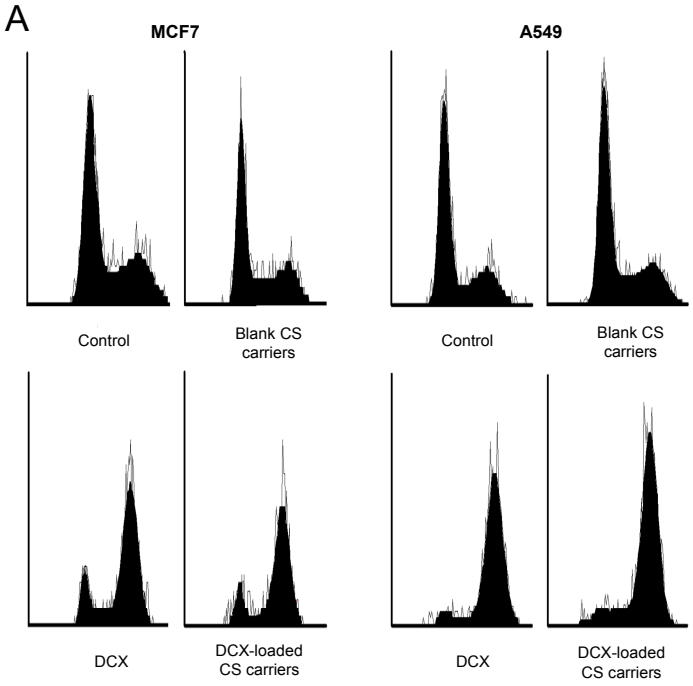

B	G0/G1	S	G2/M	G0/G1	S	G2/M
Control	56.1±0.6	28.1±4.8	15.8±4.2	67.9±1.8	19.0±4.9	13.1±6.7
Blank CS carriers	54.8±3.2	31.2±5.2	14.0±4.6	61.8±3.4	27.3±0.1	10.9±3.3
DCX	9.8±5.0	19±6.0	71.2±1.0	2.1±0.8	15.2±7.0	82.7±7.8
DCX-loaded CS carriers	12.7±3.9	16.5±4.6	70.8±8.6	0.1±0.0	16.4±0.9	83.5±0.9

Percentages of cells in each cell cycle phase. Mean ± standard deviation, n=3.

Figure 5: Representative flow cytometry profiles of the cell cycle phase distribution of MCF7 (A) and A549 (B). Cells were incubated with free docetaxel (DCX), docetaxel (DCX)-loaded CS carriers, blank CS carriers and fresh medium (Control) for 48 h. They were subsequently fixed and stained with propidium iodide for DNA content analysis.

In addition to this, confocal microscopy showed that both control (without treatment) and blank CS carrier-treated cells had a more or less homogeneous microtubule network, which was clearly present throughout the cell. In contrast, docetaxel-loaded CS carriers and free docetaxel-treated cells presented a pattern of unevenly distributed staining with clear aggregation and anchorage of the microtubules into thicker fibers (depolymerisation was inhibited by docetaxel, therefore, causing aggregation; Figure 6), which again suggests that docetaxel-loaded carriers and free docetaxel cause cytostasis by the same microtubule-interfering mechanisms.

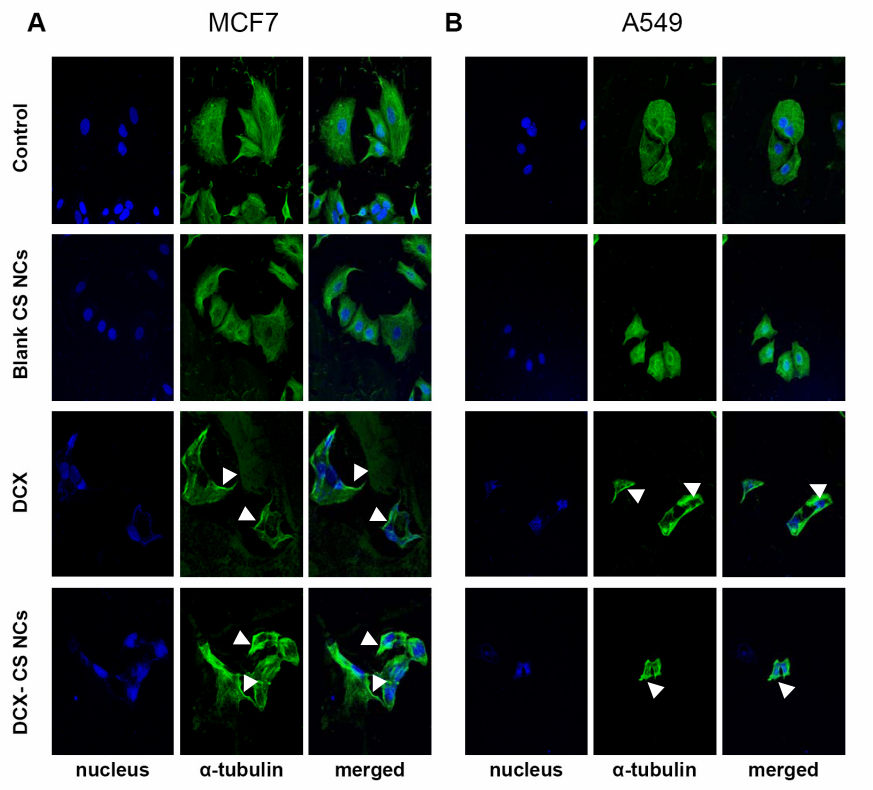

Figure 6: Confocal microscopy of MCF7 (A) and A549 (B) cells after incubation with free docetaxel (DCX), docetaxel (DCX)-loaded CS carriers, blank CS carriers and fresh medium (Control). Cells were incubated for 48 h with 100 nM of the drug or the equivalent concentration for the controls. They were subsequently processed by staining nuclear DNA (DAPI) and -tubulin microtubules (monoclonal mouse anti -tubulin antibody and goat anti mouse antibody conjugated with Alexa 488). Micronuclear abnormalities formation and microtubules condensation (arrow head) are visible in docetaxel treated cells (DCX and DCX-loaded CS carriers).

Overall, these findings indicate that docetaxel-loaded CS carriers exhibit a higher antiproliferative effect on the two studied cancer cell lines when compared with that of the free drug. This took place during the first hours of the study and was probably related to an early uptake of the systems by the cancer cells. In addition to this, it was also demonstrated that the mechanism of action of docetaxel included in the colloidal carriers was unchanged. Future work on CS carriers will aim at determining the efficacy of docetaxel entrapped in these systems in appropriate tumor models.

CONCLUSIONS

In conclusion, it can be stated that CS oligomer carriers are a very efficient system for the delivery of docetaxel into human cancer cells. More specifically, CS carriers favor a fast and efficient uptake of the encapsulated drug into tumor cells. It can also be stated that encapsulated docetaxel is maintained fully active and its mechanism of action unaltered. Consequently, the efficacy of CS carriers for intracellular delivery of docetaxel combined with their low toxicity points to the potential of this system for cancer therapy. Further *in vivo* studies need to be performed in order to fully assess the potential of CS carriers in the development of new anticancer agents.

ACKNOWLEDGEMENTS

This work has been financed by the Spanish Ministry of Science and Technology (SAF 2004-08319CO2-01) and Consolider Nanobiomed (CSD 2006-00012). The first author acknowledges the fellowship received from the Spanish Government (AP2005-1701). A.V. is an investigator of the “Ramón y Cajal” Program financed by the Ministry of Science and Education, Spain. The authors also express their gratitude to Ramón Novoa Carballal for CS oligomer SEC measurements. We thank Peter Rees for the English editing.

REFERENCES

1. Rowinsky R.K.; Donehower R.C.N. (1995). Drug Therapy: Paclitaxel (Taxol). Engl. J. Med. 332: 1004-1014.
2. Trudeau M.E.; Eisenhauer E.A.; Higgins B.P.; Letendre F.; Lofters W.S.; Norris B.D.; Vandenberg T.A.; Delorme F.; Muldal A.M. (1996). Docetaxel in patients with metastatic breast cancer: A phase II study of the National Cancer Institute of Canada - Clinical Trials Group. J. Clin. Oncol. 14: 422-428.
3. Piccart M.J.; Gore M.; Huinink W.T.B.; Vanoosterom A.; Verweij J.; Wanders J.; Franklin H.; Bayssas M.; Kaye S. (1995). Docetaxel - An Active New Drug for Treatment of Advanced Epithelial Ovarian-Cancer. J. Natl. Cancer Inst. 87: 676-681.
4. Jones S.E.; Erban J.; Overmoyer B.; Budd G.T.; Hutchins L.; Lower E.; Laufman L.; Sundaram S.; Urba W.J.; Pritchard K.I.; Mennel R.; Richards D.; Olsen S.; Meyers M.L.; Ravdin P.M. (2005). Randomized phase III study of docetaxel compared with paclitaxel in metastatic breast cancer. J. Clin. Oncol. 23: 5542-5551.
5. van Zuylen L.; Verweij J.; Sparreboom A. (2001). Role of formulation vehicles in taxane pharmacology. Invest. New Drugs. 19: 125-141.
6. Engels F.K.; Mathot R.A.A.; Verweij J. (2007). Alternative drug formulations of docetaxel: a review. Anti-Cancer Drugs. 18: 95-103.
7. Heath J.R.; Davis M.E. (2008). Nanotechnology and Cancer. Annu. Rev. Med. 59: 251-265.
8. Peer D.; Karp J.M.; Hong S.; Farokhzad O.C.; Margalit R.; Langer R. (2007). Nanocarriers as an emerging platform for cancer therapy. Nat. Nanotechnol. 2: 751-760.
9. Brigger I.; Dubernet C.; Couvreur P. (2002). Nanoparticles in cancer therapy and diagnosis. Adv. Drug Deliv. Rev. 54: 631-651.
10. Green M.R.; Manikhas G.M.; Orlov S.; Afanasyev B.; Makhson A.M.; Bhar P.; Hawkins M.J. (2006). Abraxane®, a novel Cremophor®-free, albumin-bound particle form of paclitaxel for the treatment of advanced non-small-cell lung cancer. Ann. Oncol. 17: 1263-1268.
11. Khalid M.N.; Simard P.; Hoarau D.; Dragomir A.; Leroux J.C. (2007). Long Circulating Poly(Ethylene Glycol)-Decorated Lipid Nanocapsules Deliver Docetaxel to Solid Tumors. Pharm. Res. 23: 752-758.
12. Jakate A.S.; Einhaus C.M.; DeAnglis A.P.; Retzinger G.S.; Desai P.B. (2003). Preparation, characterization, and preliminary application of fibrinogen-coated olive oil droplets for the targeted delivery of docetaxel to solid malignancies. Cancer Res. 63: 7314-7320.

13. Bae K.H.; Lee Y.; Park T.G. (2007). Oil-Encapsulating PEO-PPO-PEO/PEG Shell Cross-Linked Nanocapsules for Target-Specific Delivery of Paclitaxel. Biomacromolecules. 8: 650-656.
14. Prego C.; Fabre M.; Torres D.; Alonso M.J. (2006). Efficacy and mechanism of action of chitosan nanocapsules for oral peptide delivery. Pharm. Res. 23: 549-556.
15. Prego C.; Torres D.; Alonso M.J. (2006). Chitosan nanocapsules: a new carrier for nasal peptide delivery. J. Drug Del. Sci. Tech. 16: 331-337.
16. De Campos A.M.; Sanchez A.; Gref R.; Calvo P.; Alonso M.J. (2003). The effect of a PEG versus a chitosan coating on the interaction of drug colloidal carriers with the ocular mucosa. Eur. J. Pharm. Sci. 20: 73-81.
17. Mao S.R.; Shuai X.T.; Unger F.; Simon M.; Bi D.Z.; Kissel T. (2004). The depolymerization of chitosan: effects on physicochemical and biological properties. Int. J. Pharm. 281: 45-54.
18. Prashanth K.V.H.; Tharanathan R.N. (2005). Depolymerized products of chitosan as potent inhibitors of tumor-induced angiogenesis. Biochim. Biophys. Acta. 1722: 22-29.
19. Janes K.A.; Alonso M.J. (2003). Depolymerized chitosan nanoparticles for protein delivery: Preparation and characterization. J. Appl. Polymer Sci. 88: 2769-2776.
20. Lee S.H.; Yoo S.D.; Lee K.H. (1999). Rapid and sensitive determination of paclitaxel in mouse plasma by high-performance liquid chromatography. J. Chromatogr. B Analyt. Technol. Biomed. Life Sci. 724: 357-363.
21. Vidal A.; Millard S.S.; Miller J.P.; Koff A. (2002). Rho activity can alter the translation of p27 mRNA and is important for Ras(V12)-induced transformation in a manner dependent on p27 status. J. Biol. Chem. 277: 16433-16440.
22. Prego C.; Torres D.; Alonso M.J. (2006). Chitosan nanocapsules as carriers for oral peptide delivery: Effect of chitosan molecular weight and type of salt on the *in vitro* behaviour and *in vivo* effectiveness. J. Nanosci. Nanotechnol. 6: 2921-2928.
23. Garcia-Fuentes M.; Prego C.; Torres D.; Alonso M.J. (2005). A comparative study of the potential of solid triglyceride nanostructures coated with chitosan or poly(ethylene glycol) as carriers for oral calcitonin delivery. Eur. J. Pharm. Sci. 25: 133-143.
24. Park J.H.; Kwon S.; Lee M.; Chung H.; Kim J.H.; Kim Y.S.; Park R.W.; Kim I.S.; Seo S.B.; Kwon I.C.; Jeong S.Y. (2002). Self-assembled nanoparticles based on glycol chitosan bearing hydrophobic moieties as

carriers for doxorubicin: In vivo biodistribution and anti-tumor activity. Biomaterials. 27: 119-126.

25. Campbell R.B.; Fukumura D.; Brown E.B.; Mazzola L.M.; Izumi Y.; Jain R.K.; Torchilin V.P.; Munn L.L. (2002). Cationic charge determines the distribution of liposomes between the vascular and extravascular compartments of tumors. Cancer Res. 62: 6831-6836.
26. Liang H.F.; Chen S.C.; Chen M.C.; Lee P.W.; Chen C.T.; Sung H.W. (2006). Paclitaxel-loaded poly(gamma-glutamic acid)-poly(lactide) nanoparticles as a targeted drug delivery system against cultured HepG2 cells. Bioconjug. Chem. 17: 291-299.

Article III

Freeze-dried polysaccharide nanocapsules: efficient vehicles for the intracellular delivery of docetaxel

Lozano, M.V.[1]; Esteban, H. [1]; Brea, J.[2]; Loza, M.I. [2];Torres, D. [1]; Alonso, M.J.[1*]

[1] Department of Pharmaceutical Technology.
[2] Department of Pharmacology.

Faculty of Pharmacy. University of Santiago de Compostela (USC)
15782 Santiago de Compostela, Spain.

* Corresponding author: Prof. Mª José Alonso.

ABSTRACT

Here we describe the development of a freeze-dried formulation of chitosan (CS) nanocapsules containing docetaxel (DCX) and the evaluation of its efficacy in the NCI-H460 cell line. More specifically, we developed two prototypes of nanocapsules differing in their coating, CS alone or in combination with Poloxamer 188. Both prototypes exhibited high encapsulation efficiencies of DCX and very similar release profiles. The nanocapsules could be freeze-dried in the presence of adequate amounts of sugar; however, those consisting of solely CS presented better reconstitution properties than those made of CS and Poloxamer. Namely, nanocapsules made of CS preserved their original size distribution and mean size of about 200 nm, whereas those of CS/Poloxamer suffered a size increase upon freeze-drying and reconstitution. In the last step, CS nanocapsules, were tested for their ability to deliver intracellularly the anticancer drug in NCI-H460 cancer cells. The results showed that CS nanocapsules were able to improve the antiproliferative effect of the drug and that this effect was not affected by the freeze-drying process. Moreover, we could observe that this improved effect of DCX was related to its intracellular delivery in the cancer cells.

INTRODUCTION

Nanomedicine is currently attracting a widespread interest with particular impact in the development of new therapeutic strategies in cancer therapy [1]. The benefit of these systems relies in their ability to facilitate the accumulation of the anticancer drug in the tumor environment, either by passive diffusion or active targeting to the cancer cells [2]. In addition, the inclusion of antitumor molecules in these nanocarriers prevents the use of organic solvents and solubilizers involved in many adverse reactions of the medication [3; 4]. Overall, these benefits are expected to result in an improvement in the survival and the quality of life of cancer patients by the use of safer and more effective anticancer drugs formulations [5].

Among the different nanocarriers under development for cancer therapy, nanocapsules are gaining a position of great interest. Nanocapsules are vesicular systems formed by an inner cavity, aqueous or oily, surrounded by a polymeric shell [6]. This specific structure makes them quite versatile: their lipid core allows the very efficient encapsulation of lipophilic drugs (most anticancer drugs are lipophilic), whereas their polymer shell may have the role of improving the stability of the oily droplets and facilitating their uptake by the cancer cells. Moreover, the presence of the polymer around the oily cores offers the possibility of chemical modifications, which may further improve the stability, the cellular uptake and the biodistribution of the nanocarrier. Although at the moment there is no nanocapsule-based anticancer drug formulation in the market, the accumulated information reported in the literature makes evidence of the interesting potential of these drug nanocarriers [79].

Besides the reported interesting properties of nanocarriers for anticancer drug delivery, one of their known limitations is their deficient stability during long-term storage. Indeed, these nanosystems are known to suffer destabilization phenomena such as gelling, creaming, fusion or aggregation during storage [10]. These phenomena could be avoided by converting the aqueous suspensions of nanocarriers into a freeze-dried powder. However, this freeze-drying process becomes especially difficult in the case of fluid nanostructures, i.e. nanocapsules, due to their destabilization in the freezing phase and its subsequent aggregation [11]. Therefore, efforts have been focused on the optimization of the process in order to obtain successful lyophilized nanocapsules formulations [12; 13]. For example, we have previously shown that the incorporation of an additional CS coating onto poly-ε-caprolactone (PECL) nanocapsules resulted in a significant improvement of the stability of PECL nanocapsules during freeze-drying [14].

With regard to the potential of CS nanostructures for anticancer drug delivery, we have previously reported the intracellular sustained delivery of doxorubicin from CS nanomatrices [15]. The same delivery vehicle based in CS has been evaluated in vivo for its capacity to increase the therapeutic efficacy of anticancer drugs such as doxorubicin and paclitaxel. The inclusion of the drugs in the nanocarriers produced effective systems with the same or even higher activity than the commercial drugs with less side-effects [16; 17]. More recently, we reported some interesting data on the efficacy of CS nanocapsules for the delivery of DCX in MCF-7 (human breast adenocarcinoma) and A549 (human lung carcinoma) cells [18]. The activity study of the released drug from the nanocapsules showed that DCX maintained its mechanism of action unaltered and was fully active. Furthermore, CS nanocapsules were found to promote the intracellular delivery of the drug, thereby enhancing its cytostatic effect.

Within this frame, the main goal of the work reported here has been to develop and characterize a new prototype of freeze-dried CS nanocapsules and to evaluate their potential for intracellular delivery of DCX. For this purpose, we first evaluated the influence of different parameters (nanocapsules coating composition, nanocapsules concentration, sugar concentration) on the properties of the freeze-dried nanocapsules. Secondly, we investigated the biological activity and internalization of the nanocarrier in the non-small cell lung cancer (NCI-H460) cell line.

MATERIALS AND METHODS

Chemicals

DCX (from Fluka), Poloxamer 188 (Pluronic® F68) and trehalose dihydrate were purchased from Sigma-Aldrich (Spain). Miglyol® 812, neutral oil formed by esters of caprylic and capric fatty acids and glycerol, was kindly provided by Sasol Germany GmbH (Germany). The surfactant Epikuron 145V, a phosphatidylcholine enriched fraction of soybean lecithin, was donated by Cargill (Spain). The product N-(fluorescein-5-thiocarbamoyl)-1.2-dihexa decanoyl-sn-glycero-3-phosphoethanol amine triethylammonium salt (fluorescein-DHPE) was obtained from Molecular Probes. Protasan® Cl 113, medium molecular weight CS chloride salt (medium Mw CS) with a deacetylation degree of 85%, was purchased from FMC Biopolymer Novamatrix (Norway). Sodium nitrite was purchased from Probus (Spain)

Preparation of CS oligomers

CS oligomers were prepared by oxidative depolymerization of medium MW CS using sodium nitrite ($NaNO_2$) following the procedure described by Janes *et al* [19]. Briefly, 0.1 mL of $NaNO_2$ (0,1 M) were added to 2 mL of a CS solution (1% w/v) at room temperature under magnetic stirring. After overnight reaction, the resultant CS oligomer solution was freeze-dried to obtain a dry powder. The molecular size of CS oligomers was verified by size exclusion chromatography (SEC).

Preparation of CS nanocapsules

Blank CS nanocapsules were prepared by the solvent displacement technique following the procedure described previously in our group [20]. Therefore, an organic phase was prepared containing 40 mg of Epikuron 145V dissolved in 0.5 mL ethanol, 125 µL of Miglyol® 812 and 9.5 mL of acetone. This organic phase was immediately poured over an aqueous phase that contained CS oligomers (0.05% w/v) and Pluronic® F68 (0.25% w/v) in order to obtain the CS/Poloxamer nanocapsules. Meanwhile, only CS oligomers (0.05% w/v) were added in the preparation of CS nanocapsules in absence of Poloxamer. The formation of both CS nanocapsules was instantaneous, as could be seen by the milky appearance of the mixture. Finally, solvents were eliminated from the suspension under reduced pressure to a constant volume of 10 mL.

The incorporation of DCX or the fluorescent probe fluorescein-DHPE in the nanocapsule formulations required a previous dissolution of the molecules in ethanol to a final concentration of 2 mg/mL. Afterwards, an aliquot of the stock solution was added to the organic phase and the same procedure was followed yielding a final DCX concentration of 12.4 µM.

Characterization, DCX encapsulation and release studies of CS nanocapsules

CS nanocapsules were characterized according to their particle size, zeta potential, morphology and DCX encapsulation efficiency as detailed elsewhere [18].

In vitro release studies of DCX from CS nanocapsules were performed by incubating a sample of the formulation with acetate buffer (pH=5) at an appropriate concentration to assure sink conditions. The vials were placed at 37º

C with horizontal shaking. At different time points (1, 3, 6, 24 and 48 h), 4 mL of the nanocapsule suspension were ultrafiltered (Amicon Ultra®, Millipore, Spain). The DCX released was calculated indirectly by determining by HPLC the amount of drug still associated to the system.

Freeze-dried studies of CS nanocapsules

Concentrations of CS nanocapsules (0.25, 0.5 and 1% w/v) and of trehalose (5 and 10% w/v) were considered the variables for the lyophilization study. Therefore, 1 mL dilutions of CS formulations were placed in 5 mL volume glass vials and were quickly frozen in liquid nitrogen. The lyophilization procedure consisted in an initial drying step for 60 h at -35º C, followed by a secondary drying for 24 h in a high vacuum atmosphere. Finally, temperature was slowly increased up to 20º C till the end of the process (Labconco Corp., USA).

CS nanocapsule formulations were recovered by adding 1mL of ultrapure water to the freeze-dried powders followed by manual resuspension and were characterized as explained above.

Cell viability assay and IC_{50} estimation

Human non-small cell lung cancer cell line NCI-H460 was cultured in RPMI-1640 medium (ATCC), supplemented with 10% (v/v) foetal bovine serum (FBS) at 37º C in a humidified atmosphere containing 5% carbon dioxide. Tetrazolium salt 3-(4,5-dimethylthiazol-2-yl)2,5diphenyltetrazolium bromide (MTT, Acros Organics) was used for mitochondrial activity evaluation. Briefly, cells were plated onto 96-well plates, with a seeding density of $15x10^3$ cells/well in 100 µL culture medium. After 24 h, dilutions of the different formulations in medium were added to the wells. Finally, after 48 h of incubation cell survival was measured by the MTT assay [21]. In brief, medium was removed and the cells were washed twice with 100 µL Hank's Balanced Salt Serum (HBSS). Then, 20 µL of a MTT solution (5 mg/mL in PBS) and 100 µL HBSS were added to the wells and maintained at 37º C in an atmosphere with 5% CO_2 for 4 h. Afterwards, buffers were replaced by 100 µL DMSO per well and maintained at 37ºC in an atmosphere with 5% CO_2 overnight. Absorbance (λ=490 nm) was measured in a BioRad 680 spectrophotometer removing background absorbance (λ=655 nm).

Moreover, short incubation times of 2 h were assayed in order to determine the ability of CS nanocapsules to quickly interact with the cells and deliver the

drug intracellularly. Thus, after 2 h of incubation time, medium was replaced by fresh one and cells were grown for 48 h. Finally, cell viability was measured as described.

The percentage of cell viability was calculated by the absorbance measurements of control growth and test growth in the presence of the formulations at various concentration levels. IC_{50} values were obtained by fitting the data with non-linear regression, with Prism 2.1 software (GraphPad, San Diego, CA).

Uptake studies

Cells were seeded in a multiwell-12 plate (Falcon) at $220x10^3$ cells/well for 24 h over sterile glass covers. Next, medium was removed and dilutions of the fluorescent dispersion and fluorescent CS/P nanocapsules were added to the wells. After 2 h of incubation, cells were washed three times with cold acidic phosphate saline buffer (PBS, Sigma). Next, they were fixed with paraformaldehyde 4% for 10 min, washed and counterstained with Bodipy® phalloidin during 30 min in darkness. Finally, after adding a drop of fluorescent mounting medium on the surface of the holders, covers were placed on them for confocal microscope analysis.

Statistical analysis

Cell culture results were evaluated in order to determine the statistical significance between the different formulations studied. The statistical evaluation of the cell viability results was performed by an ANOVA test followed by a multiple comparison analysis (Origin Program, Microcal, version 7.5). Differences were considered to be significant at level of 0.05. IC_{50} values were compared by means of a T test for independent samples using SPSS v 15.0 (SPSS Inc.).

RESULTS AND DISCUSSION

Our main goal in this work has been to develop a freeze-dried formulation of CS nanocapsules and to evaluate its efficacy for the effective intracellular delivery of the anticancer drug DCX. We first developed two prototypes of CS nanocapsules which differed in the presence of Poloxamer in their formulation.

We characterized both prototypes according to their size, zeta potential, DCX encapsulation efficiency and release profile. In addition, we defined the optimal freeze-drying conditions for the conversion of the aqueous suspension of the nanocapsules into a powder. Finally, we compared the efficacy of fresh and freeze-dried CS nanocapsules as intracellular drug delivery carriers for DCX using the NCI-H460 cell line.

Preparation and characterization of CS nanocapsules

A while ago we reported the potential of CS nanoparticles for the intracellular delivery of the anticancer drug doxorubicin [15]. The results of this previous work showed that CS nanoparticles were internalized in the A375 melanoma cells and provided a controlled intracellular delivery of the anticancer drug. In the present work we have chosen an alternative nanocarrier, CS nanocapsules, because of their versatility and important capacity for the encapsulation of lipophilic drugs. In addition, for the shell of the nanocapsules, we have selected low molecular weight (MW) CS (MW=10KDa) in order to accelerate its degradation and elimination. This low MW CS was obtained by oxidative degradation using sodium nitrite according to the technique previously described [19].

For the preparation of CS nanocapsules we have adopted the solvent displacement technique as previously reported [20]. This technique, allows the emulsification of an oily phase into an aqueous phase in the presence of surfactants, without the need of high energy sources. In addition, it allows the formation of a CS coating around the oily droplets due to the ionic interactions between the negatively charged lipophilic surfactant (lecithin) and the positively charged CS. Classically, this technique has used two different tensoactive agents: a lipohilic one, i.e. lecithin, and a hydrophilic one, i.e.

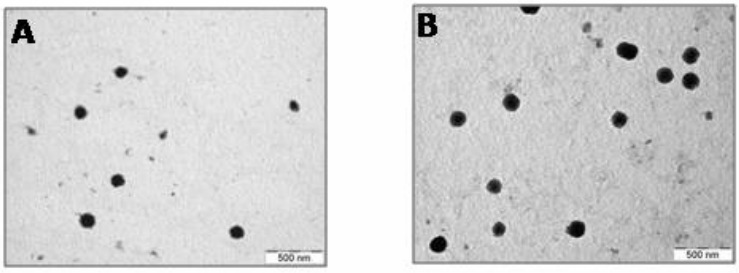

Figure 1. Transmission electron micrograph of CS nanocapsules: A) CS/P nanocapsules, B) CS/WP nanocapsules.

Table 1: Physicochemical properties of CS nanocapsules. PI: polydispersity index (Mean ± s.d.; n = 3)

	Size (nm)	**PI**	**ζ Potential (mV)**	**DCX encapsulation efficiency**
Blank CS/P nanocapsules	151 ± 1	0.1	+47 ± 1	-
Blank CS/WP nanocapsules	152 ± 1	0.1	+45 ± 1	-
DCX-loaded CS/P nanocapsules	162 ± 4	0.1	+47 ± 3	72 ± 4
DCX-loaded CS/WP nanocapsules	168 ± 5	0.1	+42 ± 2	78 ± 1
Fluorescent CS nanocapsules	185 ± 3	0.1	+38 ± 2	-

Poloxamer. Recently, we verified that the use of Poloxamer is not strictly required for the formation of nanocapsules, a fact that could be assigned to the stabilizing properties of the CS coating around the oily droplets [22]. In the present work we have confirmed that blank nanocapsules, prepared in the presence or absence of Poloxamer, show very similar characteristics: a size of less than 200 nm and a positive surface charge, which is attributed to the prevalence of the CS layer disposed over the oily core (lecithin and the oil Miglyol® 812) (Table 1). The transmission electron microscopy (TEM) images illustrated that both formulations have a low polidispersion index and exhibit a round shape (Figure 1). Moreover, both formulations could be ultracentrifuged and redispersed and were stable after storage up to six months (data not shown). Consequently, overall, the presence of Poloxamer in the formulation did not affect the morphology and physicochemical properties of the resulting nanocapsules.

DCX-loaded CS nanocapsules characterization, encapsulation efficiency and release studies

As previously stated, CS nanocapsules are excellent vehicles for the encapsulation of lipophilic compounds such as DCX [23]. As expected, both CS nanocapsules formulations, with or without Poloxamer, showed high encapsulation efficiencies of DCX due to the affinity of the drug for the components of the core. In addition, as shown in Table 1, the surface characteristics of DCX-loaded CS nanocapsules were not modified by the encapsulation of DCX.

The release study of DCX-loaded CS nanocapsules revealed that both formulations presented a similar biphasic profile (Figure 2). This profile is characterized by an initial fast release of the 40% of the encapsulated drug, followed by a second phase of very slow release. The initial fast release phase, typically observed for polymer nanocapsules and nanoemulsions [24], indicates that the release process is governed by the oil-water partition and that the polymer coating does not affect the release rate [25]. The second phase of very slow release could be related to the affinity of the drug for the phospholipid/polymer coating of the nanocapsules.

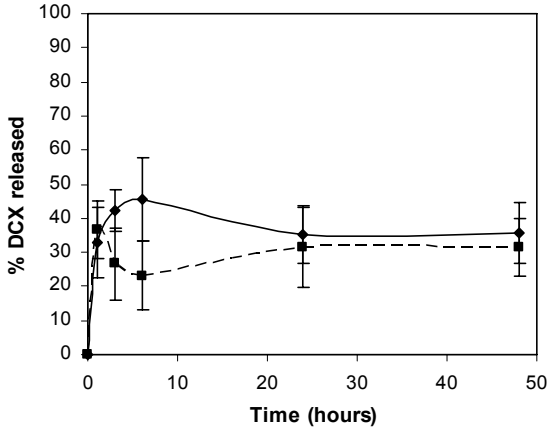

Figure 2. In vitro DCX release from DCX-loaded CS nanocapsules: DCX-loaded CS/P nanocapsules (solid line), DCX-loaded CS/WP nanocapsules (dash line). Mean ± s.d. (n=3).

Freeze-drying of CS nanocapsules

Freeze-drying is one of the most efficient methods to preserve the long-term integrity of the nanoparticulate systems. Nevertheless, this process becomes quite complex in the case of nanocapsules due to the fluidity of the polymer shell and also to the presence of the oil core, which is susceptible of leakage [26].

In order to facilitate the lyophilization of nanocarriers and avoid their collapse, the use of cryoprotectants agents is necessary. Previous studies by our group have shown that trehalose is an adequate cryoprotectant for the lyophilization of CS nanocapsules [27]. Trehalose has also been used as a cryoprotectant agent for the lyophilization of other nanocarriers such as liposomes [28], nanoparticles [29; 30], complexes [31] or nanocapsules [32]. Thus, in the present work, we studied the

lyophilization process of the two formulations of blanck CS nanocapsules, with or without Poloxamer, prior to the lyophilization of DCX-loaded nanocapsules.

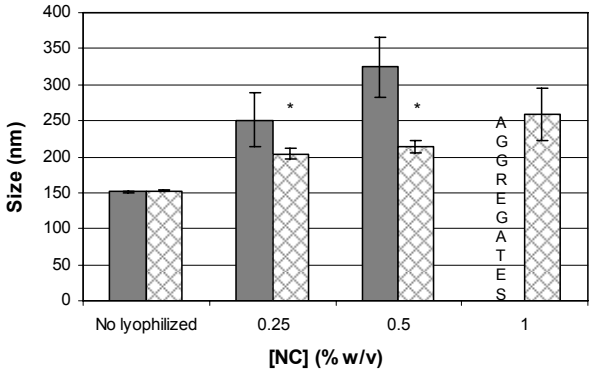

Figure 3. Mean particle size after the reconstitution of lyophilized CS/P nanocapsules (grey bars) and lyophilized CS/WP nanocapsules (diamond bars) with 10% trehalose. (Mean ± s.d.; n = 3).

The results showed that the recovery of the initial properties of CS nanocapsules upon freeze-drying and reconstitution varied with the concentrations of nanocapsules and cryoprotectant. The best results were obtained for low nanocapsules concentrations (0.25% w/v) and high trehalose concentrations (10% w/v). Figure 3 summarizes the changes in particle size of CS nanocapsules and CS/Poloxamer nanocapsules after freeze-drying in the presence of 10% w/v of trehalose. CS nanocapsules experienced a slight increase in their size and an adequate size distribution following freeze-drying and reconstitution. However, those containing Poloxamer suffered a significant increase in the size values, a result that suggested that Poloxamer interferes in the lyophilization process. This result disagrees with previous reports which have shown that Poloxamer can be used as a lyoprotective agent in combination with saccharides [33; 34]. In order to find an explanation for our observation, we studied the interaction between Poloxamer and cryoprotectants by differential scanning calorimetry (DSC) and X-ray diffraction. The results suggested an increase in the crystallinity of the cryoprotectant trehalose when Poloxamer formed part of the glassy matrix (results not shown). This increased crystallinity could be responsible of the reduction of the stabilizing effect of trehalose.

Based on these preliminary results, we proceeded with the freeze-drying of the formulation of DCX-loaded CS nanocapsules in the absence of Poloxamer.

The results showed that the drug-loaded nanocapsules could be freeze-dried in the same range of trehalose and nanocapsules concentrations tested for the unloaded nanocapsules and that the resulting freeze-dried product could be adequately reconstituted without changing the properties of the formulation. This freeze-dried formulation was subsequently tested in the cell line NCI-H460.

Cytotoxicity studies

We have recently reported the ability of CS nanocapsules to enter the MCF7 (human breast adenocarcinoma) and A549 (human lung carcinoma) cells [18]. In this work our objective was to confirm this internalization capacity and to evaluate the efficacy of freeze-dried DCX-loaded CS nanocapsules in a different cell line, i.e. the NCI-H460 non-small lung cancer cell line.

The results of the cell viability assays (Figures 4 and 5) of the DCX-loaded CS/Poloxamer nanocapsules show that the antiproliferative effect of the drug was significantly enhanced as a consequence of their incorporation into the nanocapsules. This effect was apparent either at 2 h (Figure 4) or 48 h post-incubation (Figure 5). Accordingly, the IC_{50} values were significantly higher for the free drug than for the drug incorporated into the nanocapsules (Figure 6). In addition, we observed that blank CS nanocapsules were completely innocuous (Table 2).

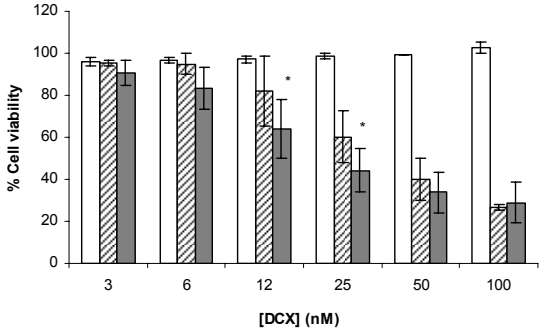

Figure 4. Effect on NCI-H460 cell viability of blank CS/P nanocapsules (white bars), free DCX (striped bars) and DCX-loaded CS/P nanocapsules (grey bars) after 2 h of incubation (n=3).
* Shows significant differences between free DCX and DCX-loaded CS/P nanocapsules ($p<0,05$).

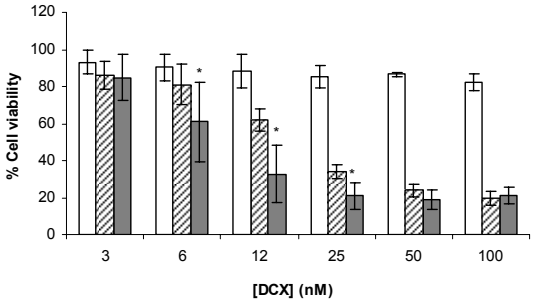

Figure 5. Effect on NCI-H460 cell viability of blank CS/P nanocapsules (white bars), free DCX (striped bars) and DCX-loaded CS/P nanocapsules (grey bars) after 48 h of incubation (n=3).

* Shows significant differences between free DCX and DCX-loaded CS/P nanocapsules ($p<0,05$).

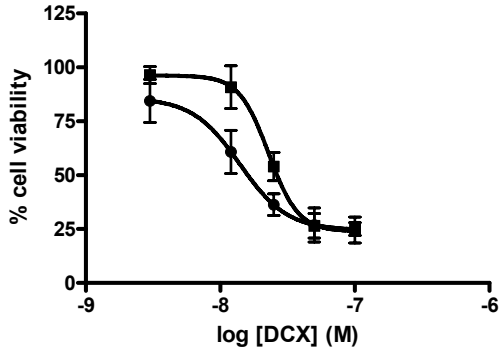

Figure 6. Concentration-response curves of free DCX (■) and lyophilized DCX-loaded CS/WP nanocapsules (●) measuring cell viability of NCI-H460 cells after 48 h of incubation. Points represent the mean ± S.D. (vertical bars) of three independent experiments.

Table 2: IC_{50} (nM) values of NCI-H460 cells after incubation with DCX and DCX-loaded CS/P nanocapsules.

	48 h	**2 h**
DCX	14.7 ± 0.3	24.6 ± 10.1
DCX-loaded CS/P nanocapsules	6.9 ± 2.1	13.6 ± 3.2

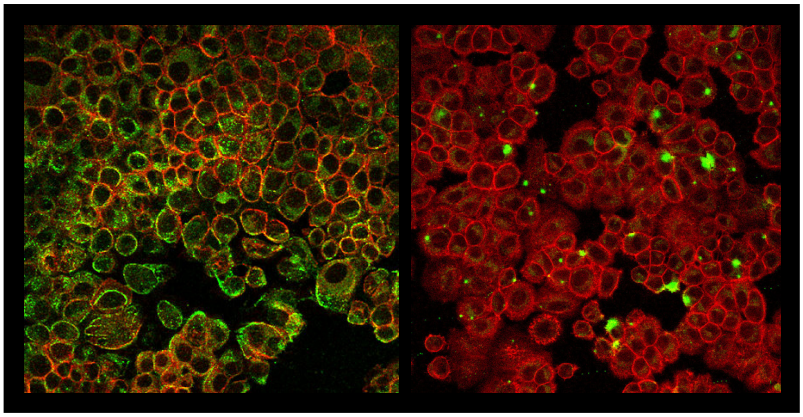

Figure 7. NCI-H460 cualitative uptake assay of fluorescent chitosan nanocapsules (left) and control fluorescent dispersion (right) after 2h of incubation. Images are a projection of x-y sections, at a magnification of 63x. The nanocapsules encapsulated fluorescein-DHPE (green channel), and the actin filaments were counterstained with Bodipy® phalloidin (red channel).

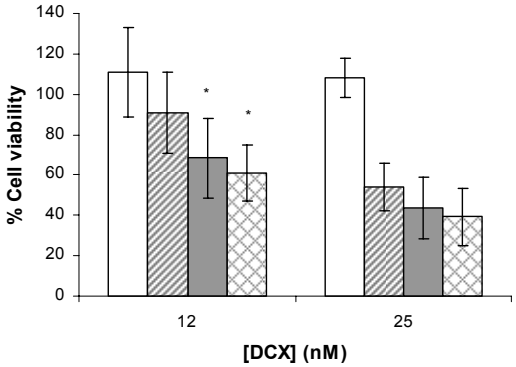

Figure 8. Effect on NCI-H460 cell viability of lyophilized blank CS/WP nanocapsules (white bars), free DCX (striped bars), DCX-loaded CS/WP nanocapsules (grey bars) and lyophilized DCX-loaded CS/WP nanocapsules (diamond bars) after 48 h of incubation (n=3).

* Shows significant differences between DCX-loaded CS/WP nanocapsules and lyophilized DCX-loaded CS/WP nanocapsules compared to free DCX ($p<0,05$).

Afterwards, in order to understand the mechanism of action of the nanocapsules, we incubated them with the NCI-H460 cells and studied their internalization by confocal microscopy. With this purpose, fluorescent nanocapsules were formulated and characterized (Table 1). Strong fluorescent

signals could be detected inside the majority of the cells, upon treatment with fluorescent nanocapsules for up to 2 h (Figure 7). These results, which confirm those previously observed for CS nanoparticles and the A375 melanoma cell line [15], evidence the favorable uptake of chitosan-based nanocarriers by cancer cells.

As a final step of this work, we have evaluated the performance of the freeze-dried DCX-loaded CS nanocapsules for inhibiting cell viability on NCI-H460 cell line. As shown in Figure 8, freeze-dried and reconstituted CS nanocapsules were able to enter the cells and deliver the encapsulated drug intracellularly. Consequently, these results clearly indicated that the lyophilization process did not alter the efficacy of the nanocapsules as intracellular delivery vehicles for DCX.

CONCLUSIONS

We have developed an optimized formulation of CS nanocapsules containing DCX, which could be obtained and freeze-dried without the use of the surfactant Poloxamer 188 (classically used for this type of formulations). This new prototype exhibited a capacity to enter the tumor cells and deliver the associated drug intracellularly, thus resulting in a significant enhancement of the drug efficacy.

ACKNOWLEDGEMENTS

This work was supported by the Spanish Ministry of Science and Technology (SAF 2004-08319-CO2-01) and Consolider Nanobiomed (CSD 2006-00012). The first author acknowledges the fellowship received from the Spanish Government (AP2005-1701). J. Brea is recipient of an Isabel Barreto contract from Xunta de Galicia (Spain). Authors also express their gratitude to Ramón Novoa Carballal for CS SEC measurements.

REFERENCES

1. Couvreur P.; Vauthier C. (2006). Nanotechnology: intelligent design to treat complex disease. Pharm. Res. 23: 1417-1450.
2. Hervella P.; Lozano V.; Garcia-Fuentes M.; Alonso M.J. (2008). Nanomedicine: New Challenges and Opportunities in Cancer Therapy. J. Biomed. Nanotechnol. 4: 276-292.
3. Gelderblom H.; Verweij J.; Nooter K.; Sparreboom A. (2001). Cremophor EL: The drawbacks and advantages of vehicle selection for drug formulation. Eur. J. Cancer. 37: 1590-1598.
4. Hennenfent K.L.; Govindan R. (2006). Novel formulations of taxanes: a review. Old wine in a new bottle? Ann. Oncol. 17: 735-749.
5. Brannon-Peppas L.; Blanchette J.O. (2004). Nanoparticle and targeted systems for cancer therapy. Adv. Drug Deliv. Rev. 56: 1649-1659.
6. Couvreur P.; Barratt G.; Fattal E.; Legrand P.; Vauthier C. (2002). Nanocapsule technology: a review. Crit. Rev. Ther. Drug Carrier Syst. 19: 99-134.
7. Bae K.H.; Lee Y.; Park T.G. (2007). Oil-encapsulating PEO-PPO-PEO/PEG shell cross-linked nanocapsules for target-specific delivery of paclitaxel. Biomacromolecules. 8: 650-656.
8. Burger K.N.; Staffhorst R.W.; de Vijlder H.C.; Velinova M.J.; Bomans P.H.; Frederik P.M.; de Kruijff B. (2002). Nanocapsules: lipid-coated aggregates of cisplatin with high cytotoxicity. Nat. Med. 8: 81-84.
9. Jakate A.S.; Einhaus C.M.; DeAnglis A.P.; Retzinger G.S.; Desai P.B. (2003). Preparation, characterization, and preliminary application of fibrinogen-coated olive oil droplets for the targeted delivery of docetaxel to solid malignancies. Cancer Res. 63: 7314-7320.
10. Heurtault B.; Saulnier P.; Pech B.; Proust J.E.; Benoit J.P. (2003). Physico-chemical stability of colloidal lipid particles. Biomaterials. 24: 4283-4300.
11. Abdelwahed W.; Degobert G.; Fessi H. (2006). Freeze-drying of nanocapsules: impact of annealing on the drying process. Int. J. Pharm. 324: 74-82.
12. Abdelwahed W.; Degobert G.; Fessi H. (2006). Investigation of nanocapsules stabilization by amorphous excipients during freeze-drying and storage. Eur. J. Pharm. Biopharm. 63: 87-94.
13. Dulieu C.; Bazile D. (2005). Influence of lipid nanocapsules composition on their aptness to freeze-drying. Pharm. Res. 22: 285-292.

14. Calvo P.; Remuñan-Lopez C.; Vila-Jato J.L.; Alonso M.J. (1997). Development of positively charged colloidal drug carriers: Chitosan-coated polyester nanocapsules and submicron-emulsions. Colloid Polym. Sci. 275: 46-53.
15. Janes K.A.; Fresneau M.P.; Marazuela A.; Fabra A.; Alonso M.J. (2001). Chitosan nanoparticles as delivery systems for doxorubicin. J. Control. Release. 73: 255-267.
16. Mitra S.; Gaur U.; Ghosh P.C.; Maitra A.N. (2001). Tumour targeted delivery of encapsulated dextran-doxorubicin conjugate using chitosan nanoparticles as carrier. J. Control. Release. 74: 317-323.
17. Kim J.H.; Kim Y.S.; Kim S.; Park J.H.; Kim K.; Choi K.; Chung H.; Jeong S.Y.; Park R.W.; Kim I.S.; Kwon I.C. (2006). Hydrophobically modified glycol chitosan nanoparticles as carriers for paclitaxel. J. Control. Release. 111: 228-234.
18. Lozano M.V.; Torrecilla D.; Torres D.; Vidal A.; Dominguez F.; Alonso M.J. (2008). Highly efficient system to deliver taxanes into tumor cells: docetaxel-loaded chitosan oligomer colloidal carriers. Biomacromolecu les. 9: 2186-2193.
19. Janes K.A.; Alonso M.J. (2003). Depolymerized Chitosan Nanoparticles for Protein Delivery: Preparation and Characterization. J. Appl. Polym. Sci. 88: 2769-2776.
20. Prego C.; Torres D.; Alonso M.J. (2006). Chitosan nanocapsules: a new carrier for nasal peptide delivery. J. Drug Del. Sci. Tech. 16: 331-337.
21. Mosmann T. (1983). Rapid colorimetric assay for cellular growth and survival: application to proliferation and cytotoxicity assays. J. Immunol. Methods. 65: 55-63.
22. Santander-Ortega M.J.; Lozano M.V.; Bastos-Gonzalez D.; Peula-Garcia J.M.; Ortega-Vinuesa J.L. Characterization of Core-Shell Lipid-Chitosan and Lipid-Poloxamer Nanocapsules. Submitted to Colloid Polym. Sci.
23. Khalid M.N.; Simard P.; Hoarau D.; Dragomir A.; Leroux J.C. (2007). Long Circulating Poly(Ethylene-Glycol)-Decorated Lipid Nanocapsules Deliver Docetaxel to Solid Tumors. Pharm. Res. 23: 752-758.
24. Prego C.; Torres D.; Alonso M.J. (2006). Chitosan nanocapsules as carriers for oral peptide delivery: Effect of chitosan molecular weight and type of salt on the in vitro behaviour and in vivo effectiveness. J. Nanosci. Nanotechnol. 6: 2921-2928.
25. Calvo P.; Vila-Jato J.L.; Alonso M.J. (1997). Evaluation of cationic polymer-coated nanocapsules as ocular drug carriers. Int. J. Pharm. 153: 41-50.

26. Choi M.J.; Briançon S.; Andrieu J.; Min S.G.; Fessi H. (2004). Effect of freeze-drying process conditions on the stability of nanoparticles. Dry. Technol. 22: 335-346.
27. Prego C.; Brasa B.; Fernandez-Megia E.; Novoa-Carballal R.; Torres D. (2006). Proc. 33rd CRS, Vienna (Austria).
28. Van Winden E.C.A. (2004). Freeze-drying of liposomes: A critical review of mechanisms involved in lyoprotection and solid-state stability. Costantino H.R. AAPS Press**:** 563-604.
29. Sameti M.; Bohr G.; Ravi Kumar M.N.; Kneuer C.; Bakowsky U.; Nacken M.; Schmidt H.; Lehr C.M. (2003). Stabilisation by freeze-drying of cationically modified silica nanoparticles for gene delivery. Int. J. Pharm. 266: 51-60.
30. Zimmermann E.; Muller R.H.; Mader K. (2000). Influence of different parameters on reconstitution of lyophilized SLN. Int. J. Pharm. 196: 211-213.
31. Molina M.C.; Armstrong T.K.; Zhang Y.; Patel M.M.; Lentz Y.K.; Anchordoquy T.J. (2004). The stability of lyophilized lipid/DNA complexes during prolonged storage. J. Pharm. Sci. 93: 2259-2273.
32. Abdelwahed W.; Degobert G.; Fessi H. (2006). A pilot study of freeze drying of poly(epsilon-caprolactone) nanocapsules stabilized by poly(vinyl alcohol): formulation and process optimization. Int. J. Pharm. 309: 178-188.
33. Saez A.; Guzman M.; Molpeceres J.; Aberturas M.R. (2000). Freeze-drying of polycaprolactone and poly(D,L-lactic-glycolic) nanoparticles induce minor particle size changes affecting the oral pharmacokinetics of loaded drugs. Eur. J. Pharm. Biopharm. 50: 379-387.
34. Wolf M.; Wirth M.; Pittner F.; Gabor F. (2003). Stabilisation and determination of the biological activity of L-asparaginase in poly(D,L-lactide-co-glycolide) nanospheres. Int. J. Pharm. 256: 141-152.

Article IV

Polyarginine nanocapsules: a new platform for intracellular drug delivery

M. V. Lozano[1], G. Lollo[1], J. Brea[2], D. Torres[1], M. I. Loza[2], M. J. Alonso[1*].

[1] Department of Pharmaceutical Technology.
[2] Department of Pharmacology.

Faculty of Pharmacy. University of Santiago de Compostela (USC) 15782
Santiago de Compostela, Spain

* Corresponding author: Prof. María José Alonso

ABSTRACT

Here we report for the first time a new nanocarrier, consisting of an oily core (Miglyol® 812 and lecithin) and a shell made of polyarginine (PArg), named PArg nanocapsules. This nanocarrier was specifically designed for the intracellular delivery of drugs. PArg nanocapsules were produced by the solvent displacement technique and were characterized for their size, zeta potential and also for their loading ability of different types of drugs. Additionally, we explored the ability of these nanocarriers to enter cancer cells and to inhibit proliferation in the NCI-H460 cell culture model. The results showed the feasibility of the solvent displacement technique for producing nanocapsules of a size in the range of 120-160 nm and a positive surface charge of around +50 mV. These nanocapsules could accommodate in their structure significant amounts of lipophilic drugs i.e. docetaxel and also highly polar molecules such as plasmid DNA with high association efficiency. In addition, the in vitro cell culture studies evidenced that PArg nanocapsules are rapidly and massively accumulated inside NCI-H460 lung cancer cells and that the PArg shell played a critical role in the internalization process. Moreover, upon incubation of the cells with docetaxel-loaded nanocapsules we observed an enhanced inhibition of cancer cells proliferation, as compared to the free drug. Consequently, PArg nanocapsules could be considered as a new versatile platform of nanocarrier for intracellular delivery of lipophilic and hydrophilic negatively charged molecules.

INTRODUCTION

One of the main focus of nanomedicine is the targeting and delivery of already known and oncoming therapeutics [1]. In fact, it is known that the incorporation of therapeutics in nanocarriers increases the efficacy of the treatments, reduces drug-associated side-effects and improves the quality of life of patients [2]. Overall, cancer, genetic or metabolic disorders are some of the diseases that benefit most of this extensive research.

Over the last years a focus of our research has been the design of nanocarriers for intracellular delivery of anticancer drugs and also gene molecules [3; 4]. For example, we already reported the potential of polysaccharide-based nanostructures for the intracellular delivery of antitumoral drugs [5; 6]. Recently, we also reported the in vivo proof-of-principle of polysaccharide nanostructures for ocular gene therapy [7].

Our goal in the present work was to develop a new intracellular drug delivery platform based upon the use of polyaminoacids for the formation of nanostructures. Currently, polyaminoacids have raised great expectancy in the development of drug delivery systems for anticancer drugs, peptides, vaccines and gene delivery [8]. Polyaminoacids safety is one of the most attractive characteristics of these molecules, as they maintain a structural resemblance to polypeptides, making possible the degradation by human enzymes, thus avoiding the polymer accumulation in the body [9; 10]. Moreover, their unique structure converts them in attractive polymers for the chemical attachment of PEG or other molecules [9; 11].

One of these polyaminoacids lately applied to drug delivery is polyarginine (PArg), a polymer enclosed in the family of the protein transduction domains (PTD). This cationic homopolymer is able to efficiently translocate through the mammalians cell membranes and facilitate the uptake of the molecules attached [12]. The cell penetrating properties of PArg are attributed to the presence of the guanidine moiety in its side chain. The guanidine group is thought to form bidentate hydrogen bonds with the anionic groups of the surface of the cells and, subsequently, this interaction facilitate its internalization into the cells [13]. This interesting feature has been the rational of its use in gene therapy [14] and protein/vaccine delivery [15; 16]. More specifically, Kim *et al*. have recently reported the synthesis of a cholesteryl oligo-D-arginine conjugate as a siRNA delivery vehicle for the silencing of the vascular endothelial growth factor (VEGF), an angiogenic growth factor involved in the vascularization of solid tumors. The

complexation of siRNA with the hydrophobically modified oligoarginine efficiently delivered siRNA into cells *in vitro*. Moreover, the local administration of the siRNA-complexes to a mouse xenograft model led to the regression of the tumoral mass [17]. Oligoarginines have also been successfully applied for the enhancement in the transfection efficiency of DNA/protamine complexes. Thus, the oligoarginine coating significantly increased the transfection in mice bearing HeLa tumor xenografts compared to the complexes of DNA/protamine [18]. Additionally, several articles reported the benefits of PArg for peptide and protein delivery. In fact, Yang *et al*. used the cell permeable properties of PArg for the obtaining of a pro-apoptotic Smac-peptide/oligoarginine conjugate that selectively reversed the apoptosis resistance of H460 cells, increasing cell death induced by chemotherapy [19]. Likewise, the cardioprotective peptide ψεRACK conjugated to oligoarginine increased its permeability and intracellular delivery, thus protecting the myocardium from ischemic episodes [20]. PArg is also a promising polymer that has been used as an adjuvant in vaccines. The results obtained in the clinical trials of a hepatitis C vaccine showed that PArg helped to induce immunoresponse in T cells, with no antigenic activity [21; 22].

Since PArg is a homopolymer constituted by an essential amino acid, it mimics the properties of endogenous proteins, and subsequently PArg have shown low toxicity and biodegradability. Thus, Rawat *et al*. have reported a PArg-based formulation for low molecular weight heparin that was well tolerated by the respiratory epithelium [23]. Intramucosal routes, such as nasal or ocular have also been explored. The results showed that PArg can efficiently promote the transport of the associated drugs through the mucosa without producing a destructive or inflammation effect on it [24-26].

Based on these excellent properties, we propose the design of an original formulation of nanocapsules which consist of a lipid core surrounded by a coating of PArg, in order to be applied for targeted cancer delivery or gene therapy. The selection of the coating was justified by the cell penetration properties of the polypeptide and to its capacity to associate genes. Besides, the oil core is an exceptional reservoir structure for the inclusion of highly hydrophobic molecules, although highly hydrophilic drugs can be also associated to their surface of the system. Thus, the main objective of his work was to develop and evaluate the potential of PArg nanocapsules as a new drug delivery system for gene material and low soluble molecules for cancer therapy.

MATERIALS AND METHODS

Chemicals

PArg (MW 5000-15000), docetaxel, Trizma® base, agarose, xylene cyanole, bromophenol blue, ethidium bromide (purity 95%) were purchased from Sigma-Aldrich (Spain). Miglyol 812®, neutral oil formed by esters of caprylic and capric fatty acids and glycerol, was a kind gift from Sasol Germany GmbH (Germany), and the surfactant Epikuron 145V, a phosphatidylcholine enriched fraction of soybean lecithin was donated by Cargill (Spain). The product N-(fluorescein-5-thiocarbamoyl)-1.2-dihexadecanoyl-sn-glycero-3-phosphoethanolamine triethylammonium salt (fluorescein-DHPE) was obtained from Molecular Probes. Plasmid DNA (pDNA) encoding green fluorescent protein (pEGFP-C1) driven by a CMV promoter was purchased from Elim. Biopharmaceutical (USA).

Preparation of PArg nanocapsules

Blank PArg nanocapsules were obtained by a modification of the solvent displacement technique based on a polymer ionic interaction after solvents diffusion [27]. Briefly, an organic phase was formed by dissolving 20 mg of Epikuron 145V in 0.25 mL ethanol, followed by 62 µL of Miglyol® 812 and 4.7 mL acetone. This organic phase was immediately poured over a solution of PArg (0.05% w/v) causing the immediate formation of PArg nanocapsules. Finally, solvents were eliminated from the suspension to constant volume and under reduced pressure yielding a nanocapsule concentration of 16.6 mg/mL.

PEG surface modified PArg nanocapsules were obtained following the same method explained above, but in this case, 40 mg of PEG stearate were additionally included in the organic phase to obtain the PEG incorporation onto the surface of the nanocapsules.

In order to achieve the incorporation of the hydrophobic molecules docetaxel or the fluorescent probe fluorescein-DHPE on PArg nanocapsules, aliquots of the stock solutions were added to the organic phase and the same procedure was followed.

Fluorescent nanoemulsion and fluorescent dispersion controls used for the cell uptake studies were obtained by the method previously described. Unlike nanocapules, nanoemulsion is only formed by the hydrophobic cores without the

polymer cover. With respect to the fluorescent dispersion, an aliquot of the dye was diluted in the ethanol/acetone mixture following the same process.

Physicochemical characterization of PArg nanocapsules

The different PArg nanocapsules formulations were characterized with regard to size, zeta potential and morphology as follows.

Particle size and polydispersion index were determined by photon correlation spectroscopy (PCS). Samples were diluted to the appropriate concentration with filtered water. Each analysis was carried out at 25ºC with an angle detection of 90º. The zeta potential values were calculated from the mean electrophoretic mobility values, which were determined by laser Doppler anemometry (LDA). Samples were diluted with KCl 1 mM and placed in the electrophoretic cell where a potential of ±150 mV was established. PCS and LDA analysis were performed in triplicate using a NanoZS® (Malvern Instruments, Malvern, UK).

Nanocapsules were isolated in order to assess the adhesion strength of the PArg layer to the droplet surface. Therefore, a 5 mL aliquot was ultracentrifuged at 20000 rpm for 1 h and the remaining nanocapsule-rich fraction was collected and diluted with ultrapure water. Isolated PArg nanocapsules were also characterized according to particle size and zeta potential.

The morphological examination of the nanocapsules was performed by transmission electron microscopy (TEM, CM12 Philips, The Netherlands). Samples were stained with 2% w/v phosphotungstic acid solution, and placed on copper grids with Formvar® films for analysis.

Long-term stability studies of PArg nanocapsules

The suspension stability of PArg nanocapsules was evaluated according to time and temperature of storage. Therefore, aliquots of the nanocapsules suspension without dilution were placed in sealed tubes at 4º C and 37º C for storage. Size and polydispersity index of the nanocapsules were measured for a nine months period, meanwhile zeta potential values were controlled at the end of the study. Each sample corresponds to a different PArg nanocapsules batch.

For the lyophilization studies, dilutions of 1 mL suspension with concentrations of 0.25, 0.5 and 1% w/v PArg nanocapsules and 5 or 10% w/v

trehalose were placed in 5 mL volume glass vials. Then, samples were quickly frozen in liquid nitrogen. The lyophilization procedure consisted in an initial drying step for 60 h at -35º C, followed by a secondary drying for 24 h in a high vacuum atmosphere. Finally, temperature was slowly increased up to 20º C till the end of the process (Labconco Corp., USA).

PArg nanocapsules were recovered by adding 1 mL of ultrapure water to the freeze-dried powders followed by manual resuspension. Finally, their size distribution was measured as indicated above.

pDNA association to PArg nanocapsules

Plasmid DNA (pDNA) encoding green fluorescent protein was adsorbed on the surface of PArg nanocapsules at different theoretical loadings (3%, 10% and 30%), defined as the percentage between the mass of pDNA and the total mass of the formulation. For the adsorption procedure, a pDNA solution (50 µL) was added to an isolated PArg nanocapsules suspension (200 µL) and subsequently vortexed for 30 seconds. Formulations were left at room temperature for 1 h before being analyzed. pDNA concentration was varied in order to achieve the desired weight ratios, meanwhile the concentration of PArg nanocapsules was maintained constant at 1.4 mg/mL.

The association of pDNA to the nanocapsules was studied by a conventional agarose gel electrophoresis assay. In order to displace the pDNA adsorbed to the nanocapsules, a far excess of heparin (15 mg/mL) was added to the suspension and was incubated for 2 h. Then, the samples and the control of free pDNA were placed in 1% agarose gel containing ethidium bromide, and ran for 90 min at 60 V in TAE buffer (Sub-Cell GT 96/192, Bio-Rad Laboratories Ltd., England).

Finally, pDNA-associated nanocapsules were characterized according to size and zeta potential as detailed previously.

Afterwards, pDNA-associated nanocapsules were compared to pDNA/PArg complexes previously described in the literature [28] for their potential as delivery vehicles of pDNA. For that purpose, complexes were prepared in the range pDNA/PArg weight ratio 5:1-1:5. The preparation method consisted on adding equal volumes of pDNA and PArg aqueous solutions (final volume of 100 µL) and shaking the mixture for 30 min at room temperature. Then, complexes were characterized with respect to size and zeta potential. Additionally, the different formulations of nanocapsules and complexes were studied according to their

stability in phosphate buffer by diluting the samples with the buffer to a final ionic strength of 75 mM and measuring their size values after an incubation of 30 min.

Moreover, pDNA-associated nanocapsules were evaluated for the premature release of the plasmid after their incubation in phosphate buffer. Free pDNA was determined by an agarose gel electrophoresis as explained before.

Encapsulation of Docetaxel into the nanocapsules

The incorporation of docetaxel in PArg nanocapsules was achieved by adding aliquots of an ethanolic stock solution to the organic phase in order to obtain a final drug concentration of 10 µg/mL, and the process was continued as described previously. Docetaxel encapsulation efficiency in PArg nanocapsules was determined indirectly by the difference between the total amount of docetaxel in the formulation and the free drug measured in the infranatant of the nanocapsules. Therefore, the total amount of drug was estimated by dissolving an aliquot of non-isolated docetaxel-loaded PArg nanocapsules with acetonitrile. This sample was centrifuged during 20 min at 4000 xg and the supernatant was measured with a high-performance liquid chromatography (HPLC) system. The non-encapsulated drug was determined by the same method following separation of the PArg nanocapsules from the aqueous medium by ultracentrifugation.

Docetaxel was assayed by a slightly modified version of the method proposed by Lee *et al*. [29]. The HPLC system consisted of an Agilent 1100 Series instrument equipped with a UV detector set at 227 nm and a reverse phase Zorbax Eclipse® XDB- C8 column (4.6 x 150 mm i.d., pore size 5 µm Agilent U.S.A.). The mobile phase consisted of a mixture of acetonitrile and 0.1% v/v ortophosphoric acid (55:45 v/v) and the flow rate was 1 mL/min. The standard calibration curves of docetaxel were linear (r^2> 0.999) in the range of concentrations between 0.3-2 µg/mL.

The encapsulation efficiency (E.E.) was calculated as follows:

E.E. % = [(A-B)/A] x 100

where A is the experimental total drug concentration (mg/mL), and B is the drug concentration measured in the external aqueous medium, corresponding to unloaded drug (mg/mL).

The release studies of docetaxel from PArg nanocapsules were performed by incubating a sample of the formulation with acetate buffer (pH=5) at an appropriate concentration to assure sink conditions. The vials were placed in an incubator at 37º C with horizontal shaking. 4 mL of the suspension were collected and centrifuged by using Amicon Ultra® devices (Millipore, Spain) at different time intervals (1, 3, 6, 24 and 48 h). The docetaxel released was calculated indirectly by determining the amount of drug remaining in the system by processing the isolated PArg nanocapsules with acetonitrile before HPLC analysis.

Growth inhibition of tumor cells

Human non-small cell lung cancer cell line NCI-H460 was cultured in RPMI-1640 medium (ATCC), supplemented with 10% (v/v) foetal bovine serum (FBS) at 37º C in a humidified atmosphere containing 5% carbon dioxide. Tetrazolium salt 3-(4,5-dimethylthiazol-2-yl)-2,5diphenyltetrazoliumbromide (MTT, Acros Organics) was used for mitochondrial activity evaluation. Briefly, cells were plated onto 96-well plates, with a seeding density of $15x10^3$ cells/well in 100 µL culture medium. After 24 h, medium was removed and dilutions of docetaxel solution, docetaxel-loaded PArg nanocapsules and blank PArg nanocapsules in medium were added to the wells. Finally, after 48 h of incubation cell survival was measured by the MTT assay [30]. Briefly, medium was removed and the wells were washed twice with 100 µL Hank's Balanced Salt Serum (HBSS). Then, 20 µL of a MTT (5 mg/mL in PBS) and 100 µL HBSS were added to the wells and maintained at 37º C in an atmosphere with 5% CO_2 for 4 h. Afterwards, buffers were removed and 100 µL DMSO were added to each well and maintained at 37ºC in an atmosphere with 5% CO_2 overnight. Absorbance (λ=490 nm) was measured in a BioRad 680 spectrophotometer removing background absorbance (λ=655 nm).

The percentage of cell viability was calculated by the absorbance measurements of control growth and test growth in the presence of the formulations at various concentration levels.

IC_{50} values were obtained by fitting the data with non-linear regression, with Prism 2.1 software (GraphPad, San Diego, CA).

Cellular translocation of PArg nanocapsules

Cells were plated in a multiwell-12 plate (Falcon) at $15.7x10^4$ cells/well in supplemented medium for 24 h. Next, medium was removed and dilutions of the

fluorescent dispersion, fluorescent nanoemulsion and fluorescent PArg nanocapsuless were added to the wells. After 2 h of incubation, cells were washed with acidic phosphate saline buffer (PBS, Sigma), trypsinized and resuspended in PBS supplemented with 3% (v/v) of FBS.

Living cell suspensions were analyzed for green fluorescence by flow cytometry in a FACScan (Becton Dickinson).

Statistical analysis

Cell culture results were evaluated in order to determine the statistical significance between the different formulations studied. The statistical evaluation of the cell viability results was performed by an ANOVA test followed by a multiple comparison analysis (SigmaStat Program, Jandel Scientific, version 3.5). Differences were considered to be significant at level of 0.05. IC_{50} values were compared by means of a T test for independent samples using SPSS v 15.0 (SPSS Inc.).

RESULTS AND DISCUSSION

This article describes for the first time a new drug nanocarrier consisting of an oily core surrounded by a PArg shell. The rational behind the design of this nanocarrier, named PArg nanocapsules, was as follows: the oily core is intended to allocate significant amounts of lipophilic active ingredients whereas the external polymer shell is expected to have three differentiated roles: (i) to associate negatively charged molecules, i.e. nucleic acid molecules; (ii) to facilitate the interaction and internalization of the nanocarrier with the cells; (iii) to prevent the stability of the nanocarrier in biological media and during storage.

These expected properties are justified by the positive nature of PArg and also by the previous documentation of its ability to interact and get across the cell membrane. In fact, there is significant evidence on the internalization of this polymer into the cell and its ability to deliver intracellularly the attached molecules [13].

Moreover, PArg nanocapsules are able to include a PEG protecting shield just by the addition of a hydrophobic derivative of PEG to the organic phase, avoiding the need of chemical PEGylation of the polymer. This modification

enlarges the scope of applicability of the nanocapsules, giving rise to an appropriate nanosystem for parenteral administration. PEGylation is an usual approach to improve the stability of the nanosystems in biological media as well as a strategy to avoid the clearance by the mononuclear phagocytes system (MPS).

Therefore, the main goals of this work are: (i) to construct the defined nanocarrier, (ii) to evaluate its ability to associate lipophilic drugs (docetaxel) and polar molecules (pDNA), (iii) to determine its stability, and (iv) to validate the expected internalization of the nanocarrier into cancer cells.

The construction of the nanocarrier

Three are the key elements of the construction: an oil (Miglyol® 812), a polymer shell (PArg) and a surfactant that facilitates the formation of nanodroplets as well as the attachment of the PArg shell (lecithin). These three elements were combined according to the solvent displacement technique, that we have previously applied to the formation of other types of nanocapsules [31]. This procedure is based on the controlled nanodispersion of lipid components in an aqueous solution followed by electrostatic interaction between the negatively charged lecithin and a cationic polymer. Using this experimental approach we

Table 1: Physicochemical properties of polyarginine nanocapsules (PArg NCs). PI: polydispersity index. (Mean ± s.d.; n = 3).

	Size (nm)	PI	Zeta potential (mV)
PAG NCs	145 ± 13	0.1	+ 53 ± 6
Isolated PAG NCs	123 ± 7	0.2	+56 ± 2
PAG-PEG NCs	119 ± 3	0.1	+15 ± 2
3% pDNA/PAG NCs	129 ± 4	0.2	+47 ± 2
10% pDNA/PAG NCs	136 ± 9	0.2	+31 ± 6
DCX-loaded PAG NCs	170 ± 10	0.1	+ 56 ± 6

could obtain a monodispersed population of PArg nanocapsules with a mean size close to 200 nm. As expected, these nanocarriers exhibit a high positive net charge due to the PArg layer disposed over the hydrophobic core, formed by

lecithin and the oil Miglyol® 812 (Table 1). It was also interesting to observe that PArg nanocapsules could be separated from the suspension medium and resuspended without altering their original properties (Table 1). This possibility of manipulation in order to obtain the desired concentration of the nanocarrier in an external aqueous medium is very important from a pharmaceutical standpoint.

The morphological appearance of the systems was observed by transmission electron microscopy. The micrograph presented in Figure 1 indicates that the

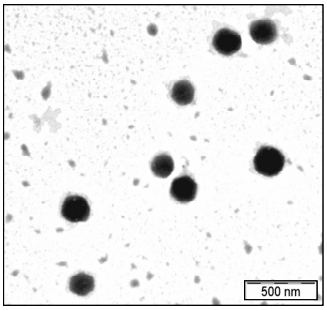

Figure 1: Transmission electron micrograph of polyarginine nanocapsules.

PArg nanocapsules have a round shape and a size of less than 200 nm, similar to the values obtained by photonic correlation spectroscopy. In addition, it was possible to observe the presence of a polymer corona covering the nanodroplets, thus confirming the existence of the PArg layer.

Furthermore, we attempted to modify the surface characteristics of PArg nanocapsules by the incorporation of PEG-stearate in the oily phase. The resulting PEG-surface modified PArg nanocapsules experienced a slight reduction of their size values in comparison with the uncoated nanocapsules. Concerning to the zeta potential, it was observed a clear decrease in the net charge of the system, most probably due to the presence of the PEG coating as we have previously reported for other PEG surface modified nanoparticles [32].

pDNA association to PArg nanocapsules and quantification

We are aware of previous reports describing the potential of PArg for the intracellular delivery of gene material such as siRNA [33; 34] and DNA [35]. In most of these studies the polymer was directly associated to the polynucleotide molecules.

In this work we have adopted a different strategy consisting on adsorbing the gene material onto a preformed PArg nanocarrier. We hypothesized that the nanostructured polymer would further promote the cellular uptake of the genetic material while allowing the co-administration of an auxiliary ingredient in the oily core.

pDNA was associated to PArg nanocapsules by simple electrostatic interaction. The results presented in Table 1 indicate that it is possible to associate significant amounts of pDNA with loadings of 3 and 10% of pDNA/nanocapsules, equivalent to the ratios 1:5 and 1:2 of pDNA/PArg respectively. In addition, the results of the particle size analysis show that the association of pDNA did not affect the mean size and polydispersity index of the nanocapsules (Table 1). On the other hand we observed, as expected, a significant reduction in the zeta potential values; a result that is attributed to the masking of the positive charge due to the interaction of PArg with the negatively charged pDNA molecules. Accordingly, the zeta potential reduction was related to the amount of pDNA associated (more remarkable for the 10% than for the 3% pDNA loading) (Table 1). Despite the surface charge reduction, pDNA-associated nanocapsules exhibit a significant positively charge (above +30 mV). This preservation of the positive charge evidences the prevalence of PArg at the shell of the nanocapsules, a characteristic that is critical in order to preserve the expected cell surface interaction of the shell.

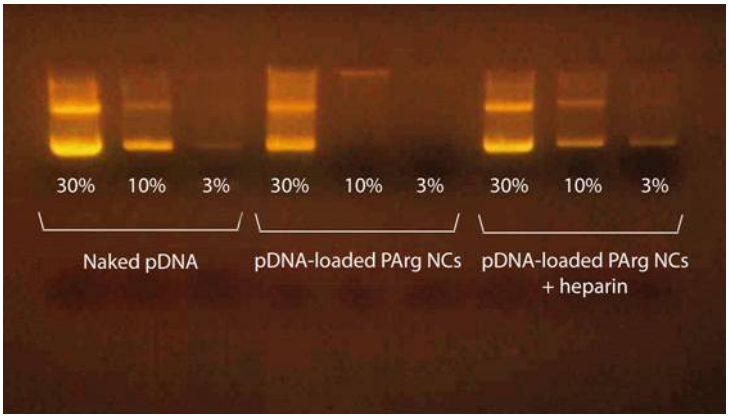

Figure 2: Gel electrophoresis of naked pDNA, pDNA-loaded polyarginine nanocapsules and pDNA-loaded polyarginine nanocapsules pretreated with heparin.

The association of pDNA onto PArg nanocapsules was visualized by agarose gel electrophoresis. As shown in Figure 2, no migration of free pDNA was observed for the theoretical loadings of 3% and 10%, suggesting the effective association of pDNA onto the PArg nanocapsules. Nevertheless, when a 30% of theoretical loading was incorporated to the systems, an excess of pDNA was clearly visualized in the gel, thus indicating that PArg did not interact with the whole amount of plasmid.

Table 2: Physicochemical properties of pDNA/polyarginine complexes (pDNA/PArg). PDI: polydispersity index. (Mean ± s.d.; n = 3)

Complex ratio (pDNA/PArg)	Size (nm)	PI	Zeta Potential (mV)
5:1	176 ± 63	0.3	-11 ± 2
3:1	101 ± 42	0.2	-12 ± 2
1:1	79 ± 13	0.2	+19 ± 3
1:3	150 ± 77	0.3	+14 ± 1
1:5	132 ± 20	0.3	+9 ± 1

In order to verify if the DNA molecules were efficiently associated to the nanocapsules, we incubated the 3% and 10% pDNA-associated PArg nanocapsules with a far excess of heparin in order to displace the pDNA from the surface of the nanocapsules. The appearance of the bands after the heparin treatment, corresponding to the released pDNA, confirmed that the molecule was firmly associated to the PArg shell of the nanocapsules. Therefore, based on the previous results we selected the formulation of PArg nanocapsules with the 3% loading for the rest of the studies.

Besides, the physicochemical characterization of the pDNA/PArg complexes showed polydispersed systems, although their size values were of less than 200 nm (Table 2). The zeta potential of the complexes varied with the ratio pDNA/PArg tested, having negative charge the complexes with an excess of pDNA with respect to PArg (ratios 5:1 and 3:1) meanwhile the higher amount of PArg to pDNA led to positively charged complexes (ratios 1:1, 1.3 and 1:5). Nevertheless, the main drawback of pDNA/PArg complexes was their poor stability in simulated biological fluids. In fact, the whole range of the complexes experienced an immediate and massive aggregation in the presence of

phosphate buffer (Figure 3). On the other hand, pDNA/PArg and pDNA/PArg-PEG nanocapsules had a more favorable behavior: pDNA/PArg-PEG nanocapsules were stable maintaining size values close to the original ones (Table 1); with respect to the size of pDNA/PArg nanocapsules it could be observed an initial increase of 200 nm, but they were not massively aggregated like happened with the complexes.

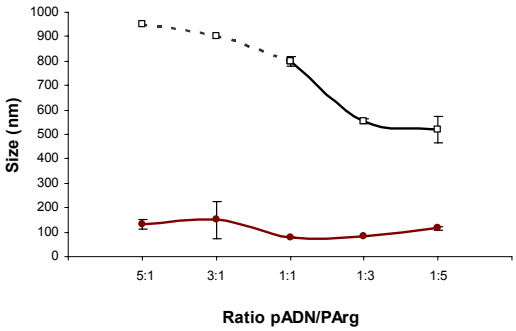

Figure 3: Size values of pDNA/PArg complexes in water (●) and phosphate buffer (□).

Likewise, pDNA-loaded nanocapsules were evaluated for a premature release of the associated plasmid as a consequence of their incubation in phosphate buffer. The results of the Figure 4 showed that PArg and PArg-PEG nanocapsules efficiently associate the pDNA and they do not release it after incubation in phosphate buffer.

As a conclusion, PArg and PArg-PEG nanocapsules are nanosystems of higher homogenicity that provide the possibility of co-encapsulating other drugs in their inner core. Moreover, their enhanced stability provided by the coating polymers upgrades the potential of PArg nanocapsules.

Docetaxel encapsulation and release studies

The defined nanocapsules may represent an interesting approach for overcoming a frequent limitation of anticancer drugs, i.e. poor water-solubility. The cytotoxic drug docetaxel was selected in order to validate this hypothesis. Docetaxel could be efficiently encapsulated within the core of PArg nanocapsules (encapsulation efficiency of 74%) without altering the original size and zeta-potential values of the nanocapsules.

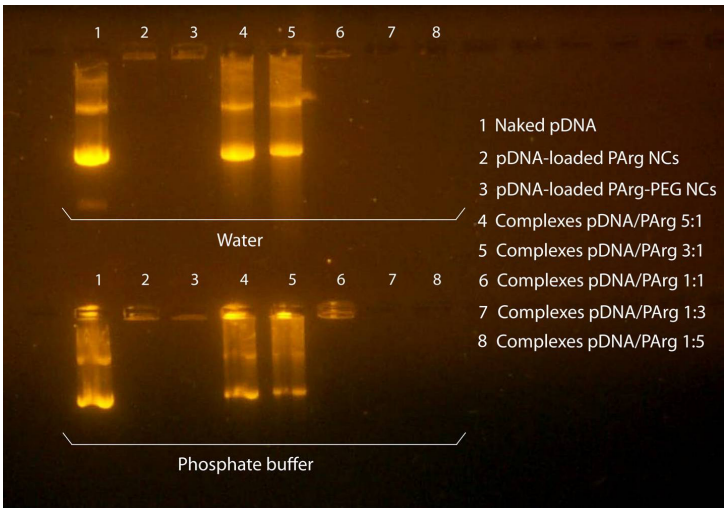

Figure 4: Gel electrophoresis of naked pDNA, pDNA-loaded polyarginine nanocapsules, pDNA-loaded poliarginine-PEG nanocapsules and complexes pDNA/PArg in water and phosphate buffer.

In an additional experiment we evaluated the release pattern of the encapsulated docetaxel upon incubation of highly diluted nanocapsules in simulated biological media. The results showed that docetaxel is released from

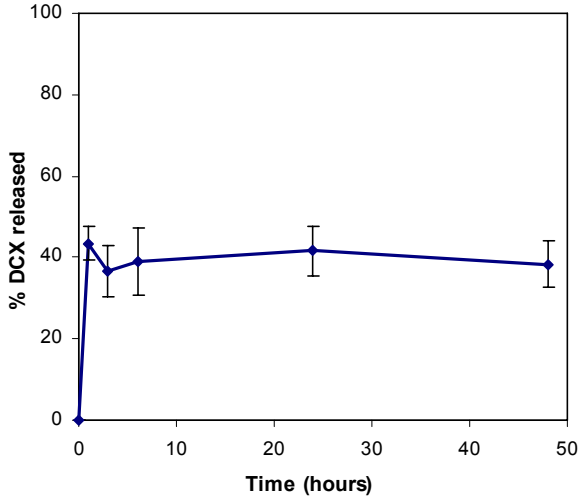

Figure 5: In vitro docetaxel release from docetaxel-loaded polyarginine nanocapsules. (Mean ± s.d.; n=3).

PArg nanocapsules according to a biphasic profile, characterized by a rapid initial release (40% of the encapsulated drug), followed by a second phase in which no further drug release was observed (Figure 5). The initial release phase, typically observed in oily systems [6; 27; 31], is related to the dilution of the nanocapsules in the incubation medium and the subsequent partition of the drug between the oily core and the external aqueous aqueous phase. On the other hand, the absence of release in the second phase confirms the high affinity of the drug by the oil core. These results showed that PAG nanocapsules are suitable nanocarriers for the encapsulation and targeted delivery of low soluble molecules.

Long-term stability of PArg nanocapsules

Frequently, stability is a critical issue in the development of a nanocarrier formulation. There are several factors, such as temperature, light or packing material, which may compromise their stability upon storage as a suspension [36]. The surface charge of the nanocarrier, usually plays a significant role in its stability: highly charged nanocarriers do not normally suffer aggregation due to the repulsion between particles [37]. In the present study we evaluated the stability of PArg nanocapsules suspension under storage at 4º C and 37º C, during a period of 9 months. The results showed that there was no effect of the temperature on the particle size evolution, neither on the zeta potential of the nanocapsules, which maintained their values under 200 nm and at +50 mV throughout the study (Figure 6). This prolonged stability, which could be strictly to

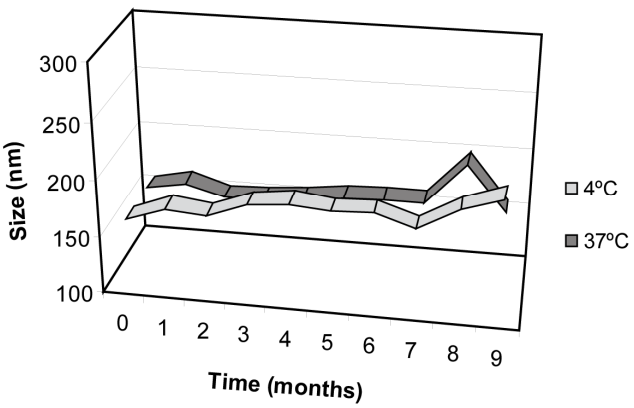

Figure 6: Stability study of polyarginine nanocapsule suspension after 9 months storage at 4º C and 37º C. (Mean ± s.d.; n=3).

the high zeta potential of PArg nanocapsules,

On the other hand, lyophilization is the most frequent and efficient method used to preserve the properties of nanocarriers. However, to obtain adequate lyophilizates of colloidal carriers is often a complex issue due to the fragility of the structure upon freezing and drying and requires the use of cryoprotectants [38]. In this study we have selected trehalose as a cryoprotectant because it has many advantages in comparison with other sugars such as less hygroscopicity and higher glass transition temperature [39].

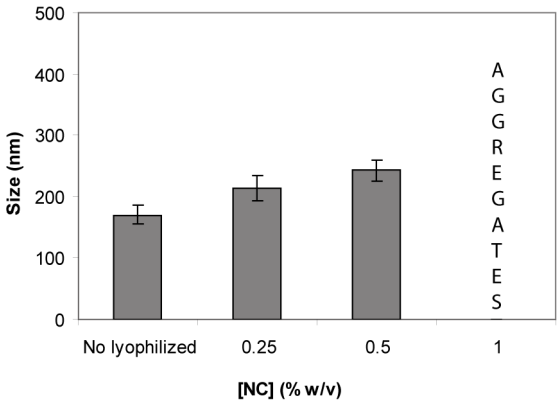

Figure 7: Lyophilization study of polyarginine nanocapsules with 10% w/v trehalose. (Mean ± s.d.; n=3).

The results showed that the size of PArg nanocapsules remained close to its initial values after lyophilization with 10% of trehalose (Figure 7), for the concentrations of 0.25 and 0.5% w/v. It was also observed that the concentration of nanocapsules is an important factor in the recovery of the initial size values after lyophilization.

The efficacy of PArg nanocapsules for the intracellular delivery of docetaxel

Cell viability studies were performed in order to assess the efficacy of docetaxel-loaded PArg nanocapsules in the non-small cell lung cancer NCI-H460 cell line. Figure 8 shows the cell viability profiles after 48 h of treatment with docetaxel-loaded PArg nanocapsules, in comparison with a docetaxel solution or

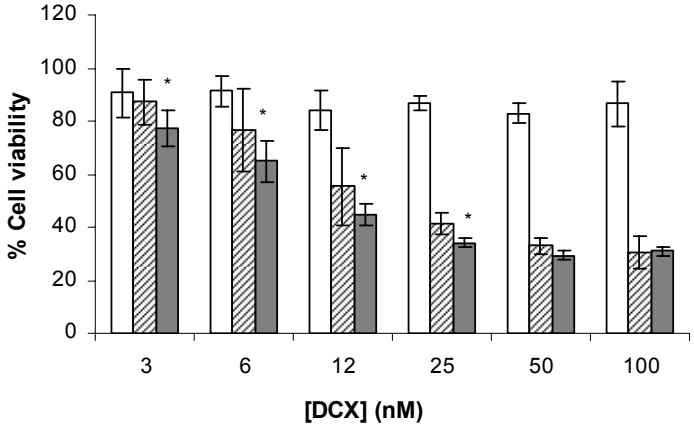

Figure 8: Cell viability profiles of blank polyarginine nanocapsules, docetaxel and docetaxel-loaded polyarginine nanocapsules on NCI-H460 cell line. (Mean ± s.d.; n=3).

the unloaded-PArg nanocapsules. The results indicate that the encapsulated drug decreased the cell viability in a concentration dependent manner, reaching a 30% reduction for the highest concentrations tested (100 nM). As expected, this reduction was significantly greater for the encapsulated than for the free drug. In fact, the IC_{50} value determined for docetaxel-loaded PArg nanocapsules was four times lower (3.11 nM) than the corresponding to the docetaxel solution (11.8 nM). Theoretically, this improvement of the antiproliferative effect of docetaxel could be related to the uptake of the nanocarriers by the cells and the more efficient transport of the drug into them. Additionally, the internalization of the nanocarrier could lead to an intracellular delivery of the associated drug in a more prolonged and efficient manner. Perhaps, this facilitated internalization of PArg nanocapsules could be the reason of their more favorable behavior in the cell proliferation inhibition compared to other docetaxel drug delivery systems, that showed inhibition levels similar to the control drug [40; 41]. Another interesting result from these studies is the lack of toxicity of blank PArg nanocapsules under the range of concentrations investigated, in agreement with previous studies that provided evidence of the safety of PArg-based nanosystems. Indeed, Holowka *et al*. for PArg-polyleucine polymeric vesicles, as well as Rawat *et al*. for PArg-heparin complexes have shown the cell biocompatibility of PArg with epithelial and endothelial cells [23; 42].

Internalization of PArg nanocapsules in cancer cells

In order to corroborate the hypothesis of the intracellular drug delivery, as stated in the efficacy studies, we studied the internalization of fluorescently labelled nanocarriers into the NCI-H460 cells by FACS analysis. For the correct evaluation of the contribution of PArg coat to the uptake of the nanocarriers, we used the uncoated nanoemulsion and a dispersion of the fluorescent probe fluorescein-DHPE as controls. The results in Figure 9 clearly illustrate that the PArg shell has a critical role in the internalization of PArg nanocapsules by the NCI-H460 cells. Indeed, the fluorescent PArg nanocapsules could be detected inside every cell after 2 h of incubation. In contrast, the nanoemulsion was internalized in a very low extent and the fluorescent dispersion was almost excluded from the cells.

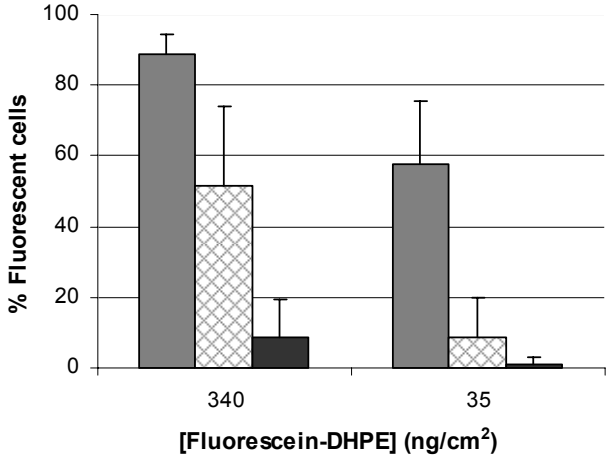

Figure 9: Cell uptake of polyarginine nanocapsules (grey bars), uncoated nanoemulsion (diamond bars) and free-fluorescent probe (black bars). (Mean ± s.d.; n=3).

The effect of PArg on the intracellular accumulation of different nanostructures has been shown despite de molecular weight of the polymer used. Thus, arginine octamer-modified liposomes as well as PArg-polyleucine vesicles (60 arginine monomers) showed more extent uptake compared to the systems that did not incorporate PArg [33; 42]. Nevertheless, there is a certain disparity related to the optimal PArg molecular weight for efficient translocation of the cargoes. Whereas some authors have reported that the maximal uptake is seen

for 15 arginines and longer oligomers lead to impaired translocation [43], others have shown the inefficient delivery of large monoclonal antibodies, anti-fullerene and anti-HIV-1 Gag when octaarginine was used compared to large molecular weight poly-L-arginine (MW 10.750 Da) [44].

Moreover, the precise mechanism of cellular entry of cell penetrating peptides (CPPs) and of PArg, as a member of this family, is a matter of mayor controversy. Until not so long ago, it was thought that endocytosis was not involved in the internalization [45]. Authors claimed that internalization was an independent receptor-, energy- or temperature-process, based on a transduction mechanism (direct membrane penetration and inverted micelle) [46; 47]. However, nowadays, the hypothesis of an unique transduction mechanism for cellular internalization has generally been deserted [48]. Up to now, it is believed that endocytosis (constituted by clathrin mediated, caveolin mediated, clathrin and caveolin independent endocytosis and macropinocytosis), is the main mechanism for cellular entry into living cells [49]. Thus, it is important to take into account that the internalization pathway may be modified by parameters such as the PArg length or the PArg surface density which may determine the intracellular fate of the cargo molecules and subsequently the success of their action [50; 51].

CONCLUSIONS

Here we report the construction and the properties of an original nanocapsule prototype, consisting of a hydrophobic core surrounded by a PArg shell. PArg nanocapsules are able to successfully associate pDNA on their surface as well as to encapsulate the hydrophobic molecule docetaxel in their inner core. Results from the NCI-H460 cell culture studies showed that the encapsulation of the antitumor drug docetaxel in PArg nanocapsules maximized its pharmacological effect. According to that, it was found that PArg shell contributed to an efficient uptake of the nanosystem in the cell line. In conclusion, it can be stated that PArg nanocapsules are effective nanocarriers for cancer treatment, although *in vivo* future studies will fully assess their potential for targeted drug delivery.

ACKNOWLEDGEMENTS

This work was supported by the Spanish Ministry of Science and Technology (SAF 2004-08319-CO2-01) and Consolider Nanobiomed (CSD 2006-00012). The first author acknowledges the fellowship received from the Spanish Government (AP2005-1701). Authors also thank Dr. Vidal for his valuable help in the cell cytometry analysis.

REFERENCES

1. Farokhzad O.C.; Langer R. (2006). Nanomedicine: developing smarter therapeutic and diagnostic modalities. Adv. Drug Deliv. Rev. 58: 1456-1459.
2. Couvreur P.; Vauthier C. (2006). Nanotechnology: intelligent design to treat complex disease. Pharm. Res. 23: 1417-1450.
3. Hervella P.; Lozano V.; Garcia-Fuentes M.; Alonso M.J. (2008). Nanomedicine: New Challenges and Opportunities in Cancer Therapy. J. Biomed. Nanotechnol. 4: 276-292.
4. de la Fuente M.; Csaba N.; Garcia-Fuentes M.; Alonso M.J. (2008). Nanoparticles as protein and gene carriers to mucosal surfaces. Nanomedicine. 3: 845-857.
5. Janes K.A.; Fresneau M.P.; Marazuela A.; Fabra A.; Alonso M.J. (2001). Chitosan nanoparticles as delivery systems for doxorubicin. J. Control. Release. 73: 255-267.
6. Lozano M.V.; Torrecilla D.; Torres D.; Vidal A.; Dominguez F.; Alonso M.J. (2008). Highly efficient system to deliver taxanes into tumor cells: docetaxel-loaded chitosan oligomer colloidal carriers. Biomacromolecu les. 9: 2186-2193.
7. de la Fuente M.; Seijo B.; Alonso M.J. (2008). Bioadhesive hyaluronan-chitosan nanoparticles can transport genes across the ocular mucosa and transfect ocular tissue. Gene Ther. 15: 668-676.
8. Chiang C.H.; Yeh M.K. (2003). Contribution of poly(amino acids) to advances in pharmaceutical biotechnology. Curr. Pharm. Biotechnol. 4: 323-330.
9. Lavasanifar A.; Samuel J.; Kwon G.S. (2002). Poly(ethylene oxide)-block-poly(L-amino acid) micelles for drug delivery. Adv. Drug Deliv. Rev. 54: 169-190.
10. Romberg B.; Metselaar J.M.; Baranyi L.; Snel C.J.; Bunger R.; Hennink W.E.; Szebeni J.; Storm G. (2007). Poly(amino acid)s: promising enzymatically degradable stealth coatings for liposomes. Int. J. Pharm. 331: 186-189.
11. Nakanishi T.; Fukushima S.; Okamoto K.; Suzuki M.; Matsumura Y.; Yokoyama M.; Okano T.; Sakurai Y.; Kataoka K. (2001). Development of the polymer micelle carrier system for doxorubicin. J. Control. Release. 74: 295-302.
12. Lundberg M.; Wikström S.; Johansson M. (2003). Cell Surface Adherence and Endocytosis of Protein Transduction Domains. Mol. Ther. 8: 143-150.

13. Patel L.N.; Zaro J.L.; Shen W.C. (2007). Cell penetrating peptides: intracellular pathways and pharmaceutical perspectives. Pharm. Res. 24: 1977-1992.
14. Torchilin V.P. (2008). Tat peptide-mediated intracellular delivery of pharmaceutical nanocarriers. Adv. Drug Deliv. Rev. 60: 548-558.
15. Lührs P.; Schmidt W.; Kutil R.; Buschle M.; Wagner S.N.; Stingl G.; Schneeberger A. (2002). Induction of specific immune responses by polycation-based vaccines. J. Immunol. 169: 5217-5226.
16. Lingnau K.; Riedl K.; Von Gabain A. (2007). IC31® and IC30, novel types of vaccine adjuvant based on peptide delivery systems. Expert Rev. Vaccines. 6: 741-746.
17. Kim W.J.; Christensen L.V.; Jo S.; Yockman J.W.; Jeong J.H.; Kim Y.H.; Kim S.W. (2006). Cholesteryl Oligoarginine Delivering Vascular Endothelial Growth Factor siRNA Effectively Inhibits Tumor Growth in Colon Adenocarcinoma. Mol. Ther. 14: 343-350.
18. Fujita T.; Furuhata M.; Hattori Y.; Kawakami H.; Toma K.; Maitani Y. (2008). High gene delivery in tumor by intratumoral injection of tetraarginine-PEG lipid-coated protamine/DNA. J. Control. Release. 129: 124-127.
19. Yang L.; Mashima T.; Sato S.; Mochizuki M.; Sakamoto H.; Yamori T.; Oh-Hara T.; Tsuruo T. (2003). Predominant suppression of apoptosome by inhibitor of apoptosis protein in non-small cell lung cancer H460 cells: therapeutic effect of a novel polyarginine-conjugated Smac peptide. Cancer Res. 63: 831-837.
20. Chen L.; Wright L.R.; Chen C.H.; Oliver S.F.; Wender P.A.; Mochly-Rosen D. (2001). Molecular transporters for peptides: Delivery of a cardioprotective εPKC agonist peptide into cells and intact ischemic heart using a transport system, R7. Chem. Biol. 8: 1123-1129.
21. Firbas C.; Jilma B.; Tauber E.; Buerger V.; Jelovcan S.; Lingnau K.; Buschle M.; Frisch J.; Klade C.S. (2006). Immunogenicity and safety of a novel therapeutic hepatitis C virus (HCV) peptide vaccine: a randomized, placebo controlled trial for dose optimization in 128 healthy subjects. Vaccine. 24: 4343-4353.
22. Klade C.S.; Wedemeyer H.; Berg T.; Hinrichsen H.; Cholewinska G.; Zeuzem S.; Blum H.; Buschle M.; Jelovcan S.; Buerger V.; Tauber E.; Frisch J.; Manns M.P. (2008). Therapeutic Vaccination of Chronic Hepatitis C Nonresponder Patients With the Peptide Vaccine IC41. Gastroenterology. 134: 1385-1395.

23. Rawat A.; Yang T.; Hussain A.; Ahsan F. (2008). Complexation of a poly-L-arginine with low molecular weight heparin enhances pulmonary absorption of the drug. Pharm. Res. 25: 936-948.
24. Nemoto E.; Ueda H.; Akimoto M.; Natsume H.; Morimoto Y. (2007). Ability of poly-L-arginine to enhance drug absorption into aqueous humor and vitreous body after instillation in rabbits. Biol. Pharm. Bull. 30: 1768-1772.
25. Miyamoto M.; Natsume H.; Iwata S.; Ohtake K.; Yamaguchi M.; Kobayashi D.; Sugibayashi K.; Yamashina M.; Morimoto Y. (2001). Improved nasal absorption of drugs using poly-L-arginine: Effects of concentration and molecular weight of poly-L-arginine on the nasal absorption of fluorescein isothiocyanate-dextran in rats. Eur. J. Pharm. Biopharm. 52: 21-30.
26. Zaki N.M.; Mortada N.D.; Awad G.A.S.; ElHady S.S.A. (2006). Rapid-onset intranasal delivery of metoclopramide hydrochloride. Part II: Safety of various absorption enhancers and pharmacokinetic evaluation. Int. J. Pharm. 327: 97-103.
27. Calvo P.; Vila-Jato J.L.; Alonso M.J. (1997). Evaluation of cationic polymer-coated nanocapsules as ocular drug carriers. Int. J. Pharm. 153: 41-50.
28. Rudolph C.; Plank C.; Lausier J.; Schillinger U.; Müller R.H.; Rosenecker J. (2003). Oligomers of the arginine-rich motif of the HIV-1 TAT protein are capable of transferring plasmid DNA into cells. J. Biol. Chem. 278: 11411-11418.
29. Lee S.H.; Yoo S.D.; Lee K.H. (1999). Rapid and sensitive determination of paclitaxel in mouse plasma by high-performance liquid chromatogra phy. J. Chromatogr. B Biomed. Sci. Appl. 724: 357-363.
30. Mosmann T. (1983). Rapid colorimetric assay for cellular growth and survival: application to proliferation and cytotoxicity assays. J. Immunol. Methods. 65: 55-63.
31. Prego C.; Torres D.; Alonso M.J. (2006). Chitosan nanocapsules: a new carrier for nasal peptide delivery. J. Drug Del. Sci. Tech. 16: 331-337.
32. Garcia-Fuentes M.; Torres D.; Alonso M.J. (2003). Design of lipid nanoparticles for the oral delivery of hydrophilic macromolecules. Colloids Surf. B Biointerfaces. 27: 159-168.
33. Zhang C.; Tang N.; Liu X.; Liang W.; Xu W.; Torchilin V.P. (2006). siRNA-containing liposomes modified with polyarginine effectively silence the targeted gene. J. Control. Release. 112: 229-239.

34. Kim H.H.; Choi H.S.; Yang J.M.; Shin S. (2007). Characterization of gene delivery in vitro and in vivo by the arginine peptide system. Int. J. Pharm. 335: 70-78.
35. Theodossiou T.A.; Pantos A.; Tsogas I.; Paleos C.M. (2008). Guanidinylated dendritic molecular transporters: Prospective drug delivery systems and application in cell transfection. ChemMedChem. 3: 1635-1643.
36. Freitas C.; Müller R.H. (1998). Effect of light and temperature on zeta potential and physical stability in solid lipid nanoparticle (SLN^{TM}) dispersions. Int. J. Pharm. 168: 221-229.
37. Heurtault B.; Saulnier P.; Pech B.; Proust J.E.; Benoit J.P. (2003). Physico-chemical stability of colloidal lipid particles. Biomaterials. 24: 4283-4300.
38. Abdelwahed W.; Degobert G.; Fessi H. (2006). Investigation of nanocapsules stabilization by amorphous excipients during freeze-drying and storage. Eur. J. Pharm. Biopharm. 63: 87-94.
39. Crowe L.M.; Reid D.S.; Crowe J.H. (1996). Is trehalose special for preserving dry biomaterials? Biophys. J. 71: 2087-2093.
40. Elsabahy M.; Perron M.É.; Bertrand N.; Yu G.E.; Leroux J.C. (2007). Solubilization of docetaxel in poly(ethylene oxide)-block-poly(butylene/styrene oxide) micelles. Biomacromolecules. 8: 2250-2257.
41. Immordino M.L.; Brusa P.; Arpicco S.; Stella B.; Dosio F.; Cattel L. (2003). Preparation, characterization, cytotoxicity and pharmacokinetics of liposomes containing docetaxel. J. Control. Release. 91: 417-429.
42. Holowka E.P.; Sun V.Z.; Kamei D.T.; Deming T.J. (2007). Polyarginine segments in block copolypeptides drive both vesicular assembly and intracellular delivery. Nat. Mater. 6: 52-57.
43. Wender P.A.; Galliher W.C.; Goun E.A.; Jones L.R.; Pillow T.H. (2008). The design of guanidinium-rich transporters and their internalization mechanisms. Adv. Drug Deliv. Rev. 60: 452-472.
44. Chen B.X.; Erlanger B.F. (2002). Intracellular delivery of monoclonal antibodies. Immunol. Lett. 84: 63-67.
45. Silhol M.; Tyagi M.; Giacca M.; Lebleu B.; Vivès E. (2002). Different mechanisms for cellular internalization of the HIV-1 Tat-derived cell penetrating peptide and recombinant proteins fused to Tat. Eur. J. Biochem. 269: 494-501.
46. Nagahara H.; Vocero-Akbani A.M.; Snyder E.L.; Ho A.; Latham D.G.; Lissy N.A.; Becker-Hapak M.; Ezhevsky S.A.; Dowdy S.F. (1998).

Transduction of full-length TAT fusion proteins into mammalian cells: TAT-p27(Kip1) induces cell migration. Nat. Med. 4: 1449-1452.

47. Schwarze S.R.; Ho A.; Vocero-Akbani A.; Dowdy S.F. (1999). In vivo protein transduction: Delivery of a biologically active protein into the mouse. Science. 285: 1569-1572.
48. Richard J.P.; Melikov K.; Vives E.; Ramos C.; Verbeure B.; Gait M.J.; Chernomordik L.V.; Lebleu B. (2003). Cell-penetrating peptides: A reevaluation of the mechanism of cellular uptake. J. Biol. Chem. 278: 585-590.
49. Kaplan I.M.; Wadia J.S.; Dowdy S.F. (2005). Cationic TAT peptide transduction domain enters cells by macropinocytosis. J. Control. Release. 102: 247-253.
50. Furuhata M.; Izumisawa T.; Kawakami H.; Toma K.; Hattori Y.; Maitani Y. (2009). Decaarginine-PEG-liposome enhanced transfection efficiency and function of arginine length and PEG. Int. J. Pharm. 371: 40-46.
51. Khalil I.A.; Kogure K.; Futaki S.; Harashima H. (2006). High density of octaarginine stimulates macropinocytosis leading to efficient intracellular trafficking for gene expression. J. Biol. Chem. 281: 3544-3551.

ANNEXES

Annex I

In vivo efficacy of anti-TMEFF-2 modified nanocapsules in non-small cell lung cancer tumors

D. Torrecilla[1#], M. V. Lozano[2#], E. Lallana[3#], R. Novoa-Carballal[3], A. Vidal[1], D. Torres[2], E. Fernández-Megía[3], R. Riguera[3], M. J. Alonso[2], F. Domínguez[1*].

[1] Department of Physiology. Faculty of Medicine.
[2] Department of Pharmaceutical Technology, Faculty of Pharmacy.
[3] Department of Organic Chemistry, Faculty of Chemistry.

University of Santiago de Compostela (USC)
15782 Santiago de Compostela, Spain

# Authors equally contributed to the paper.

* Corresponding author: Prof. Fernando Domínguez

ABSTRACT

The goal of the present work has been the development of monoclonal antibody (mAb, anti-TMEFF-2) chitosan (CS) nanocapsules for the selective delivery of the cytostatic drug docetaxel (DCX) to cancer cells that over-express the target protein TMEFF. Therefore, CS nanocapsules were obtained and afterwards efficiently functionalized with the mAb, yielding nanometric systems of around 200 nm and with positive surface charge. The cell cycle analysis of the cancer cells pretreated with the formulations indicated that the encapsulated drug was fully active and had similar effect to the free drug. The in *vivo* efficacy studies on a mouse xenograft model that overexpress TMEFF-2 showed that mAb-functionalized CS nanocapsules were as effective as the commercial DCX (Taxotere®). Nevertheless, differences were observed on the pharmacodinamic behaviour of the formulations. Meanwhile Taxotere® exerted a fast and short in period effect on the tumor volume, TMEFF-2-modified nanocapsules obtained a delayed but more prolonged action of DCX.

INTRODUCTION

Active targeting of nanosystems is an interesting approach for cancer therapy, because the functionalization of these carriers with selective entities leads to their specific targeting to the cancer cells. This facilitated vehiculization of the systems favors the local delivery of the loaded anticancer drug in the tumor tissue, producing a decrease in the toxic effects of the drug and promoting a more effective treatment.

Previous studies recently reported have shown that chitosan (CS) nanocapsules efficiently delivered the cytostatic drug docetaxel (DCX) to the cancer cell lines MCF-7 (human breast adenocarcinoma) and A549 (human lung carcinoma). The results indicated that CS nanocapsules were rapidly and massively internalized by the tumor cells. Moreover, the nanoencapsulation process induced an increase in the antiproliferative effect of the drug in both cell lines. Altogether, these studies indicated that CS nanocapsules accelerate the internalization of DCX by a non-selective pathway and promote the pharmacological activity of the drug encapsulated.

TMEFF-2 is a transmembrane protein enclosed in the family of EGF-like genes. This protein is usually overexpressed in non-microcytic tumors (NSCLC, non-small cell lung carcinomas). Therefore, this enhancement could transform TMEFF-2 as a good target molecule for NSCLC treatment.

Based on these evidences, the aim of this study has been the development of functionalized CS nanocapsules with the mAb anti-TMEFF-2 for the active targeting of DCX to cancer cells. For that purpose, the association of the mAb to the nanocapsules surface was achieved by the avidin-biotin technology. This technology was selected by its exceptional selectivity and strong interaction, making possible the functionalization of the nanocapsules with the mAb. Moreover, we have used a PEGylated derivative of CS for the preparation of the nanocapsules in order to obtain a formulation of CS nanocapsules with *Stealth*® properties and long-circulation times after intravenous injection.

Therefore, first we have carried out the development and characterization of mAb-functionalized CS nanocapsules. Afterwards we assessed the efficacy of the nanocapsules in cell culture studies for their subsequent evaluation in an *in vivo* model of NSCLC tumor cells.

MATERIALS AND METHODS

Chemicals

Docetaxel (DCX) and poloxamer 188 (Pluronic F-68®) were purchased from Sigma-Aldrich (Spain). Miglyol 812®, neutral oil formed by esters of caprylic and capric fatty acids and glycerol, was donated by Sasol Germany GmbH (Germany). The surfactant Epikuron 145V, phosphatidylcholine enriched fraction of soybean lecithin was donated by Cargill (Spain). Ultrapure chitosan (CS) hydrochloride salt [Protasan® UP CL 113, degree of acetylation (DA) 14% by ^{1}H NMR] was purchased from Biopolymer Novamatrix (Norway). MeO-PEG-CO_2H (M_n 5114 by MALDI-TOF) has been synthesized following known procedures [1; 2] from a commercially available MeO-PEG-OH (M_n 5055, M_w 5088, by MALDI-TOF) purchased from Fluka (Spain). Biotin-PEG-CO_2H (M_n 4030, M_w 4060, by MALDI-TOF) has been previously synthesized [2] from a commercially available NHS-PEG-NHFmoc (M_n 3837, M_w 3890, by MALDI-TOF) obtained from Nektar (USA). Biotin-$(PEG)_4$-NHS was purchased from Pierce. Avidin from egg white (14 units/mg protein) and 2-(4-hydroxyphenylazo)benzoic acid (HABA) were purchased from Sigma-Aldrich (Spain). All other reagents used were of analytical grade.

Anti-TMEFF2 mAb development

Cloning and expression of TMEFF2 and ECD-TMEFF2

Total RNA was isolated from A549 tumor cells in two steps using TRIzol reagent (Invitrogen) and RNeasy Micro Kit (Quiagen). cDNA was produced from total RNA using SuperScrip II (Invitrogen) and specific PCR were performed to obtain the codificant region for TMEFF2 complete form (374 aminoacids) and the codificant region for the TMEFF2 extracellular domain (ECD) with a 6 x His tag (307 aminoacids). Three different primers with recognition sequence for Hind III endonuclease were used for this purpose (TMEFF2 fw and ECD fw 5´-GGCAGCAAGCTTCCACCATGGTGCTG, TMEFF2 rev 5´- CGGGCCAAGCTTA GATTAACCTCGT and ECD rev 5´- CGGGCCAAGCTTAGTGATGGTGATGGTG ATGTTCACAGTGTTGTCCAGT) in a PCR using FastStart Taq Polimerase (Roche). The products of this reaction were cloned with TOPO TA Cloning System (Invitrogen) and subcloned to pCDNA3.1 vector to generate two expression vectors, pC-TMEFF2 and pC-ECD.

Complete form of TMEFF2 and extracellular domain of TMEFF2 were expressed in HEK293 cells transfected by calcium phosphate transfection method. Briefly, cells were seeded and incubated with complete culture medium 24 h for recovery. Once cells growed to 90 % of confluency they were washed twice with PBS and changed to culture medium only with DMEM; 1 h later they were transitory transfected with calcium phosphate cristals prepared with the expression plasmid. Cells were returned to complete culture medium 16 h after transfection and expression was tested 48 h later.

Culture medium of ECD expression was concentrated 10 X by centrifugation with Amicon 50 (Millipore) at 4º C and tagged protein was purified using B-PER 6 x His Spin Purification Kit (Pierce). All proteins were identified by Coomassie Blue staining and Western blotting.

Anti-TMEFF2 mAb generation and characterization

Female BALB/c mice were immunized directly with plasmid codifying for extacellular domain of TMEFF2 as DNA vaccine. mAbs were generated by standard techniques with fusion of spleen cells and myeloma tumor cells for hibridoma formation and clonal selection by Genovac GmbH. A panel of anti-TMEFF2 antibody containing clone culture supernatants were characterized by flow cytometry on TMEFF2-superexpressing HEK293 cells transfected as described before. Transfected cells were washed twice with PBS and they were detached and resuspended in PBS with 3 % of foetal bovine serum. Cells were incubated 1 h at 4º C with anti-TMEFF2 culture supernatants, washed twice and incubated 45 min at 4º C with 2.5 µg/mL of Alexa Fluor 488 anti-mouse IgG (Molecular Probes) in PBS, washed twice and fluorescence intensenty was assessed in a FACScan (Becton Dickinson) compared to control cells. Selected clone was continued and used to express and purify the anti-TMEFF2 mAb.

Ag-Ab binding studies

To evaluate Ag-Ab recognition of 11D1C1 anti-TMEFF2 mAb to the native form the extracellular domain of TMEFF2 a binding experiment with conditioned medium were performed. Briefly, 200 µL of anti-TMEFF2 mAb dilution (5 µg/mL in PBS) was incubed 1 h with gently shaking at 4º C with different amounts of concentrated culture medium from HEK293 transfected cells with pC-ECD plasmid and pCDNA3.1 as a control. After binding process, anti-TMEFF2 mAb solutions were tested by flow cytometry on TMEFF2-superexpressing HEK293 cells transfected as described before.

Biotinylation of anti-TMEFF2 mAb

The biotinylation of anti-TMEFF2 mAb was performed with Biotin-$(PEG)_4$-NHS following a slightly modified procedure for the amine acylation of proteins reported by Smith [3]. Briefly, Biotin-$(PEG)_4$-NHS was freshly dissolved in ultrapure water (2.0 mg/mL) by vigorous vortex mixing. Working as rapidly as possible, 34 µL of this solution were pipetted into 1.0 mL of a solution of anti-TMEFF2 mAb (1.0 mg/mL) in 10 mM PBS (pH 7.4). The resulting solution was orbitally shaken for 60 min at room temperature, and then, dialyzed against 10 mM PBS (pH 7.4) overnight at 4 ºC to remove the excess of biotinylating reagent. The concentration of the biotinylated anti-TMEFF2 mAb was quantified spectrophotometrically at 280 nm (ε_{molar} = 195000 $M^{-1}cm^{-1}$).

The accessible biotin label incorporation was quantified by measuring the absorbance at 500 nm of an avidin-HABA solution before and after addition of the biotinylated mAb [4]. Briefly, the absorbance of a solution of avidin and HABA (0.5 mg/mL and 73 µg/mL, respectively) in 100 mM PBS (pH 7.2) was measured at 500 nm. Afterwards, an aliquot of the biotinylated anti-TMEFF2 mAb (1.0 mg/mL) was added to the cuvette containing the avidin-HABA complex, and the absorbance was measured again at 2 min time intervals until a constant value

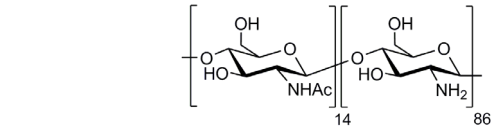

Chitosan (CS)

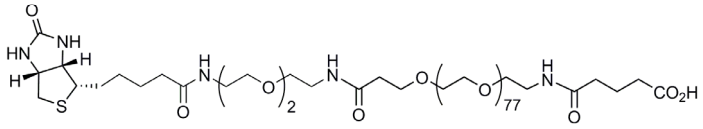

Biotin-PEG-CO_2H

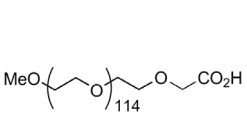

MeO-PEG-CO_2H

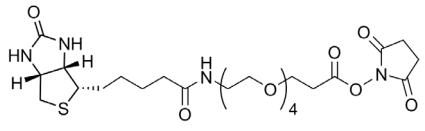

Biotin-$(PEG)_4$-NHS

Scheme 1

was reached. From the measured absorbance decay, an average of 3.0 biotin labels per mAb was determined.

Preparation and characterization of PEGylated CS derivatives

Depolymerization of CS

Depolymerized CS was prepared from a commercial CS hydrochloride salt by oxidative degradation using sodium nitrite ($NaNO_2$) [5]. Briefly, 0.1 mL of $NaNO_2$ (0.1M) were added to 2 mL of a CS solution (1% w/v) at room temperature and left under magnetic stirring overnight. Then, the resulting CS solution was freeze-dried to obtain a dry powder. The molecular weight of depolymerized CS was measured by SEC-MALLS.

Determination of molecular weight of CS by SEC-MALLS

Number- and weight-average molecular weights (M_n and M_w) of commercial and depolymerized CS were determined by size exclusion chromatography-multiangle laser-light scattering (SEC-MALLS) [6]. An Iso Pump G1310A (Hewlett Packard) was connected to two PSS Novema GPC columns (10 µm, 30 Å, 8×300 mm; and 10 µm, 3000 Å, 8×300 mm). A PSS SLD7000 MALLS detector (Brookhaven Instruments Corporation) operating at 660 nm and a G1362A refractive index detector (Agilent) were connected on line. A 0.15M NH_4OAc/0.2M AcOH buffer (pH 4.5) was used as eluent. Polymer solutions were filtered through 0.2 µm pore size membranes before injection. Polymer concentrations were in the range 1 to 5 mg/mL depending on CS molecular weight. Refractive index increment dn/dC was set at 0.188 according previous reports [7]. Average molecular weights M_n $5.4 \cdot 10^4$ and M_w $8.0 \cdot 10^4$ resulted for commercial CS Protasan UP CL 113. For depolymerized CS the values were M_n $8.5 \cdot 10^3$ and M_w $1.3 \cdot 10^4$.

Synthesis of CS-PEG-OMe

CS·HCl (100 mg, 0.5 mmol), MeO-PEG-CO_2H (30.7 mg, 6.0 µmol), and NHS (3.4 mg, 30 µmol, 100 µL of a 34 mg/mL solution in H_2O) were dissolved in H_2O (14.3 mL). Then, EDC (69.1 mg, 0.36 mmol) was added in four equal portions every 30 min. The resulting solution was stirred at room temperature for 22 h, and then was ultrafiltered (Amicon YM1) with H_2O, and lyophilized to afford CS-PEG-OMe (117 mg, 99% yield, 78% mass recovery, degree of PEGylation 1.1% by ^1H NMR) as a white foam: ^1H NMR (400 MHz, 2% DCl in D_2O, 300K) δ: 2.00-2.20

(m, 41.1H), 3.10-3.30 (m, 86H), 3.31-4.30 (m, 1040H), 4.55-4.70 (m), 4.80-4.95 (m). NMR experiments of CS samples were acquired at an Inova 400 Varian spectrometer operating at 400 MHz ^{1}H frequency. ^{1}H chemical shifts are reported in ppm referred to internal sodium 3-trimethylsilylpropane sulfonate (TSP). Mestre-C Software (Mestrelab Research) was used for spectral processing.

Synthesis of CS-PEG-Biotin

From a solution of CS·HCl (100.0 mg, 0.5 mmol), MeO-PEG-CO_2H (27.6 mg, 5.4 μmol), Biotin-PEG-CO_2H (2.4 mg, 0.6 μmol, 100 μL of a 24 mg/mL solution in H_2O) and NHS (3.4 mg, 30 μmol, 100 μL of a 34 mg/mL solution in H_2O) in H_2O (14.3 mL), and EDC (69.1 mg, 0.36 mmol), and following the same procedure as above, CS-PEG-Biotin (118 mg, 99% yield, 80% mass recovery, degrees of PEGylation by ^{1}H NMR: 1.0% for PEG-OMe, and 0.1% for PEG-Biotin) was obtained as a white foam: ^{1}H NMR (400 MHz, 2% DCl in D_2O, 300K) δ: 2.00-2.20 (m, 41.1H), 3.10-3.30 (m, 86H), 3.31-4.30 (m, 1010H), 4.55-4.70 (m), 4.80-4.95 (m).

Development of nanocapsules formulations

Preparation of the nanocapsule formulations

Blank CS-PEG-OMe nanocapsules were prepared by the solvent displacement technique following the procedure described previously by our group [8]. More specifically, 40 mg of Epikuron 145V were dissolved in 0.5 mL of ethanol. Afterwards 125 μL of Miglyol 812® and 9.5 mL of acetone were added. This organic phase was immediately poured over an aqueous phase composed of CS-PEG-OMe or CS-PEG-Biotin (0.05% w/v) and Pluronic 188 (0.25% w/v), and the corresponding CS-PEG-OMe or CS-PEG-Biotin nanocapsules were instantaneously obtained. Then, solvents were evaporated under vacuum to a constant final volume of 10 mL.

DCX-loaded nanocapsules were obtained as previously described by adding 0.5 mL of an ethanolic DCX solution (20 mg/mL) to the organic phase and following the procedure afore mentioned [9].

Characterization and concentration of DCX-loaded nanocapsules

The different formulations of nanocapsules were physicochemically characterized according to particle size, zeta potential, and drug association efficiency as previously described [9].

To accomplish the requirements for the *in vivo* dosing of DCX-loaded nanocapsules, and taking into account the limitation in the administration volume, it was necessary to increase considerably the DCX loading of the formulations. Therefore, purification and concentration processes had to be follow in order to increase the final DCX concentration from 0.1 mg/mL to 4 mg/mL. Firstly, CS-PEG-OMe and CS-PEG-Biotin nanocapsules were isolated by ultracentrifugation to eliminate the excess of free polymer. Afterwards, 5 mL of formulation were floated by ultracentrifugation at 20000 g for 1 h, and 3 mL of the resulting infranatant were removed. The remaining nanocapsule-rich fraction was dispersed in ultrapure water. The resultant nanocapsule suspension was concentrated under vacuum using a rotaevaporator to afford a final nanocapsule suspension with a DCX concentration of 4 mg/mL. The physicochemical properties of the concentrated nanocapsules were also determined.

The commercial formulation (Taxotere®) was prepared according to the manufacturer's instructions. Afterwards, it was diluted with ultrapure water to a final drug concentration of 4 mg/mL.

Preparation of CS-PEG-anti-TMEFF2 nanocapsules for in vitro experiments

CS-PEG-anti-TMEFF2 nanocapsules were obtained from CS-PEG-Biotin nanocapsules following a two-step functionalization procedure based on the avidin-biotin technology. Firstly, CS-PEG-Biotin nanocapsules were incubated with avidin, and the resulting avidin-coupled nanocapsules with the biotinylated anti-TMEFF2 mAb. More precisely, 4.0 mL of CS-PEG-Biotin nanocapsules were added to 36.3 mL of a solution of avidin (10.7 µg/mL) in Dulbecco´s Modified Eagle´s Medium (DMEM, Sigma). For the A549 cancer cell line, a 1:1 mixture of DMEM and Ham´s F12 Medium (Sigma) supplemented with 10% (v/v) of fetal bovine serum (FBS, GIBCO - Invitrogen) and 1% (v/v) of L-glutamine, penicillin, and streptomycin solution (GPS, Sigma) was used. The resulting mixtures were shaken in the dark for 90 min at room temperature. Afterwards, 91 µL of a solution of biotinylated anti-TMEFF2 mAb (1.0 mg/mL) were added to each mixture, and shaking continued for additional 90 min. As a result of the avidin and

anti-TMEFF2 mAb incubations, DCX-loaded CS-PEG-anti-TMEFF2 nanocapsule formulations with a final DCX concentration of 10.0 µg/mL were obtained.

Preparation of CS-PEG-anti-TMEFF2 nanocapsules for in vivo experiments

Nanocapsule formulations for *in vivo* experiments were obtained following a procedure analogous to the one described above for the *in vitro* experiments. Namely, 1.0 mL of CS-PEG-Biotin nanocapsules was added to 1.2 mL of a solution of avidin (320 µg/mL) in DMEM supplemented with 10% (v/v) of FBS and 1% (v/v) of GPS solution. The resulting mixture was shaken in the dark for 90 min at room temperature. Then, 378 µL of a solution of biotinylated anti-TMEFF2 mAb (1.0 mg/mL) were added, and shaking continued for additional 6 h. As a result of the avidin and anti-TMEFF2 mAb incubations, DCX-loaded CS-PEG-anti-TMEFF2 nanocapsule formulations with a final DCX concentration of 1.5 mg/mL were obtained.

***In vitro* cell culture studies**

Cell Culture

The human lung carcinoma derived cell line A549 was obtained from American Tissue Culture Collection (ATCC) and cultured in a 1:1 mixture of Dulbecco´s Modified Eagle´s Medium (DMEM, Sigma-Aldrich) and Ham´s F-12 Medium (Sigma-Aldrich), supplemented of 10 % (v/v) foetal bovine serum (FBS, GIBCO-Invitrogen) and 1 % (v/v) of L-glutamin, penicillin and streptomycin solution (GPS, Sigma-Aldrich). The human embrionic kidney derived cell line HEK293 was obtained from the same source and cultured with DMEM with same supplements as culture medium.

Cell Cycle Analysis

Distribution of cell cycle phases was determined measuring DNA content by flow cytometry after a propidium iodide staining as described [10]. Blank nanocapsules, free DCX, DCX-loaded nanocapsules, mAb functionalized DCX-loaded nanocapsules and free biotinylated mAb were tested as treatments at 100 nM or equivalent concentration and compared with control cells. Whole cells suspension were washed in PBS, fixed in 70 % ethanol overnight at 4º C and stained with 50 µg/mL propidium iodide (Calbiochem), 1 mg/mL RNase (Invitrogen), 0.1 Triton X-100 (Sigma-Aldrich). Fluorescence was measured in

FACScan cytometer (Becton Dickinson) and data were analized using ModFit software.

***In vivo* efficacy studies**

All experiments with animals were carried out under Santiago de Compostela University Bioethics Commite Rules and in compliance with Principles of Laboratoy Animal Care of national laws. Mice with severe combined immunodeficiency (SCID) between 8 and 14-weeks-old were used to grow xenotransplant flank tumors, one by mouse, by subcutaneous injection of 20 x 10^6 A549 tumor cells. For monitoring, tumors were measured three times weekly and the tumor volume was determined by the formula $V = (A \times B^2) / 2$, where A is the largest diameter and B is the shorter diameter measured by caliper. After 4-5 weeks, once the tumor volumes were ≥ 100 mm^3 and mean tumor size had reached 300 mm^3, mice were divided into four groups of eight mice for treatments, minimizing weight and tumor size differences. Tumor-bearing immunodefficient mice were treated by intratumoral injection of 9 mg/kg of free comercial DCX (Taxotere®, Sanofi Aventis), 9 mg/kg of DCX-loaded nanocapsules, 9 mg/kg of mAb-functionalized DCX-loaded nanocapsules, and controls were maintained without treatment. Treatments were administered in anesthetized mice by intra-peritoneal injection of 2,2,2-tribromoethanol-2-methyl-2-butanol (Avertine®, Sigma Aldrich) three times every four days for a complete dose of 27 mg/kg in all treatments. Mice were monitored for a maximum of 14 days after first dose to avoid excessive tumor burden, and mice weight and body weight loss were also monitored according with good laboratory practices to check excessive toxicity of treatments. Complete tumors of all animals were extracted and weighted at endpoint of efficacy studies.

RESULTS

In the present work we aimed at investigating the potential of the functionalization process of CS nanocapsules for a more selective effect of the anticancer drug DCX. The rationale behind this approach has been the previous evidence of the enhanced delivery and pharmacological effect of DCX when it was encapsulated in CS nanocapsules. As this uptake mechanism was shown to be non-selective, in this work we have developed an active targeting strategy by the modification of CS nanocapsules with the mAb anti-TMEFF2, in order to achieve a specific accumulation of the drug in the target cells.

Anti-TMEFF2 mAb development

cDNA codifiying for ECD-TMEFF2 were used to generate the mAb against TMEFF2 by DNA immunization of mice. Positive clones were isolated and tested. 11D1C1 clone was selected by flow cytometry assays. 11D1C1 clone was used to produce and purify the 11D1C1 anti-TMEFF2 mAb, wich conserved a clear recognition profile versus control without antibody in TMEFF2-overexpressing cells (Figure 1C).

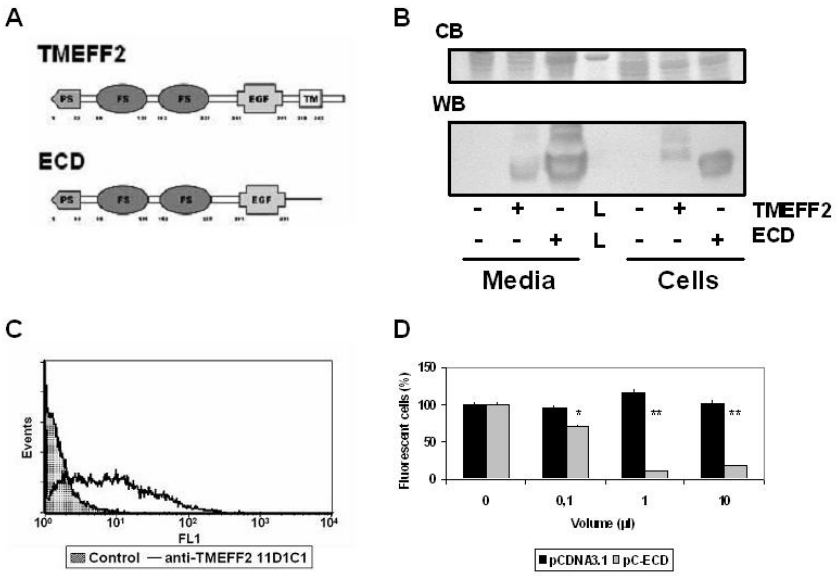

Figure 1. Anti-TMEFF2 mAb development. A) Schemathic structure of the two forms of the protein cloned for the study, the full protein (TMEFF2) and the histidine-tagged extracellular domain (ECD), with domains situation. PS: signal peptide, FS: follistatin-like domain, EGF: epidermal growth factor-like domain, TM: transmembrane domain. B) Characterization by Coomassie Blue staining (CB) and western-blotting (WB) of anti-TMEFF2 mAb 11D1C1 in TMEFF2 and ECD-overexpressing HEK293 cells, in culture medium and in cellular extracts. L: molecular weight ladder. C) Representative flow cytometry profile of anti-TMEFF2 mAb 11D1C1 staining versus control mAb in TMEFF2-overexpressing HEK293 cells. D) "Competition" flow cytometry of anti-TMEFF2 mAb 11D1C1 staining in TMEFF2-overexpressing HEK293 cells after incubation with conditioned media of ECD expression and control. * $p<0,05$ ** $p<0,01$.

Proteins of 374 and 307 aminoacids for TMEFF2 and ECD-TMEFF2 respectively (Figure 1A), including 6 x His tag in ECD-TMEFF2, were overexpressed in HEK293 cells and detected in 58 and 54 KDa by Coomassie

Blue staining and Western blotting under reducing conditions, both in cell extracts and in culture media (Figure 1B). These sizes and broad bands are characteristic of these proteins and they are motivated for the presence of disulfide bonds in the follistatin-like and EGF-like domains, and for glycosylation as post-translational modification.

To be sure of the recognition of the native form of TMEFF2 by the 11D1C1 mAb we performed binding assays of the antibody with different quantities of conditioned medium with ECD, the soluble form of the protein. Subsequent flow cytometry analysis of the blocked mAb confirmed that binding with the soluble ECD significantly decreases its binding capacity in posterior process (Figure 1D). All these data of affinity and selectivity together support the use of 11D1C1 mAb as a targeting molecule for the functionalization of the nanocapsules and for their guiding to TMEFF2-expressing cells.

The design and development of mAb functionalized nanocapsules

For the preparation of the CS-PEG-Biotin nanocapsules functionalized with the anti-TMEFF2 mAb we have relied on the strong non-covalent interaction associated with avidin-biotin (K_D=10^{-15} M^{-1}) [11]. With this aim, we have followed the strategy depicted in Figure 2 where CS-PEG-Biotin nanocapsules, incorporating biotin at the end of some of the PEG chains, were firstly incubated with tetrameric

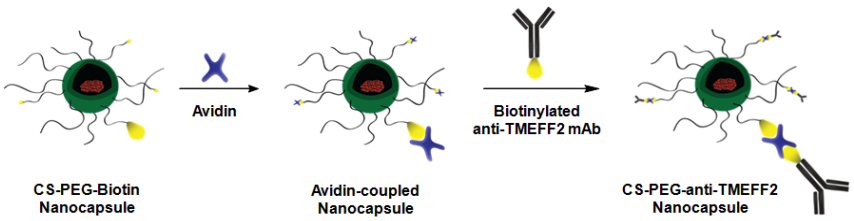

Figure 2. Functionalization of CS-PEG-Biotin nanocapsules with anti-TMEFF2 mAb.

avidin, and afterwards with a biotinylated anti-TMEFF2 mAb. Similar approaches have been recently executed successfully by us and other authors in the preparation of PEGylated immuno-nanoparticles from various polymers, including CS [12-14]. The advantages of such a strategy include an absolute control of the location and density of the mAb at the periphery of the nanocapsules to ensure an effective ligand-receptor interaction [15].

CS-PEG synthesis

The required CS-PEG-Biotin copolymer, incorporating biotin at the end of some of the PEG chains, has been prepared by the simultaneous grafting of Biotin-PEG-CO_2H (M_n 4030) and MeO-PEG-CO_2H (M_n 5114) to the amino groups of a low molecular weight CS (M_w $1.3 \cdot 10^4$) in the presence of EDC and NHS (Scheme 1) [2]. By controlling the reaction conditions and the ratio between the two PEG chains, degrees of PEGylation of 1.0% for PEG-OMe and 0.1% for PEG-Biotin were obtained in the resulting graft copolymer as determined by ^1H NMR. In the same way, a CS-PEG-OMe copolymer with identical degree of PEGylation, but lacking biotin tags, has been prepared for control experiments.

Nanocapsules preparation method and characterization

CS-PEG-OMe and CS-PEG-Biotin nanocapsule formulations were obtained following the solvent-displacement technique. This procedure allows the formation of a coating constituted by CS-PEG-OMe or CS-PEG-Biotin around the oily droplets (formed by lecithin and Miglyol® 812) due to the ionic interactions between the negatively charged lipophilic surfactant (lecithin) and the positively charged CS. All of the formulations studied showed very similar values of particle size, with a mean value around 200 nm. The zeta potential was also highly positive due to the CS layer surrounding the cores.

Table 1: Physicochemical properties of unprocessed and processed blank CS-PEG-OMe, docetaxel (DCX)-loaded CS-PEG-OMe and DCX-loaded CS-PEG-Biotin nanocapsules. PI: polydispersity index. Values are given as mean ± s.d.; n=3.

	UNPROCESSED			PROCESSED		
	Size (nm)	PI	Z-Potential (mV)	Size (nm)	PI	Z-potential (mV)
Blank CS-PEG-OMe NCs	160 ± 2	0.1	39 ± 2	186 ± 20	0.2	32 ± 5
DCX-loaded CS-PEG-OMe NCs	155 ± 5	0.1	33 ± 6	197 ± 24	0.2	27 ± 9
DCX-loaded CS-PEG-Biotin NCs	161 ± 10	0.1	27 ± 6	204 ± 20	0.2	25 ± 5

Afterwards, an optimization of the DCX-loaded nanocapsules formulation was carried out in order to increase the drug loading which was essential to achieve the required dosing for the subsequent *in vivo* experiments. As expected, the incorporation of DCX to the nanocapsules did not modify their

physicochemical characteristics, even at high drug to polymer ratios. The reservoir structure of the system allowed the inclusion of the hydrophobic molecule DCX in the inner core, enabling the scaling up of the formulation from an initial drug loading of 0.05 % to a final value of 2.8 % in the processed nanocapsule formulation.

Moreover, the different formulations were also concentrated facing the *in vivo* experiments. The concentration process of the nanosystems induced a slight increase in particle size, although the surface remained still positive, confirming the presence of a CS coating in the processed nanocapsules (Table 1).

mAb decoration of nanocapsules

With a reliable method for the preparation of DCX-loaded nanocapsules in hand, we decided to face their decoration with the anti-TMEFF2 mAb. With this aim, the mAb was firstly biotinylated with Biotin-$(PEG)_4$-NHS (Scheme 1), a water-soluble reagent carrying an active ester for amine functionalization. Since the biotin binding site of avidin is located 9 Å below its surface, the presence of the short polyethylene glycol (PEG) linker was envisaged to facilitate the interaction of the resulting biotinylated mAb with avidin. Both the incorporation of biotin to anti-TMEFF2 mAb and the recognition of the conjugate by avidin have been demonstrated colorimetrically by means of the avidin-HABA assay, a technique based on the stoichiometric displacement of the dye HABA by biotin in the avidin-HABA complex [4]. According to these experiments, an average of 3.0 accessible biotin labels per mAb resulted, what represents a standard density for bioconjugation purposes.

CS-PEG-Biotin nanocapsules were consecutively incubated with avidin and the biotinylated anti-TMEFF2 mAb. The use of substoichiometric amounts of both proteins not only ensured their complete incorporation, but also avoided the necessity of subsequent purification steps. In the formulations for *in vitro* experiments, a PEG-Biotin:avidin:anti-TMEFF2 mAb ratio 100:65:6.5 was employed, which rendered CS-PEG-anti-TMEFF2 nanocapsules with an mAb density of 2.3 μg/mL, and a DCX loading of 10.0 μg/mL. These nanocapsules resulted to be stable by DLS (MilliQ water, 25 ºC), as neither sign of aggregation, nor change in hydrodynamic size and polydispersity index were observed.

Incubation of the more concentrated formulations for *in vivo* experiments under identical PEG-Biotin:avidin:mAb ratio (100:65:6.5) led to aggregation of

nanocapsules by DLS. However, by reducing the density of tetrameric avidin (ratio 100:2.8:2.8), stable nanocapsules by DLS (MilliQ water, 25 ºC) were obtained, carrying a mAb density of 145 µg/mL, and a DCX loading of 1.5 mg/mL.

In vitro cellular assays

The efficacy of the different formulations of nanocapsules was determined by flow cytometry assays in which we evaluated the percentage of cells in each phase of the cell cycle after their treatment with the different formulations. These experiments will assess the efficacy of the DCX loaded formulations by measuring the population of cells arrested in the G2/M phase as a consequence of the action of the drug. Moreover, the safety of the controls formulations could be also determined.

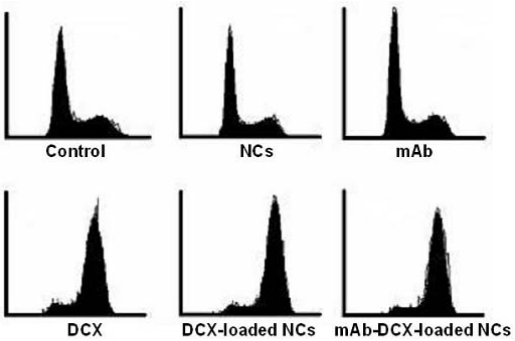

	G0/G1	S	G2/M
Control	59,3 ± 2,3	29,7 ± 1,7	11,1 ± 1,1
NCs	58,8 ± 2,3	30,6 ± 1,7	10,7 ± 0,9
mAb	61,9 ± 0,8	30,3 ± 2,5	8,5 ± 1,4
DCX	4,2 ± 1,9	25,0 ± 3,6	70,8 ± 5,5
DCX-loaded NCs	2,3 ± 0,8	25,8 ± 2,3	72,1 ± 3,4
mAb-DCX-loaded NCs	3,1 ± 0,8	26,9 ± 5,8	70,0 ± 3,4

Figure 3. Representative flow cytometry profiles of the cell cycle phase distribution of A549 cells after treatment with blank nanocapsules (NCs), anti-TMEFF2 mAb (mAb), docetaxel (DCX), docetaxel-loaded nanocapsules (DCX-loaded NCs), anti-TMEFF2 mAb functionalizated docetaxel -loaded nanocapsules (mAb-DCX-loaded NCs) and fresh medium (Control) for 48 h. The table shows the mean ± standard deviation of cell cycle percentage of three independent experiments.

Figure 3 shows the cell cycle distribution of the A549 tumor cells after treatment with DCX-based systems (DCX, DCX-loaded nanocapsules and functionalized mAb-DCX-loaded nanocapsules). These formulations were able to accumulate cells in the G2/M phase, in contrast of cells treated with blank NCs, free mAb and control cells without treatment that conserved the normal profile. The results herein exposed indicate that both formulations of nanocapsules were as effective as the free drug. Additionally, cells treated with blank nanocapsules

had a profile similar to the control cells, suggesting that the nanocapsules caused no toxic effects to the cells.

In vivo efficacy studies using mouse NSCLC xenograft model

We next evaluated the efficacy of the formulations using a xenograft model of NSCLC developed by s.c. injection of A549 in the flank of SCID mice and developed comparative efficacy studies. Using commercial docetaxel (Taxotere®)

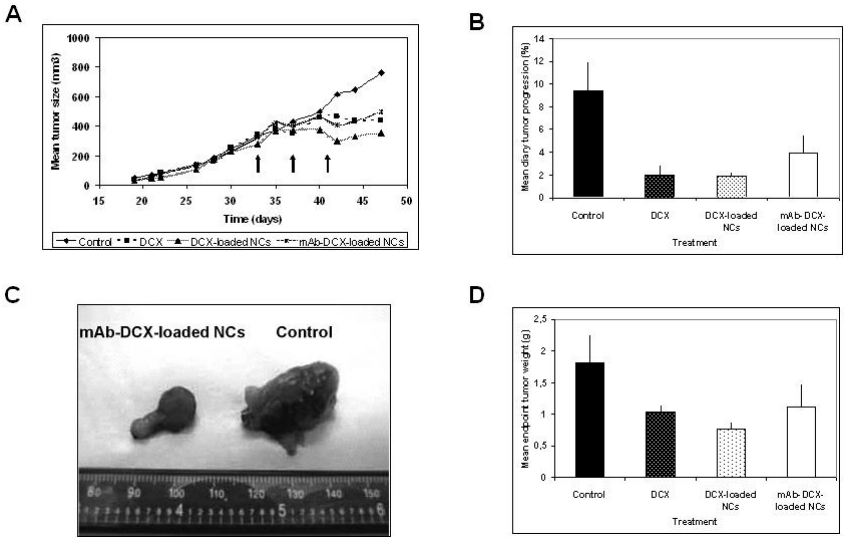

Figure 4. Comparative efficacy study in A549 tumor xenograft model of commercial docetaxel (Taxotere®, Sanofi Aventis) (DCX), 9 mg/kg of docetaxel-loaded nanocapsules (DCX-loaded NCs), 9 mg/kg of anti-TMEFF2 mAb-functionalized docetaxel-loaded nanocapsules (mAb-DCX-loaded NCs), meanwhile controls were maintained without treatment. A) Mean volume progression of the four groups (black arrows point the injection days. B) Evaluation of the diary tumor progression in the 14 days of treatment for the formulations tested (Mean ± SEM). C) Representative image of extracted tumors at endpoint of anti-TMEFF2 mAb functionalizated docetaxel-loaded nanocapsules treated tumor versus control tumor. D) Mean ± SEM tumor weight of the four groups at endpoint.

as reference point, the following regimens were administered: nothing in control group, DCX (Taxotere®), DCX-loaded nanocapsules and mAb-DCX-loaded nanocapsules, all of them by 3 intratumoral injections for a total dose of 27 mg/kg. The results in tumor volume monitoring showed that all of the 3 DCX-based treatments were efficient stopping tumor development compared with control group (Figure 4A). Moreover, Figure 5 shows that the decrease of tumor volume

was statistically significant for the DCX-based systems compared to the control group.

In addition, we used the mean diary tumor progression value to show this effect of the treatments during the 14 days from the first dose to the endpoint of the experiment. The three treatments with DCX achieved a reduction of the same magnitude, from 2.25 times in mAb-DCX-loaded nanocapsules to 4.5 times in DCX and DCX-loaded nanocapsules versus control (Figure 4B). These data were consistent with size and weight of extracted tumors after the experiment, with clearly smaller tumors in the 3 treatments with DCX (Figure 4C). In terms of tumor weight, the treatments decreases tumor growth to the half, from 1.8 g of mean in control group to 0.8-1.0 g in treated groups (Figure 4D).

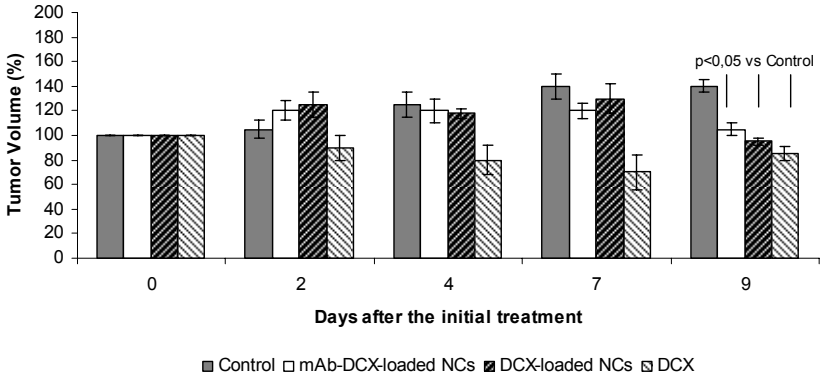

Figure 5. Treatment effects in animal model. A) Mean mice body weight after treatment with the formulations: commercial docetaxel (Taxotere®, Sanofi Aventis) (DCX), docetaxel-loaded nanocapsules (DCX-loaded NCs), anti-TMEFF2 mAb-functionalized docetaxel-loaded nanocapsules (mAb-DCX-loaded NCs), and controls (black arrows point the injection days). B) Automatized biochemistry of mice blood samples of the four groups and wild type mice (WT) without tumor xenografts. The table shows the mean results of two to four animals for each group.

We have also analyzed the effect of any single injection in tumor size in order to clarify the differential pharmacodinamic between free DCX and the encapsulated forms. The first dose did not result in any significant effect of the DCX-based treatments versus control, probably due to the low dose of DCX (9 mg/kg) in all treatments when the maximum tolerated dose (MTD) of docetaxel is 40 mg/kg i.v., as well as to the short time of measurement between doses, only four days. After second dose, we clearly observed the free DCX effect translated in mean tumor size reduction and still no effect was detected in any of the

encapsulated DCX treatments. Instead of this, after the third dose, the effect of free DCX was reduced, meanwhile both encapsulated DCX treatments showed tumor size reduction; dramatically in case of DCX-loaded nanocapsules that achieve a 12 % of reduction in tumor size (Figure 6). This data suggest that free DCX has faster effect but in shorter time and that encapsulated DCX-based treatments need more time to achieve their effect but they can continue their antiproliferative action for longer periods of time.

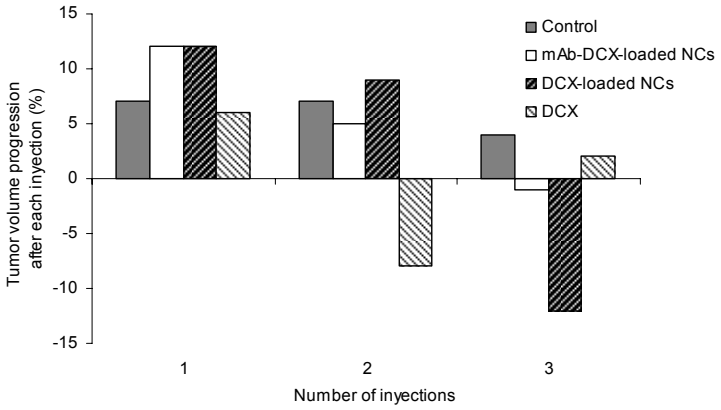

Figure 6. Variation in tumor size after each single injection of commercial docetaxel (Taxotere®, Sanofi Aventis) (DCX), docetaxel-loaded nanocapsules (DCX-loaded NCs), anti-TMEFF2 mAb-functionalized docetaxel-loaded nanocapsules (mAb-DCX-loaded NCs), and control.

REFERENCES

1. Royer G.P.; Anantharmaiah G.M. (1979). Peptide synthesis in water and the use of immobilized carboxypeptidase Y for deprotection. J. Am. Chem. Soc. 101: 3394-3396.
2. Fernandez-Megia E.; Novoa-Carballal R.; Quiñoá E.; Riguera R. (2007). Conjugation of bioactive ligands to PEG-grafted chitosan at the distal end of PEG. Biomacromolecules. 8: 833-842.
3. Smith G.P. (2006). Kinetics of amine modification of proteins. Bioconjug. Chem. 17: 501-506.
4. Green N.M. (1965). A Spectrophotometric Assay for Avidin and Biotin Based on Binding of Dyes by Avidin. Biochem. J. 94: 23c-24c.
5. Janes K.A.; Alonso M.J. (2003). Depolymerized Chitosan Nanoparticles for Protein Delivery: Preparation and Characterization. J. Appl. Polym. Sci. 88: 2769-2776.
6. Lamarque G.; Lucas J.M.; Viton C.; Domard A. (2005). Physicochemical behavior of homogeneous series of acetylated chitosans in aqueous solution: Role of various structural parameters. Biomacromolecules. 6: 131-142.
7. Schatz C.; Viton C.; Delair T.; Pichot C.; Domard A. (2003). Typical physicochemical behaviors of chitosan in aqueous solution. Biomacromolecules. 4: 641-648.
8. Prego C.; Torres D.; Alonso M.J. (2006). Chitosan nanocapsules: a new carrier for nasal peptide delivery. J. Drug Del. Sci. Tech. 16: 331-337.
9. Lozano M.V.; Torrecilla D.; Torres D.; Vidal A.; Domínguez F.; Alonso M.J. (2008). Highly efficient system to deliver taxanes into tumor cells: Docetaxel-loaded chitosan oligomer colloidal carriers. Biomacromolecu les. 9: 2186-2193.
10. Vidal A.; Sean Millard S.; Miller J.P.; Koff A. (2002). Rho activity can alter the translation of p27 mRNA and is important for RasV12-induced transformation in a manner dependent on p27 status. J. Biol. Chem. 277: 16433-16440.
11. Savage M.D.; Mattson G.; Desai S.; Nielander G.W.; Morgensen S.; Conklin E.J. (1992). Avidin-Biotin Chemistry: A Handbook. Rockford, Illinois, Pierce Chemical Company.
12. Aktas Y.; Yemisci M.; Andrieux K.; Gürsoy R.N.; Alonso M.J.; Fernandez-Megia E.; Novoa-Carballal R.; Quiñoá E.; Riguera R.; Sargon M.F.; Çelik H.H.; Demir A.S.; Hincal A.A.; Dalkara T.; Çapan Y.; Couvreur P. (2005). Development and brain delivery of chitosan-PEG

nanoparticles functionalized with the monoclonal antibody OX26. Bioconjug. Chem. 16: 1503-1511.

13. Wartlick H.; Michaelis K.; Balthasar S.; Strebhardt K.; Kreuter J.; Langer K. (2004). Highly specific HER2-mediated cellular uptake of antibody-modified nanoparticles in tumour cells. J. Drug Target. 12: 461-471.
14. Gref R.; Couvreur P.; Barratt G.; Mysiakine E. (2003). Surface-engineered nanoparticles for multiple ligand coupling. Biomaterials. 24: 4529-4537.
15. Allen T.M.; Hansen C.B.; Stuart D.D. (1998). Targeted sterically stabilized liposomal drug delivery. D. D. Lasic; D. Papahadjopoulos. Amsterdam, Elsevier Science B. V. 4.6.

Annex II

Characterization of Core-Shell Lipid-Chitosan and Lipid-Poloxamer Nanocapsules

M.J. Santander-Ortega[1], M.V. Lozano-López[2], D. Bastos-González[1], J.M. Peula-García[3], J.L. Ortega-Vinuesa[1*].

[1]*Biocolloid and Fluid Physics Group, Department of Applied Physics, University of Granada, 18071 Granada, Spain*

[2]*Department of Pharmacy and Pharmaceutical Technology, University of Santiago de Compostela, 15782 Santiago de Compostela, Spain.*

[3]*Department of Applied Physics, University of Málaga, 29071 Málaga, Spain.*

* Corresponding author: Dr. J.L. Ortega-Vinuesa.

ABSTRACT

In this paper, different core-shell structured lipid nanocapsules have been synthesized and characterized looking for incoming applications of these systems as drug carriers. Although this type of carriers have already been used as delivery systems, it is difficult to find in the literature a deep physicochemical characterization of them. Hence, the aim of this work was to achieve a deeper knowledge of the properties of these colloidal particles, paying special attention to the role played by the components that constituted them. Lipid nanocapsules were formed by a triglyceride-lecithin core surrounded by a chitosan and/or poloxamer (Pluronic® F68) shell. Four different systems were formulated by varying the chitosan and poloxamer contents. The electrokinetic characterization and the colloidal stability studies revealed that Pluronic® F68 presented a secondary role during the nanocapsule formation, obtaining final systems with low incorporation of poloxamer. However, the incorporation of chitosan was very significant in all cases. In addition, the stability studies, performed not only in ideal solutions but also in simulated physiological fluids, showed that hydration forces play a crucial role to maintain the integrity of these nanocapsules under physicochemical conditions that match those found in real physiological fluids.

I. INTRODUCTION

The research in Nanotechnology has intensively increased in the last three decades. Colloidal carriers, such as liposomes, nanoparticles and polymeric micelles [1-3], have been widely investigated for drug delivery applications. Although vesicular systems, mainly nanoemulsions and nanocapsules, experimented a contemporary finding compared to other nanosystems, their development has not been so wide. Nevertheless, they are lately receiving increasing attention in different fields such as cosmetics or as drug carriers.

Nanoemulsions are vesicular reservoir systems formed by an oil or aqueous core, which is surrounded by a thin polymeric membrane in case of nanocapsules. Therefore, highly hydrophobic drugs are likely to be encapsulated in lipidic cores [4] or hydrophilic molecules in case of aqueous core nanocapsules [5]. The versatility of these systems for the encapsulation of a wide variety of drugs such as low molecular weight molecules, peptides or gene material enlarges their appealing characteristics [6-8]. On the other hand, the presence of a thin polymeric shell surrounding the inner compartment exhibited by nanocapsules in comparison to nanoemulsions, awards higher drug protection from degradation by preventing direct contact of the encapsulated drug with the environment. Moreover, the polymeric shell is crucial in the long term stability of the system [9]. The shell can be formed by a wide variety of polymers capable to stabilize the oil/water emulsion and to confer stability, long-circulating properties after intravenous administration, and to modulate the interaction of the nanosystems with the biological environment at which they are immersed.

A major drawback after intravenous injection of drug delivery systems is their recognition by the mononuclear phagocytes system (MPS) with the subsequent undesirable accumulation of the colloidal carriers in the liver or the spleen. This problem can be overcome by using the so-called *Stealth*® nanosystems, which have reduced opsonization by grafting onto their surfaces non-ionic amphiphilic macromolecules, for example polyethylene glycol (PEG) derivatives [10]. In addition to the previous strategy, nanosystems surface can be modified by adsorbing cationic polymers that offer additional advantages over the conventional negatively charged emulsions [11], like the improvement of the nanocapsules interaction with different epithelia. Thus, it has been proved that cationic nanosystems interact more intensely with the negatively charged cell membranes of skin, eye, and gastrointestinal mucosa [12; 13], leading to better uptake of the encapsulated drug. Therefore, obtaining nanocapsules with a combined PEG-cationized shell would be desirable.

With this scenario in mind, the goal of the present investigation was to perform a deep characterization study of chitosan nanocapsules containing a polyoxyethylene/cationized shell, to determine their *in vitro* properties as possible vehicles for either oral or intravenous administration. Therefore, the present study was mainly focused on analysing the colloidal stability of these systems, since the aggregation induced by the physicochemical characteristics of the physiological medium would hamper the effectiveness of the carriers.

Therefore, we have studied four systems of nanocapsules characterized by the progressively increasing complexity of their shell nature. All of them shared the same oil core, composed by medium-chain triglycerides – that were liquid at room and physiological temperature – and emulsified by lecithin. The first system was constituted by this simple nanoemulsion where lecithin molecules located at the oil/water interface acted by themselves as stabilizers. The second system was formed adding a polyoxyethylene derivative emulsifier in order to supply some *Stealth*® properties to the lipid core. Pluronic® F68 poloxamer was chosen for this purpose. A cationic shell was sought for the third system; in this case, chitosan was thought to be an ideal candidate due to its advantageous biological properties, such as biodegradability, biocompatibility, and nontoxicity [14; 15]. Finally, the fourth system was formed by adding simultaneously both poloxamer and chitosan chains in order to achieve a heterogeneous shell where the previously described favourable effects given by both types of molecules would coexist. It is also important to take into account that the components of the formulations are safe and biodegradable (polysaccharides and lipids), which are essential characteristics for future *in vivo* studies and other applications of the systems.

II. MATERIALS AND METHODS

2.1. Reagents.

In order to study the electrophoretic mobility and colloidal stability at different pH values, several buffered solutions with a low ionic strength (I = 0.002 M) were prepared: pH 4 and 5 were buffered with acetate, pH 6 and 7 with phosphate, and pH 8 and 9 with borate. In some cases, stability was evaluated in simulated protein free physiological fluids: simulated gastric (pH 1.2) and intestinal (pH 6.8) fluids were prepared according to the USP XXIX. Hanks buffer was used for simulating plasma physicochemical conditions. Nanocapsule hydrophobic core was formed by the oil Miglyol 812®, kindly donated by Sasol Germany GmbH

(Germany), and by Epikuron 145V (which is deoiled, wax-like, phosphatidilcholine enriched fraction of soybean lecithin (min 45% phosphatidilcholine)) that was donated by Cargill (Spain). Pluronic® F68 was acquired from Sigma-Aldrich (Spain). Protasan® Cl 113, medium molecular weight chitosan chloride salt (medium Mw chitosan) with a deacetylation degree of 85%, was supplied from FMC Biopolymer Novamatrix (Norway). All the chemicals and electrolytes used were of the highest grade commercially available.

2.2. Nanocapsules synthesis.

The nanosystems herein studied were prepared by the solvent displacement technique following the procedure previously described by Prego *et al*. [16]. This is a well-known technique widely reported for the preparation of nanocapsules. Traditionally, hydrophilic surfactants should be presented in the aqueous phase before the emulsion formation [17; 18]. These molecules were responsible of the nanocapsules properties and their future stability [19].

The procedure used consisted on the preparation of an organic phase constituted by 40 mg of Epikuron 145V dissolved in 0.5 ml ethanol, 125 µl of Miglyol 812® and 9.5 ml of acetone. This organic phase was immediately poured onto an aqueous phase that had different components depending on the systems formulated. Therefore, the composition of this solution determined the interfacial properties of the nanocapsules obtained. For example, when nothing was added to the aqueous phase, a nanoemulsion formed by Miglyol® cores stabilized by lecithin external layers was obtained. This nanoemulsion will be referred to as "LC" hereafter. When the aqueous phase contained Pluronic® F68 at a 0.25% w/v concentration, a nanoemulsion (called "PX") coated by poloxamer shells was generated. The presence of chitosan (0.05% w/v) as the only component in the aqueous phase yielded nanocapsules that were named "CS". Finally, the forth system, called "CS+PX", was obtained by mixing chitosan and Pluronic® F68 (at the same concentrations mentioned above for the other systems) in the aqueous phase.

2.3. Size and storage stability.

The average size of the nanocapsules was determined by photon correlation spectroscopy (PCS) with a commercial light-scattering setup, 4700C, Malvern Instruments (Malvern, UK), with an argon laser of wavelength λ_0 = 488 nm,

working at a fixed angle (90º) at 25ºC. PCS gives information about the average diffusion coefficient of the particles, which can be easily related to the mean diameter (∅) by using the Stokes-Einstein equation for spheres. The mean diameter of the four systems in purified water (pH~5.8, 25ºC) was $\varnothing_{LC}$ = (118 ± 4) nm, $\varnothing_{PX}$ = (153 ± 3) nm, $\varnothing_{CS}$ = (212 ± 9) nm, and $\varnothing_{CS+PX}$ = (196 ± 5) nm. At present, there is no doubt on the fact that the size is a critical variable for the nanosystems to cross biological barriers and to elude their uptake by macrophages [14; 20; 21]. Generally, a mean diameter around 200 nm is advised in specialised literature. In this sense, all of the systems are potentially useful for future *in vivo* applications. The average size of the four samples – which was measured each week – was constant for months (data not shown), which is an indication of high stability, at least when kept in the storage medium (purified water, 4ºC).

2.4. Electrophoretic mobility.

A ZetaPALS instrument (Brookhaven, USA) was used to measure the electrophoretic mobility (μ_e). The study was focused on measuring the μ_e as a function of pH keeping constant a low ionic strength value (0.002 M). Each μ_e mobility data was obtained by averaging 45 individual measurements.

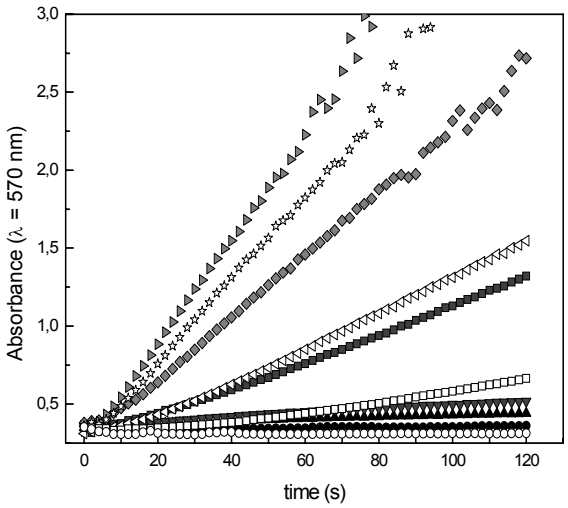

Figure 1a. Variation of the optical absorbance with time for the PX sample at different $CaCl_2$ concentrations (pH7): (●) 2.5 mM; (▲) 5 mM; (▼) 7.5 mM; (■) 12.5 mM; (◆) 18.8 mM; (▶) 37.5 mM; (★) 50 mM; (◁) 87.5 mM; (□) 125 mM; and (○) 500 mM.

2.5. Colloidal stability.

NaCl and $CaCl_2$ were used as destabilizing agents. According to the classical DLVO theory [15], a salinity increment triggers the coagulation of a lyophobic colloidal system. During aggregation, the turbidity of the system increases when the average size of the scattering particles increases. Therefore, a simple spectrophotometer (Beckman DU 7400) working with a visible wavelength (λ = 570 nm) is clearly able to detect and to analyze the aggregation kinetics. Figure 1a shows a typical coagulation experiment, in which the PX sample was forced to aggregate at different $CaCl_2$ concentrations. Information about the kinetics aggregation constant "*k*" of dimmer formation can be derived from these curves. The initial slopes of the *absorbance vs time* curves (dAbs/dt) can be directly related to *k* by [22; 23]:

$$\frac{dAbs}{dt} = \frac{\left(C_2/2 - C_1\right) N_0^2 \, l}{2.3} k \qquad (1)$$

where C_1 and C_2 are the scattering cross-sections of a monomer and a dimmer, respectively, N_0 is the initial particle concentration, and *l* is the optical path through the cuvette. Nevertheless, stability is usually evaluated by calculating the Fuchs factor (*W*), instead of calculating the *k* values by using equation 1. The

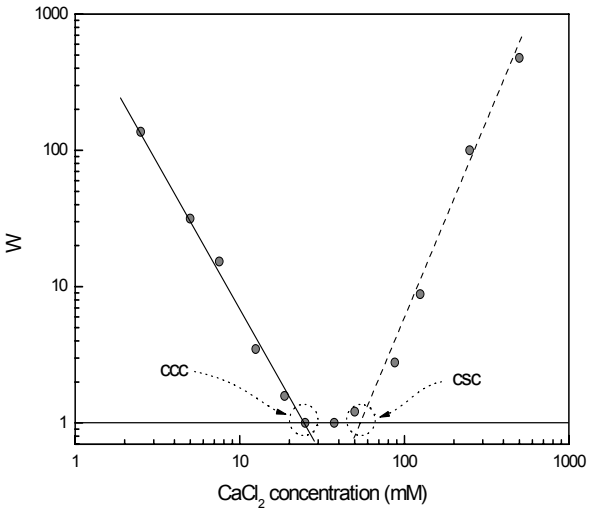

Figure 1b. Dependence of the stability factor (W) on the $CaCl_2$ concentration for the PX sample at pH7. Lines serve to guide the eye for locating the ccc and csc values.

Fuchs factor (also called “stability factor”) can be experimentally obtained by:

$$W = \frac{k_f}{k_s} = \frac{(dAbs/dt)_f}{(dAbs/dt)_s} \quad (2)$$

where “k_f” refers to the fastest aggregation kinetics constant, and the subscript “*s*” refers to slower coagulation rates. Therefore, when $W = 1$ the system is completely unstable, while $W = \infty$ indicates total stability. It is easy to calculate the Fuchs factor at every salt concentration from those data shown in Figure 1a, and using equation 2. This is shown in Figure 1b, where the dependence of W on the $CaCl_2$ concentration has been plotted. The double-logarithmic scale becomes very useful to estimate the critical coagulation concentration (ccc) and the critical stabilization concentration (csc), which are fundamental parameters in colloidal stability studies. The ccc value is related to destabilization processes and it indirectly gives information about the surface charge density of the particles; a low ccc means low stability. However, the csc value – defined as the minimum salt concentration at which the system begins to re-stabilize when salinity is increased even more – is associated to the surface hydrophilicity. This kind of restabilization phenomenon at high salt concentration is well known in colloidal systems, and it is governed by hydration forces [24-29]. For a specific electrolyte, the lower the csc, the higher the hidrophilicity of the particle surface.

III. RESULTS AND DISCUSSIONS

The analysis of the particle size values (shown in the previous section) can give initial information about the role played by poloxamer and/or chitosan during the nanocapsule formation. Lecithin appears to be the best emulsifier, since the mean diameter was lower when this molecule acts by itself stabilizing the formulation (see the LC case). Poloxamer, however, seems to be a poorer emulsifier than lecithin because when both surfactants were mixed the particle size increased (see the PX diameter). This size increment became even higher when chitosan (instead Pluronic® F68) was added together with lecithin. In this case, the positive chitosan chains can interact electrostatically with the negative lecithin molecules reducing the effective concentration of this last emulsifier and, consequently, producing bigger nanocapsules (see CS). Finally, when poloxamer was also added together with chitosan and lecithin (CS+PX) the mean diameter values practically coincided with the CS sample. This suggests that the non-ionic

surfactant does not play any role in this blend formulation, and subsequently, the nanocapsule size only depends on the chitosan/lecithin mixture. As will be shown afterwards, the electrophoretic mobility and stability data appear to corroborate that Pluronic® F68 is practically unable to anchor at the NC/water interface in the CS+PX system.

The next set of experiments was designed to establish the electrical state of the nanocapsules at different pH values. The electrophoretic mobility data, obtained at low ionic strength media, are shown in Figure 2. We will analyse the results sample by sample. The LC nanocapsules showed a typical behaviour of colloids with weak acid groups at the surface, giving lower μ_e values at acid pH than those obtained at neutral and basic pH. These results are in agreement with the nature of the shell of these capsules, which is exclusively formed by lecithin, (note that lecithin is a mixture of phospholipids that contains negatively charged components, although the major component is phosphatidylcholine).

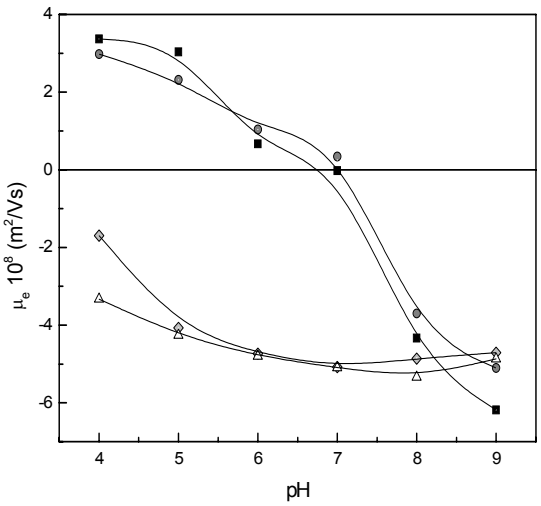

Figure 2. Electrophoretic mobility versus pH for the (△) LC, (◇) PX, (●) CS, and (■). CS+PX samples.

Surprisingly, when Pluronic® F68 is added to the formulation, the mobility of the resulting capsules (see the PX case in Figure 2) is almost identical to the LC sample. A μ_e reduction was expected after the incorporation of this non-ionic surfactant onto the lecithin surface, since the presence of PEO chains would shift outwards the shear plane where the ζ-potential is defined, which subsequently

would diminish the electrophoretic mobility. At least, for PLGA particles the μ_e reduction was significant and directly related to the poloxamer coating [30]. Only at pH4, a decrease of the mobility (with regard to the LC case) is observed. The similar μ_e behaviour among these two samples (excepting the pH 4 data) suggests the low poloxamer incorporation onto the particle surface, probably because that the lecithin shell supplies an important hydrophilic character to the surface that hinders the adsorption of this non-ionic surfactant (note that for uncharged polymers, as Pluronic® F68, adsorption only can be led by hydrophobic interactions). Similar reasoning can be applied when comparing the μ_e results of the CS and CS+PX systems. We will start analysing the CS sample. Incorporation of chitosan seems to be clearly effective when this polysaccharide is added to the formulation. Mobility of the LC nanocapsules radically changes in presence of chitosan chains (see the CS curve in Figure 2), yielding particle surfaces that show mobility behaviours totally similar to those obtained with pure chitosan nanogels [31]. It can be seen that mobility goes from positive values (at acid pH) to large negative values at more basic pH, presenting an isoelectric point (i.e.p.) at pH 7. The positive charge of nanocapsules is provided by the glucosamine groups of chitosan, which present weak basic character. At basic pH, chitosan chains are uncharged, so the negative μ_e may come from the phosphate groups of lecithin. These μ_e results suggest a shell structure practically formed (in its outer part) by a chitosan layer. The clear incorporation of this polycationic polymer at the nanocapsule shell can be understood by considering the attractive interaction existing between the (negative) lecithin and the (positive) chitosan molecules. Sonvico *et al.* [32] have experimentally evidenced a strong electrostatic interaction between these two components, which are capable to form by themselves self-organized lecithin/chitosan nanoparticles by means of purely ionic interactions. On the other hand, the CS+PX sample practically match the CS mobility, which would indicate a very low or almost negligible incorporation of poloxamer when this surfactant is added during the synthesis process (note that both chitosan and Pluronic® F68 chains are simultaneously added to the formulation, and thus, a competitive adsorption onto an enriched lecithin layer must take place). In this competitive situation chitosan molecules are much more attracted by the negatively charged lecithin layer than poloxamer, which does not experiment any specific attraction (neither by means of electrostatic nor hydrophobic interactions) toward the hydrophilic surface of the nanocapsules. Therefore, is reasonable to believe that the surface will be mainly coated by chitosan, remaining the poloxamer molecules dissolved (or forming micelles) in the bulk solution. As will be shown, the stability experiment will confirm this assumption. Finally, as the isoelectric point for the CS and CS+PX nanocapsules

was around pH 7, it is more than likely that these samples become unstable at neutral pH, unless the action of any steric contribution could prevent the system coagulation.

Table 1a. Critical coagulation concentration (ccc) and critical stabilization concentration (csc) data, in mM units of *LC* and *PX* at different pH values.

	LC				PX			
	NaCl		$CaCl_2$		NaCl		$CaCl_2$	
	ccc	csc	ccc	csc	ccc	csc	ccc	Csc
pH4	100	---	10	220	~200	~	18	60
pH7	310	1000	10	150	- stable -		21	53
pH9	- stable -		12	>40	- stable -		12	90

Table 1b. Critical coagulation concentration (ccc) and critical stabilization concentration (csc) data, in mM units of *CS* and *CS+PX* at different pH values.

	CS				CS + PX			
	NaCl		$CaCl_2$		NaCl		$CaCl_2$	
	ccc	csc	ccc	csc	ccc	csc	ccc	csc
pH4	32	280	10	20	32	235	10	20
pH7	*- aggr. -*		*- aggr. -*		*- aggr. -*		*- aggr. -*	
pH9	20	---	6	40	30	---	7	40

In the third set of experiments the colloidal stability was studied at different pH values, in order to analyze several situations in which nanocapsules varied their corresponding electrical states. The selected pH values were 4, 7 and 9. Aggregations were induced by salinity using independently NaCl and $CaCl_2$. The results obtained at each pH will be discussed separately. Figures 3a and 3b show

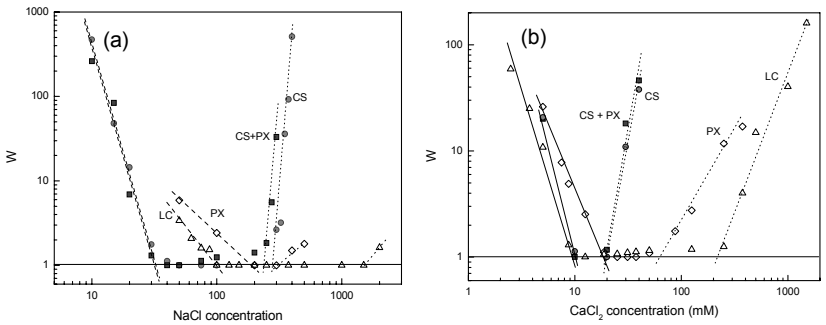

Figure 3. Stability factor versus (a) NaCl or (b) $CaCl_2$ concentration at pH 4. (△) LC, (◇) PX, (●) CS, and (■) CS+PX samples.

the stability patterns at pH 4. The corresponding ccc and csc values are shown in Tables 1a-b. With regard to the ccc data, calcium exerts a much higher destabilizating power than sodium, above all in those samples where these cations act as counterions (LC and PX cases). The coincidence of ccc values in the CS and CS+PX samples appears to corroborate the conclusions extracted from the mobility experiments. These experiments showed that both systems practically share the same superficial nature, indicating that the non-ionic surfactant was hardly able to adsorb onto the lecithin shell when competing for adsorption with chitosan chains. However, some differences exist between the ccc data of the LC and PX nanocapsules. The PX sample is more stable, suggesting that some poloxamer molecules achieve to adsorb onto the lecithin shell in formulation media free of chitosan.

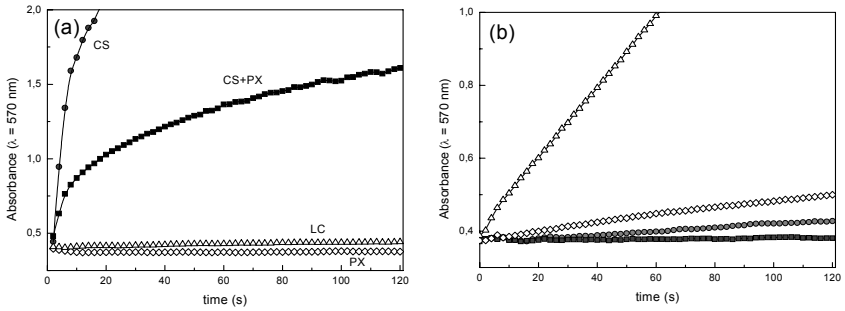

Figure 4. Aggregation kinetics at pH4 under maximum instability conditions, salt concentration value above the ccc and below the csc: (a) 100 mM of NaCl (excepting the PX sample, in which 200 mM of NaCl was used); and (b) 12.5 mM of $CaCl_2$, (excepting the PX sample, in which 20 mM of $CaCl_2$ was used). (△) LC, (◇) PX, (●) CS, and (■) CS+PX samples.

With regard to the csc values, they are dependent on the *hydration forces* acting between two approaching nanocapsules. It should be noted that hydration forces are structural repulsive interactions that arises from the local order of water layers adjacent to a surface. The magnitude of this force is not only correlated to the hydrophilicity of the surface but also depends strongly on the concentration and hydration degree of the ions that surround the surface [24; 26; 28; 33]. This is why restabilization, by means of hydration forces, is often found when great amounts of hydrated ions are accumulated at the proximities of any hydrophilic surface. According to data shown in Tables 1a-b, calcium clearly shows higher restabilization trends when compared to sodium. This is an expected result, since Ca^{2+} is much more hydrated than Na^{+}. On the other hand, if only one electrolyte is considered (NaCl or $CaCl_2$), differences in csc data give a qualitative

information about the hydrophilicity of the nanocapsule surface. The clear restabilization phenomena observed in the CS and CS+PX samples, even with NaCl, indicate that these samples are much more hydrophilic than LC or PX ones. This result is expectable because water behaves as a good solvent at room temperature for the deacetylated chitosan chains that are located at the particle shell.

Additional information about the surface composition can be obtained analysing the aggregation kinetics. Figures 4a and 4b show the fastest coagulation kinetics for every system at pH4, using NaCl and $CaCl_2$, respectively; that means coagulation regimes produced at salt concentrations above the ccc but below the csc. There are some expectable results, as those related to the aggregation kinetics given by $CaCl_2$ (Figure 4b). At this acid pH, the CS and CS+PX particles present a positive surface, while the LC and PX nanocapsules are negative. Therefore, calcium acts as counterion for LC and PX, while chloride does for CS and CS+PX, and thus, the surface potential screening given by the divalent cation is much more effective, producing more rapid aggregation than the one obtained by the monovalent anion [15]. In addition, the existence of repulsive structural interactions (mediated by hydration forces) in the most hydrophilic systems (CS and CS+PX) – even at low calcium concentrations (note that the csc is around 20 mM for both samples) – contributes to slow down the kinetics in the CS and CS+PX samples with regard to the LC and PX ones. The high aggregation kinetics shown by the LC sample can be understood not only taking into account the strong screening effect exerted by this divalent counterion, but also considering that Ca^{2+} form a poorly soluble ionic pair with phosphate groups. Consequently, the phosphate charges in the lecithin shell would be rapidly neutralized by calcium, and thus, the LC particles would rapidly collapse in absence of repulsive electrostatic forces. In addition, these experiments permit to infer that incorporation of poloxamer molecules onto the nanocapsule surface was not negligible, since the PX aggregation kinetics was significantly slower than that of LC. Kinetics results appear to indicate that some PEO chains are present in the particle/water interface, creating some kind of steric repulsive barrier, which would explain why the PX and CS+PX kinetics are lower than those of the LC and CS cases, respectively. Note that this feature is also observable when working with NaCl (see Figure 4a). Nevertheless, a striking result is observed when working with the CS sample in the 100 mM NaCl solution (see Figure 4a): an extremely rapid coagulation process is found. If there was only one aggregating mechanism – i.e. the well-known electric double layer compression – lower kinetics would be obtained (as that observed for the LC case in NaCl). The very rapid aggregation occurring in the CS system suggests the participation of other

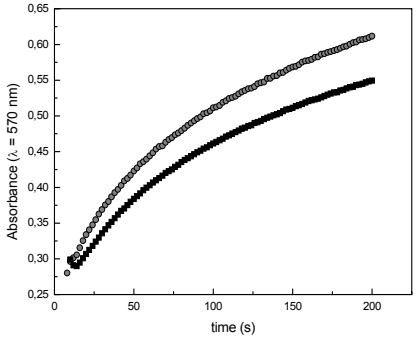

Figure 5a. Aggregation kinetics of (●) CS and (■) CS+PX nanocapsules when they were immersed at pH 7 in a low strength buffered solution (I = 0.002 M).

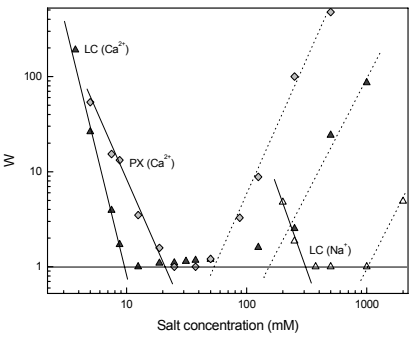

Figure 5b. Stability factor versus salt concentration at pH 7. (△) LC with NaCl, (▲) LC with $CaCl_2$, and (◇) PX with $CaCl_2$.

specific destabilization mechanism. It is known that chitosan easily tends to form ion pairs with non-monovalent anions, a property which is broadly used in ionic gelation processes by using tripolyphosphate [34-36] or sulphate [37; 38] as cross-linking molecules. However, to our knowledge, chitosan is not able to form this type of specific ion pairs with chloride; consequently, giving a convincing explanation to this point becomes rather complicated. Table 2 summarizes, following a qualitative scale, the aggregation kinetics patterns obtained under maximum instability conditions, salt concentration values above the ccc and below the csc.

Table 2. Qualitative classification of aggregation kinetics above the ccc and below the csc: (-) no aggregation, (+) very low, (++) low, (+++) rapid, (++++) very rapid, and (+++++) extremely rapid kinetics.

	LC		PX		CS		CS + PX	
	NaCl	$CaCl_2$	NaCl	$CaCl_2$	NaCl	$CaCl_2$	NaCl	$CaCl_2$
pH4	++	+++	+	++	+++++	+	+++++	+
pH7	+	+++	-	++++	- *aggr.* -	- *aggr.* -	- *aggr.* -	- *aggr.* -
pH9	-	++++	-	+++++	+	+++	+	++++

The next set of experiments was aimed to analyze the stability at neutral pH. It should be noted that aggregation studies by using NaCl and $CaCl_2$ were not carried out with the CS and CS+PX samples, since these two systems coagulated as soon as they were immersed into the pH7 buffer. This feature is shown in Figure 5a. The isoelectric point of both samples coincided with the neutral pH (see Figure 2), and thus, this spontaneous aggregation is a result of charge cancellation. Once more, the CS+PX system shows lower aggregation kinetics than that of the CS one, suggesting that, at least, some poloxamer molecules

were able to adsorb together with the chitosan chains to form the external shell of the nanocapsules. With regard to the other two systems (LC and PX), their electrokinetic charges were higher than those at pH4 (see Figure 2), and thus, it is presumable to find higher stability. The stability results are shown in Figure 5b, and the corresponding ccc and csc values are given in Table 1. The PX sample became completely stable when using NaCl. This can be explained as follows. Data obtained with $CaCl_2$ clearly inform us about the presence of Pluronic® F68 molecules on the PX surface, since its ccc is higher than that of LC (which must be a result of the action of a stabilizing agent), and also its csc is lower than that of LC, which is a signal of a higher hydrophilic character that is given by the PEO fragments. When NaCl is used instead, the ccc values become higher than those at pH4, even making the ccc and csc overlap for the most hydrophilic system (PX). Thus, restabilization mechanisms effectively act on this hydrophilic system even for moderate NaCl concentrations, avoiding aggregation in all the NaCl concentration range. This does not occur in the less hydrophilic sample (LC), where restabilization phenomena also take place at very high salt concentrations,

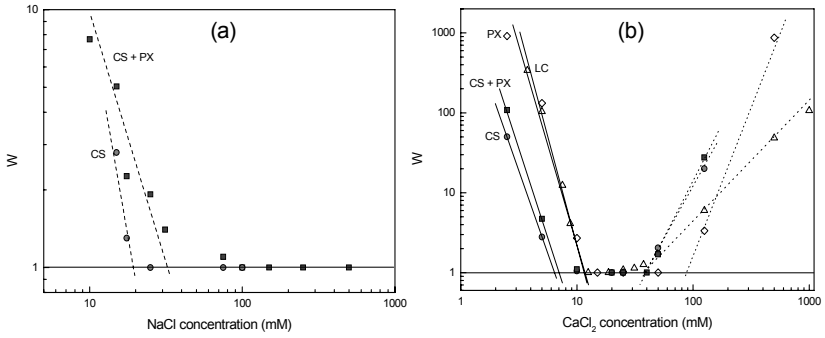

Figure 6. Stability factor versus (a) NaCl or (b) $CaCl_2$ concentration at pH 9. (△) LC, (◇) PX, (●) CS, and (■) CS+PX samples.

although in this case the ccc and csc values did not attain to overlap completely; nevertheless, the fastest LC aggregation kinetics became rather low when working with this salt (see Table 2).

Finally, the aggregation at pH9 was studied. Figures 6a and 6b show the stability factor versus NaCl and $CaCl_2$ concentration, respectively. At this basic pH the lecithin ionizable groups must be completely charged, making the surface even more hidrophilic than that at pH 7. This would explain why not only the PX but also the LC nanocapsules were completely stable, since (as just explained

previously) the ccc and csc values overlap in both samples, and thus, no aggregation was found in all the NaCl concentration range. On the other hand, low stability is found for the CS and CS+PX systems (see the ccc data in Table 1). It should be noted that at pH9 the chitosan shell is not charged, as the pKa values for chitosan usually goes from 6 to 7, depending on the deacetylation degree [31; 39]. In this situation, electrostatic repulsive forces become weak, which favours the colloidal instability. This lack of charge does not only explain the low ccc values, but also the absence of csc, since the uncharged chitosan shell is much less hydrophilic than a fully charged one. It is necessary the participation of a high hydrated ion (i.e. calcium) at moderate and high concentrations to observed restabilization by means of hydration forces (see Figure 6b). Once more, the minor differences existing among the CS and CS+PX results suggest low incorporation of poloxamer at the particle interface. Additionally, at this basic pH a partial desorption of uncharged chitosan might take place, since the electrostatic attraction between the (negative) lecithin layer and the (positive) chitosan chains would disappear when the polysaccharide becomes uncharged (which occurs at pH9). This partial desorption would explain why the mobility of CS and CS+PX is almost equal to that of the LC sample at pH9 (see Figure 2); or why the stability patterns of both samples are similar to that of LC at pH9 (i.e. compare the ccc and csc data with $CaCl_2$). Nevertheless, chitosan desorption must not be fully complete as differences appears with NaCl: the LC sample was totally stable while some unstability was found with the CS and CS+PX systems, although it should be noted that they showed very low aggregation kinetics (see Table 2).

If one combines all the stability results shown in Tables 1 and 2, it is possible to extract some general conclusions. With regard to the ccc values, all of them are concordant, at least qualitatively, with the electrophoretic mobility data shown in Figure 2, indicating that electric repulsive forces are the main responsible of the stability of the systems. Incorporation of Pluronic® F68 at the nanocapsule surface is not high in the PX case or even very poor in the CS+PX case, and consequently no stabilization mechanisms based on steric hindrance of PEO chains have been observed. However, the hydrophilic character of the surfaces has become an advantage against aggregation due to the effect caused by stabilization processes governed by hydration forces at moderate and high ionic strengths. The csc results permit to conclude that hidrophilicity increased as follows: LC < PX < CS ≤ CS+PX. With regard to the maximum aggregation kinetics (Table 2), calcium exerts rapid aggregation mechanisms only when this divalent cation acts as counter-ion. When it acts as co-ion (see the CS and CS+PX cases at pH4) the kinetics become rather low, although in such cases

NaCl rapidly destabilized both systems. Finally, if we compare the kinetics between LC and PX, and the ones of CS and CS+PX (see Table 2), the presence of some poloxamer molecules at the nanocapsule interface slightly speeds up aggregation at neutral and basic pH with $CaCl_2$. This feature may be caused by the natural tendency of calcium to form chemical complexes with the oxygens of PEO groups, a reaction catalyzed by traces of multivalent voluminous anions (as phosphate or borate which are present in the buffers used) [40-42]. In these cases, additionally to the coagulation caused by charge screening, a bridging mechanism – mediated by complexation of calcium with PEO groups of two different particles – also participates, speeding up somehow the aggregation kinetics.

Despite stability has been analysed in ideal solutions, the obtained ccc values may help to predict aggregation or stability regimes of the nanocarriers in some physiological solutions. For example, taking into account that sodium and calcium concentrations in blood (pH 7.4) are 145 mM and 1.2 mM, respectively, or that they are 140 mM and 2.5 mM in the intestinal fluid (pH 6.8) [43], a stability of LC and PX systems and a destabilization of CS and CS+PX ones may be predictable according to the data shown in Table 1. Nevertheless, the best way to check these assumptions, at least *in vitro*, is to analyze the potential aggregation kinetics in simulated fluids. Figures 7a-d show the results in three different simulated solutions: gastric, intestinal and plasma. As will be justified soon afterwards, a forth solution was also used, namely, a simulated intestinal fluid in which the sodium concentration was reduced ten-fold.

We will start discussing the results of the gastric fluid, where the pH was 1.2 and the sodium concentration was 34 mM. Note that this sodium concentration matched the ccc found at pH4 for the CS and CS+PX samples. However, we have significantly shifted the pH towards a more acidic value in which CS and CS+PX present a fully charged positive shell, making these nanocapsules stable even at 34 mM in Na^+. The other two samples (LC and PX) clearly aggregate by means of a charge cancellation mechanism, since the phosphate groups in the lecithin molecules become totally protonated at pH 1.2. The stability behaviour of the systems changed when they were immersed in intestinal fluid. In this medium LC and PX were stable, as predicted by the data shown in Tables 1a-b. Surprisingly, CS and CS+PX systems became completely stable. This could be a striking result, as the intestinal pH matches the CS and CS+PX isoelectric points (see Figure 2). It is worth reminding that both samples aggregated as soon as they were immersed into the low ionic strength pH7 buffer (see Figure 5a). There is only one logical explanation to justify the clear stability found in the intestinal

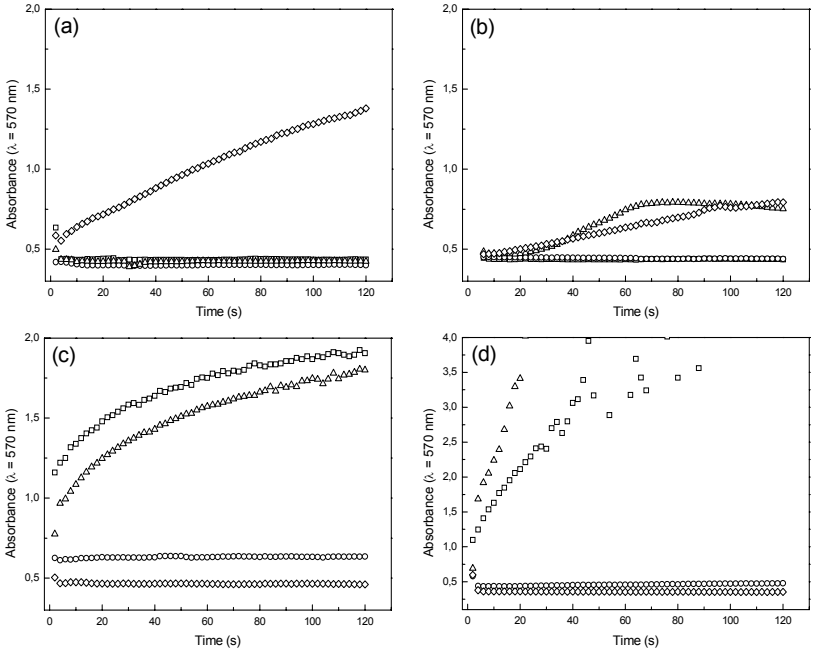

Figure 7. Aggregation kinetics of (a) LC, (b) PX, (c) CS, and (d) CS+PX nanocapsules when they were immersed in (◇) simulated gastric fluid, (○) simulated intestinal fluid, (□) simulated intestinal fluid with a low Na^+ concentration (15 mM), and (△) Hanks buffer.

fluid: the sodium concentration is around 150 mM, which is a moderate (but high enough) value capable to restabilize both hydrophilic systems by means of hydrations forces. To corroborate this hypothesis, aggregation kinetics were repeated in a simulated intestinal medium where the sodium concentration was reduced to 15 mM. As can be seen in Figure 7c and 7d, both systems immediately began to coagulate in this low salinity medium, which confirms our assumption. Therefore, hydration forces are capable to convert by themselves an uncharged and unstable system into a stable one, provided that the particle surface is hydrophilic enough.

Finally, the stability in Hanks buffer shows that LC nanocapsules are stable (as predicted), while PX is partially unstable (not predicted initially), and CS and CS+PX are totally unstable. It may be surprising not to observe restabilization phenomena mediated by hydration forces in the last two samples (above all reminding the stability in intestinal fluid), since the buffer contains hydrated Na^+, Ca^{2+} and Mg^{2+}, that significantly contribute to create a repulsive barrier against coagulation. The reason may lie on the fact that Hanks buffer also contains

sulphate and phosphate anions, with which (as mentioned previously) chitosan easily tends to form ion pairs [34-38] and, consequently, they can induce coagulation not only by charge cancellation, but also by a bridging mechanism. In addition, when comparing the results between LC and PX, with the one of CS and CS+PX, the presence of Ca^{2+} and Mg^{2+} in Hanks speeds up the aggregation kinetics of those particles that have PEO chains adhered on their surfaces. This is due to the previously mentioned tendency of divalent cations to form complexes with the oxygens of PEO fragments, increasing the aggregation of the system by bridging. It should be noted that PX initially aggregates and then it reaches a steady state, which reproduces the patterns observed with the aggregation of PLGA-Pluronic® F68 complexes in presence of calcium (see Figure 6 of reference 42). This would confirm the complexation reaction between Ca^{2+} and Mg^{2+} and PEO groups as responsible of the rare aggregation behaviour found with the PX sample in Hanks.

As a general conclusion, administration of LC and PX particles via oral is not advisable, since both types of nanoemulsions, despite being stable in the intestinal tract, would aggregate in the stomach losing their colloidal identity. However, nanocapsules covered by chitosan (either CS or CS+PX) are potentially useful for oral administration, since they are completely stable not only in the stomach (by means of repulsive electrostatic forces), but also in the small intestine thanks to the action of the hydration forces. In fact, various drug delivery carriers based on chitosan formulations have been successfully used *in vivo* when using oral, ocular and nasal routes [16; 44; 45]. With regard to intravenous administration, nanocapsules coated by chitosan would aggregate rapidly, and, in principle, their use would be discarded. Stability is only observed for LC and PX (at least partially), although the presumable low concentration of poloxamer molecules in their interface would make these carriers to be rapidly uptaken by the MPS. This handicap may be solved if PEG, instead of PEO, derivatives were used. For example, following the usual strategy of covalent-modification with polyethylenglycol, chitosan pegylation could be an interesting approach to improve the stability of cationized nanocapsulate systems with *Stealth*® properties. Moreover, the covalent pegylation would become an advantage for intravenous administrations because the PEG desorption or dilution after contact with blood components could be reduced [13].

IV. CONCLUSIONS

Four core-shell lipid nanocapsules differing in the shell nature have been synthesized with innocuous compounds. In all cases, the mean diameter was optimum and appropriate to be potentially used as drug delivery carriers.

The colloidal characterization (performed by electrophoretic mobility and stability measurements) has allowed us to conclude that incorporation of Pluronic® F68 at the particle/water interface was not high. It should be noted that this non-ionic surfactant is only capable to adsorb by means of hydrophobic forces, and the external (hydrophilic) lecithin layer in the nanocapsules does not favour such type of adsorption mechanism. The poloxamer incorporation was even poorer when chitosan chains were added together with the surfactant molecules during the synthesis. In this situation, the competitive adsorption between both types of polymers is much more favourable for chitosan, which is strongly adhered to the lecithin coat by means of intense attractive electrical forces. This is why performing a sequential adsorption (adding first the PEO derivative) instead of a competitive adsorption would be recommended to increase the surfactant/chitosan ratio at the particle interface. Nevertheless, there are better strategies available in order to obtained cationized *Stealth*® nanocapsules using shells based on chitosan: For example, 1) coadsorbing chitosan and a poloxamine instead of a poloxamer, since the poloxamines possess positive charges that would help to enhance the incorporation of this PEO derivative on the outer lecithin layer; or 2) forming a shell of chitosan covalently modified by polyethylenglycol derivatives. In this manner, a higher durable shell would be obtained and, moreover, changing the PEO by PEG groups the undesired complexes formed by PEO fragments with divalent cations (i.e. Ca^{2+}, Mg^{2+}) in the presence of phosphate traces would disappear.

It has been shown in this work that hydration forces play a crucial role in the colloidal stability of hydrophilic nanocapsules. In fact, total destabilized nanocapsules in low salinity media (i.e. CS and CS+PX in the pH7 buffer) become completely stable at physiological ionic strength values (see data in simulated intestinal fluid) due to the action exerted by these structural forces.

Finally, it should be noted that it is absolutely mandatory to carry out *in vivo* studies to test the viability of lipidic nanocapsules as potential drug delivery systems. However, *in vitro* studies, as those presented in this paper, become very useful, since they serve to delimit and diminish the number of variables to study in

the *in vivo* analysis, which in turn also helps to reduce the number of sacrificed animals.

ACKNOWLEDGEMENTS

The authors wish to thank the financial support granted by the “Ministerio de Educación y Ciencia” (MEC, Spain), project MAT2007-66662-C02-01 (European FEDER support included), and from the “Conserjería de Innovación, Ciencia y Tecnología de la Junta de Andalucía” (Spain), projects of excellence FQM 392 and FQM03099. Moreover, M.V. Lozano-Lopez acknowledges the fellowship received from de Spanish Government (AP2005-1701). Finally, we wish to thank Professor M.J. Alonso for her supervision.

REFERENCES

1. Drummond D.C.; Meyer O.; Hong K.; Kirpotin D.B.; Papahadjopoulos D. (1999). Optimizing liposomes for delivery of chemotherapeutic agents to solid tumors. Pharmacol. Rev. 51: 691-743.
2. Brigger I.; Dubernet C.; Couvreur P. (2002). Nanoparticles in cancer therapy and diagnosis. Adv. Drug Deliv. Rev. 54: 631-651.
3. Jones M.C.; Leroux J.C. (1999). Polymeric micelles - A new generation of colloidal drug carriers. Eur. J. Pharm. Biopharm. 48: 101-111.
4. Bae K.H.; Lee Y.; Park T.G. (2007). Oil-encapsulating PEO-PPO-PEO/PEG shell cross-linked nanocapsules for target-specific delivery of paclitaxel. Biomacromolecules. 8: 650-656.
5. Lambert G.; Fattal E.; Pinto-Alphandary H.; Gulik A.; Couvreur P. (2000). Polyisobutylcyanoacrylate nanocapsules containing an aqueous core as a novel colloidal carrier for the delivery of oligonucleotides. Pharm. Res. 17: 707-714.
6. Khalid M.N.; Simard P.; Hoarau D.; Dragomir A.; Leroux J-C. (2006). Long circulating poly(ethylene glycol)-decorated lipid nanocapsules deliver docetaxel to solid tumors. Pharm. Res. 23: 752-758.
7. Prego C.; Torres D.; Fernandez-Megia E.; Novoa-Carballal R.; Quiñoa E.; Alonso M.J. (2006). Chitosan-PEG nanocapsules as new carriers for oral peptide delivery: Effect of chitosan pegylation degree. J. Control. Release. 111: 299-308.
8. Lee S.H.; Choi S.H.; Kim S.H.; Park T.G. (2008). Thermally sensitive cationic polymer nanocapsules for specific cytosolic delivery and efficient gene silencing of siRNA: Swelling induced physical disruption of endosome by cold shock. J. Control. Release. 125: 25-32.
9. Rübe A. (2006). Development and physico-chemical characterization of nanocapsules. Thesis, Martin-Luther-University, Germany.
10. Gabizon A.; Catane R.; Uziely B.; Kaufman B.; Safra T.; Cohen R.; Martín F.; Huang A.; Barenholz Y. (1994). Prolonged circulation time and enhanced accumulation in malignant exudates of doxorubicin encapsulated in polyethylene-glycol coated liposomes. Cancer Res. 54: 987-992.
11. Tobio M.; Sánchez A.; Vila A.; Soriano I.; Evora C.; Vila-Jato J.L.; Alonso M.J. (2000). The role of PEG on the stability in digestive fluids and in vivo fate of PEG-PLA nanoparticles following oral administration. Colloids Surf. B. 18: 315-323.
12. Moghimi S.M.; Hunter A.C. (2001). Capture of stealth nanoparticles by the body's defences. Crit. Rev. Ther. Rug. Carrier Syst. 18: 527-550.

13. Barrat G. (2003). Colloidal drug carriers: achievements and perspectives. Cell. Mol. Life Sci. 60: 21-37.
14. Desai M.P.; Labhasetwar V.; Walter E.; Levy R.J.; Amidon G.L. (1997). The mechanism of uptake of biodegradable microparticles in Caco-2 cells is size dependent. Pharm. Res. 14: 1568-1573.
15. Hiemenz P.C.; Rajagopalan R. (1997). Principles of Colloidal and Surface Chemistry. Dekker, New York.
16. Prego C.; Fabre M.; Torres D.; Alonso M.J. (2006). Efficacy and mechanism of action of chitosan nanocapsules for oral peptide delivery. Pharm. Res. 23: 549-556.
17. Soppimath K.S.; Aminabhavi T.M.; Kulkarni A.R.; Rudzinski W.E. (2001). Biodegradable polymeric nanoparticles as drug delivery devices. J. Control. Release. 70: 1-20.
18. Letchford K.; Burt H. (2007). A review of the formation and classification of amphiphilic block copolymer nanoparticulate structures: micelles, nanospheres, nanocapsules and polymersomes. Eur. J. Pharm. Biopharm. 65: 259-269.
19. Fessi H.; Puisieux F.; Devissaguet J.Ph.; Ammoury N.; Benita S. (1989). Nanocapsule formation by interfacial polymer deposition following solvent displacement. Int. J. Pharm. 55: R1-R4.
20. Allen T.M.; Austin G.A.; Chonn A.; Lin L.; Lee K.C. (1991). Uptake of liposomes by cultured mouse bone marrow macrophages: Influence of liposome composition and size. Biochim. Biophys. Acta. 1061: 56-64.
21. Florence A.T. (1997). The oral absorption of micro- and nanoparticulates: Neither exceptional nor unusual. Pharm. Res. 14: 259-266.
22. Singer J.M.; Vekermans F.C.A.; Lichtenbelt J.W.Th.; Hesselkink Th.; Wiersema A.P.H. (1973). Kinetics of flocculation of latex particles by human gamma globulin. J. Colloid Interface Sci. 45: 608-614.
23. Quesada M.; Puig J.; Delgado J.M.; Hidalgo-Álvarez R. (1998). Modelling the kinetics of antigen-antibody reactions at particle enhanced optical immunoassays. J. Biomater. Sci. Polymer Edn. 9: 961-971.
24. Pashley R.M. (1982). Hydration forces between mica surfaces in electrolyte solutions. Adv. Colloid Interface Sci. 16: 57-62.
25. Churaev N.V.; Derjaguin B.V. (1985). Inclusion of structural forces in the theory of stability of colloids and films. J. Colloid Interface Sci. 103: 542-553.
26. Israelachvili J.N. (1992). Intermolecular and Surface Forces. Academic Press, London.

27. Molina-Bolívar J.A.; Galisteo-González F.; Hidalgo-Álvarez R. (1997). Colloidal stability of protein-polymer systems: A possible explanation by hydration forces. Phys. Rev. E 55: 4522-4530.
28. Molina-Bolívar J.A.; Ortega-Vinuesa J.L. (1999). How proteins stabilize colloidal particles by means of hydration forces. Langmuir. 15: 2644-2653.
29. Molina-Bolívar J.A.; Galisteo-González F.; Hidalgo-Álvarez R. (2001). Specific cation adsorption on protein-covered particles and its influence on colloidal stability. Colloids Surf. B. 21: 125-135.
30. Santander-Ortega M.J.; Jódar-Reyes A.B.; Csaba N.; Bastos-González D.; Ortega-Vinuesa J.L. (2006). Colloidal stability of Pluronic F68-coated PLGA nanoparticles: A variety of stabilisation mechanisms. J. Colloid Interface Sci. 302: 522-529.
31. López-León T.; Carvalho E.L.S.; Seijo B.; Ortega-Vinuesa J.L.; Bastos-González D. (2005). Physicochemical characterization of chitosan nanoparticles: Electrokinetic and stability behavior. J. Colloid Interface Sci. 283: 344-351.
32. Sonvico F.; Cagnani A.; Rossi A.; Motta S.; Di Bari M.T.; Cavatorta F.; Alonso M.J.; Deriu A.; Colombo P. (2006). Formation of self-organized nanoparticles by lecithin/chitosan ionic interaction. Int. J. Pharm. 324: 67-73.
33. Christenson H.K. (1988). Non-DLVO forces between surfaces – solvation, hydration and capillary effects. J. Dispersion Sci. Technol. 9: 171-206.
34. Calvo P.; Remuñán-López C.; Vila-Jato J.L.; Alonso M.J. (1997). Novel hydrophilic chitosan-polyethylene oxide nanoparticles as protein carriers. J. Appl. Polym. Sci. 63: 125-132.
35. Janes K.A.; Fresneau M.P.; Marazuela A.; Fabra A.; Alonso M.J. (2001). Chitosan nanoparticles as delivery systems for doxorubicin. J. Control. Release. 73: 255-267.
36. Vila A.; Sánchez A.; Tobío M.; Calvo P.; Alonso M.J. (2002). Design of biodegradable particles for protein delivery. J. Control. Release. 78: 15-24.
37. Berthold A.; Kremer K.; Kreuter J. (1996). Preparation. J. Control. Release. 39: 17-25.
38. van der Lubben I.M.; Verhoef J.C.; Van Aelst A.C.; Borchard G.; Junginger H.E. (2001). Chitosan microparticles for oral vaccination: Preparation, characterization and preliminary in vivo uptake studies in murine Peyer's patches. Biomaterials. 22: 687-694.

39. Schatz C.; Pichot C.; Delair T.; Viton C.; Domard A. (2003). Static light scattering studies on chitosan solutions: From macromolecular chains to colloidal dispersions. Langmuir. 19: 9896-9903.
40. Nuyssink J.; Koopal K. (1982). The effect of the polyethylene oxide molecular weight on determination of its concentration in aqueous solution. Talanta. 29: 495-501.
41. Thima R.T.; Tammishetti S. (2001). Barium chloride crosslinked carboxymethyl guar gum beads for gastrointestinal drug delivery. J. Appl. Polym. Sci. 82: 3084-3090.
42. Santander-Ortega M.J.; Csaba N.; Alonso M.J.; Ortega-Vinuesa J.L.; Bastos-González D. (2007). Stability and physicochemical characteristics of PLGA, PLGA:poloxamer and PLGA:poloxamine blend nanoparticles. A comparative study. Colloids Surf. A. 296: 132-140.
43. Fordtran J.S.; Locklear T.W. (1966). Ionic constituents and osmolality of gastric and small-intestinal fluids after eating. Am. J. Digestive Diseases. 11: 503-521.
44. Calvo P.; Vila-Jato J.L.; Alonso M.J. (1997). Evaluation of cationic polymer-coated nanocapsules as ocular drug carriers. Int. J. Pharm. 153: 41-50.
45. Prego C.; Torres D.; Alonso M.J. (2006). Chitosan nanocapsules: A new carrier for nasal peptide delivery. J.D.D.S.T. 16: 331-337.

DISCUSIÓN GENERAL

DISCUSIÓN GENERAL

En los últimos años, las nanocápsulas poliméricas, constituidas por un núcleo oleoso y una cubierta polimérica, han sido utilizadas con éxito para la encapsulación de moléculas pequeñas de baja solubilidad en agua y, más concretamente, de antitumorales con estas características [1-3]. El núcleo oleoso ofrece unas propiedades únicas en cuanto a la capacidad de incorporación de gran cantidad de fármaco hidrofóbico, en comparación con otros sistemas como son las nanopartículas [4].

El otro elemento clave de estos sistemas es el polímero de recubrimiento. Esta capa de polímero confiere estabilidad a la nanocápsula así como al principio activo encapsulado, protegiéndolo frente a la degradación [5]. Además, en función del polímero que se emplee para recubrir el núcleo oleoso es posible modular el comportamiento biológico del sistema. De esta forma, gracias a una cubierta hidrofílica de PEG, por ejemplo, es posible elaborar nanocápsulas que evitan el reconocimiento por los macrófagos, obteniéndose sistemas con un elevado tiempo de permanencia en circulación sanguínea [6]. Eligiendo una cubierta mucoadhesiva, se puede favorecer el paso del fármaco a través de vías mucosas [7], o bien, si la cubierta tiene propiedades que facilitan la penetración celular, se puede ver favorecida la internalización celular [8]. A este respecto, es importante resaltar los interesantes resultados obtenidos en nuestro laboratorio con sistemas nanocapsulares en los que el polímero de recubrimiento es el quitosano. El quitosano es un polisacárido de origen natural ampliamente utilizado en la formulación de sistemas coloidales. Sus propiedades de biodegradabilidad, mucoadhesividad y promotoras de la absorción han, y continúan suscitando, un gran interés en la formulación de nuevos vehículos

---

[1] **Bae K.H.; Lee Y.; Park T.G.** (2007). Biomacromolecules. 8: 650-656.
[2] **Khalid M.N.; Simard P.; Hoarau D.; Dragomir A.; Leroux J.C.** (2007). Pharm. Res. 23: 752-758.
[3] **Peltier S.; Oger J.M.; Lagarce F.; Couet W.; Benoit J.P.** (2006). Pharm. Res. 23: 1243-1250.
[4] **Rübe A.** (2006). Mathematisch-Naturwissenschaftlich-Technischen Fakultät. Halle-Wittenberg, Martin-Luther-Universität Halle-Wittenberg.
[5] **Legrand P.; Barratt G.; Mosqueira V.; Fessi H.; Devissaguet J.P.** (1999). S.T.P. Pharm. Sci. 9: 411-418.
[6] **Cahouet A.; Denizot B.; Hindre F.; Passirani C.; Heurtault B.; Moreau M.; Le Jeune J.J.; Benoit J.P.** (2002). Int. J. Pharm. 242: 367-371.
[7] **Prego C.; Torres D.; Alonso M.J.** (2006). J. Nanosci. Nanotechnol. 6: 2921-2928.
[8] **Lozano M.V.; Brea J.; Loza M.I.; Torres D.; Alonso M.J.** (Unpublished results).

transportadores de fármacos [9-11]. Como constituyente de la cubierta de nanocápsulas, se ha podido demostrar que favorece la interacción de las nanoestructuras con las mucosas, tanto intestinal como nasal u ocular, hecho que se traduce en un aumento de la biodisponibilidad del péptido calcitonina [7], o de la penetración intraocular de la indometacina [12].

Por otro lado, en los últimos años se han descrito diferentes sistemas transportadores de fármacos en los que el poliaminoácido poliarginina constituye un elemento esencial [13-16]. La poliarginina es un poliaminoácido catiónico perteneciente a la familia de los *"protein transduction domains"*. Recientemente, se ha descrito que la presencia de los grupos guanidino en las cadenas laterales del polímero, sería la responsable de la notable capacidad de la poliarginina para atravesar las membranas celulares y aumentar la entrada celular de las moléculas asociadas [17; 18].

En este contexto, y teniendo en cuenta los comentarios recogidos en la sección "Antecedentes, Hipótesis y Objetivos", en el desarrollo de este trabajo, nos hemos planteado la elaboración de formulaciones de nanocápsulas poliméricas para la vehiculización del antitumoral docetaxel. Las formulaciones propuestas comparten la composición del núcleo hidrófobo pero difieren en su cubierta polimérica. De este modo, se han estudiado dos sistemas nanocapsulares que difieren en el polímero de recubrimiento: el quitosano y la poliarginina. Hemos optado, en el caso del quitosano, por la utilización de oligómeros en vez del polímero, ya que ofrecen ventajas en cuando a mayor biodegradabilidad y menor toxicidad.

---

[9] **Peniche C.; Argüelles-Monal W.; Goycoolea F.M.. Belgman M.N.G.** (2008). Amsterdam, Elsevier. B.V.: 517-542.
[10] **de la Fuente M.; Seijo B.; Alonso M.J.** (2008). Gene Therapy. 15: 668-676.
[11] **Garcia-Fuentes M.; Prego C.; Torres D.; Alonso M.J.** (2005). Eur. J. Pharm. Sci. 25: 133-143.
[12] **Calvo P.; Vila-Jato J.L.; Alonso M.J.** (1997). Int. J. Pharm. 153: 41-50.
[13] **Firbas C.; Jilma B.; Tauber E.; Buerger V.; Jelovcan S.; Lingnau K.; Buschle M.; Frisch J.; Klade C.S.** (2006). Vaccine. 24: 4343-4353.
[14] **Suzuki R.; Yamada Y.; Harashima H.** (2007). Biol. Pharm. Bull. 30: 758-762.
[15] **Zhang C.; Tang N.; Liu X.; Liang W.; Xu W.; Torchilin V.P.** (2006). J. Control. Release. 112: 229-239.
[16] **Theodossiou T.A.; Pantos A.; Tsogas I.; Paleos C.M.** (2008). ChemMedChem. 3: 1635-1643.
[17] **Lundberg M.; Wikström S.; Johansson M.** (2003). Mol. Ther. 8: 143-150.
[18] **Patel L.N.; Zaro J.L.; Shen W.C.** (2007).Pharm. Res. 24: 1977-1992.

La discusión general la hemos dividido en dos partes para facilitar la comprensión de los resultados.

- Parte I. Nanocápsulas de quitosano para la liberación intracelular de fármacos antitumorales.

  I.a. Desarrollo de nanocápsulas de quitosano conteniendo docetaxel.

  I.b. Funcionalización de las nanocápsulas de quitosano y evaluación *in vivo* de la actividad antitumoral.

- Parte II. Nanocápsulas de poliarginina para la liberación intracelular de fármacos antitumorales.

Parte I. Nanocápsulas de quitosano para la liberación intracelular de fármacos antitumorales.

I.a. Desarrollo de nanocápsulas de quitosano conteniendo docetaxel.

Preparación y caracterización físico-química de las nanocápsulas de quitosano.

Las nanocápsulas de quitosano se prepararon mediante la técnica de desplazamiento de disolvente [19], siguiendo el procedimiento previamente adaptado en nuestro laboratorio [20]. Básicamente, el proceso consiste en la adición, bajo agitación, de una fase oleosa sobre una fase acuosa en la que se incorporan oligómeros de quitosano y poloxámero 188, tras la cual se produce la difusión de los disolventes orgánicos al agua. De este modo se forman pequeñas gotículas de tamaño nanométrico, constituidas por el aceite (Mygliol® 812) y el tensoactivo lecitina, sobre las que se dispone el quitosano gracias a la interacción iónica entre los oligómeros cargados positivamente y la lecitina cargada negativamente.

La caracterización físico-química de las nanocápsulas de quitosano permitió apreciar una población de baja polidispersión y tamaño nanométrico, siempre inferior a 200 nm. Con respecto al potencial zeta, se observaron valores

[19] **Fessi H.; Piusieux F.; Devissaguet J.P.; Ammoury N.; Benita S.** (1989). Int. J. Pharm. 55: R1-R4.
[20] **Prego C.; Torres D.; Alonso M.J.** (2006). J. D.D.S.T. 16: 331-337.

altamente positivos, lo que confirmó la presencia de la cubierta de quitosano sobre las nanogotículas de la emulsión (Tabla 1). La morfología de los sistemas también se estudió mediante microscopía electrónica de transmisión. Como se muestra en la Figura 1, las nanocápsulas de quitosano constituyen una población homogénea, de morfología esférica.

Tabla 1. Propiedades físico-químicas de las nanocápsulas de quitosano (CS) blancas, conteniendo docetaxel (DCX) y fluorescentes. (Media ± d.e.; n=3); [a] índice de polidispersión.

Formulación	Tamaño (nm)	IP[a]	Potencial zeta (mV)
Nanocápsulas CS blancas	151 ± 1	0,1	+47 ± 1
Nanocápsulas CS-DCX	162 ± 4	0,1	+47 ± 3
Nanocápsulas CS fluorescentes	185 ± 3	0,1	+38 ± 2

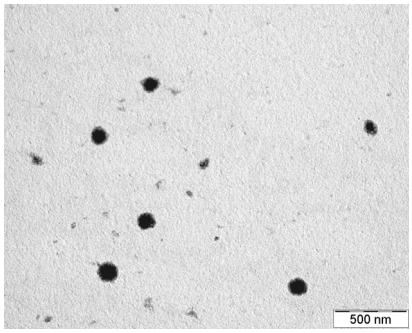

Figura 1. Imagen de microscopía electrónica de transmisión de las nanocápsulas de quitosano blancas.

Eficacia de encapsulación y liberación del docetaxel a partir de las nanocápsulas de quitosano.

La inclusión del fármaco citostático docetaxel en las nanocápsulas de quitosano se logró mediante la incorporación en la fase orgánica de una alícuota de la solución stock de la molécula disuelta en etanol. Las nanocápsulas resultantes no experimentaron cambios significativos en sus propiedades físico-químicas respecto a las nanocápsulas blancas (Tabla 1).

La eficacia de encapsulación del docetaxel en los sistemas se determinó de forma indirecta midiendo la concentración del fármaco en el infranadante, correspondiente al fármaco no encapsulado. Las nanocápsulas de quitosano mostraron una elevada eficacia de encapsulación, en torno al 70%, lo cual era esperable teniendo en cuenta la afinidad que el fármaco hidrófobo presenta por el núcleo oleoso [1, 2].

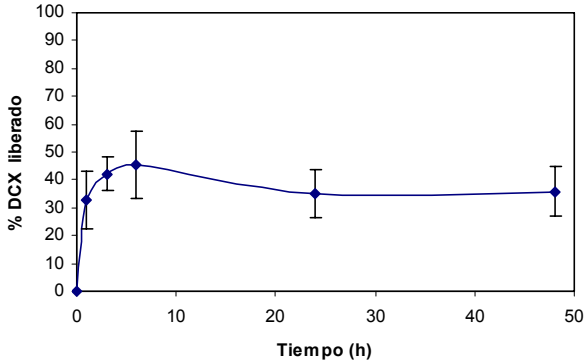

Figura 2. Perfil de liberación del docetaxel a partir de las nanocápsulas de quitosano. (Media ± d.e.; n=3).

En relación al proceso de liberación del docetaxel a partir de las nanocápsulas, se observó un perfil bifásico típico de estos sistemas, caracterizado por una liberación inicial del 50% en las primeras 8 h, que se continúa con, prácticamente, una ausencia de liberación en el resto del estudio (Figura 2). La fase inicial se relaciona con el reparto del docetaxel entre el núcleo hidrófobo y la fase externa acuosa, mientras que la segunda fase refleja la gran afinidad que la molécula tiene por el núcleo oleoso.

Estudios en cultivos celulares.

Para evaluar el potencial de las nanocápsulas de quitosano como vehículos de antitumorales como el docetaxel, se consideró esencial el estudio de la capacidad antiproliferativa del fármaco incluido en los nanosistemas en contacto con cultivos de células tumorales. Estos ensayos se llevaron a cabo en dos líneas celulares, MCF7 (cáncer de mama) y A549 (carcinoma humano de

pulmón). Los resultados se recogen en la Figura 3 en la que se indica la existencia de diferencias significativas en relación al fármaco libre al cabo de 24 h de incubación, que no se aprecian sin embargo al cabo de 48 h. La Tabla 2 muestra los valores de concentración inhibitoria del 50% del crecimiento (IC_{50}) del fármaco, cuando se encuentra libre o incluido en las nanocápsulas, demostrándose también para el mismo período de tiempo, la existencia de diferencias significativas entre ellos. Estos resultados sugieren que las nanocápsulas promueven la internalización del fármaco con una cinética más rápida que la del fármaco libre.

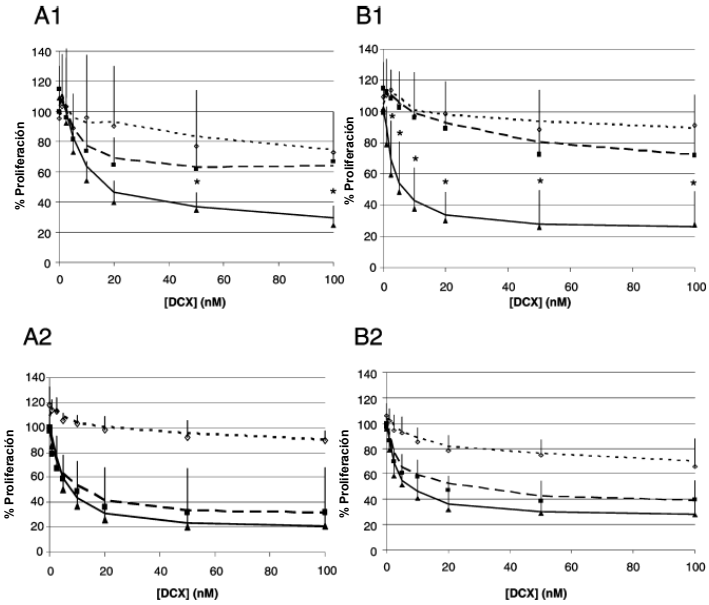

Figura 3. Efecto sobre la proliferación celular de MCF7 y A549 de docetaxel (DCX) (línea discontinua), nanocápsulas de quitosano con docetaxel (línea continua) y nanocápsulas de quisosano blancas (línea punteada) a diferentes tiempos de incubación y concentraciones. MCF7 tras 24 h (A1) y 48 h (A2), A549 tras 24 h (B1) y 48 h (B2). (n=4, *p < 0,05, nanocápsulas de CS con docetaxel frente al docetaxel).

Un aspecto a destacar es la ausencia de toxicidad de las nanocápsulas blancas, lo cual está en consonancia con estudios previos realizados con otras formulaciones de nanocápsulas de quitosano, en contacto con cultivos celulares Caco-2 [7].

Teniendo en cuenta los resultados de inhibición de la proliferación, nos planteamos estudiar la interacción de las nanocápsulas de quitosano con ambas

líneas celulares. El objetivo de este estudio consistió en determinar si efectivamente se producía la internalización de los sistemas, lo cual favorecería la liberación intracelular del fármaco. Para ello, en primer lugar, se prepararon nanocápsulas de quitosano fluorescentes, modificando el procedimiento anteriormente descrito mediante la adición del fluoróforo en la fase orgánica. En la caracterización físico-química de las nanocápsulas fluorescentes se observó un ligero aumento del tamaño de partícula respecto a las nanocápsulas blancas,

Tabla 2. Valores de IC_{50} expresados en nM (concentración que inhibe el 50% del crecimiento celular) de la solución de docetaxel (DCX) y de las nanocápsulas de quitosano conteniendo DCX (CS-DCX), en líneas celulares MCF7 y A549.

	MCF7		A549	
	24h	48h	24h	48h
DCX	62,5	5,6	36,5	12,8
Nanocápsulas CS-DCX	4,7	2,7	5,3	4,5

manteniéndose el potencial zeta altamente positivo (Tabla 1). Los estudios de internalización celular, realizados mediante citometría de flujo, demostraron que las nanocápsulas marcadas con fluorescencia eran capaces de entrar masivamente en ambas líneas celulares tras una corta incubación de 2 h (Figura 4), hecho que contrasta con los resultados obtenidos con el marcador libre, que prácticamente no fue captado intracelularmente. Estos resultados ratificaron, por lo tanto, la hipótesis expuesta anteriormente.

Por otra parte, con el fin de determinar si el proceso de encapsulación o la interacción con las células tumorales modificaban la actividad biológica del fármaco, se plantearon dos estudios diferentes. En primer lugar, se comparó mediante citometría de flujo, el efecto del fármaco libre o encapsulado sobre el ciclo celular y, además, se estudió mediante microscopía confocal la distribución de la α-tubulina en las células previamente tratadas con el fármaco libre o encapsulado. Los resultados mostrados en la Figura 5 indicaron que el fármaco incorporado en las nanocápsulas de quitosano mantenía intacta su actividad biológica. Tras la acción de los tratamientos, ambos grupos de células tumorales se acumulaban en la fase G2/M, lo cual es característico de la parada del ciclo celular, provocada por la acción del fármaco [15]. El mecanismo de acción del docetaxel consiste en la inhibición de los microtúbulos que constituyen el citoesqueleto, la formación de núcleos de estructura anómala y posteriormente la

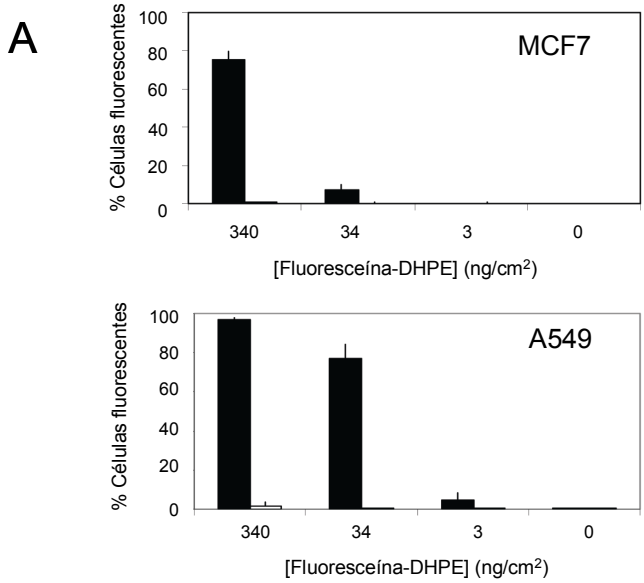

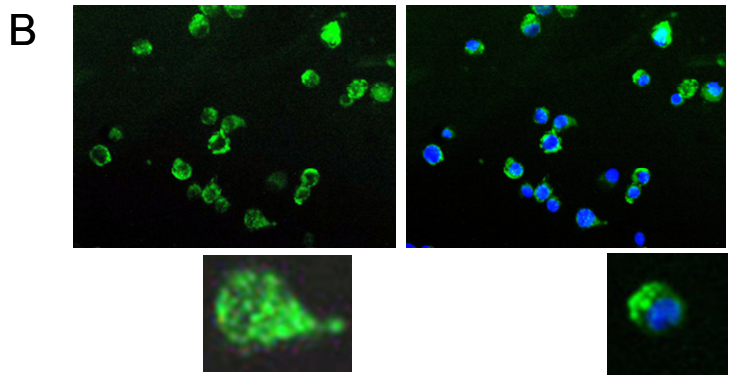

Figura 4. Estudios de captura celular de las nanocápsulas de quitosano. (A) Porcentaje de células fluorescentes tras 2 h de incubación con las nanocápsulas de quitosano fluorescentes (negro) o con una dispersión del marcador fluorescente (blanco). (Media ± d.e.; n=3) (B) Imagen de microscopía de fluorescencia de las células MCF7 incubadas con las nanocápsulas de quitosano fluorescentes. Izquierda, el marcaje verde corresponde a las nanocápsulas cargadas con el marcador fluorescente fluoresceína-DHPE. Derecha, imagen conjunta de los núcleos celulares marcados con DAPI (azul) y la señal de la fluoresceína-DHPE (verde). La imagen aumentada indica que el marcador fluorescente se encuentra internalizado dentro de vesículas.

parada del ciclo celular. En las imágenes obtenidas mediante microcopía confocal se puede observar mediante la tinción de la α-tubulina y de los núcleos, la existencia de estas estructuras anómalas en las células tratadas con las formulaciones que contienen docetaxel **(Artículo 2, Figura 6)**.

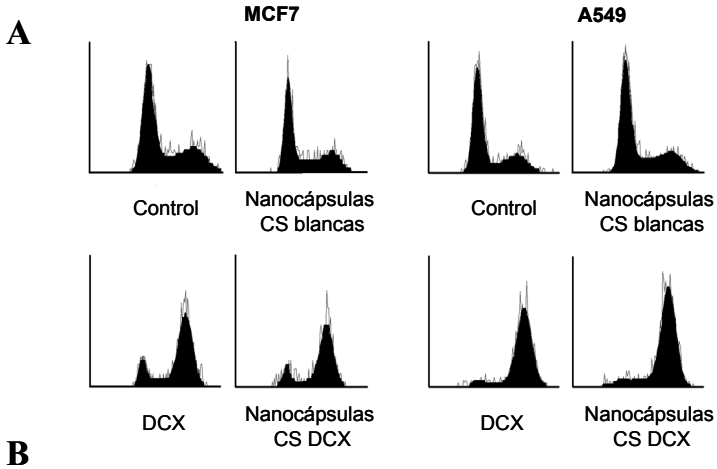

B

	MCF7			A549		
	G0/G1	S	G2/M	G0/G1	S	G2/M
Control	56,1 ± 0,6	28,1 ± 4,8	15,8 ± 4,2	67,9 ± 1,8	19,0 ± 4,9	13,1 ± 6,7
Nanocápsulas CS blancas	54,8 ± 3,2	31,2 ± 5,2	14,0 ± 4,6	61,8 ± 3,4	27,3 ± 0,1	10,9 ± 3,3
DCX	9,8 ± 5,0	19 ± 6,0	71,2 ± 1,0	2,1 ± 0,8	15,2 ± 7,0	82,7 ± 7,8
Nanocápsulas CS DCX	12,7 ± 3,9	16,5 ± 4,6	70,8 ± 8,6	0,1 ± 0,0	16,4 ± 0,9	83,5 ± 0,9

Figura 5. Resultados que muestran el ciclo celular de las líneas MCF7 y A549 sin tratamiento, o en contacto con las nanocápsulas de quitosano (CS) blancas, conteniendo docetaxel (DCX) o con el DCX libre. (A) Perfiles representativos de citometría de flujo. (B) Porcentaje de células que se encontraron en cada fase del ciclo celular.

Optimización de la formulación de nanocápsulas de quitosano: Estudios de liofilización.

El principal objetivo de estos estudios consistió en la obtención de una formulación de nanocápsulas de quitosano conteniendo docetaxel, que tras un proceso de liofilización mantuviese las propiedades iniciales del sistema. Para ello, en primer lugar, se tomaron en consideración los resultados de un reciente estudio en el que se determinó la aportación de cada componente de las nanocápsulas de quitosano a las propiedades finales del sistema **(Anexo II)**. En este estudio, se pudo comprobar que durante la formación de las nanocápsulas, el quitosano presentaba una adhesión preferente a las nanogotículas oleosas, dando lugar a la formación de nanocápsulas con muy bajo contenido en poloxámero 188. Así, en el estudio de liofilización se incluyó una nueva

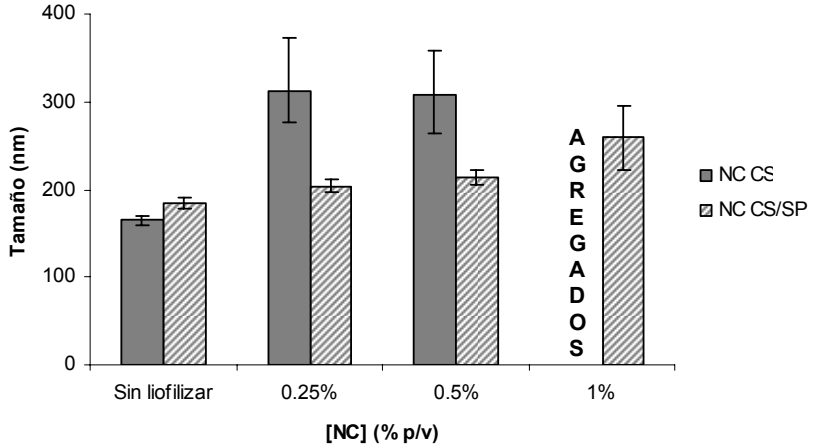

Figura 6. Tamaño de partícula tras la reconstitución de los liofilizados de las nanocápsulas de quitosano (CS) (gris) y de las nanocápsulas de quitosano sin poloxámero (CS/SP) (rayas). (Media ± d.e.; n=3).

formulación de nanocápsulas cuya cubierta polimérica estaba constituida únicamente por quitosano. Estas nanocápsulas, sin poloxámero, presentaron valores de tamaño, potencial zeta, eficacia de encapsulación y perfil de liberación de docetaxel muy similares a los de las nanocápsulas de quitosano **(Artículo 3, Tabla 1, Figuras 1 y 2)**. Sin embargo, se apreciaron diferencias significativas en la liofilización de las nanocápsulas blancas en presencia del crioprotector trealosa, obteniéndose mejores resultados en la recuperación del tamaño de partícula en el caso de la formulación sin poloxámero (Figura 6). La explicación de este comportamiento podría residir en el aumento de la cristalinidad de la trealosa en presencia del poloxámero, hecho comprobado mediante calorimetría diferencial de barrido y rayos X (resultados no mostrados). Debido a este comportamiento, la capacidad crioprotectora de la trealosa se reduciría al disminuir su componente amorfo, produciendo la desestabilización de las nanocápsulas.

Estos resultados nos llevaron a seleccionar las nanocápsulas de quitosano sin poloxámero para encapsular el docetaxel y proceder a la liofilización de la formulación. La liofilización se llevó a cabo en el mismo rango de concentraciones de trealosa y nanocápsulas utilizado para las formulaciones blancas. Los resultados mostraron que la presencia del fármaco no modificaba el proceso de liofilización, obteniéndose un liofilizado que se puede reconstituir fácilmente y que recupera el tamaño inicial de las nanocápsulas, de aproximadamente 200 nm.

Estudios en cultivos celulares de las nanocápsulas liofilizadas.

El análisis del comportamiento de las nanocápsulas de quitosano con docetaxel liofilizadas, en contacto con cultivos celulares, se realizó en la línea de cáncer de pulmón NCI-H460. Para ello, se ensayaron en primer lugar las nanocápsulas de quitosano con docetaxel, para comprobar si la liofilización modificaba la eficacia de los nanosistemas.

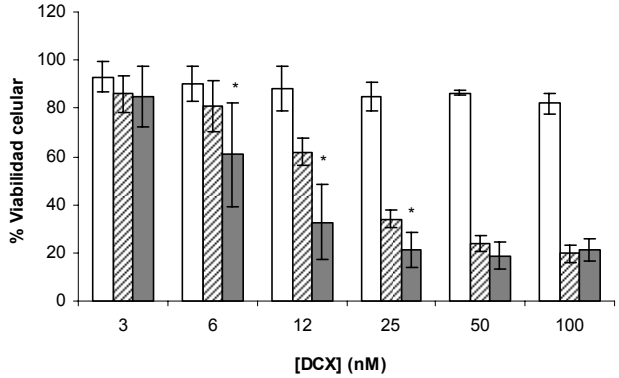

Figura 7. Efecto de las nanocápsulas de quitosano blancas (blanco), docetaxel (DCX) libre (rayas) y nanocápsulas de quitosano conteniendo DCX (gris) sobre la viabilidad celular, tras 48 h de incubación con células NCI-H460. * Diferencias significativas entre DCX y nanocápsulas de quitosano conteniendo DCX ($p<0,05$).

Como se refleja en la Figura 7, las nanocápsulas de quitosano conteniendo docetaxel aumentaron significativamente el efecto antiproliferativo del fármaco, para un rango de concentraciones de 6 a 25 nM, tras tiempos de incubación de 2 y 48 h **(Artículo 3, Figuras 4 y 5)**. Los estudios de internalización celular, realizados mediante microscopía confocal, demostraron que las nanocápsulas de quitosano también son captadas masivamente por las células NCI-H460, como sucedió con las otras dos líneas previamente estudiadas (Figura 8). Finalmente, se pudo comprobar que el docetaxel, incluido en las nanocápsulas sin poloxámero y liofilizadas, vio incrementado su efecto antiproliferativo con una intensidad similar a la observada con las nanocápsulas sin liofilizar (Figura 9).

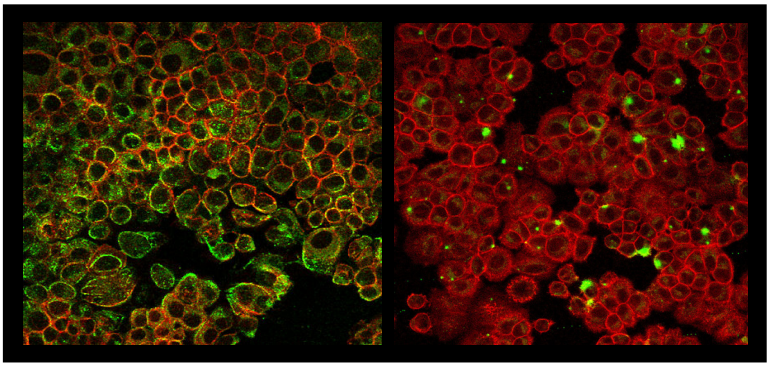

Figura 8. Imagen de microscopía confocal de células NCI-H460 tras una incubación de 2 h con las nanocápsulas quitosano fluorescentes (izquierda) o con una dispersión acuosa del marcador fluorescente (derecha). Las imágenes son secciones x-y con un aumento de 63x. Las nanocápsulas contienen fluoresceína-DHPE (canal verde) mientras que los filamentos de actina fueron teñidos con Bodipy® faloidina (canal rojo).

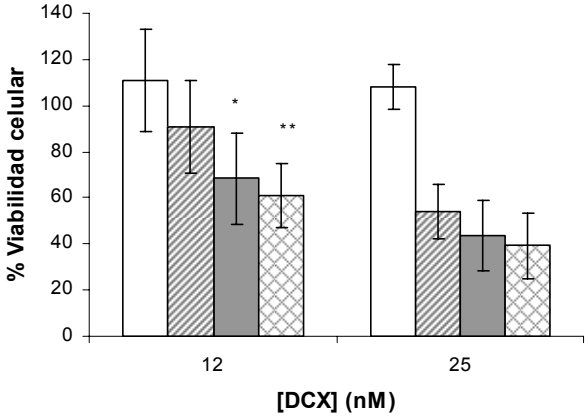

Figura 9. Efecto de las nanocápsulas de quitosano sin poloxámero blancas liofilizadas (blanco),docetaxel (DCX) libre (rayas), nanocápsulas de quitosano sin poloxámero conteniendo DCX (gris) y nanocápsulas de quitosano conteniendo DCX liofilizadas (diamantes) sobre la viabilidad celular, tras 48 h de incubación con células NCI-H460.
* Diferencias significativas entre DCX y nanocápsulas de quitosano sin poloxámero conteniendo con DCX ($p < 0,05$).
** Diferencias significativas entre DCX y nanocápsulas de quitosano sin poloxámero conteniendo DCX liofilizadas ($p < 0,05$).

I.b. Funcionalización de las nanocápsulas de quitosano y evaluación *in vivo* de la actividad antitumoral.

Preparación y caracterización de nanocápsulas de quitosano-PEG y quitosano-PEG-biotina funcionalizadas.

El objetivo de la funcionalización de las nanocápsulas de quitosano mediante el uso de anticuerpos fue conseguir un reconocimiento selectivo por parte de las células cancerosas que sobreexpresan el antígeno en su superficie, favoreciendo la internalización de los sistemas y la liberación del fármaco a nivel intracelular. Esta estrategia ha sido ampliamente estudiada para conseguir el direccionamiento selectivo de diversas nanoestructuras hacia las células tumorales [21-23]. Por lo tanto, basándonos en el conocimiento previo de la sobreexpresión del antígeno tomoregulina por las células de cáncer de pulmón no microcítico, el grupo del Prof. Domínguez desarrolló el correspondiente anticuerpo monoclonal anti-tomoregulina. Asimismo, el grupo del Prof. Riguera se encargó de la modificación del quitosano con PEG y con PEG-biotina, así como de la unión del anticuerpo a las nanocápsulas ya formadas mediante la unión del sistema biotina/avidina.

Las nanocápsulas se prepararon siguiendo la metodología descrita previamente, con la particularidad de que en estos estudios la cubierta polisacarídica de quitosano estaba modificada con PEG o con PEG-biotina. Se desarrollaron tres sistemas: nanocápsulas de quitosano-PEG blancas, nanocápsulas de quitosano-PEG con docetaxel y nanocápsulas de quitosano-PEG-biotina con docetaxel. Todas las formulaciones de nanocápsulas estudiadas mostraron valores muy similares de tamaño medio, siempre inferiores a 200 nm, y carga superficial altamente positiva, debido a la presencia del quitosano en la superficie. Estos valores fueron comparables a los obtenidos para las nanocápsulas de quitosano anteriormente descritas, con la excepción de una pequeña reducción del potencial zeta debido a la presencia de PEG (Tabla 3). No obstante, las etapas de aislamiento y concentración a las que fueron sometidos los sistemas, para incrementar el contenido en docetaxel para su posterior administración *in vivo*, ocasionaron un ligero aumento en el tamaño y

---

[21] **Aktas Y.; Yemisci M.; Andrieux K.; Gürsoy R.N.; Alonso M.J.; Fernandez-Megia E.; Novoa-Carballal R.; Quiñoá E.; Riguera R.; Sargon M.F.; Çelik H.H.; Demir A.S.; Hincal A.A.; Dalkara T.; Çapan Y.; Couvreur P.** (2005). Bioconjug. Chem. 16: 1503-1511.

[22] **Nielsen U.B.; Kirpotin D.B.; Pickering E.M.; Hong K.; Park J.W.; Shalaby M.R.; Shao Y.; Benz C.C.; Marks J.D.** (2002). Biochim. Biophys. Acta. 1591: 109-118.

[23] **Chen H.; Gao J.; Lu Y.; Kou G.; Zhang H.; Fan L.; Sun Z.; Guo Y.; Zhong Y.** (2008) J. Control. Release. 128: 209-216.

polidispersión, pero siempre manteniéndose en torno a los 200 nm.

Tabla 3. Propiedades físico-químicas de las nanocápsulas de quitosano-PEG (CS-PEG) blancas, con docetaxel (DCX) y de CS-PEG-biotina con DCX, concentradas y sin concentrar. (Media ± d.e.; n=3); [a] índice de polidispersión.

	SIN CONCENTRAR			CONCENTRADAS		
Formulación	Tamaño (nm)	IP[a]	Potencial Zeta (mV)	Tamaño (nm)	IP[a]	Potencial Zeta (mV)
NCs CS-PEG blancas	160 ± 2	0,1	39 ± 2	186 ± 20	0,2	32 ± 5
NCs CS-PEG DCX	155 ± 5	0,1	33 ± 6	197 ± 24	0,2	27 ± 9
NCs CS-PEG-Biotina DCX	161 ± 10	0,1	27 ± 6	204 ± 20	0,2	25 ± 5

La encapsulación del docetaxel en las nanocápsulas de quitosano-PEG y quitosano-PEG-biotina no dio lugar a modificaciones apreciables en sus características físico-químicas. Finalmente, se logró incrementar la carga de docetaxel en las nanocápsulas desde valores iniciales del 0.05% hasta el 2.8%, tras someter el sistema a sucesivos procesos de aislamiento y concentración.

La funcionalización de las nanocápsulas se llevó a cabo tras la incubación del nanosistema conteniendo docetaxel, con avidina y, posteriormente, con el anticuerpo anti-tomoregulina biotinilado. De este modo, se consiguió la incorporación del anticuerpo a la superficie del sistema, para asegurar posteriormente una correcta interacción ligando-receptor [24].

Estudios en cultivos celulares

Los estudios en cultivos celulares se realizaron en la línea celular A549 de carcinoma humano de pulmón no microcítico. El objetivo de estos estudios fue evaluar si el proceso de encapsulación alteraba la actividad biológica del docetaxel. Este citostático se une a la tubulina, lo que provoca la estabilización de los microtúbulos causando la parada del ciclo celular o apoptosis. Como se observa en la Figura 10, todas las formulaciones que contienen docetaxel (docetaxel libre, nanocápsulas de quitosano-PEG con docetaxel, y nanocápsulas

[24] **Allen T.M.; Hansen C.B.; Stuart D.D.** (1998). Targeted sterically stabilized liposomal drug delivery. Lasic D.D.; Papahadjopoulos D. Amsterdam, Elsevier Science B. V. 4.6.

de quitosano-PEG-mAb con DCX) produjeron acumulación de células en la fase G2/M, mientras que el resto de los sistemas (nanocápsulas de quitosano-PEG blancas, anticuerpo libre, y células control) no mostraron alteración en el perfil del ciclo celular.

A

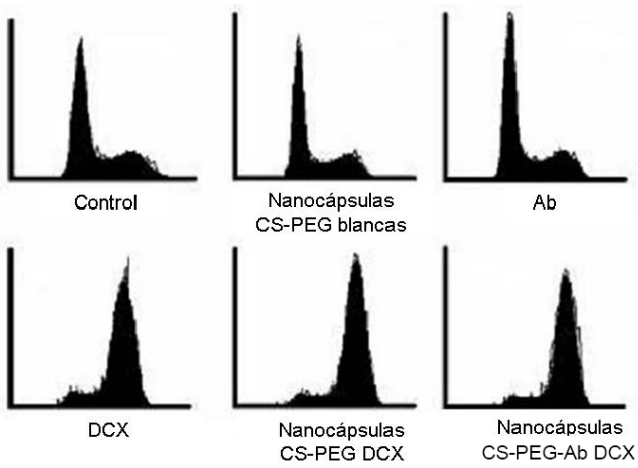

B

	G0/G1	S	G2/M
Control	59,3 ± 2,3	29,7 ± 1,7	11,1 ± 1,1
Nanocápsulas CS-PEG blancas	58,8 ± 2,3	30,6 ± 1,7	10,7 ± 0,9
Ab	61,9 ± 0,8	30,3 ± 2,5	8,5 ± 1,4
DCX	4,2 ± 1,9	25,0 ± 3,6	70,8 ± 5,5
Nanocápsulas CS-PEG DCX	2,3 ± 0,8	25,8 ± 2,3	72,1 ± 3,4
Nanocápsulas CS-PEG-Ab DCX	3,1 ± 0,8	26,9 ± 5,8	70,0 ± 3,4

Figura 10. Resultados que muestran el ciclo celular de la línea A549 sin tratamiento, o tras incubación con las nanocápsulas de quitosano-PEG (CS-PEG) blancas, con el anticuerpo antitomoregulina (mAb), con docetaxel (DCX) libre, con las nanocápsulas de CS-PEG conteniendo DCX o con las nanocápsulas de CS-PEG-mAb conteniendo DCX. (A) Perfiles representativos de citometría de flujo; (B) porcentaje de células que se encontraron en cada fase del ciclo celular.

Estudios *in vivo*

La evaluación biológica de los sistemas desarrollados se realizó en un modelo de cáncer de pulmón de células no microcíticas implantado en ratones. Para ello se realizaron tres administraciones intratumorales de las siguientes formulaciones con una dosis total de docetaxel de 27 mg/Kg: nanocápsulas de quitosano-PEG, nanocápsulas de quitosano-PEG-mAb y el control comercial Taxotere®. Como blanco, se utilizó el grupo sin tratar. Los resultados de progresión del volumen del tumor (Figura 11), indicaron que tanto las nanocápsulas conteniendo docetaxel, como la formulación comercial, frenaron eficazmente el desarrollo del tumor en comparación al grupo control. Este efecto también se observó en la reducción del tamaño y peso de los tumores (Figura 12). Asimismo, la progresión diaria del volumen del tumor determinada en los 14 días siguientes a la primera dosis, reflejó un desarrollo similar de los tumores tras la administración de cada una de las formulaciones (Figura 13). La formulación de nanocapsulas funcionalizadas no mejoró, sin embargo, el efecto de las que no contienen el anticuerpo.

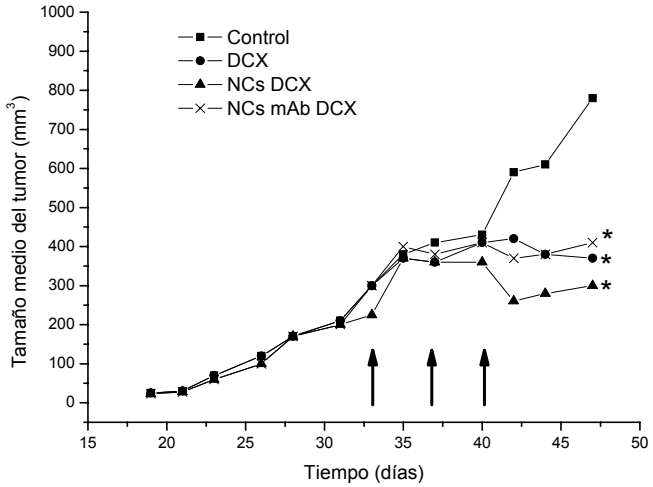

Figura 11. Desarrollo del volumen del tumor tras la administración de la formulación de docetaxel (DCX) comercial Taxotere®, nanocápsulas de quitosano-PEG conteniendo DCX (NCs DCX) y nanocápsulas de quitosano-PEG-funcionalizadas conteniendo DCX (NCs mAb DCX), en comparación con el grupo control sin tratar (las flechas negras indican las administraciones). * Diferencias significativas con el grupo control ($p<0,05$).

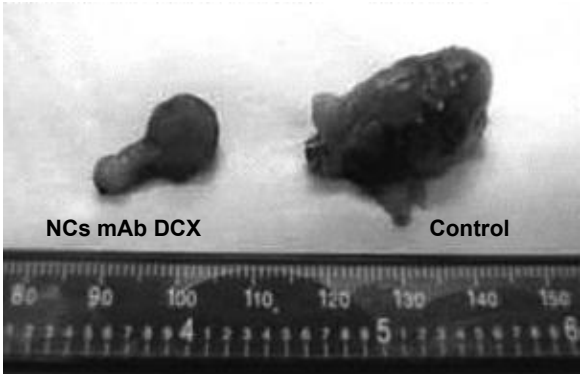

Figura 12. Imagen de los tumores extraídos al final del estudio, en la que se compara un tumor tratado con las nanocápsulas funcionalizadas conteniendo docetaxel (NCs mAb DCX) con un tumor perteneciente al grupo control.

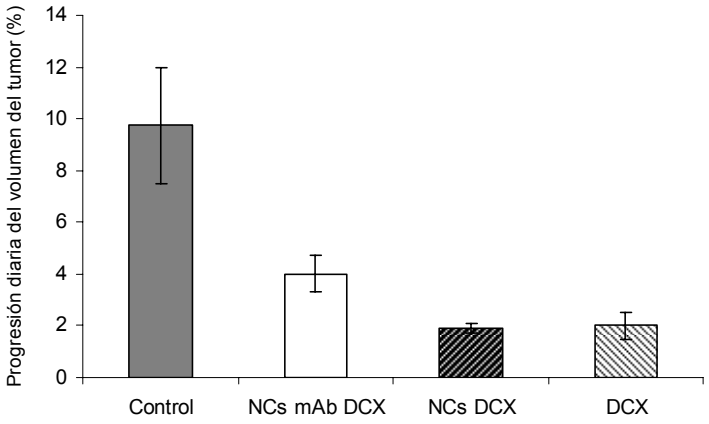

Figura 13. Progresión diaria del volumen del tumor durante el tratamiento con la formulación de docetaxel (DCX) comercial Taxotere®, nanocápsulas de quitosano-PEG conteniendo DCX (NCs DCX) y nanocápsulas de quitosano-PEG-funcionalizadas conteniendo DCX (NCs mAb DCX) en comparación con el grupo control sin tratar.

El análisis del efecto de cada inyección sobre el volumen del tumor, que recoge la Figura 14, indica las diferencias existentes entre el efecto del docetaxel libre (Taxotere®) y el encapsulado. La primera dosis no causó reducción en el volumen del tumor, muy probablemente debido a que la cantidad de fármaco administrado (9 mg/Kg) no fue suficiente, aunque también pudo ser debido a que el fármaco precisa de tiempos más largos para que su efecto sea significativo, ya que la medida se realizó a los 4 días postadministración. En cambio, tras la

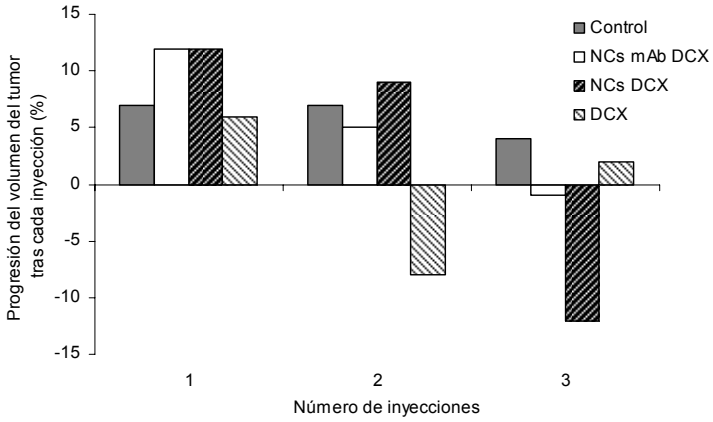

Figura 14. Variación del tamaño del tumor tras cada una de las 3 inyecciones de los siguientes tratamientos: control (sin tratamiento), nanocápsulas funcionalizadas conteniendo docetaxel (NCs mAb DCX), nanocápsulas conteniendo DCX (NCs DCX) y formulación de DCX comercial Taxotere®.

segunda dosis, se observó que el fármaco libre redujo el tamaño medio del tumor, sin apreciarse cambio alguno para el fármaco encapsulado. No obstante, tras la tercera dosis, es cuando se aprecia la reducción del tumor provocada por la formulación de nanocápsulas sin funcionalizar. Estos resultados sugieren que el efecto del docetaxel (Taxotere®) es más acentuado y breve en comparación al producido por el sistema de nanocápsulas que incluye docetaxel, tras el cual se observa que el fármaco necesita más tiempo para ejercer su acción pero ésta es más prolongada. Esta posibilidad se relacionaría con la facilidad de internalización de las nanocápsulas observada *in vitro*, que permitiría una liberación más prolongada del docetaxel y, por lo tanto, maximizar su eficacia. Sin embargo, las diferencias observadas no han sido muy rotundas, si se compara el fármaco libre y el encapsulado. Un incremento de dosis de docetaxel, permitiría quizás poner de manifiesto de manera más significativa el efecto de la inclusión del fármaco en las nanocápsulas, como ha ocurrido en estudios muy similares.

Así, Koziara *et al.* han publicado un estudio en el que se demuestra el efecto de la pauta de administración de las formulaciones en su eficacia antitumoral *in*

vivo en modelo animal de ratón [25]. De este modo, tanto el aumento de la dosis de paclitaxel (1.5 frente a 0.75 mg/Kg) como el menor volumen del tumor al inicio del estudio (150 frente a 300 mm^3), fueron claves a la hora de demostrar la mejora significativa de la actividad antitumoral de las nanopartículas que asociaban paclitaxel con respecto al control comercial (Taxol®).

Por otro lado, aunque diversos autores han demostrado que el proceso de funcionalización de nanosistemas con anticuerpos monoclonales mejora la acumulación de los mismos en el tejido tumoral, aumentando así su actividad antitumoral en comparación con la formulación comercial y con los nanosistemas sin funcionalizar [26; 27], en nuestro caso no ha sido así. La modificación de los nanosistemas mediante la unión de anticuerpos en su superficie suele favorecer la internalización de los mismos a través de la interacción antígeno-anticuerpo, obteniéndose un aumento de la actividad antitumoral en comparación con los sistemas sin modificar [28]. Las nanocápsulas ensayadas en este estudio presentan alta capacidad de internalización, por lo que podría suceder que el efecto de los anticuerpos se viese encubierto, observándose similar actividad antitumoral para ambos sistemas. No obstante, otras causas que explicarían la ausencia de mejoras tras la funcionalización de las nanocápsulas podrían estar relacionadas con una escasa expresión del antígeno TMEFF-2 en la superficie de las células tumorales o debido a una falta de especificidad por parte del anticuerpo frente al antígeno expresado por las células tumorales implantadas [29-31]. La confirmación de estas hipótesis plantea un estudio más profundo que explique cómo se desarrolla esta interacción *in vivo*.

---

[25] **Koziara J.M.; Whisman T.R.; Tseng M.T.; Mumper R.J.** (2006). J. Control. Release. 112: 312-319.

[26] **Chen H.; Gao J.; Lu Y.; Kou G.; Zhang H.; Fan L.; Sun Z.; Guo Y.; Zhong Y.** (2008). J. Control. Release. 128: 209-216.

[27] **Torchilin V.P.; Lukyanov A.N.; Gao Z.; Papahadjopoulos-Sternberg B.** (2003). Proc. Natl. Acad. Sci. USA. 100: 6039-6044.

[28] **Kirpotin D.B.; Drummond D.C.; Shao Y.; Shalaby M.R.; Hong K.; Nielsen U.B.; Marks J.D.; Benz C.C.; Park J.W.** (2006). Cancer Res. 66: 6732-6740.

[29] **Yang T.; Choi M.K.; Cui F.D.; Lee S.J.; Chung S.J.; Shim C.K.; Kim D.D.** (2007). Pharm. Res. 24: 2402-2411.

[30] **Goren D.; Horowitz A.T.; Zalipsky S.; Woodle M.C.; Yarden Y.; Gabizon A.** (1996). Br. J. Cancer. 74: 1749-1756.

[31] **Park J.W.; Hong K.; Carter P.; Asgari H.; Guo L.Y.; Keller G.A.; Wirth C.; Shalaby R.; Kotts C.; Wood W.I.; Papahadjopoulos D.; Benz C.C.** (1995). Proc. Natl. Acad. Sci. U.S.A. 92: 1327–1331.

Parte II. Nanocápsulas de poliarginina conteniendo docetaxel para la liberación intracelular de fármacos antitumorales.

Preparación y caracterización físico-química de las nanocápsulas de poliarginina.

En esta etapa, nos planteamos el diseño de un nuevo sistema de nanocápsulas poliméricas, en el que la cubierta está constituída por el poliaminoácido poliarginina, también de carga positiva. Resulta especialmente novedosa la elección de la poliarginina como recubrimiento, ya que hasta ahora no se había descrito ningún sistema similar. El interés de la poliarginina radica en sus demostradas propiedades como potenciador de la internalización celular de moléculas activas. Las nanocápsulas se prepararon igualmente mediante la técnica de desplazamiento del disolvente [19]. El procedimiento utilizado fue análogo al anteriormente descrito para la preparación de las nanocápsulas de quitosano, con la diferencia de que, en este caso, en la fase acuosa se incorporó únicamente la poliarginina. Asimismo, se incorporaron fosfolípidos peguilados, como el estearato de PEG, en la fase orgánica para dar lugar a las nanocápsulas de poliarginina-PEG. El valor adicional de esta formulación es la mejora de la estabilidad en fluidos biológicos así como la posibilidad de su administración por vía endovenosa, puesto que la cubierta de PEG reduce el reconocimiento de los nanosistemas por el sistema fagocítico mononuclear. En la Tabla 4, se muestran los valores de tamaño, índice de polidispersión y potencial zeta de las nanocápsulas de poliarginina y de poliarginina-PEG. Se observa que las nanocápsulas presentan una población con baja polidispersión, tamaño nanométrico inferior a 200 nm y potencial altamente positivo para las nanocápsulas de poliarginina, que se redujo en el caso de las nanocápsulas de poliarginina-PEG debido a la cubierta de PEG, manteniéndose aún así el sistema cargado positivamente.

Eficacia de encapsulación y liberación de docetaxel a partir de las nanocápsulas de poliarginina.

La encapsulación del fármaco docetaxel en las nanocápsulas de poliarginina se realizó por el mismo procedimiento anteriormente descrito para las nanocápsulas de quitosano. Del mismo modo, la eficacia de encapsulación y el perfil de liberación de la molécula fueron muy similares a los obtenidos para las nanocápsulas de quitosano **(Artículo 4, Figura 5)**. Estos resultados indican que tanto la encapsulación como la liberación están determinadas principalmente por

las propiedades de la molécula incorporada, así como por las del núcleo oleoso, sin influir prácticamente la naturaleza de la cubierta polimérica.

Tabla 4. Propiedades físico-químicas de las nanocápsulas de poliarginina (PArg) blancas, PArg-PEG blancas, conteniendo docetaxel (DCX) o el marcador fluorescente fluoresceína-DHPE. (Media ± d.e.; n=3); [a] índice de polidispersión.

Formulación	Tamaño (nm)	IP[a]	Potencial zeta (mV)
Nanocápsulas PArg	145 ± 13	0,1	+ 53 ± 6
Nanocápsulas PArg-PEG	125 ± 5	0,1	+ 28 ± 3
Nanocápsulas PArg-DCX	170 ± 10	0,1	+ 56 ± 6
Nanocápsulas PArg fluorescentes	172 ± 8	0,1	+ 42 ± 4

Estudios en cultivos celulares.

Los estudios de viabilidad celular realizados en la línea NCI-H460 demostraron que las nanocápsulas de poliarginina con docetaxel también son eficaces vehículos que aumentan significativamente el efecto antiproliferativo del fármaco para concentraciones situadas en el rango 3-25 nM (Figura 15). De hecho, los valores de concentración inhibitoria 50 (IC_{50}) de las nanocápsulas de poliarginina fueron 4 veces inferiores a los obtenidos para el fármaco en solución,

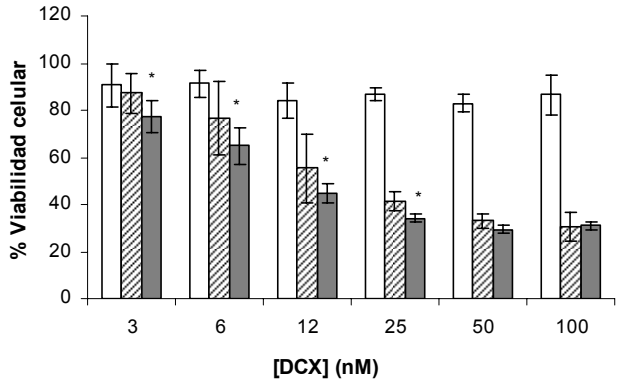

Figura 15. Efecto de las nanocápsulas de poliarginina blancas (blanco), docetaxel (DCX) libre (rayas) y nanocápsulas de poliarginina conteniendo DCX (gris) sobre la viabilidad celular, tras 48 h de incubación con las células NCI-H460. ***** Diferencias significativas entre DCX y nanocápsulas de poliarginina conteniendo DCX ($p<0,05$).

disminuyendo de 11,8 nM a 3,11 nM. Por otro lado, las nanocápsulas de poliarginina blancas no disminuyeron la viabilidad celular en grado alguno, lo cual demuestra la inocuidad del sistema.

Se realizaron estudios de captura celular para determinar si la presencia de la cubierta de poliarginina favorecía la internalización de las nanocápsulas. Para ello se analizaron mediante citometría de flujo las células incubadas previamente con las nanocápsulas de poliarginina fluorescentes y con los controles. Los resultados indicaron que las nanocápsulas de poliarginina son eficazmente internalizadas, en una proporción significativamente superior a la observada para la nanoemulsión y la dispersión acuosa del marcador libre (Figura 16). Así pues, se pone de manifiesto que la cubierta polimérica de poliarginina desempeña un papel esencial en la captura celular de los nanosistemas.

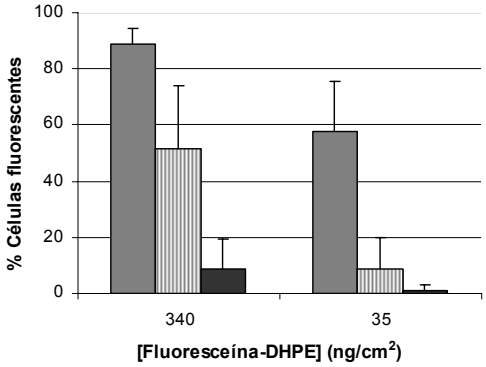

Figura 16. Captura celular de las nanocápsulas de poliarginina fluorescentes (gris), nanoemulsión (rayas) y dispersión acuosa del marcador fluorescente (negro) tras 2 h de incubación con las células NCI-H460. (Media ± d.e.; n=3).

Asociación de ADN plasmídico a las nanocápsulas de poliarginina.

El interés de la incorporación de material genético a las nanocápsulas de poliarginina es notable, si se tiene en cuenta la capacidad de internalización celular de este poliaminoácido. Con el objetivo de reducir el estrés que pueden sufrir los fármacos durante el proceso de encapsulación, especialmente si se trata de biomoléculas, la opción de asociar el principio activo a la superficie de las nanoestructuras aparece como una interesante alternativa [32; 33]. Así, en este

[32] **Singh M.; Briones M.; Ott G.; O'Hagan D.** (2000). Proc. Natl. Acad. Sci. U.S.A. 97: 811-816.
[33] **Messai I.; Lamalle D.; Munier S.; Verrier B.; Ataman-Önal Y.; Delair T.** (2005). Colloids Surf. A Physicochem. Eng. Asp. 255: 65-72.

estudio incorporamos ADN plasmídico (pADN) a las nanocápsulas de poliarginina y de poliarginina-PEG mediante la adsorción del mismo sobre la superficie del sistema. Dicha asociación se realizó con diferentes proporciones de material genético/nanocápsulas. Los resultados del estudio indicaron que las proporciones óptimas eran las del 3 y 10%. Los valores de la Tabla 5 muestran que los nanosistemas presentan tamaños inferiores a 200 nm, y potenciales zeta que se redujeron con respecto a las nanocápsulas blancas. Esta disminución puede atribuirse a la presencia de los grupos fosfato del pADN adsorbido en la superficie de las nanocápsulas.

Tabla 5. Propiedades físico-químicas de las nanocápsulas de poliarginina (PArg) y PArg-PEG conteniendo pADN asociado en relaciones 3 y 10%. (Media ± d.e.; n=3); [a] índice de polidispersión.

Formulación	Tamaño (nm)	IP[a]	Potencial zeta (mV)
Nanocápsulas PArg 3% pADN	129 ± 4	0,2	+47 ± 2
Nanocápsulas PArg 10% pADN	136 ± 9	0,2	+31 ± 6
Nanocápsulas PArg-PEG 3% pADN	167 ± 13	0,2	+ 9 ± 1
Nanocápsulas PArg-PEG 10% pADN	186 ± 17	0,2	-1 ± 2

La eficacia de asociación del pADN a las nanocápsulas de poliarginina se determinó cualitativamente mediante electroforesis, evaluando el pADN libre. Como se puede apreciar en la Figura 17, para las proporciones del 3 y 10% se

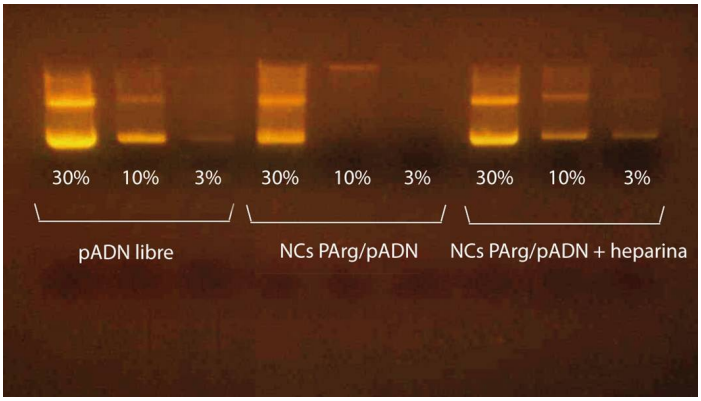

Figura 17. Gel de electroforesis de pADN libre, nanocápsulas de poliarginina con pADN asociado y nanocápsulas de poliarginina con pADN asociado tratadas con heparina, para distintas relaciones pADN/nanocápsulas.

observó una total asociación del pADN a las nanocápsulas, no detectándose la presencia de plásmido libre en el gel. Además, dicha interacción se producía de manera intensa, siendo necesaria la adición de elevadas concentraciones de heparina (15 mg/mL) para conseguir el desplazamiento del pADN. Para la proporción del 30% se observó una asociación significativa, aunque también se detectó la presencia de plásmido libre en el gel. La proporción del 3% fue la seleccionada para el resto de los estudios con pADN.

A continuación se evaluó el potencial de las nanocápsulas de poliarginina y de poliarginina-PEG como sistemas para la vehiculización de pADN, en comparación con los complejos pADN/poliarginina previamente descritos en la literatura [34]. Para ello se prepararon una serie de complejos pADN/poliarginina de relaciones de peso 5:1-1:5. Los valores de diámetro medio, índice de polidispersión, así como de carga eléctrica superficial (potencial zeta) de los complejos se encuentran recogidos en la Tabla 6.

Tabla 6. Propiedades físico-químicas de los complejos pADN/poliarginina elaborados en las relaciones pADN/poliarginina que se indican (Media ± d.e.; n=3); [a] índice de polidispersión.

Formulación	Tamaño (nm)	PI[a]	Potencial Zeta (mV)
Complejos 5:1	176 ± 63	0,32	-11 ± 2
Complejos 3:1	101 ± 42	0,24	-12 ± 2
Complejos 1:1	79 ± 13	0,21	+19 ± 3
Complejos 1:3	150 ± 77	0,31	+14 ± 1
Complejos 1:5	132 ± 20	0,28	+9 ± 1

Como se observa en la Figura 18, los complejos de pADN/poliarginina presentan tamaños inferiores a 200 nm cuando se encuentran suspendidos en agua. Sin embargo, tras su dilución en tampón fosfato se produce la agregación masiva de los complejos, lo que pone de manifiesto su inestabilidad en fluidos biológicos. Por el contrario, las nanocápsulas de pADN/poliarginina, y también las de pADN/poliarginina-PEG, mostraron un comportamiento mucho más favorable: las nanocápsulas de pADN/poliarginina-PEG permanecieron estables tras su dilución en tampón fosfato y las de pADN/poliarginina experimentaron un incremento inicial de su tamaño de 200 nm, pero en ningún caso fueron objeto de agregación masiva.

[34] **Rudolph C.; Plank C.; Lausier J.; Schillinger U.; Müller R.H.; Rosenecker J.** (2003). J. Biol. Chem. 278: 11411-11418.

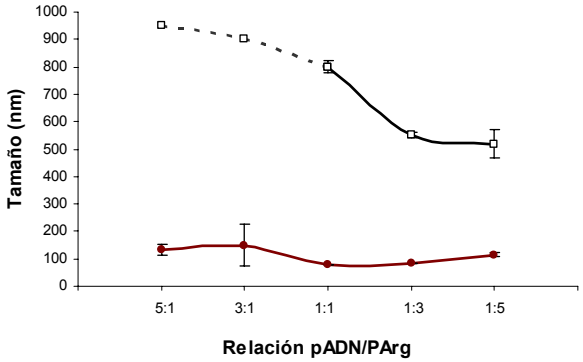

Figura 18. Tamaño de los complejos de pADN/poliarginina en agua (●) y en tampón fosfato (□), para distintas relaciones pADN/poliarginina.

Asimismo, se evaluó la posible liberación prematura del ADN a partir de las nanocápsulas tras su incubación en tampón fosfato. Los resultados de gel de electroforesis mostrados en la Figura 19 muestran que tanto las nanocápsulas de poliarginina como las de poliarginina-PEG asocian eficazmente el pADN y no lo liberan tras su incubación en tampón fosfato.

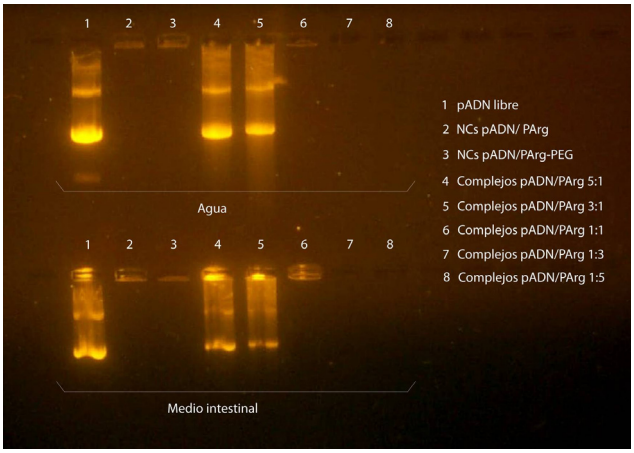

Figura 19. Evaluación del grado de asociación de pADN a las nanocápsulas de poliarginina, a las nanocápsulas de poliarginina-PEG y a los complejos con poliarginina.

CONCLUSIONES

CONCLUSIONES

El trabajo experimental recogido en la presente memoria, se ha dirigido al diseño de nuevas formulaciones de nanocápsulas poliméricas para la vehiculización de fármacos citostáticos. Los resultados obtenidos nos han permitido extraer las siguientes conclusiones:

Parte I. Nanocápsulas de quitosano para la liberación intracelular de fármacos antitumorales.

Parte Ia. Desarrollo de nanocápsulas de quitosano conteniendo docetaxel.

1. La técnica de desplazamiento de disolvente ha permitido la obtención de nanocápsulas constituidas por un núcleo oleoso y una cubierta polimérica a base de oligómeros de quitosano. Las nanocápsulas resultantes tienen tamaño nanométrico (inferior a 200 nm), baja polidispersión y carga superficial altamente positiva (en torno a +40 mV). El fármaco citostático docetaxel se ha incorporado eficazmente en los sistemas nanocapsulares desarrollados, sin que ello haya modificado significativamente sus propiedades físico-químicas.

2. Los estudios realizados sobre células tumorales de cáncer de mama (MCF 7) y pulmón (A549), han evidenciado una internalización más rápida del fármaco cuando se encuentra encapsulado en las nanoestructuras, hecho que se refleja en una eficacia antitumoral significativamente superior del fármaco encapsulado durante un período de estudio de 24 h.

3. La optimización de las nanocápsulas de quitosano, tras la eliminación del tensoactivo poloxámero 188 de su composición, ha dado lugar a la obtención de una formulación liofilizable que vehiculiza eficazmente el docetaxel a las células tumorales.

Parte I.b. Funcionalización de las nanocápsulas de quitosano y evaluación *in vivo* de la actividad antitumoral.

1. Se han funcionalizado en superficie las nanocápsulas de quitosano con el anticuerpo antitomoregulina mediante la reacción biotina-avidina entre las nanocápsulas de quitosano-PEG-avidina y el anticuerpo biotinilado.

2. Tras su administración intratumoral, las nanocápsulas de quitosano conteniendo docetaxel frenaron eficazmente el desarrollo del tumor implantado en ratones desnudos, de modo comparable a la formulación comercial de docetaxel (Taxotere®). El proceso de funcionalización no aportó mejoras relacionadas con una mayor localización del nanosistema en las células tumorales.

Parte II. Nanocápsulas de poliarginina para la liberación intracelular de fármacos antitumorales

1. Los resultados de la caracterización físico-química de las nanocápsulas de poliarginina revelaron que el poliaminóacido interacciona fuertemente con la superficie del núcleo oleoso, dando lugar a nanocápsulas de tamaño inferior a 200 nm, y con potencial zeta altamente positivo (+50 mV). Asimismo, las nanocápsulas de poliarginina pueden ser modificadas con una cubierta externa de PEG, que amplía la aplicación del sistema para su administración endovenosa.

2. Las formulaciones desarrolladas muestran una gran versatilidad para encapsular eficazmente fármacos de distintas características, desde los muy hidrofóbicos como el docetaxel, a polinucleótidos de carácter hidrofílico, como el ADN plasmídico.

3. En la evaluación biológica, se ha demostrado la validez de las nanocápsulas de poliarginina como vehículos de fármacos antitumorales, puesto que potencian la acción del docetaxel al favorecer su internalización celular.

CONCLUSIONS

The experimental work included in this manuscript was aimed to design novel formulations of polymeric nanocapsules to target antitumor drugs. The results obtained enabled us to conclude the following points:

Part I. Chitosan nanocapsules as vehicles for the intracellular delivery of antitumor drugs.

Part Ia. Development of chitosan nanocapsules containing docetaxel.

1. The solvent displacement technique has enabled the formation of nanocapsules constituted by an oil core and a polymer shell of chitosan oligomers. The resulting nanocapsules have nanometric size (less than 200 nm), low polydispersity and highly positive superficial charge (about 200 nm). The cytostatic drug docetaxel has been efficiently incorporated to the nanocapsules without significant modification in their physicochemical properties.

2. The cell culture studies performed on breast cancer tumor cells (MCF 7) and lung cancer cells (A549) showed the fast internalization of the drug when it is included in the nanosystems. This process produced a significant enhancement of the antitumor effect of the drug in a period of 24 h.

3. The optimization process of chitosan nanocapsules, by the elimination of the tensioactive Pluronic® F68 from the formulation, has produced an improved lyophilized formulation that transport efficiently the drug to the tumor cells.

Part I.b. Functionalization of chitosan nanocapsules and *in vivo* evaluation of their antitumor activity.

1. The surface of chitosan nanocapsules has been functionalized with the antibody antitomoregulin by the reaction biotin-avidin with chitosan-PEG-avidin nanocapsules and the biotinylated antibody.

2. By intratumoral administration of the formulations, it could be clearly seen that docetaxel-loaded chitosan nanocapsules efficiently

hindered the development of the xenografts as the commercial formulation of docetaxel did (Taxotere®). Nevertheless, the functionalization of the nanocapsules did not improve the internalization of the system in the tumor cells.

Part II. Polyarginine nanocapsules as vehicles for the intracellular delivery of antitumor drugs.

1. The physicochemical characterization of polyarginine nanocapsules showed that the polyaminoacid massively interacts with the oil core surface, producing nanocapsules of less that 200 nm and highly positive surface charge (+50 mV). Moreover, polyarginine nanocapsules can be modified by an external shell of PEG that maximizes the scope of the nanosystem for its intravenous administration.

2. The developed formulations showed high versatility to efficiently encapsulate drugs of different characteristics, such as hydrophobic drugs like docetaxel or polynucleotides of hydrophilic character like plasmid DNA.

3. The biological evaluation of the formulations showed that polyarginine nanocapsules are efficient systems for the vehiculization of antitumor drugs. These nanocapsules have shown to promote the effect of docetaxel by improving its internalization.